UNIVERSITY OF
CAMBRIDGE

Some more problems of geodynamics

Matthew Alexander Maitra

Trinity College

This dissertation is submitted on June 14, 2021 for the degree of Doctor of Philosophy.

Declaration

This dissertation is the result of my own work and includes nothing which is the outcome of work done in collaboration except as declared in the Preface and specified in the text. It is not substantially the same as any that I have submitted, or am concurrently submitting, for a degree or diploma or other qualification at the University of Cambridge or any other University or similar institution except as declared in the Preface and specified in the text. I further state that no substantial part of my dissertation has already been submitted, or is being concurrently submitted, for any such degree, diploma or other qualification at the University of Cambridge or any other University or similar institution except as declared in the Preface and specified in the text. This dissertation does not exceed the prescribed limit of 275 numbered pages of which not more than 225 pages are text, appendices, illustrations and bibliography.

Two chapters of this dissertation are based on research published in scientific journals, Chapter 2 as Maitra & Al-Attar (2019) and Chapter 3 as Maitra & Al-Attar (2020). An expanded version of Chapter 4 is expected to be submitted later in 2021; that chapter, in turn, builds on work that was begun during my Part III Project.

Matthew Alexander Maitra
June 14, 2021

Abstract

Some more problems of geodynamics

Matthew Alexander Maitra

This dissertation presents new theoretical methods that could contribute to constraining the deep Earth's long-wavelength density structure.

In Chapter 2 we present a numerically exact method for calculating the internal and external gravitational potential of aspherical and heterogeneous planets. Such calculations are crucial in computing Earth's long-period deformation. Our approach is based on the transformation of Poisson's equation into an equivalent equation posed on a spherical computational domain. This new problem is solved in an efficient iterative manner based on a hybrid pseudo-spectral/spectral-element discretisation. The main advantage of our method is that its computational cost reflects the planet's geometric and structural complexity, being in many situations only marginally more expensive than boundary perturbation theory. Several numerical examples are presented to illustrate the method's efficacy and potential range of applications.

In Chapter 3 we investigate theoretically the dependence of the elastic tensor on the equilibrium stress, our aim being to understand the effect of nonzero stress on seismic wave propagation and Earth's long-period motion. Using ideas from finite elasticity, it is first shown that both the equilibrium stress and elastic tensor are given uniquely in terms of the equilibrium deformation gradient relative to a fixed choice of reference body. Inversion of the relation between the deformation gradient and stress might, therefore, be expected to lead neatly to the desired expression for the elastic tensor. Unfortunately, the deformation gradient can only be recovered from the stress up to a choice of rotation matrix. Hence it is not possible in general to express the elastic tensor as a unique function of the equilibrium stress. By considering material symmetries, though, it is shown that the degree of non-uniqueness can sometimes be reduced, and in some cases even removed entirely. These results are illustrated through a range numerical calculations, and we also obtain linearised relations applicable to small perturbations in equilibrium stress. Finally, we make a comparison with previous studies before considering implications for geophysical forward- and inverse-modelling.

Finally, in Chapter 4 we present a theoretical framework for modelling the rotational dynamics of solid elastic bodies. It takes full account of: Earth's variable rotation, aspherical topography, and lateral variations in density and wave-speeds. It is based on an exact decomposition of the body's motion that separates out the motion's elastic and rotational components, in a way that

we make precise in the main text. As a prelude to the elastic problem, we show how Hamilton's principle provides an elegant means of deriving the exact and linearised equations of *rigid* body motion, then study the normal modes of a rigid body in uniform rotation. We subsequently build on these ideas to write down the exact equations of motion of a variably rotating elastic body. We linearise the equations and discuss their numerical solution, before showing how to extend these ideas to analyse N elastic bodies interacting through gravity.

We conclude in Section 4.7 by discussing the extensions that would be necessary in order to describe layered fluid-solid bodies. Importantly, with those extensions the framework will bypass the numerical difficulties commonly associated with the Earth's fluid layers, and could therefore readily be used to model diurnal tides. Thus, it would allow the abundant data provided by diurnal tides to be used to constrain lateral variations in mantle density. Furthermore, it would allow for a systematic investigation of the effect of lateral density heterogeneities on the Earth's rotation; this has never yet been undertaken, and will provide additional constraints on mantle density and other parameters of interest.

Acknowledgements

First and foremost I thank my supervisor, Dr David Al-Attar, for his unwavering support throughout my PhD. There are a number of reasons for which it cannot always have been easy, not least among them my occasional mathematical recalcitrance. In spite of those hurdles DAA – through his immense insight, experience and generosity – has overhauled my approach to physics in ways I could not have conceived of four years ago. Ultimately, he has permitted me to undertake work that I am proud of. All errors in this thesis are, naturally, my own.

Throughout this work I have been supported financially by an EPSRC studentship and a CASE award from BP. I am grateful to BP for sponsoring work whose ultimate motivation is to understand how mass is distributed within the lower mantle and core. It is not impossible that this work will contribute to that firm's putative 'pivot' towards green energy over the next decades, but I'm not holding my breath.

Chapter 2 benefitted from the insights of Frédéric Chambat, an anonymous reviewer and GJI editor Gaël Choblet, all of whom provided helpful comments and suggestions. In writing Chapter 3 I was aided greatly by Jeroen Tromp, Brent Delbridge and GJI editor Juan Carlos Afonso. I would particularly like to thank Prof. Tromp for taking the time to discuss our initial results with us at length. Those conversations contributed greatly to the shaping of Section 3.1, Section 3.3.1 and Appendix B.4, and they significantly improved my own understanding of the work.

Prof. John Woodhouse has left an indelible mark on this work, not only by providing us with computer code that gives new meaning to the words "speed" and "illegibility", but also by influencing my thinking on a profound level through his former student DAA. It should be mentioned too that the titular homage to the essay of Love (1911) was – as with so many things – originally suggested by John.

My friends and parents have helped me more than I can say. Georg and Attila have been superb non-specialist sounding boards, and it is only thanks to my parents' support that I have managed to complete this work.

Finally, no piece of work written by me can truly be complete until it has included special thanks to Dr Anson Cheung, of Trinity College and the Cavendish Laboratory's 'Theory of Condensed Matter' department, and to whom this work is dedicated. Without his guidance during my formative years it is unlikely that this thesis would exist; it certainly would not have been written by me.

Contents

CHAPTER 1

Introduction

The Earth's mantle is believed to convect on long timescales, but several features of that convection remain elusive. In particular, it is not known whether convection in the lowermost mantle is driven purely by thermal variations, or whether compositional effects are important too (e.g. Garnero et al., 2016). To answer that question we would like measurements of the temperature, composition and density of the mantle. But these are hard to obtain directly. Given that our planet's interior is off limits beyond the depth of a few kilometres, we can only constrain its interior properties through observations made at the surface. In order to paint a detailed global picture of the deep Earth one must turn to seismology. Geochemistry also provides important insights into the nature of the lower mantle, but within this introduction we will focus on the geophysical aspect.

Using seismology to learn about the deep Earth involves some trade-offs. For a start, seismology only provides a snapshot of the present-day Earth, along with a little information about the Earth's recent history. Secondly, much as seismic waves are able to probe areas of the planet that we cannot hope to observe directly, the quantities that they allow us to measure are not necessarily those that we are most interested in. Broadly speaking, through seismology we can constrain: *seismic wave speeds*, which contain information on Earth's elastic structure; *quality factors* pertaining to anelastic structure; and *density*. Seismic observations can therefore act only as proxies for temperature and composition. Nevertheless, seismology is an important tool for studying laterally varying temperature, composition and density in the lower mantle.

1.1 Constraining Earth's interior structure through seismology

The seismological study of Earth's interior was initiated around the turn of the nineteenth century. Oldham (1906) inferred the existence of the Earth's core, and Gutenberg (1913) provided the first constraint on the depth of the core-mantle boundary (CMB). Lehmann (1936) later inferred the existence of the inner core, while the analyses of Jeffreys (1939, 1949) and Birch (1952) provided strong evidence that the outer core should be fluid and the inner core solid. This work culminated 40 years ago when Dziewonski & Anderson (1981) established the Earth's spherically-averaged elastic, anelastic and density structure. Those authors inverted a large data-set – consisting of normal mode periods and Q values, travel times, and mass and moment of inertia – to produce

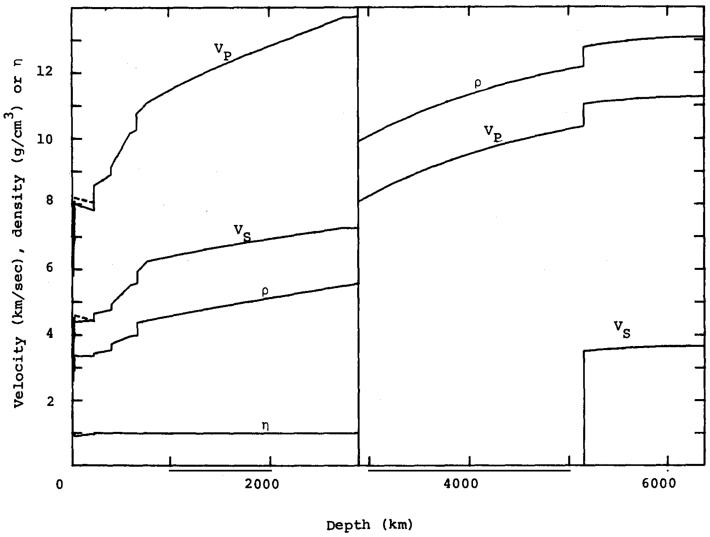

Figure 1.1: PREM's density and S- and P-wave velocities plotted as functions of radius. The dashed lines represent horizontal components of the velocity. Also plotted is the parameter η, which equals unity when the model is isotropic. η is not plotted in the isotropic core. Figure from Dziewonski & Anderson (1981).

the 'Preliminary Reference Earth Model' (PREM). PREM's S- and P-velocities and density are plotted in Fig 1.1 as a function of radius. This approach, whereby aspherical structure is ignored, is justified *a priori* by observations and physical arguments that suggest the Earth is unlikely to deviate too much from spherical symmetry. It was especially well motivated in the early 1980s due to the quality of available normal mode data and existing computational resources. It is also justified *a posteriori* by the fact that modern models (such as Ritsema et al.'s (2010) S-wave tomographic model S40RTS) measure their lateral deviations from PREM by little more than a few percent.

S40RTS is one of the many S-wave tomographic models that have been produced in the decades since PREM. Fig. 1.2 presents a comparison of several such models. They all show broad – though not perfect – agreement among themselves on the distribution of S-wave speeds (e.g. Masters et al., 2000; Ritsema et al., 2010). P-wave tomographic models (e.g. Su & Dziewonski, 1997) exist too, but they are outnumbered by S-wave models because shear velocity has the largest effect on most observables and it is also thought that shear velocity variations in the mantle will be larger than those in other parameters. Of particular interest is the fact that the vast majority of tomographic models contain continent-sized regions at the base of the mantle – one under Africa, the other under the Pacific – within which both S- and P-waves travel anomalously slowly. These enigmatic regions are known as LLSVPs ('Large Low Shear Velocity Provinces'; see Garnero et al. (2016) and McNamara (2019) for comprehensive recent reviews). Fig. 1.3 gives a more detailed illustration of an LLSVP according to the model S20RTS of Ritsema et al. (1999, 2004). Their provenance is not known. Are they simply evidence of upwelling mantle at the base of a thermal convection cell? Or are they a 'slab graveyard' (e.g. Tackley, 2011)? The answers are not known, but are surely related intimately to the more general question of the nature of lower mantle convection.

From S- and P-wave tomography one can start to constrain the temperature and composition

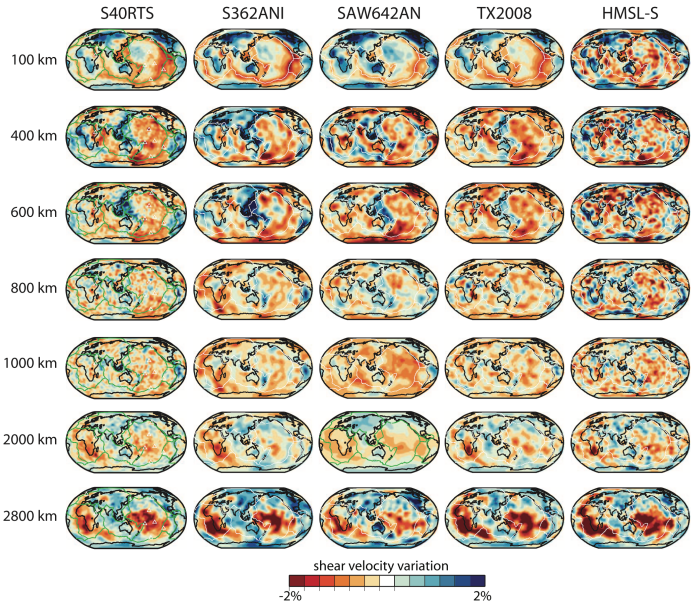

Figure 1.2: A comparison of some different S-wave tomographic models, each plotted at several different depths. From left to right: S40RTS (Ritsema et al., 2010), S362ANI (Kustowski et al., 2008), SAW642AN (Panning & Romanowicz, 2006), TX2008 (Simmons et al., 2009), HMSL-S (Houser et al., 2008). The velocities vary by $\pm 2\%$ about the average value, except for the 100km maps where that variation is $\pm 7\%$. Although the models disagree on small-scale details, there is broad agreement at large length-scales. In particular, they all display large negative shear velocity anomalies at the base of the mantle, interpreted to be LLSVPs. Figure from Ritsema et al. (2010).

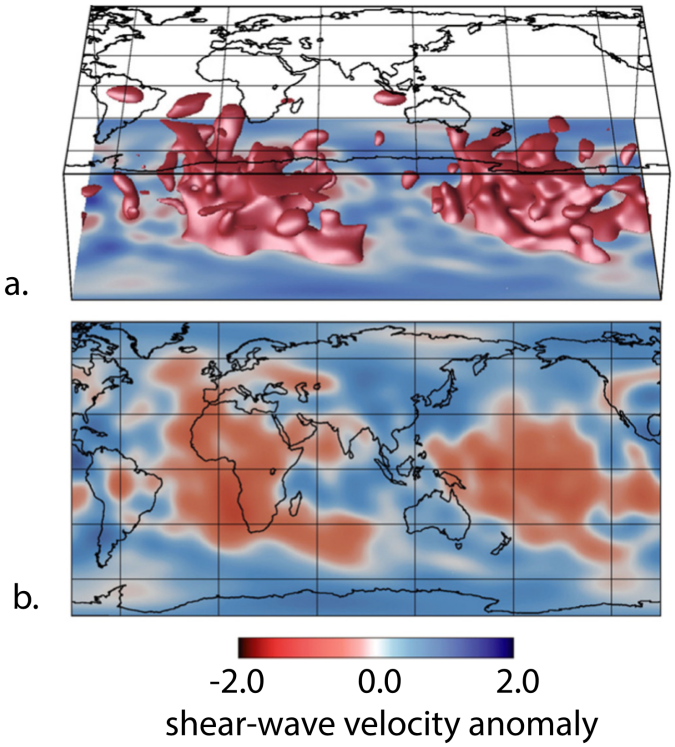

Figure 1.3: Global shear-wave velocity anomalies of the model S20RTS (Ritsema et al., 1999, 2004). Panel (a) shows in red an iso-surface representing 0.6% shear-wave anomaly, with the core-mantle boundary at the bottom of the box. Panel (b) shows a map of shear-wave anomalies at a depth of 2750km. Figure from McNamara (2019).

of LLSVPs and the rest of the deep Earth. Schematically, for small deviations in temperature T and composition X, the S- and P-wave velocities will vary as

$$\delta v_S = \frac{\partial v_S}{\partial T}\delta T + \frac{\partial v_S}{\partial X}\delta X \tag{1.1a}$$

$$\delta v_P = \frac{\partial v_P}{\partial T}\delta T + \frac{\partial v_P}{\partial X}\delta X, \tag{1.1b}$$

where the partial derivatives can be measured in laboratories and/or computed theoretically. For normal materials $\partial v_S/\partial T$ and $\partial v_P/\partial T$ are both negative, so regions of low velocity might be thought to correspond to material that is hot and therefore buoyant. But compositional variations complicate this picture; cold material could turn out to be buoyant and vice versa. For a better understanding of LLSVPs it is crucial to obtain measurements of their *density*.

However, as pointed out by Kuo & Romanowicz (2002) lateral density variations are notoriously hard to invert seismic data for, much more so than seismic wave speeds. There are still relatively few studies of mantle density (most prominently Ishii & Tromp, 1999, 2001, 2004; Moulik & Ekström, 2016; Lau et al., 2015, 2016, 2017; Koelemeijer et al., 2017), and taken together they present a rather blurry picture. If we go by majority voting then they suggest that LLSVPs are *dense* and must therefore be compositionally distinct. But before we can review these studies and identify paths forward, we must understand more precisely the problems that density poses.

1.2 Modelling the effects of density

1.2.1 Only long-period phenomena are sensitive to density

In the notation of Dahlen & Tromp (1998), the *elastodynamic equations* governing the motion of a rotating, self-gravitating Earth model are

$$\partial_t^2\mathbf{s} - \frac{1}{\rho^0}\nabla\cdot(\boldsymbol{\Lambda}:\nabla\mathbf{s}) + 2\boldsymbol{\Omega}\times\partial_t\mathbf{s} + \nabla\phi^{E1} + \mathbf{s}\cdot\nabla\nabla\left(\phi^0+\psi\right) = 0 \tag{1.2a}$$

$$\nabla^2\phi^{E1} = -4\pi G\nabla\cdot\left(\rho^0\mathbf{s}\right), \tag{1.2b}$$

for an Earth model initially at equilibrium with density ρ^0 and gravitational potential ϕ^0, and which rotates at constant angular velocity $\boldsymbol{\Omega}$ giving rise to the centrifugal potential ψ; the displacement from equilibrium is $\mathbf{s}$, with ϕ^{E1} the corresponding perturbation to the gravitational potential, while $\boldsymbol{\Lambda}$ is the elastic tensor (ibid. p.84). Density's broad role within these equations can be understood by scaling analysis. Let the displacement have typical amplitude S, time-scale T and length-scale L, and denote by $\bar{\rho}$ and $\bar{\mu}$ the typical values of the Earth model's density and elastic moduli respectively, from which we can construct a typical wave-velocity $\bar{v} = \sqrt{\bar{\mu}/\bar{\rho}}$. For an Earth-model *without* rotation or gravity we need only balance the product of density and acceleration against the divergence of elastic stress, and we obtain

$$\frac{\bar{\rho}S}{T^2} \sim \frac{\bar{\mu}S}{L^2}, \tag{1.3}$$

from which it follows trivially that

$$L \sim \bar{v}T. \tag{1.4}$$

It is important that $\bar{\rho}$ only enters this problem *implicitly* through $\bar{v}$. This is a manifestation of the standard *ray theoretic* result that high-frequency, small-wavelength seismic waves are sensitive to wave-speeds, but not density itself (e.g. Dahlen & Tromp, 1998, Chapter 15). Indeed, it is because of this that the mantle's S- (and P-) velocity structure has been so thoroughly studied whilst we know rather little about its density. Including now the terms from eq.(1.2) that involve gravity and rotation, balance (1.3) is augmented to

$$\frac{\bar{\rho}S}{T^2} + \underbrace{\frac{2\bar{\rho}\Omega S}{T}}_{\text{Coriolis}} + \underbrace{\bar{\rho}\Omega^2 S}_{\text{Centrifugal}} \sim \frac{\bar{\mu}S}{L^2} + 4\pi G\bar{\rho}^2 S, \tag{1.5}$$

where Ω is the typical magnitude of the Earth model's angular velocity and G is Newton's constant. We cannot really 'solve' (1.5) as we did in eq.(1.4), but we *can* identify its three natural time-scales:

1. $T_{\text{rot}} = \Omega^{-1}$;
2. $T_{\text{seis}} = L/\bar{v}$, which gives the typical time for a disturbance to propagate across the model;
3. and a gravitational timescale $T_{\text{grav}} = (4\pi G\bar{\rho})^{-\frac{1}{2}}$.

Substituting the parameter values $L = 6371\text{km}$ (Earth's average radius), $\bar{\rho} = 5000\text{kgm}^{-3}$, $\bar{v} = 8000\text{ms}^{-1}$, $G = 6.67 \times 10^{-11}\text{m}^3\text{kg}^{-1}\text{s}^{-2}$ and $\Omega = (24\text{hr})^{-1}$, those timescales take the values

$$T_{\text{rot}} \sim 24\text{hr} \tag{1.6a}$$

$$T_{\text{seis}} \sim 800\text{s} \tag{1.6b}$$

$$T_{\text{grav}} \sim 500\text{s}. \tag{1.6c}$$

The rotational timescale is a couple of orders of magnitude larger than the other two, a separation that is large, but not so much so as to be trivial. Most interestingly, perhaps, is that

$$4\pi G\bar{\rho}L^2\bar{v}^{-2} = (T_{\text{seis}}/T_{\text{grav}})^2 \sim 1, \tag{1.7}$$

which confirms that gravity cannot be neglected when working at a length scale comparable to the Earth's radius. Crucially, density enters independently of $\bar{\mu}$ now that we have included gravity. The smaller we take L, the further T_{seis} drifts from T_{grav}, and the less sensitive the motions will be to gravity and density.

It follows from these arguments that gravity should have a marked effect on the largest-scale vibrational motions of the Earth – and because of that we expect those motions to be sensitive to the Earth's long-wavelength density structure. For that reason we will need to consider long-wavelength, long-period motions if we are to probe density. The canonical example of such motions are the Earth's *long-period free-oscillations* or *normal-modes* (e.g. Woodhouse & Deuss,

2015). Any of the Earth's motions can be viewed as a certain superposition of its normal modes. Such long-period dynamics arise from the tidal forces acting on the Earth due to the Moon and Sun (e.g. Agnew, 2015), as well as from variations in the Earth's rotation (e.g. Lambeck, 2005); large earthquakes can also excite long-period normal-modes. It is these phenomena that we must observe if our measurements are to be sensitive to the deep Earth's density. Moreover, in generating the synthetic data required for inversions we will need to account for both the Earth's rotation and its self-gravitation. From a theoretical point of view, the problem thus reduces to solving the equations of motion of a rotating, self-gravitating, aspherical, heterogeneous body composed of alternating fluid/solid layers. This problem is dauntingly complex in principle, but great progress has been made through the technique of *normal-mode coupling*.

1.2.2 Normal mode coupling

Normal mode coupling (NMC) provides a comprehensive framework for modelling the long-period dynamics of heterogeneous, rotating, self-gravitating, slightly-aspherical Earth models with a fluid outer core (e.g. Woodhouse & Giardini (1985); Giardini et al. (1987); Dahlen & Tromp (1998); see Akbarashrafi et al. (2017) for a comprehensive recent review). The fundamental idea underlying it is to use a suitably truncated subset of the normal modes of a reference spherically symmetric, non-rotating Earth model as a basis on which to expand the motion of the non-spherically-symmetric Earth model under study. With the addition of a force term $\mathbf{f}$, eq.(1.2) can be rewritten as

$$\left(\mathcal{V} + \mathcal{W}\partial_t + \rho\partial_t^2\right)\mathbf{s} = \mathbf{f}, \tag{1.8}$$

where we follow Akbarashrafi et al. (2017) in defining the *Coriolis operator* $\mathcal{W}$, and the operator $\mathcal{V}$ that represents the effects of elasticity, anelasticity, centrifugal force and gravitation. We now represent the normal-modes of the reference Earth model by $\mathcal{S}_i$, normalising them so that

$$\int_{\mathcal{B}} \bar{\rho}\mathcal{S}_j^*\mathcal{S}_i \,\mathrm{d}V = \delta_{ij}, \tag{1.9}$$

where $\bar{\rho}$ is the spherically-symmetric density of the reference model. Expanding $\mathbf{s}$ on a suitably truncated subset of these basis functions as

$$\mathbf{s}(\mathbf{x}, t) = \sum_i u_i(t)\mathcal{S}_i(\mathbf{x}), \tag{1.10}$$

we convert eq.(1.8) into the *linear-algebraic* system

$$\left(\mathbf{V} + \mathbf{W}\partial_t + \mathbf{P}\partial_t^2\right)\cdot\mathbf{u} = \mathbf{q}, \tag{1.11}$$

with

$$V_{ij} = \int_{\mathcal{B}} \mathcal{S}_i^* \cdot \mathcal{V}\mathcal{S}_j \, \mathrm{d}V \tag{1.12a}$$

$$W_{ij} = \int_{\mathcal{B}} \mathcal{S}_i^* \cdot \mathcal{W}\mathcal{S}_j \, \mathrm{d}V \tag{1.12b}$$

$$P_{ij} = \int_{\mathcal{B}} \rho\mathcal{S}_i^* \cdot \mathcal{S}_j \, \mathrm{d}V \tag{1.12c}$$

$$q_i = \int_{\mathcal{B}} \mathcal{S}_i^* \cdot \mathbf{f} \, \mathrm{d}V. \tag{1.12d}$$

$\mathbf{P}$ is known as the *mass matrix*. We now Fourier-transform these equations in time to arrive at the frequency-domain equations of mode-coupling

$$\left(\tilde{\mathbf{V}}(\omega) + \mathrm{i}\omega\mathbf{W} - \omega^2\mathbf{P}\right) \cdot \tilde{\mathbf{u}} = \tilde{\mathbf{q}}, \tag{1.13}$$

as written by Akbarashrafi et al. (2017). The great attraction of these equations is that for Earth models that are nearly spherically-symmetric they are diagonally dominant. Indeed, for a spherically-symmetric model there is a complete decoupling of all basis functions and the equations are exactly diagonal.

At heart NMC involves just two main sources of approximation. The first approximation is the use of a spherical model's eigenfunctions as a basis on an aspherical domain. This is generally dealt with through *boundary perturbation theory*, whereby the boundary topography is assumed to be small enough that one can work on an equivalent spherical domain and account for the topography just though modified boundary conditions. It is presumably a good approximation for the Earth, and even if it isn't, Al-Attar & Crawford (2016) have recently suggested a way around the problem. Normal-mode coupling's second approximation is that the basis must be truncated and is thus rendered incomplete. However, by taking the cut-off frequency ω_c to be high enough, the method should be able to resolve up to any degree of precision. Computational resources are the sole limiting factor here, as a result of which three flavours of normal mode coupling have arisen: *full-coupling*, *group-coupling* and *self-coupling*. Full-coupling is the most complete because it accounts for coupling between all the basis functions used, that is, one solves eq.(1.13) as written. Self-coupling, on the other hand, neglects most of the matrix elements (1.12). One keeps only the matrix elements that couple together basis functions with the same radial eigenfunction and spherical harmonic degree, so that the matrix in eq.(1.13) is exactly block-diagonal. Group-coupling occupies a position somewhere in the middle, although closer to self- than full-coupling.

Full-coupling has only become computationally feasible in the last decade or so, with most early studies having had no choice but to use self-coupling. However, Al-Attar et al. (2012), Yang & Tromp (2015) and most recently Akbarashrafi et al. (2017) all advise caution when employing self-coupling. Of particular relevance here are Akbarashrafi et al.'s findings, namely that even full-coupling is perhaps not sufficient to gain reliable density measurements if the cutoff frequency is not set rather high. Akbarashrafi et al. computed synthetic seismograms for a model whose shear velocity is given by S40RTS (Ritsema et al., 2010), with compressional wave velocities and

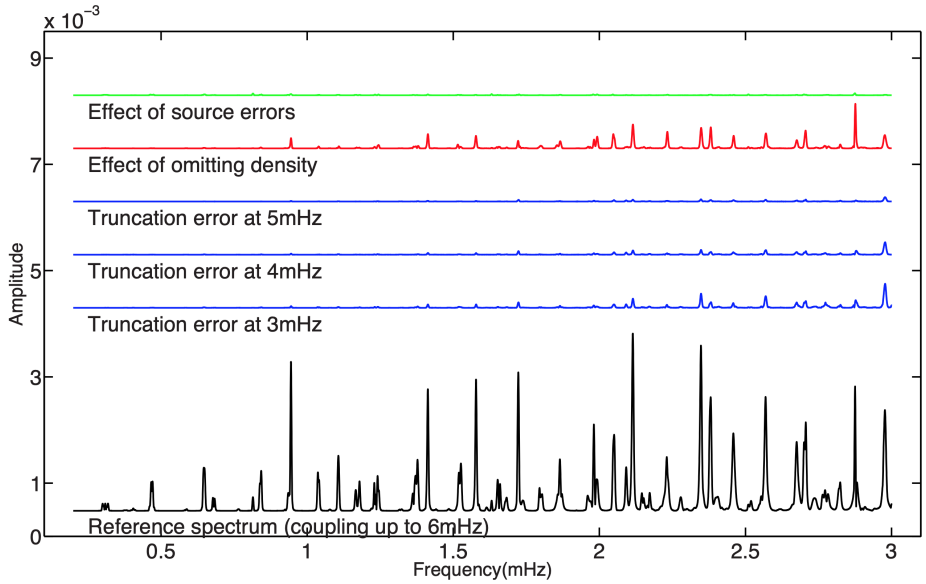

Figure 1.4: The consequences of different approximations on long-period spectra. The reference spectrum was computed for an Earth model whose shear velocities are given by S40RTS and whose P-velocities and density were obtained by suitable scaling relations; a large set of eigenfunctions was used, with the truncation at 6mHz. Each of the coloured traces gives the amplitude of the *difference* between the reference spectrum and a spectrum computed with some approximations; the difference between two spectra was found by subtracting one from the other. The sizes of these differences give an idea of the error associated with each approximation. The three blue traces correspond to truncating the normal-mode basis at the limit stated in the figure, the red line results from omitting *lateral* density variations, and the green line from ignoring source errors. Note well that the rough magnitude of the error associated with omitting density is about the same as that due to truncating the basis at 3mHz, even under full-coupling. Figure from Akbarashrafi et al. (2017).

density obtained by scaling the shear velocity. They generated a reference seismogram truncated at 6mHz, which they compared against several other seismograms generated by less precise means. As shown in Fig. 1.4, truncating at lower frequency leads to differences with the reference seismogram. Akbarashrafi et al. also applied the same procedure to many randomly-generated Earth models, and found qualitatively similar behaviour. What is most striking is that the differences caused by neglecting lateral density variations are similar in magnitude to those caused by just truncating at 3mHz. Modern full-coupling calculations rarely truncate at more than $3-4$mHz, so Akbarashrafi et al.'s results give a plausible demonstration that the numerical uncertainty inherent in existing studies of density is probably larger than the very signal due to lateral density variations.

In this connection a last general point about normal-mode coupling is in order. Although NMC can in principle accommodate any level of density heterogeneity (subject to the two main approximations mentioned above) all its modern implementations also approximate the density heterogeneity as small. Specifically, the (m,n)'th component of $\tilde{\mathbf{V}}$ is given by

$$\tilde{V}_{mn} = \int_V \mathcal{S}_m^* \mathcal{V} \mathcal{S}_n \,\mathrm{d}V. \tag{1.14}$$

Computing this matrix element depends crucially on being able to calculate $\mathcal{S}_n$'s associated gravitational potential ϕ_n, whose contribution to $\tilde{V}_{mn}$ is given by

$$\int_V \rho \mathcal{S}_m^* \cdot \nabla \phi_n \,\mathrm{d}V. \tag{1.15}$$

Now, one obtains ϕ_n by solving the Poisson equation

$$\nabla^2 \phi_n = -4\pi G \nabla \cdot (\rho \mathcal{S}_n)\,, \tag{1.16}$$

but in current implementations of NMC ρ is approximated as *spherically symmetric* for that purpose[†], even though the factor of ρ in the matrix element (1.15) is not (Al-Attar, 2021, personal communication). It follows that $\tilde{\mathbf{V}}$, and by extension the whole calculation, is limited to first-order accuracy in the density.

This might seem like splitting hairs, but the results of Woodhouse & Girnius (1982) suggest a different interpretation. Those authors note that low-frequency normal modes correspond to waves that have travelled through the Earth for a very long time. Those waves have scattered off any small heterogeneities *multiple times*, so it is not clear that those (small) heterogeneities should have a correspondingly small effect on the waveforms. Fundamentally, one cannot assess heterogeneities' effect on the normal mode spectrum just by looking at their size, but rather by their size *and the length of time over which observations are conducted*. The lower the frequency, the more important heterogeneities could be.

[†]This approximation, together with that of small topography, leads to a complete decoupling of ϕ_n's spherical-harmonic components. Solving the Poisson equation is reduced to performing multiple independent one-dimensional quadratures; see Chapter 2.

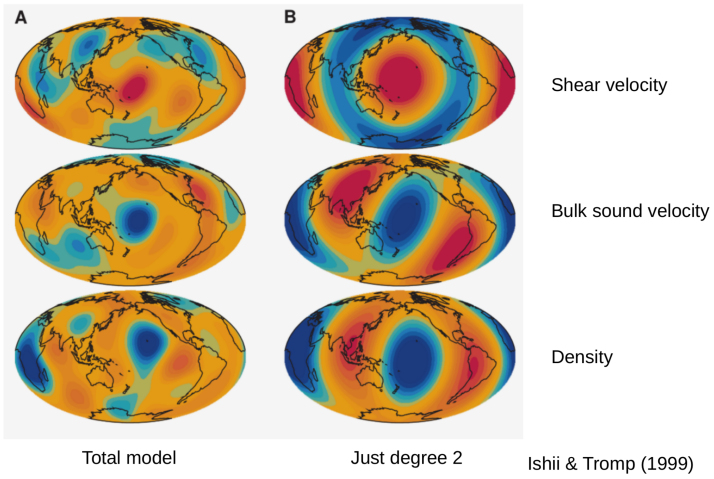

Figure 1.5: The model of Ishii & Tromp (1999), showing shear velocity, bulk sound velocity and density at 2800km depth. Blue (resp. red) colours indicate a value higher (resp. lower) than the average. This model is consistent with relatively dense LLSVPs. Figure after Ishii & Tromp (1999).

1.2.3 Review of previous work on laterally varying density

The studies of laterally varying density carried out by Ishii & Tromp (1999, 2001, 2004), Moulik & Ekström (2016), Lau et al. (2015, 2016, 2017) and Koelemeijer et al. (2017) are all based on NMC. Ishii & Tromp (1999, 2001, 2004) inverted normal-mode and free-air gravity anomaly data to produce the first models of laterally-varying mantle density that had not been obtained by scaling wavespeeds. Their studies were motivated in part by the Bolivia earthquake of 1994, which provided an important new source of high-quality normal-mode data whose analysis required greater theoretical sophistication. Ishii & Tromp's density model, part of which is reproduced in Fig. 1.5, suggests that the LLSVPs are *denser* than the surrounding medium. If the LLSVPs' low shear velocity is just a result of their being hotter than the surrounding mantle, then one might expect them to be positively buoyant. The negative buoyancy inferred by Ishii & Tromp suggests that LLSVPs could be compositionally distinct. Ishii & Tromp's study was carried out under the self-coupling approximation, so in light of Akbarashrafi et al.'s results caution is in order when interpreting their results. However, we emphasise that self-coupling was well known by past authors to be suboptimal and that its use rarely represented anything more than pragmatism.

Moulik & Ekström (2016) reached similar conclusions on mantle density:

> Our preferred joint model consists of denser-than-average anomalies ($\sim 1\%$ peak to peak) at the base of the mantle roughly coincident with the low-velocity superplumes. The relative variation of shear velocity, density, and compressional velocity in our study disfavors a purely thermal contribution to heterogeneity in the lowermost mantle, with implications for the long-term stability and evolution of superplumes.

Their data set was larger than that of Ishii & Tromp, but their treatment of normal-mode data was also based on splitting functions under the self-coupling approximation, so similar caveats presumably apply.

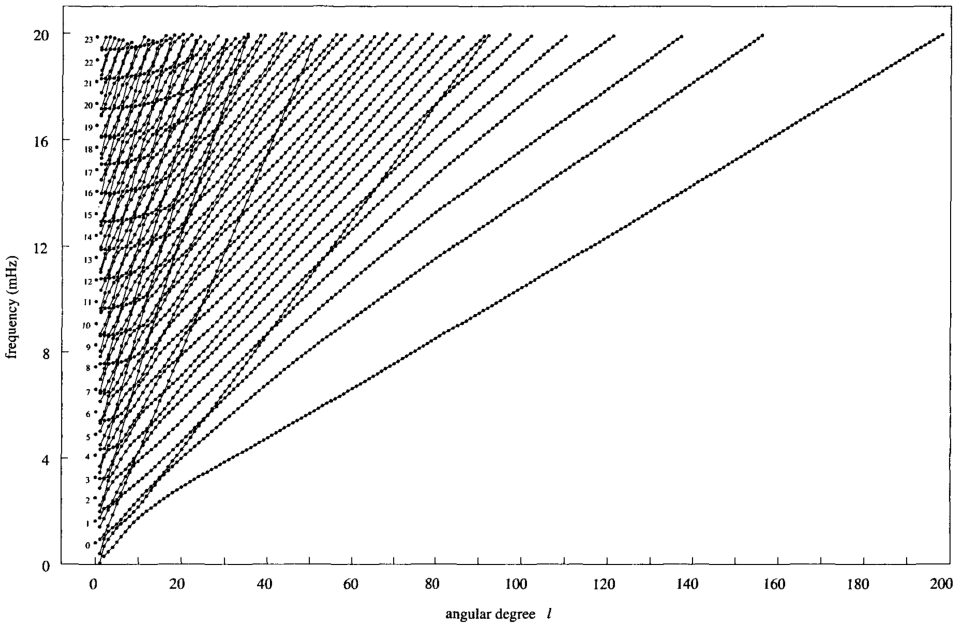

Figure 1.6: Dispersion diagram for the spheroidal modes of isotropic PREM. Looking at the mid- to top-left of the plot we see sets of eigenfrequencies that are so closely spaced that they appear to form solid lines curving gently upwards to right. Being so close in frequency, we expect these modes to interact strongly under NMC, but under the self-coupling approximation most such interactions would be neglected. Figure from Dahlen & Tromp (1998).

In contrast, Koelemeijer et al. (2017), after analysing the anomalous splitting of *Stoneley modes*, concluded that LLSVPs should be positively buoyant. Stoneley modes are expected to be highly sensitive to LLSVP density due to having a very large relative amplitude around the CMB. However, that study was conducted using small group coupling, so its results too are called into question by those of Akbarashrafi et al. (2017). Furthermore, one expects small group coupling to be especially detrimental when applied to Stoneley modes. Because they are relatively high-frequency they are close in frequency to many modes of a different spherical harmonic degree, as illustrated by Figure 1.6. They are therefore likely to interact strongly with those modes, but with small group coupling one throws away most such interactions.

The only study to employ full-coupling is that of Lau et al. (2017). Those authors also used a novel data-set: GPS measurements of the displacements due to *semi-diurnal body tides*. Their parameter search yielded negatively buoyant LLSVPs, with Figure 1.7 showing part of their "best-performing" density model. Lau et al.'s data set samples a much lower frequency-range than Ishii & Tromp's, so the two studies presumably provide independent constraints on mantle density. The theory underlying this work was developed by Lau et al. (2015, 2016). They first made important updates to the theory of body tides (e.g. Wahr, 1981b,c), updates that were inspired by the normal mode theory that had been developed within the seismological community (e.g. Lognonné, 1991; Hara et al., 1993; Dahlen & Tromp, 1998; Al-Attar et al., 2012). They then developed a normal-mode coupling theory that Lau et al. (2017) implemented under the full-coupling assumption.

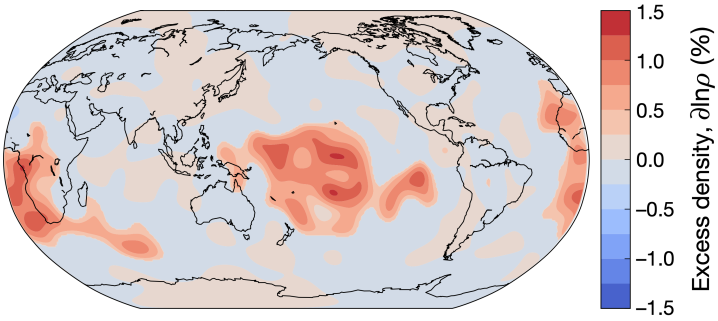

Figure 1.7: A representative view of the best-performing density model of Lau et al. (2017). Those authors' parametrisation divided the mantle into several layers, with the bottom layer extending from the CMB to a relative altitude of 350km. The figure shows the excess density within the mantle's bottom layer. This density model is "best-performing" in the sense that it fits the data best. The excess density is *positive* below Africa and the Pacific, suggesting the presence of relatively dense LLSVPs. Figure from Lau et al. (2017), where their precise statistical methodology is also described.

1.2.4 Normal mode coupling and the fluid outer core

The outer's core fluidity gives rise to two problems that are likely to be especially hard to address using NMC. The first of these has already been encountered by Lau and co-authors: their new methods cannot model dynamics at 24-hour periods because of the so-called *NDFW resonance* (e.g. Agnew, 2015, 3.06.3.2.1). The resonance occurs because the period of diurnal tidal forces is close to that of the aptly named *Nearly-Diurnal Free Wobble* (NDFW), the outer core's quasi-rigid precession driven by pressure-torques arising from CMB ellipticity. The PREM-derived mode catalogue used by Lau et al. for their mode-coupling simply does not contain any modes that can adequately represent the NDFW's associated displacement. Given that the NDFW must form an important part of Earth's response to diurnal tides, absent an adequate means of representing it one can only neglect it and work at periods far from 24 hours. Until this problem can be addressed through extended theory the abundant data available from diurnal body tides cannot be used to constrain Earth's lateral density structure.

Besides its troublesome quasi-rigid behaviour, the outer core is thought to possess extremely short-wavelength *undertone modes* that are controlled by its stratification and are almost entirely confined within it. If the outer core is approximated as perfectly inviscid, as is standard practice within much seismology, then there is no mechanism to damp these low-frequency modes and they must in principle be accounted for when modelling long-period phenomena. This is extremely challenging on a numerical level. Valette (1989a,b), Chaljub & Valette (2004) and Rogister & Valette (2009) have done much elegant work on this problem, but I expect that it is more practical to simply account for the outer core's small viscosity. Not only does a nonzero viscosity regularize the mathematical problem, but viscous effects at long periods are also of particular relevance to dynamic interactions of the core and mantle, with Buffett (2010) and Lin & Ogilvie (2017) having suggested that viscous boundary layers are responsible for a large amount of the outer core's energy dissipation. But such boundary layers pose a serious problem to NMC. They are expected to be ~ 10m in width, so one would presumably require a prohibitive number of eigenfunctions in order to resolve their behaviour.

1.2.5 Alternatives to normal-mode coupling

Normal-mode coupling is not the only method for modelling Earth's long-period dynamics, but at present it is probably more practical than its alternatives, especially for investigating density heterogeneities. A different approach would be to use a time-domain code such as SPECFEM3D (e.g. Peter et al., 2011). SPECFEM3D can simulate accurate seismic wavefields over long times in bodies of arbitrary shape. However, to my knowledge it does not yet account for self-gravity (although Gharti & Tromp (2017); Gharti et al. (2018, 2019) have made important progress) so it is not clear that it could be applied to the problems of interest in this dissertation.

Another important time-domain approach is that of Chaljub & Valette (2004), which does include self-gravitation exactly and is applicable in principle to arbitrarily shaped Earth models possessing a fluid outer core. Those authors used an innovative approach to purge spurious modes associated with the (inviscid) outer core, and their ideas have recently been adapted and extended by van Driel et al. (2021). On the other hand, investigating density requires that we capture long-period behaviour, and that in turn necessitates long runs of time-domain codes. This could prove particularly unwieldy when investigating Earth's rotational normal modes, which have periods of up to hundreds of days.

1.2.6 Outlook

Modelling density's effect on Earth's long-period dynamics is challenging. Although three of the four studies of mantle density that we have discussed agree that LLSVPs are negatively buoyant and therefore compositionally distinct, two of those studies were carried out under a numerical scheme that has the potential to introduce large errors. Modern full-coupling calculations would likely clarify previous results, and we hope that such studies will be undertaken in due course. Nevertheless, as discussed in Section 1.2.2 it remains unclear how much error is introduced by even the most advanced full-coupling calculations such as those of Lau et al. (2017). Furthermore, it is not clear how much further normal-mode coupling can be taken, given the difficulties associated with the outer core. In order to gain a better understanding of Earth's density heterogeneities we require further developments in numerical methods.

There are also theoretical problems to be solved. The theory of Lau et al. (2015) is the most advanced treatment known to me of heterogeneous Earth models' long-period deformation, but even that theory cannot readily accommodate the Earth's *wobbles* and *nutations*. Such motions have of course been studied extensively in the geodesy literature, but even the most advanced geodetic models of those motions allow for ellipticity but *no further lateral heterogeneity* (Smith, 1974; Wahr, 1981a,b; Dehant, 2013). Nor, in this author's view, do those models provide a ready enough means of addressing the possible interactions between the outer core's boundary layers and nutational modes such as the Chandler Wobble. A more complete approach would combine aspects of both the 'normal-mode' and the 'geodetic' approaches, and thus allow us to assimilate new sources of data to constrain mantle density, such as wobbles, nutations and diurnal tides. We could then carry out novel studies into, say, the effect of LLSVPs on the Chandler Wobble.

1.3 Aims of this dissertation

Without well-constrained measurements of lower mantle density it is difficult to gauge the extent to which compositional variations drive convection there. We have seen that new theoretical and numerical methods are required in order to gain a better picture of lower mantle density, both by assimilating new sources of density data, as well as by carrying out fuller analyses of extant data. This dissertation develops some methods relevant to those goals. Throughout it I work, as far as reasonably possible, without approximation. I feel that this is especially relevant to the study of Earth's lateral density variations and long-period dynamics. Can we approximate Earth's density heterogeneities as small? Can we approximate its boundary topography as small? Is its rotation a small perturbation? I would be surprised if "no" were the answer to all these, but in light of the comments of Woodhouse & Girnius (1982) discussed earlier that could be so – and without exact modelling *that cannot be verified*. I aim to show in this dissertation that exact modelling of density, topography and rotation can be achieved without either prohibitive computational cost or excessive theoretical difficulty.

A crucial part of computing the long-period deformation of an aspherical, heterogeneous Earth model is the calculation of its gravitational potential. Such potential calculations must be performed many times as the body deforms, so it is desirable to be able to carry them out quickly. In Chapter 2 we present a new method for performing these calculations. The method, which is numerically exact, can accommodate bodies of almost arbitrary shape, but it is most powerful when applied to bodies whose internal and external boundaries are approximately spherical. For such bodies we show that our method is only a little more taxing than boundary-perturbation theory, while obtaining an answer that is exact up to a specified precision. We therefore anticipate that it could usefully be applied to the study of Earth's long-wavelength density structure. Importantly, this technique points towards an alternative to normal-mode coupling within elastodynamic calculations.

In Chapter 3 we consider the stress dependence of the elastic tensor, a problem that might seem a little tangential, but could nevertheless be of some importance for mantle density studies. Inverting seismic observations for equilibrium stress could provide information on the constitutive behaviour of the mantle, and this in turn could inform studies of mantle density. It is also possible that future inversions for density could be carried out as *joint inversions* for several unknown parameters including stress, and for that one would need to know the stress dependence of the elastic tensor. I show in Chapter 3 that the various expressions for the elastic tensor as a function of equilibrium stress given by Dahlen (1972b), Dahlen & Tromp (1998), Tromp & Trampert (2018) and Tromp et al. (2019) are special cases of a more general result. My argument clarifies how a material's constitutive behaviour links the equilibrium stress and the elastic tensor.

The dissertation's final goal is to present a more complete description of the elastodynamics of rotating planets than has been achieved so far. Assembling that framework is the purview of Chapter 4. We show that the equations governing the motion of an elastic body can be *exactly* reformulated in a manner that 'decouples' elasticity and rotation as far as possible (in a sense that we will make precise later). We derive the exact equations of motion of a solid elastic body under this reformulation, and then show that they may be linearised to produce a new

set of equations of global seismology that are only a little more complicated than the standard equations of, say, Dahlen & Tromp (1998). We then give the equations of motion of $N \geq 2$ solid bodies interacting through gravity, as well as outlining how these equations could be solved with simple extensions to normal-mode coupling theory.

The conclusions of Chapter 4 sum up the whole dissertation, outlining how the results of Chapters 2–4 should be combined and extended in order to model Earth's long-period dynamics. I describe qualitatively how one could build on the method of Chapter 2 to carry out pseudo-spectral/spectral-element numerical solutions of Chapter 4's equations of motion. I also mention how Chapter 3's results have provided useful insight into the role that equilibrium stress plays in those equations. I then discuss how Chapter 4's arguments could be extended to derive the equations of motion of layered fluid-solid bodies such as the Earth. Finally, I outline the numerical difficulties that could be faced by anyone seeking to solve those equations at very low frequencies, and speculate that the numerical methods discussed in this dissertation's main body could be more practical for that purpose than normal-mode coupling.

CHAPTER 2

A NON-PERTURBATIVE METHOD FOR GRAVITATIONAL POTENTIAL CALCULATIONS WITHIN HETEROGENEOUS AND ASPHERICAL PLANETS

2.1 Introduction

The calculation of a planet's gravitational potential is required in diverse areas of geophysics and planetary science, including studies of free oscillation seismology (e.g. Woodhouse & Dahlen, 1978), body tides (e.g. Wahr, 1981b), rotational dynamics (e.g. Smith, 1977), orbital evolution (e.g. Kaula, 1964) and glacial isostatic adjustment (e.g. Peltier, 1974). Neither the Earth nor any other planetary body of interest is geometrically spherical, where we follow the terminology of Al-Attar & Crawford (2016) and define a planet to be geometrically spherical if its internal and external boundaries form a series of concentric spheres. Within a geometrically spherical planet Poisson's equation can be reduced in an exact manner to a decoupled system of ordinary differential equations for the spherical harmonic coefficients of the potential. These differential equations can be solved using numerical quadrature, making it easy to calculate the planet's gravitational potential to any desired level of accuracy.

A number of approaches have been developed to account for asphericity within calculations of the gravitational potential. It is most common to assume the deviation of a boundary from an appropriate reference sphere to be small and determine its contribution to the gravitational potential using first-order boundary perturbation theory. In fact, for many applications, lateral variations in density are also regarded as first-order quantities, and this allows for the asphericity of the planet to be handled with minimal effort. Higher-order extensions of this boundary perturbation theory have been developed (e.g. Nakiboglu 1982; Chambat & Valette 2005) and the improvements over the first-order theory are significant for some terrestrial applications (e.g. Mitrovica et al. 2005; Chambat et al. 2010). The use of higher-order boundary perturbation theory, however, is both time-consuming and cumbersome, particularly when the coupling of such calculations into dynamical problems is considered.

Non-perturbative methods for calculating the external gravitational potential of aspherical bodies have been described a number of times in both the geophysics and planetary science literature. This includes, for example, the work of Parker (1973), Parker & Shure (1985), Martinec et al. (1989) and Balmino (1994) based on spectral expansions of the exterior gravitational potential of piecewise homogeneous bodies, and studies by Barnett (1976), Waldvogel (1979), and Werner (1994) using homogeneous polyhedral models for which the necessary integrals can be performed analytically. Whilst these methods are useful within their intended applications it seems unlikely that they can be readily extended to the calculation of the internal gravitational potential of a general heterogeneous planet. We note, however, that the method of Hubbard (2012, 2013), which is based on a combination of spectral and multipole expansions, can be applied to ellipsoidally symmetric bodies, and allows for accurate calculation of both the internal and external potential.

It is only quite recently that non-perturbative methods for calculating the internal gravitational potential of aspherical planets have been considered, this being motivated largely by the desire to model their dynamics without unnecessary approximations. At first sight, it might seem that this should be a simple problem. Indeed, we need only consider a linear partial differential equation with constant coefficients, whereas problems that are ostensibly far more complicated are now solved routinely using numerical methods. The difficulty with our problem, however, is that Poisson's equation is not defined in a finite domain, but within all of space. Of course, one could attempt to approximate the whole of space by a sufficiently large computational domain, but this has been shown to be both inaccurate and inefficient (Gharti & Tromp, 2017).

Within the geophysics literature three main approaches to this "infinite-domain problem" have been discussed. First, Chaljub & Valette (2004) used a Dirichlet-to-Neumann (DtN) map to reduce Poisson's equation in $\mathbb{R}^3$ to an equivalent problem defined within a finite spherical domain containing the body of interest. The DtN map introduces non-local boundary terms into the problem, which comes with an associated computational cost. Chaljub & Valette's approach seems to have been impractical for its original application to long period seismology, but it has subsequently been employed in quasi-static deformation calculations by Métivier et al. (2006), Al-Attar & Tromp (2014), Crawford et al. (2016) and Crawford et al. (2018).

A second approach to calculating the internal potential field was described by Latychev et al. (2005) within their finite-volume method for modelling glacial isostatic adjustment. Here the internal gravitational potential was obtained through direct numerical evaluation of the Newtonian potential integrals at each point within the body. This method, however, is rather costly and care is needed in accounting for the singular nature of the integrands.

Most recently, a powerful approach known as the "spectral infinite-element method" has been described within a series of papers by Gharti & Tromp (2017), Gharti et al. (2018) and Gharti et al. (2019). This is a variant of the infinite-element method developed within the engineering literature (e.g. Bettess 1977; Beer & Meek 1981; Medina & Taylor 1983) and reduces the exterior problem to the addition of a single layer of elements onto the interior domain, but without the need for non-local boundary terms. Numerical tests show this method to be both accurate and comparatively efficient while offering the flexibility to calculate the gravitational potential of an almost arbitrarily complex object.

Given the preceding comments it might seem that there is no problem left to solve. But this view leaves us with a rather stark gap in computational cost: within a geometrically spherical planet the gravitational potential can be determined in an almost trivial manner using spherical harmonic expansions, while in an aspherical planet the problem requires the assembly and solution of a large system of linear equations associated with the spectral-infinite-element discretisation. The aim of this chapter is to present an alternative method for gravitational potential calculations that fills out the middle ground, providing a numerically exact solution to the problem, but with a computational cost that reflects the planet's geometric complexity. In doing this we must sacrifice some generality in the planet's form, but will see that a usefully large class of structures can still be accounted for. The solution is "numerically exact" in the sense that the only source of error is truncation of the radial and angular bases on which the problem is discretised: by taking sufficiently many terms in the expansion we can, in principle, achieve any desired level of accuracy.

The key idea in our method is the transformation of Poisson's equation into a new equation defined in a geometrically spherical reference domain (c.f. Woodhouse 1976; Jobert 1976; Takeuchi 2005; Al-Attar & Crawford 2016; Leng et al. 2019). The introduction of such a mapping is similar to, and can be seen as a generalisation of, Clairaut's approach to ellipsoidal equilibrium figures (e.g. Clairaut, 1743; Chambat & Valette, 2005). Whilst this transformed equation has laterally-varying and tensorial coefficients, the geometrical sphericity of its domain means that it can be solved numerically using an approach based on generalised spherical harmonic (GSPH) expansions combined with a spectral element discretisation in the radial co-ordinate (e.g. Al-Attar & Tromp 2014; Crawford et al. 2018). The lateral heterogeneity of the equation's coefficients leads to coupling between the different spherical harmonic orders and degrees, but the resulting linear system can be solved using a preconditioned iterative method similar to that of Al-Attar et al. (2012). Crucially, the closer the planet is to being geometrically spherical, the more quickly the iteration converges.

2.2 Theory

2.2.1 Poisson's Equation for the gravitational potential

We begin by recalling the Poisson equation governing a planet's gravitational potential. The planet is assumed to occupy a compact subset $\mathcal{M} \subseteq \mathbb{R}^3$ with open interior, and smooth external boundary $\partial\mathcal{M}$. Its interior is then further subdivided into a finite number of non-interpenetrating regions, with the union of all internal and external boundaries denoted by Σ. The planet's gravitational potential ϕ satisfies the Poisson equation

$$\nabla^2\phi = 4\pi G\varrho\,, \tag{2.1}$$

which is to hold within $\mathbb{R}^3$, where ϱ is the density, G the universal gravitational constant, and ∇^2 the Laplacian operator; the density is non-zero only in $\mathcal{M}$. This equation is solved subject to the boundary and regularity conditions

1. $[\phi]^+_- = [\langle \hat{\mathbf{n}}, \nabla\phi \rangle]^+_- = 0$ for $\mathbf{x} \in \Sigma$,

2. $\phi \to 0$ as $\|\mathbf{x}\| \to \infty$,

where $\hat{\mathbf{n}}$ is the outward unit normal vector to a boundary, $[\cdot]^+_-$ denotes the jump in a quantity across the boundary in the direction of $\hat{\mathbf{n}}$, ∇ is the gradient operator, $\langle \cdot, \cdot \rangle$ denotes the standard inner product on $\mathbb{R}^3$, and $\| \cdot \|$ is the associated norm.

2.2.2 Weak form of Poisson's equation

Following Chaljub & Valette (2004), we will express the problem in weak form on a bounded domain through the use of an appropriate DtN map. Let $\mathcal{B} = \{\mathbf{x} \in \mathbb{R}^3 \,|\, \|\mathbf{x}\| \leq b\}$ denote a closed ball of radius b which contains $\mathcal{M}$, and ψ be a sufficiently regular complex-valued function defined on $\mathcal{B}$. We multiply eq.(2.1) by the complex-conjugate $\overline{\psi}$ of this test function and integrate to obtain

$$\int_{\mathcal{B}} (\nabla^2 \phi) \overline{\psi} \, \mathrm{d}^3\mathbf{x} = 4\pi G \int_{\mathcal{M}} \varrho \, \overline{\psi} \, \mathrm{d}^3\mathbf{x} \,. \tag{2.2}$$

The use of complex-valued functions is to facilitate our later introduction of spherical harmonic expansions. Integrating the left hand side of eq.(2.2) by parts we arrive at

$$\int_{\mathcal{B}} \left\langle \nabla\phi, \nabla\overline{\psi} \right\rangle \, \mathrm{d}^3\mathbf{x} - \int_{\partial\mathcal{B}} \langle \hat{\mathbf{n}}, \nabla\phi \rangle \, \overline{\psi} \, \mathrm{d}S = -4\pi G \int_{\mathcal{M}} \varrho \, \overline{\psi} \, \mathrm{d}^3\mathbf{x} \,, \tag{2.3}$$

where we have used the continuity conditions on ϕ and its normal derivative across Σ. To account for the term $\langle \hat{\mathbf{n}}, \nabla\phi \rangle$ within the surface integral over $\partial\mathcal{B}$ we use the fact that ϕ is harmonic in $\mathbb{R}^3 \setminus \mathcal{B}$. It follows that the value of ϕ within this exterior domain is determined uniquely by its restriction to $\partial\mathcal{B}$, and we have, in particular, the well-known expansion

$$\phi(r, \theta, \varphi) = \sum_{lm} \left(\frac{b}{r} \right)^{l+1} \phi_{lm}(b) Y^0_{lm}(\theta, \varphi) \,. \tag{2.4}$$

valid for $r \geq b$, where Y^N_{lm} denote the fully normalised GSPHs of degree l, order m, and upper index N (e.g. Dahlen & Tromp, 1998). Here the expansion coefficients of the restriction of the potential to $\partial\mathcal{B}$ are given by the integrals

$$\phi_{lm}(b) = \int_{\mathbb{S}^2} \phi(b, \theta, \varphi) \overline{Y^0_{lm}(\theta, \varphi)} \, \mathrm{d}S, \tag{2.5}$$

where $\mathbb{S}^2$ is the unit two-sphere. Using this result, we find that

$$\langle \hat{\mathbf{n}}, \phi \rangle|_{\partial\mathcal{B}} = -\sum_{lm} \frac{l+1}{b} \phi_{lm}(b) Y^0_{lm}(\theta, \varphi), \tag{2.6}$$

and hence eq.(2.3) can be written

$$\int_{\mathcal{B}} \left\langle \nabla\phi, \nabla\overline{\psi} \right\rangle \, \mathrm{d}^3\mathbf{x} + \sum_{lm} (l+1) b \, \phi_{lm}(b) \, \overline{\psi_{lm}(b)} = -4\pi G \int_{\mathcal{M}} \varrho \, \overline{\psi} \, \mathrm{d}^3\mathbf{x} \,, \tag{2.7}$$

which is to hold for all test functions ψ. This is the desired weak form of the problem. Importantly, the role of the exterior potential has been reduced to non-local boundary terms involving its spherical harmonic expansion coefficients on $\partial\mathcal{B}$.

2.2.3 Transformation of Poisson's equation

The weak form of Poisson's equation in eq.(2.7) provides a suitable starting point for numerical discretisation using, for example, a three-dimensional spectral element method (e.g. Chaljub & Valette, 2004). However, we cannot use methods based upon GSPH expansions to tackle this problem if the planet is not geometrically spherical because the continuity conditions on ϕ across the boundaries Σ cannot be readily enforced. In order to apply such an approach we must transform the problem into an equivalent one defined on a geometrically spherical domain.

Consider a diffeomorphism $\boldsymbol{\xi} : \mathcal{B} \to \mathcal{B}$ (i.e. a smooth mapping, with a smooth inverse) with the following properties:

1. its restriction to the boundary $\partial\mathcal{B}$ is the identity mapping;
2. the inverse image $\tilde{\mathcal{M}} = \boldsymbol{\xi}^{-1}(\mathcal{M})$ is a ball with centre coincident with that of $\mathcal{B}$;
3. the inverse image $\tilde{\Sigma} = \boldsymbol{\xi}^{-1}(\Sigma)$ of the boundary set is comprised of concentric spheres in $\tilde{\mathcal{M}}$.

For general $\mathcal{M}$ such a diffeomorphism will not exist, and so we see the fundamental restriction of our method. Nonetheless, for many applications a suitable diffeomorphism can be found, and later we discuss how this can be done practically. In fact, the requirement that this mapping be smooth is more stringent than is strictly necessary, and it is possible for it to be defined in a piecewise manner with continuity enforced at interfaces.

Using this diffeomorphism, we can define a new *referential potential field*

$$\zeta(\mathbf{x}) = (\phi \circ \boldsymbol{\xi})(\mathbf{x}) := \phi[\boldsymbol{\xi}(\mathbf{x})], \tag{2.8}$$

where $\circ$ denotes the composition of two functions. Knowledge of ζ is equivalent to that of ϕ, but ζ is defined on a geometrically spherical domain. Our first aim is to show that ζ satisfies a suitably generalised form of Poisson's equation. Using $\boldsymbol{\xi}$ to change variables in eq.(2.7), we arrive at

$$\int_{\mathcal{B}} J\big\langle \mathbf{F}^{-T}\nabla\zeta, \mathbf{F}^{-T}\nabla\overline{\chi}\big\rangle \,\mathrm{d}^3\mathbf{x} + \sum_{lm}(l+1)b\,\zeta_{lm}(b)\,\overline{\chi_{lm}(b)} = -4\pi G\int_{\tilde{\mathcal{M}}} J\varrho\circ\boldsymbol{\xi}\,\overline{\chi}\,\mathrm{d}^3\mathbf{x}\,. \tag{2.9}$$

where we have defined a new test function $\chi = \psi \circ \boldsymbol{\xi}$, along with the *deformation gradient* $\mathbf{F}$ of the diffeomorphism, which has components

$$[\mathbf{F}]_{ij} \equiv \frac{\partial\xi_i}{\partial x_j}\,, \tag{2.10}$$

and its *Jacobian*,

$$J = \det\mathbf{F}\,, \tag{2.11}$$

which we assume without loss of generality to be everywhere positive. We have also applied the chain rule to arrive at the identity

$$(\nabla\phi)\circ\boldsymbol{\xi} = \mathbf{F}^{-T}\nabla\zeta, \tag{2.12}$$

along with a corresponding expression involving the gradients of the test functions. At this stage it is convenient to define the *right Cauchy-Green deformation tensor*,

$$\mathbf{C} = \mathbf{F}^T\mathbf{F}\,, \tag{2.13}$$

a tensor derived from it,

$$\boldsymbol{a} = J\mathbf{C}^{-1}\,, \tag{2.14}$$

and the *referential density*,

$$\rho = J\varrho\circ\boldsymbol{\xi}\,. \tag{2.15}$$

With these definitions, the transformed weak form for ζ can be written

$$\int_{\mathcal{B}}\langle\mathbf{a}\,\nabla\zeta,\nabla\overline{\chi}\rangle\;\mathrm{d}^3\mathbf{x} + \sum_{lm}(l+1)b\,\zeta_{lm}(b)\,\overline{\chi_{lm}(b)} = -4\pi G\int_{\tilde{\mathcal{M}}}\rho\,\overline{\chi}\,\mathrm{d}^3\mathbf{x}\,, \tag{2.16}$$

which is to hold for all test functions χ. This equation broadly resembles the original weak formulation, but involves the tensor field $\mathbf{a}$ determined from the diffeomorphism $\boldsymbol{\xi}$. By construction, these problems are mathematically equivalent: in essence we have just exchanged simplicity of the equation for simplicity of the domain in which it is posed. From a numerical perspective, however, it is only in the transformed problem that we can usefully apply methods based on GSPH expansions.

2.3 Numerical implementation

2.3.1 Numerical discretisation of the problem

Our approach to solving eq.(2.16) numerically is based on GSPH expansions for the angular dependence of the referential potential, along with a spectral-element discretisation in the radial co-ordinate. Within $\mathcal{B}$, the truncated GSPH expansion of the referential potential takes the form

$$\zeta(r,\theta,\varphi) = \sum_{l=0}^{L}\sum_{m=-l}^{l}\zeta_{lm}(r)Y_{lm}^0(\theta,\varphi)\,, \tag{2.17}$$

where the maximum expansion degree L is to be chosen based on the planet's structure and properties. Each of the radial expansion coefficients ζ_{lm} is then expanded in a finite set of radial

basis functions

$$\zeta_{lm}(r) = \sum_{n=1}^{N} \zeta_{lmn} h_n(r). \tag{2.18}$$

The specific basis functions used are Lagrange polynomials defined on a radial spectral element mesh (e.g. Komatitsch & Tromp, 1999; Al-Attar & Tromp, 2014). Importantly, the radial mesh is built to honour the discontinuities within the reference planet $\tilde{\mathcal{M}}$, and thus we can enforce the required continuity of ζ in a trivial manner. The appropriate continuity conditions on the gradient of the referential potential are built directly into the weak formulation of the problem, and so need not be considered explicitly.

The test functions for the problem are taken in turn to be $\chi = h_n Y_{lm}^0$ as the indices l, m, and n range over appropriate values, and in this manner we arrive at a system of linear equations

$$\mathsf{A}\mathsf{x} = \mathsf{f}, \tag{2.19}$$

where the vector x contains the expansion coefficients ζ_{lmn}, while the matrix A and force vector f are obtained through discretisation of the weak form in a manner detailed below. Specifically, we represent x by defining for each l and m an N-component vector x_{lm} the n'th component of which is ζ_{lmn},

$$[\mathsf{x}_{lm}]_n = \zeta_{lmn}\,. \tag{2.20}$$

All the x_{lm} are then bundled together into the $\left[N(L+1)^2\right]$-component column-vector

$$\mathsf{x} = \begin{pmatrix} \mathsf{x}_{00} \\ \mathsf{x}_{1-1} \\ \mathsf{x}_{10} \\ \vdots \\ \mathsf{x}_{lm} \\ \vdots \\ \mathsf{x}_{LL} \end{pmatrix}, \tag{2.21}$$

and the components of the force, f_{lmn} (computed below), are arranged similarly. Importantly, explicit calculation of the components of A, which can be large, is not required. Instead, we need only ever compute its action on a given vector as part of the iterative solution of the linear system.

2.3.2 Hybrid pseudo-spectral/spectral element calculations

To determine the action of the matrix A and to compute the force vector f, we use a hybrid pseudo-spectral/spectral element method similar to that of Crawford (2018) for modelling glacial isostatic adjustment in the presence of laterally varying mantle viscosity. This approach also closely resembles the method of Leng et al. (2016) and Leng et al. (2019) for modelling global

seismic wave propagation, though in their work a two-dimensional spectral element method is coupled to a Fourier-series expansion in an azimuthal variable about the source location.

To explain the key ideas, we start with the computation of the force vector, which is part of the preprocessing for the potential calculation. The components f_{lmn}, having been computed once, are stored and used at the first stage of the iterative solution. The (l, m, n)th element of the force vector is given by the integral

$$f_{lmn} = -4\pi G \int_{\tilde{\mathcal{M}}} \rho\, h_n\, \overline{Y_{lm}^0}\, \mathrm{d}^3\mathbf{x}, \tag{2.22}$$

where we note that the radial basis functions are real valued. Using spherical polar co-ordinates the volume integral can be reduced to

$$\int_{\tilde{\mathcal{M}}} \rho\, h_n\, \overline{Y_{lm}^0}\, \mathrm{d}^3\mathbf{x} = \int_0^a \rho_{lm}\, h_n\, r^2\, \mathrm{d}r, \tag{2.23}$$

where ρ_{lm} is the (l, m)th GSPH coefficient of the referential density and a denotes the radius of the reference planet $\tilde{\mathcal{M}}$; once ρ_{lm} is known, the radial integral can be evaluated using the numerical quadrature formula associated with the spectral element discretisation. How we find ρ_{lm} depends on the way in which the planet's structure is specified. On the one hand, the density might be described referentially, with ρ and $\boldsymbol{\xi}$ given, in which case we obtain ρ_{lm} by applying a fast GSPH transformation at each radial node to calculate the GSPH coefficients for an appropriate range of indices. In detail, this transformation is done using Gauss-Legendre quadrature in co-latitude coupled to a fast Fourier transformation in longitude (c.f. Lognonné & Romanowicz, 1990). On the other hand, if the model is specified by the *physical* density $\varrho(\mathbf{x})$ then we must first determine $\rho(\mathbf{x})$. To do this, we use eq.(2.15) to determine the values of ρ on an appropriate spatial grid and then proceed as before.

Turning to the action of the matrix A, suppose we wish to determine Ax, with x defined as above to contain the components of the discretised referential gravitational potential ζ. It will be useful to define an auxiliary vector field

$$\mathbf{q} = \mathbf{a}\nabla\zeta, \tag{2.24}$$

where we recall that $\mathbf{a}$ is the symmetric tensor field introduced in eq.(2.14). Working in the canonical basis of Phinney & Burridge (1973) (see Appendix A.1) the components of this vector field can be expanded as

$$q^\alpha = \sum_{lm} q_{lm}^\alpha Y_{lm}^\alpha. \tag{2.25}$$

Taking the (l, m, n)th test function, we can apply the rules for contravariant differentiation (e.g. Dahlen & Tromp, 1998, Appendix C) to reduce the left hand side of eq.(2.16) to

$$\int_0^b \left[r^2 h_n' q_{lm}^0 + \frac{k}{\sqrt{2}} r h_n (q_{lm}^+ + q_{lm}^-) \right] \mathrm{d}r + b(l+1) h_n(b) \zeta_{lm}(b), \tag{2.26}$$

where $k = \sqrt{l(l+1)}$. Assuming we know the functions q^{α}_{lm}, the radial integral can be trivially evaluated using numerical quadrature, and gives the desired element of Ax.

Calculation of the coefficient functions q^{α}_{lm} is done in a number of stages, following the standard pseudo-spectral philosophy by which we work in either the spatial or spectral domain based on what is simplest (e.g. Boyd, 2001). Starting from the expansion coefficient functions ζ_{lm}, we use the rules for contravariant differentiation along with those for Lagrange polynomial interpolation to determine $\zeta^{|\alpha}_{lm}$, the expansion coefficients of $\nabla\zeta$ relative to the canonical basis. Inverse fast GSPH transformations are then performed to find the values of $\nabla\zeta$ on a spatial mesh. Multiplication by $\mathbf{a}$ is performed spatially to obtain $\mathbf{q} = \mathbf{a}\nabla\zeta$ on this grid, and finally the required coefficient functions q^{α}_{lm} are obtained through forward fast GSPH transformations. Within this process forward and inverse fast GSPH transformations must – potentially – be performed at each node of the radial mesh, and this accounts for a substantial part of our method's computational cost. Importantly, however, in regions where the diffeomorphism is the identity we have $\mathbf{a}(\mathbf{x}) = \mathbf{1}$, so these transformations are not needed and we can make substantial computational savings.

2.3.3 Pre-conditioned iterative solution of the linear system

The numerical solution of eq.(2.19) is accomplished most efficiently using matrix-free iterative methods. From eq.(2.16) it is clear that A is an Hermitian matrix, and so we can apply the pre-conditioned conjugate gradient algorithm (e.g. Saad, 2003). In order for this algorithm to converge rapidly a good pre-conditioner B for the linear system must be found. Here a balance must be struck between B being a good approximation to the inverse operator A^{-1} – meaning the algorithm will converge in fewer iterations – and the cost of determining the action of B. The preconditioner which we have used in all our numerical examples is

$$\mathsf{B} = \left(\mathsf{A}^{(0)}\right)^{-1}, \tag{2.27}$$

where $\mathsf{A}^{(0)}$ is the system matrix for the corresponding spherical system, i.e. the matrix obtained by considering eq.(2.16) with $\boldsymbol{\xi}(\mathbf{x}) = \mathbf{x}$.

The reasoning behind this choice is similar to that of Al-Attar et al. (2012) in the context of normal mode coupling calculations. One starts by observing that when the planet is geometrically spherical there is a complete decoupling between the coefficients for different spherical harmonic degrees and orders, which gives the corresponding matrix $\mathsf{A}^{(0)}$ a block diagonal structure. The matrix $\mathsf{A}^{(0)}_l$ associated with the (l,m)th sub-system is independent of m, and can be readily computed in terms of the radial spectral element discretisation (c.f. Al-Attar & Tromp, 2014, Appendix D2). Moreover, the matrices $\mathsf{A}^{(0)}_l$ for each l are Hermitian and narrow banded, meaning that their LU-decomposition can be computed and stored in an efficient manner using standard LAPACK routines for banded matrices. Once these factorisations have been performed, the action of $\left(\mathsf{A}^{(0)}\right)^{-1}$ can be computed rapidly by carrying out $(L+1)^2$ simple backsubstitutions.

The action of the block-diagonal pre-conditioner on the vector f can then be written

$$\left(\mathsf{A}^0\right)^{-1}\mathsf{f} = \begin{pmatrix} \left(\mathsf{A}_0^{(0)}\right)^{-1}\mathsf{f}_{00} \\ \left(\mathsf{A}_1^{(0)}\right)^{-1}\mathsf{f}_{1-1} \\ \left(\mathsf{A}_1^{(0)}\right)^{-1}\mathsf{f}_{10} \\ \vdots \\ \left(\mathsf{A}_l^{(0)}\right)^{-1}\mathsf{f}_{lm} \\ \vdots \\ \left(\mathsf{A}_L^{(0)}\right)^{-1}\mathsf{f}_{LL} \end{pmatrix} . \tag{2.28}$$

Not only is the action of $\left(\mathsf{A}^{(0)}\right)^{-1}$ cheap to compute, but we also expect that $\mathsf{A}^{(0)}$ will approximate A reasonably well for a body which is nearly spherical, with the approximation improving as $\mathcal{M}$ approaches geometrical sphericity. This suggests that $\left(\mathsf{A}^{(0)}\right)^{-1}$ should act as a good preconditioner in a moderately aspherical system, and this is borne out by later numerical examples.

Within Al-Attar et al. (2012) it was found that for normal mode calculations such a "spherical earth pre-conditioner" could usually be out-performed by allowing some limited coupling between the off-diagonal sub-blocks. We have not investigated that for the present problem, but it might be worth considering in future work if applications to very aspherical planets are necessary (see Section 2.5).

2.4 Numerical examples & benchmarks

2.4.1 The form of the mapping

Finding a diffeomorphism which maps an aspherical, multi-layered planet onto a geometrically-spherical reference body is a problem in its own right. Therefore, for the rest of this work we restrict attention to mappings of the form

$$\boldsymbol{\xi}(\mathbf{x}) = \mathbf{x} + h(\mathbf{x})\hat{\mathbf{x}}\,, \tag{2.29}$$

where h is a scalar-valued function. Physically, $\boldsymbol{\xi}$ causes displacement along *radial* lines: hence, we shall describe these mappings as "radial". This choice of $\boldsymbol{\xi}$ limits our scope somewhat, but despite its apparent simplicity we can still study a broad class of planetary bodies. We emphasise, though, that the method described above is applicable, in principle, to any body that can be mapped diffeomorphically onto a ball.

For mappings of the form of eq.(2.29), we show in Appendix A.2 that its Jacobian is

$$J = \left(1 + \frac{h}{r}\right)^2 (1 + \partial_r h)\ . \tag{2.30}$$

In order for $\boldsymbol{\xi}$ to be a diffeomorphism it is necessary for J to be everywhere positive, so the form of h is restricted; we emphasise, however, that this function is not required to be small in any

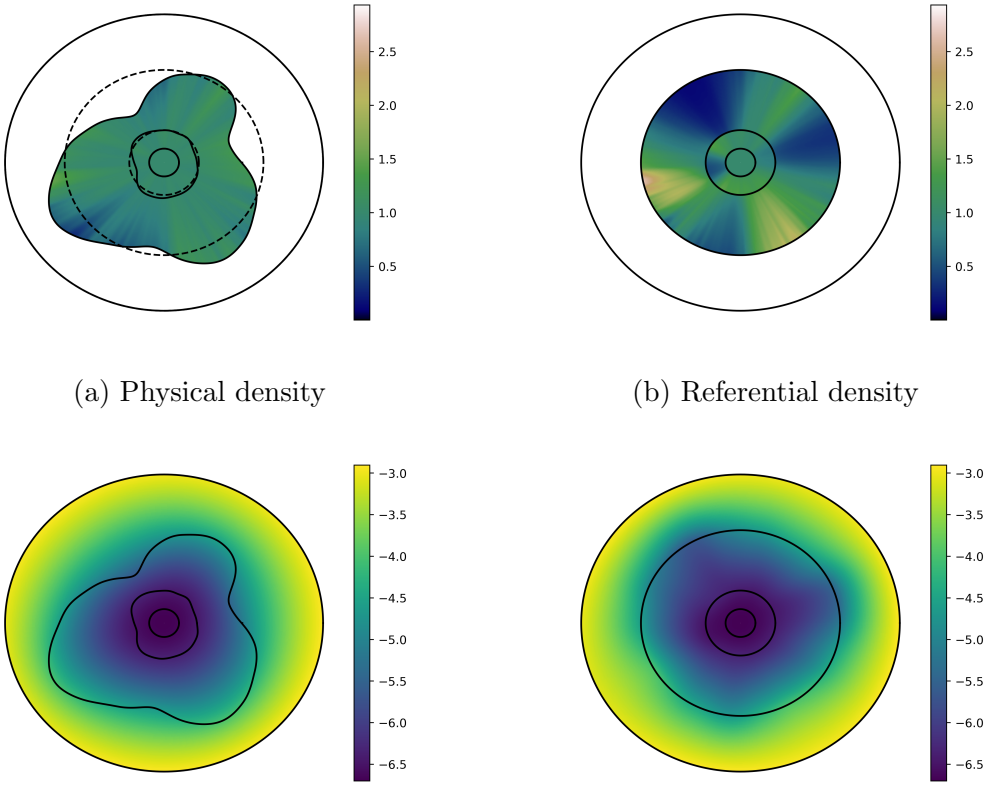

(a) Physical density

(b) Referential density

(c) Physical potential

(d) Referential potential

Figure 2.1: The stages in the calculation of ϕ for an aspherical, layered planet. Each panel shows a slice through the plane $\theta = \pi/2$, and a small, homogeneous sphere has been placed around the origin in order to ensure that $\boldsymbol{\xi}$ and ρ are both regular at the origin. Panel (a) shows the planet before performing any transformations. In panel (b) the computational domain $\mathcal{B}$ has been transformed through the action of $\boldsymbol{\xi}$: the boundaries of the planet are spherical and the density has been transformed accordingly. Panel (d) shows ζ, the solution to eq.(2.16). Moving left from (d) to (c) the planet and potential are mapped from reference space back to physical space, yielding the potential ϕ.

sense.

In practice we generate h by specifying the desired topography on each reference boundary and smoothly interpolating between them. In detail, the topography on the i'th reference boundary is defined to be h_i, with the boundary being a sphere of radius R_i, and we demand that $h|_{r=R_i} = h_i$. Since it is permissible that $\boldsymbol{\xi}$ be only piecewise-smooth and continuous across referential boundaries, hence we are free, if desired, to interpolate the form of h within each layer separately, while only enforcing continuity at the boundary radii. Once h has been specified throughout $\mathcal{B}$ we can calculate and store $a^{\alpha\beta}$, the contravariant components of $\mathbf{a}$ with respect to the canonical basis; see Appendix A.2 for details.

2.4.2 Tests, benchmarks and illustrations

In this section we present some examples and test the accuracy of our method. All physical quantities are presented non-dimensionalised, with

1. density scaled by $\tilde{\varrho} = 5150\,\mathrm{kg\,m^{-3}}$, Earth's average density,

2. length scaled by $\tilde{L} = 6.371 \times 10^6\,\mathrm{m}$, the average radius of the Earth,

3. potential itself scaled by $\tilde{\phi} = G\tilde{\varrho}\tilde{L}^2$.

2.4.2.1 Comparison with semi-analytical solution

In order to test the numerical method we must compare its results with those obtained from semi-analytical calculations. Therefore we consider the case of a planet composed of N_L layers, each layer having arbitrary topography on its surface subject to the constraint that the boundaries between the layers not interpenetrate. Furthermore, within the i'th layer the density is parametrised as a polynomial of degree N_p with laterally-varying coefficients,

$$\varrho_i(r,\theta,\varphi) = \sum_{j=1}^{N_p} \varrho_i^{(j)}(\theta,\varphi)\, r^j \,. \tag{2.31}$$

Generalising the results of Balmino (1994), the potential on a spherical surface which encloses the planet can be written analytically as a sum over the planet's layers and over spherical harmonic degrees and polynomial orders. The potential at a point $\mathbf{x}$, inside or outside the body, is of course

$$\phi(\mathbf{x}) = -G \int_{\mathcal{M}} \frac{\varrho(\mathbf{x}')}{\|\mathbf{x}-\mathbf{x}'\|} d\mathbf{x}' \,. \tag{2.32}$$

Let b be the radius of a sphere which completely bounds the body. If $\|\mathbf{x}\| \geq b$, then we may expand the above integral using the identity

$$\frac{1}{\|\mathbf{x}-\mathbf{x}'\|} = \frac{1}{r} \sum_{lm} \frac{4\pi}{2l+1} \left(\frac{r'}{r}\right)^l \overline{Y_{lm}^0(\theta',\varphi')}\, Y_{lm}^0(\theta,\varphi) \,, \tag{2.33}$$

from Dahlen & Tromp (1998, Appendix B). A simple calculation then shows that the (l,m)th component of the potential on the spherical surface $r = b$ is given by

$$\phi_{lm}(b) = -\frac{4\pi G}{(2l+1)b^{l+1}} \left\{ \sum_{i=1}^{N_L} \sum_{j=0}^{N_p} \frac{[R_i + h_i(\theta,\varphi)]^{l+N_p+j} \left[\varrho_i^{(j)}(\theta,\varphi) - \varrho_{i+1}^{(j)}(\theta,\varphi)\right]}{l+N_p+j} \right\}_{lm} , \tag{2.34}$$

where $\varrho_{N_L+1}^{(j)}$ is defined to vanish identically for all j.

For the body considered in Fig. 2.1 we have plotted in Fig. 2.2 the numerical potential anomaly,

$$\phi_{\mathrm{anom}}(r,\theta,\varphi) = \phi(r,\theta,\varphi) - \phi_{00}(r) \,, \tag{2.35}$$

the normalised difference between the numerical and analytical potentials, and the respective

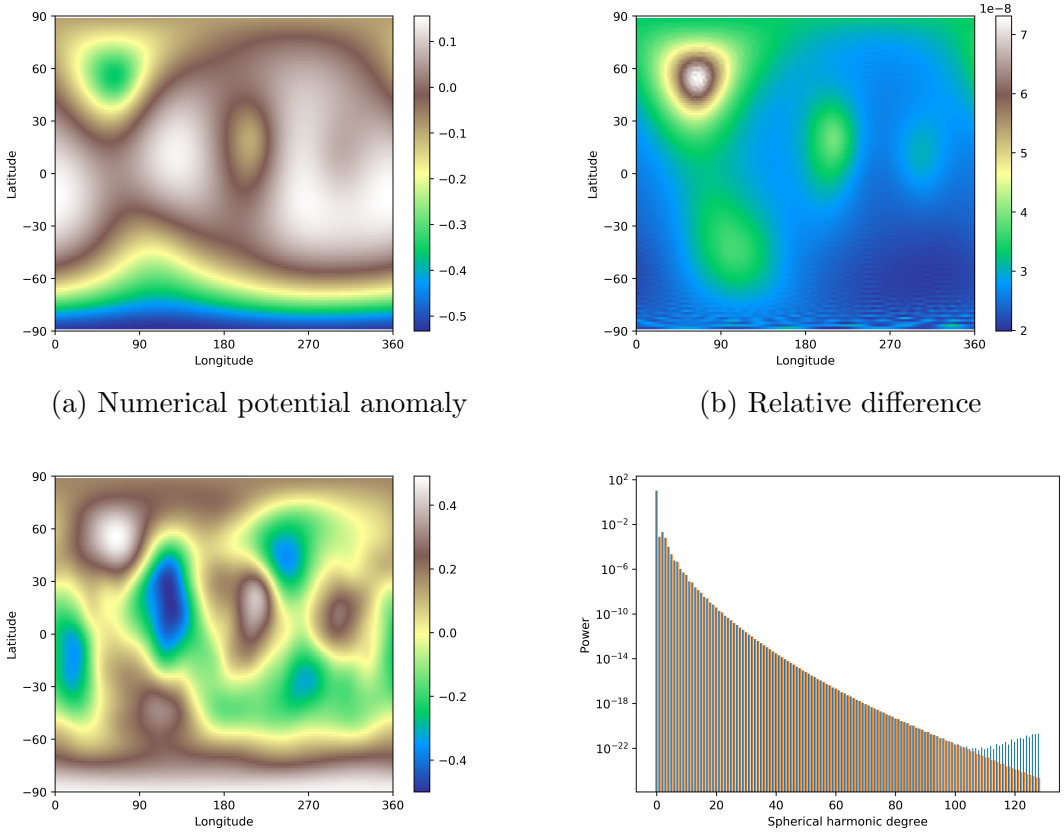

(a) Numerical potential anomaly

(b) Relative difference

(c) Surface topography

(d) Numerical and analytical power spectra

Figure 2.2: The potential and topography of the body considered in Fig. 2.1, evaluated on $\partial\mathcal{B}$. Panel (a) shows the numerical potential anomaly. Long-wavelength features of the topography –shown in panel (c) – are clearly visible. In panel (d) we have plotted the numerical (blue) and analytical (red) values of the normalised power-spectra, P_l. There is excellent agreement until about $l = 100$. Thereafter, the two spectra deviate somewhat, but the power at these higher degrees is so small that the spatial field is not affected noticeably. Indeed, the relative difference between the numerical and analytical fields, normalised by the maximum absolute value of the analytical field, is only a few parts in 10^8, as shown in panel (b).

normalised power-spectra,

$$P_l(r) = \frac{\sum_m |\phi_{lm}(r)|^2}{|\phi_{00}(r)|^2}\,, \tag{2.36}$$

on $\partial\mathcal{B}$, corresponding to a radius of $r = 1.6$. The surface topography is also shown for reference. We see from panel (d) that the numerical and analytical potentials agree closely, having identical power-spectra up to around $l = 100$. Although the power-spectra differ beyond that degree, the potential has so little power in those higher degrees that the spatial field is not affected appreciably.

The difference between the power-spectra at high degrees is due to truncation. If the planet were homogeneous with small topography, then the potential would have the same maximum degree as the topography. However, the nonlinear interactions between large topography and heterogeneous density produce a potential with power at all degrees. By truncating the spherical-harmonic expansion we necessarily neglect some of this behaviour. Therefore, the maximum

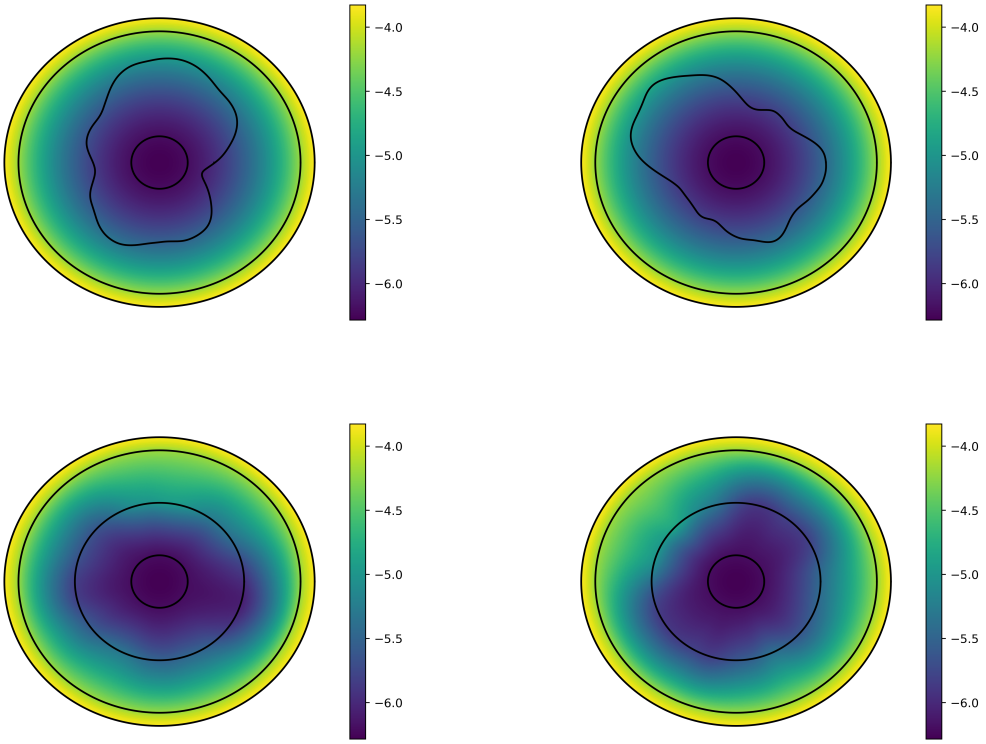

Figure 2.3: A comparison of the referential and physical potentials of two "different" homogeneous spheres, each containing a different internal "boundary" with large topography. The bottom two panels show the referential potentials which, being the result of applying different mappings to $\mathcal{B}$, are not the same. By contrast, the physical potentials, shown above, agree to numerical precision.

spherical-harmonic degree required to calculate ϕ to a given level of accuracy will not just be the larger of the maximum degree in the density and topography. Rather, it must be chosen based on the roughness of the referential density ρ and the tensor field $\mathbf{a}$. While this issue has not been investigated fully, we can easily check for convergence in each instance by repeating calculations at increasing maximum degrees.

2.4.2.2 Independence of the form of the mapping

A physical planet can be represented by many different reference bodies, each with its own diffeomorphism and associated referential density. Our numerical method must, of course, be independent of the arbitrary choice of diffeomorphism. To verify this, we consider a homogeneous, spherical planet along with two distinct referential descriptions as illustrated in Fig. 2.3. Whilst the respective referential potentials are clearly different, we see that they map to the same physical potential.

2.4.3 Further examples

Having shown that our method gives numerically-accurate answers we conclude by showing two more illustrative example calculations. First, in Fig. 2.4 we show the calculated potential of a

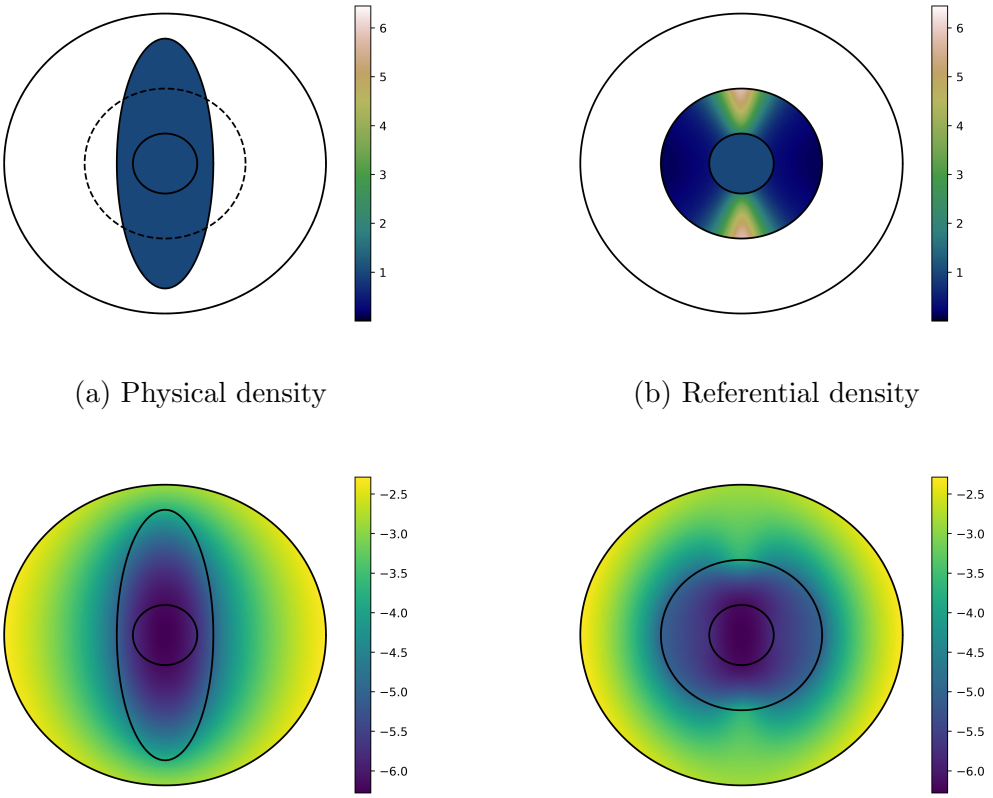

(a) Physical density

(b) Referential density

(c) Physical potential

(d) Referential potential

Figure 2.4: An illustration of the numerical method for a highly flattened ellipsoid. The body is homogeneous, which clarifies the mapping procedure visually. See Fig. 2.1 for a description of the stages.

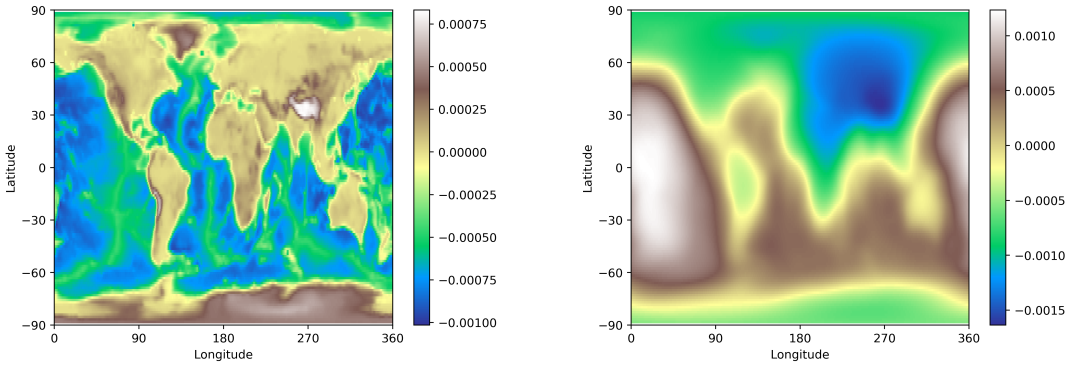

Figure 2.5: A homogeneous body with Terran topography, with the computation performed accurate to maximum degree $L = 128$. The left panel shows the topography. On the top right is plotted the potential anomaly at a radius of 1.05, corresponding to an actual altitude of about 300km.

highly flattened, homogeneous ellipsoid. Calculations of this type are required in determining hydrostatic equilibrium figures of rapidly rotating planets, this being a potential future application of this work.

Finally, Figure 2.5 shows the potential of a homogeneous body with the Earth's topography expanded up to degree 128. While the topography contains relatively short wavelengths, it is only of a very low amplitude compared to the Earth's radius. We can, therefore, chose the diffeomorphism to equal the identity mapping everywhere but a thin spherical annulus enclosing the surface. As discussed earlier, this greatly increases the speed of the calculations.

2.5 Discussion

We have presented a new method for performing numerically exact calculations of the gravitational potential of aspherical and heterogeneous planets. The novel feature of this work is the use of a diffeomorphism $\boldsymbol{\xi}$ to map $\mathcal{M}$, a heterogeneous planet with arbitrarily large topography, onto $\tilde{\mathcal{M}}$, a geometrically spherical reference body in which pseudo-spectral methods can be used in conjunction with 1D spectral element methods. The numerical examples demonstrate that the method is accurate, has an efficiency that scales with the planet's complexity, and can even be applied to markedly aspherical planets. It is worth noting that all of these examples were run on a desktop computer, and do not require the use of parallel computations.

The chief motivation behind our work is the desire to perform elastodynamics calculations in aspherical planets efficiently without approximating the effects of self-gravity and topography. In this context, the geometric transformations we have used can be interpreted physically as "particle-relabelling transformations" as described by Al-Attar & Crawford (2016) and Al-Attar et al. (2018). The necessary extensions – which we discuss qualitatively in Section 4.7 – will be undertaken in future work, with application to hydrostatic equilibrium figures, free-oscillation seismology, body tides, and rotational dynamics. Furthermore, there are bodies of interest in the planetary sciences which, although diffeomorphic to a ball, cannot be described using the radial mappings currently implemented. A particularly salient example are the "synestias" introduced

by Lock & Stewart (2017). An important extension of this work, then, is to investigate the efficient generation of more general diffeomorphisms.

CHAPTER 3

On the stress dependence of the elastic tensor

O voi che siete in piccioletta barca,
desiderosi d'ascoltar, seguiti
dietro al mio legno che cantando varca,

tornate a riveder li vostri liti:
non vi mettete in pelago, ché forse,
perdendo me, rimarreste smarriti.

Paradiso II.1-6
Dante[†]

3.1 Introduction

Approaches to seismic wave propagation within a pre-stressed Earth have a long and complicated history; see Dahlen & Tromp (1998, Chapter 1). Early work on theoretical seismology was built on the theory of classical linear elasticity (e.g. Thomson, 1863; Lamb, 1881). But classical linear elasticity is founded upon an assumption of small deformations away from a stress-free equilibrium. Its applicability to seismology is therefore unclear, given the presence of large equilibrium stresses within the Earth. In fact, it was not until the work of Dahlen (1972a) that a correct treatment was given.

Dahlen (1972a) derived the equations of motion relevant to global seismology by direct linearisation of the equations of finite elasticity. It is a result of this approach that the elastic tensor can be written as the sum of two pieces: one without explicit stress dependence, and a second piece that depends on stress linearly. There is no question that this decomposition is valid and that Dahlen's equations of motion are correct, but the decomposition is not unique in that the elastic tensor's stress dependence is left (partially) implicit.

Later that year Dahlen (1972b) used his earlier results to study plane-wave propagation

[†]See Jeffreys (1924, Chapter IX)

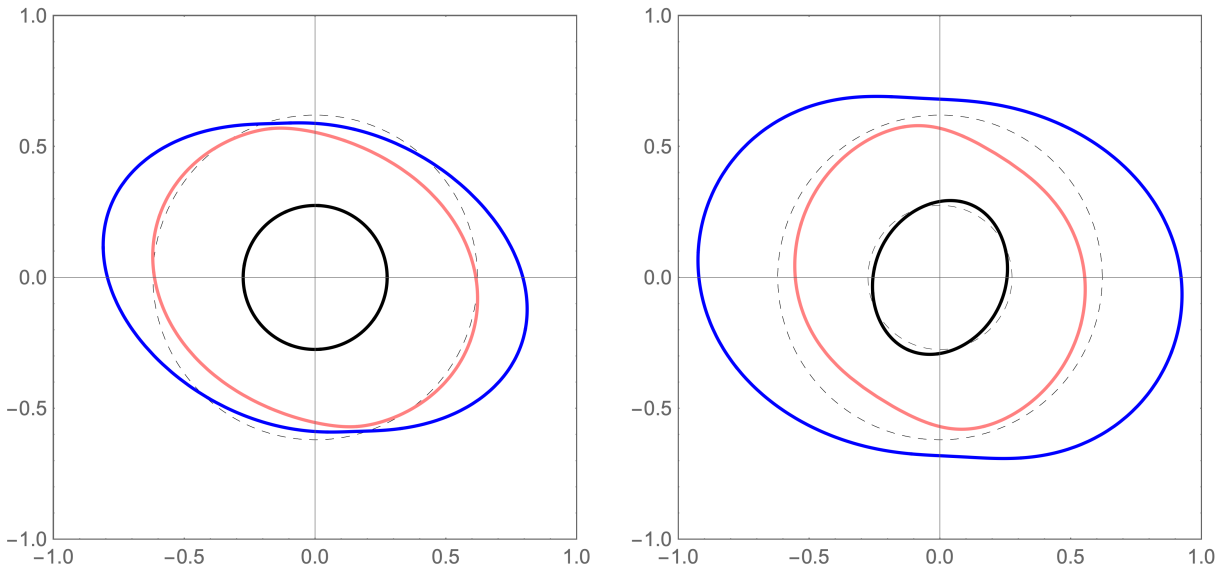

Figure 3.1: The effect of an induced deviatoric stress on plane-wave propagation within an initially isotropic body. Each panel shows a slice through the x–y plane of the slowness surface of an isotropic material in which a stress has been induced. The black line is the P-wave while the S-waves are in blue and pink, and the zero-stress result is shown dashed in the background for reference; we will adhere to this convention consistently in this chapter. The material on the left follows the theory of Dahlen (1972b). Whilst the S-waves are noticeably split the P-wave surface has not perceptibly moved from its isotropic position, illustrating Dahlen's result that P-wave speeds are not changed to first-order by a small stress. By contrast, the material on the right obeys Tromp & Trampert (2018), and there we see that P-wave speeds are indeed perturbed to first-order in small stress. There is also a marked difference in the S-wave splitting pattern. In this figure we have taken $\mu' = \kappa' = 1$, consistent with Stacey (1992).

in the presence of an arbitrary equilibrium pre-stress. To do so, he theorised that the elastic tensor's stress dependence should take a particular functional form. He assumed specifically that the only stress dependence was what his earlier formulae had made *explicit*. That theory has two important implications. Firstly, the elastic wave speeds display no explicit dependence on equilibrium pressure. Secondly, deviatoric stresses induced within an isotropic medium have no first-order effect on P-wave speeds, whilst S-waves are split to the same accuracy. This is illustrated in the left panel of Fig.3.1; as with all the figures in this chapter, the values of the physical quantities have been chosen for the sake of illustration and are not necessarily geophysically realistic.

The problem of the elastic tensor's stress dependence has since been revisited by Tromp & Trampert (2018) who were motivated by the possibility of using seismic data to image stresses within the Groningen gas field. Importantly, they arrived at a theory that predicts physical behaviour both quantitatively and qualitatively distinct from that derived by Dahlen. In direct contravention of Dahlen, Tromp & Trampert suggest that *both* P- and S-wave speeds change to first-order if a small deviatoric stress is induced in an isotropic medium (Fig.3.1, right panel).

The most recent work on the problem is that of Tromp et al. (2019). These authors not only generalised Tromp & Trampert's results beyond the framework provided by Dahlen & Tromp (1998) (see below) but also included comparisons between their new theoretical results and *ab*

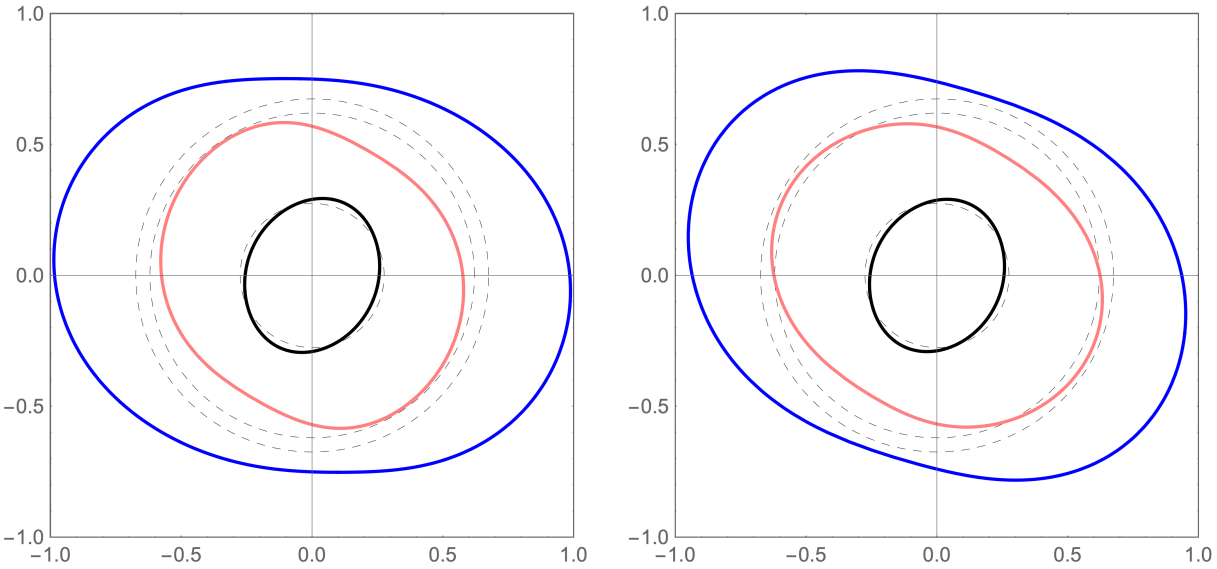

Figure 3.2: The effect of an induced deviatoric stress on plane-wave propagation within a body that is initially transversely-isotropic with its symmetry axis pointing out of the page. This figure is similar to Fig. 3.1, but now we are comparing the theories of Tromp & Trampert (2018) (left) and Tromp et al. (2019) (right). The theories give the same results for an isotropic material, so we have chosen a transversely-isotropic material in order to demonstrate that they predict distinct behaviour in general.

initio calculations. Their results reduce to those of Tromp & Trampert (2018) for an isotropic body, but make different predictions otherwise. Fig. 3.2 contrasts the two theories as applied to a transversely-isotropic body.

The seismological community is left with three distinct theories for the effect of equilibrium stress on seismic wave propagation. This has led us to undertake the present work, which revisits the elastic tensor's stress dependence and seeks to clarify it from the perspective of finite elasticity. It should be emphasised that the work of Dahlen (1972a) – which has underlain most of global seismology and related fields since its publication – is fully correct and general. The problem that we wish to address concerns only the elastic tensor's dependence on equilibrium stress. To provide more specific context we will begin by presenting a heuristic approach to the problem that slightly generalises the previous discussions and points towards their limitations.

3.1.1 A heuristic linearised theory of the elastic tensor's stress dependence

3.1.1.1 Preliminaries

In the notation of Dahlen & Tromp (1998) the equations of motion governing global seismology are (Dahlen & Tromp, 1998, p.84)

$$\partial_t^2 \mathbf{s} - \frac{1}{\rho^0} \nabla \cdot (\boldsymbol{\Lambda} : \nabla \mathbf{s}) + 2\boldsymbol{\Omega} \times \partial_t \mathbf{s} + \nabla \phi^{E1} + \mathbf{s} \cdot \nabla \nabla \big(\phi^0 + \psi\big) = 0, \tag{3.1}$$

for an Earth model initially at equilibrium with density ρ^0 and gravitational potential ϕ^0, and which rotates at constant angular velocity $\boldsymbol{\Omega}$ giving rise to the centrifugal potential ψ. The

displacement from equilibrium is $\mathbf{s}$, with ϕ^{E1} the corresponding perturbation to the gravitational potential. Most importantly for our purposes, the Earth model is assumed to be pre-stressed, supporting a nonzero *equilibrium Cauchy stress* $\mathbf{T}^0$, while $\boldsymbol{\Lambda}$ is the *elastic tensor*. (Henceforward I will always refer to equilibrium Cauchy stress simply as "stress" unless I state otherwise or the context offers no possibility of confusion; see Section 3.2.1.2 for a discussion of different stress tensors.) As discussed at length in Dahlen & Tromp's Section 3.6, $\boldsymbol{\Lambda}$ is one of a number of elastic tensors that can be used depending on how the equations of motion are formulated. It is particularly relevant for us that there exists another elastic tensor $\boldsymbol{\Xi}$ related to $\boldsymbol{\Lambda}$ by (Dahlen & Tromp, 1998, eq.3.122)

$$\Lambda_{ijkl} = \Xi_{ijkl} + T^0_{ik}\delta_{jl}. \tag{3.2}$$

$\boldsymbol{\Xi}$ is obtained as the second derivative of a strain-energy function. It therefore satisfies the *hyperelastic symmetry*

$$\Xi_{ijkl} = \Xi_{klij} \tag{3.3}$$

and the *minor symmetries*

$$\Xi_{ijkl} = \Xi_{jikl} = \Xi_{ijlk} \tag{3.4}$$

(collectively referred to as the *classical elastic symmetries*) and thus possesses 21 independent components at most. We see that $\boldsymbol{\Lambda}$ is decomposed into two parts, one with explicit, linear stress dependence, and another whose dependence on stress is *a priori* unclear. The purpose of the present work is to establish how $\boldsymbol{\Xi}$ – and hence $\boldsymbol{\Lambda}$ – depends on $\mathbf{T}^0$.

For geophysical applications it seems reasonable to restrict attention to linearised stress dependence about a hydrostatic background; finding the linearised stress dependence of $\boldsymbol{\Xi}$ is necessary and sufficient to specify that of $\boldsymbol{\Lambda}$. We regard $\mathbf{T}^0$ as being composed of a *background hydrostatic stress* $\mathbf{T}^B$ described by a large pressure p^0, with a small *incremental stress* $\Delta\mathbf{T}^0$ superimposed. The total equilibrium stress is thus written as

$$\begin{aligned}\mathbf{T}^0 &= \mathbf{T}^B + \Delta\mathbf{T}^0 \\ &= -p^0\mathbf{1} - \Delta p^0\mathbf{1} + \Delta\boldsymbol{\tau}^0,\end{aligned} \tag{3.5}$$

where Δp^0 and $\Delta\boldsymbol{\tau}^0$ are the hydrostatic and deviatoric components of $\Delta\mathbf{T}^0$. We will use this notation consistently for the rest of this section, which means that some of the expressions we quote will look slightly different from how they appear elsewhere. Now we ask what the most general linear stress dependence of $\boldsymbol{\Xi}$ could be. To that end we write $\boldsymbol{\Xi}$ as a Taylor series,

$$\Xi_{ijkl} = \Gamma_{ijkl} + \Pi_{ijklmn}\Delta T^0_{mn} + \mathcal{O}\Big(\big\|\Delta\mathbf{T}^0\big\|^2\Big), \tag{3.6}$$

and neglect all terms of quadratic and higher order in $\big\|\Delta\mathbf{T}^0\big\|$. $\boldsymbol{\Gamma}$ is then the elastic tensor of the background hydrostatic state while $\boldsymbol{\Pi}$ represents the elastic tensor's stress-derivatives

evaluated in that background state. To first-order accuracy a body's response to changes in incremental stress is thus determined entirely by $\mathbf{\Pi}$. Decomposing the stress into its hydrostatic and deviatoric parts,

$$\Delta T_{ij}^0 = -\Delta p^0 \delta_{ij} + \Delta \tau_{ij}^0, \tag{3.7}$$

we can write

$$\Xi_{ijkl} = \Gamma_{ijkl} - \Pi_{ijklaa}\Delta p^0 + \Pi_{ijklmn}\Delta \tau_{mn}^0, \tag{3.8}$$

based on which we define the pressure-derivatives of the elastic tensor as

$$\frac{\partial \Xi_{ijkl}}{\partial p} \equiv \Xi'_{ijkl} = -\Pi_{ijklaa} \tag{3.9}$$

and its derivatives with respect to deviatoric stress as

$$\frac{\partial \Xi_{ijkl}}{\partial \tau_{mn}} = \Pi_{ijklmn} - \frac{1}{3}\Pi_{ijklaa}\delta_{mn}. \tag{3.10}$$

Both $\mathbf{\Xi}$ and $\mathbf{\Gamma}$ must possess the full set of classical elastic symmetries, and the symmetry of the Cauchy stress means that $\mathbf{\Pi}$ may be taken as symmetric on its last two indices without loss of generality. Therefore $\mathbf{\Pi}$ is required at minimum to obey the relations

$$\overbrace{\Pi_{ijklnm} = \underbrace{\Pi_{ijklmn}}_{\text{Classical elastic symmetries}} = \Pi_{jiklmn} = \Pi_{ijlkmn} = \Pi_{klijmn}}^{\text{Symmetry of } \mathbf{T}^0}, \tag{3.11}$$

from which one can show that it possesses at most $21 \times 6 = 126$ independent components.

3.1.1.2 Isotropic materials

In an isotropic, hydrostatically pre-stressed material neither $\mathbf{\Gamma}$ nor $\mathbf{\Pi}$ can exhibit any preferred direction. This is true if *and only if* the material is isotropic. No matter the value of the background hydrostatic pressure, $\mathbf{\Gamma}$ therefore has just two independent components, the *bulk modulus* κ and *shear modulus* μ. According to convenience one can also use the relation

$$\kappa = \lambda + \frac{2}{3}\mu \tag{3.12}$$

to write $\mathbf{\Gamma}$ in terms of the *Lamé parameters* λ and μ. In terms of the elastic moduli $\mathbf{\Gamma}$ takes the familiar form

$$\Gamma_{ijkl} = \left(\kappa - \frac{2}{3}\mu\right)\delta_{ij}\delta_{kl} + \mu(\delta_{ik}\delta_{jl} + \delta_{il}\delta_{jk})\,. \tag{3.13}$$

The tensor $\mathbf{\Pi}$ also has considerably fewer than 126 components. It too will only be composed of Kronecker deltas, and the most general such tensor that also satisfies the required symmetries

(eq.3.11) has four independent components. Thus

$$\begin{aligned}\Pi_{ijklmn} = a\Big[\delta_{ij}\delta_{k(m}\delta_{n)l} + \delta_{kl}\delta_{i(m}\delta_{n)j} - \frac{2}{3}\delta_{ij}\delta_{kl}\delta_{mn}\Big] \\ + b\Big[\delta_{ik}\delta_{j(m}\delta_{n)l} + \delta_{il}\delta_{j(m}\delta_{n)k} + \delta_{jk}\delta_{i(m}\delta_{n)l} + \delta_{jl}\delta_{i(m}\delta_{n)k} - \frac{2}{3}\left(\delta_{ik}\delta_{jl} + \delta_{il}\delta_{jk}\right)\delta_{mn}\Big] \\ - \left[\frac{c}{3}\,\delta_{ij}\delta_{kl} + \frac{d}{3}\left(\delta_{ik}\delta_{jl} + \delta_{il}\delta_{jk}\right)\right]\delta_{mn},\end{aligned} \tag{3.14}$$

where we have explicitly symmetrised on m and n by writing parentheses around the indices, e.g.

$$\delta_{k(m}\delta_{n)l} = \frac{1}{2}(\delta_{km}\delta_{nl} + \delta_{kn}\delta_{ml})\,. \tag{3.15}$$

One can derive eq.(3.14) by splitting the incremental stress into its hydrostatic and deviatoric components,

$$\Delta T^0_{ij} = -\Delta p^0\delta_{ij} + \Delta\tau^0_{ij}, \tag{3.16}$$

and considering the pressure and deviatoric stress separately. By symmetry, the only possible effect of an induced incremental pressure is to alter the elastic moduli, which gives the terms in c and d above. Turning to the deviatoric stress, we must construct all possible tensors with the classical elastic symmetries that are permutations of $\delta_{ij}\Delta\tau^0_{kl}$ (see Dahlen & Tromp, 1998, p.79). The first possibility is

$$\delta_{ij}\Delta\tau^0_{kl} + \delta_{kl}\Delta\tau^0_{ij}. \tag{3.17}$$

Each term possesses the minor symmetries trivially, but it is only when the two terms are added together that we gain the hyperelastic symmetry. The second such tensor is a little more complicated, taking the form

$$\delta_{ik}\Delta\tau^0_{jl} + \delta_{il}\Delta\tau^0_{jk} + \delta_{jk}\Delta\tau^0_{il} + \delta_{jl}\Delta\tau^0_{ik}. \tag{3.18}$$

These are the only two tensors that fulfil our requirements, and they lead respectively to the terms in a and b above. Note that we have defined a, b, c and d so that the terms in a and b only interact with deviatoric stress (they are traceless on (mn)), while those in c and d interact with pressure alone. The components of $\boldsymbol{\Xi}$ are finally

$$\begin{aligned}\Xi_{ijkl} = \left(\kappa - \frac{2}{3}\mu + \Delta p^0 c\right)\delta_{ij}\delta_{kl} + \big(\mu + \Delta p^0 d\big)\big(\delta_{ik}\delta_{jl} + \delta_{il}\delta_{jk}\big) \\ + a\big(\delta_{ij}\Delta\tau^0_{kl} + \delta_{kl}\Delta\tau^0_{ij}\big) + b\big(\delta_{ik}\Delta\tau^0_{jl} + \delta_{il}\Delta\tau^0_{jk} + \delta_{jk}\Delta\tau^0_{il} + \delta_{jl}\Delta\tau^0_{ik}\big)\,.\end{aligned} \tag{3.19}$$

We have arrived at the most general linearised theory consistent with an isotropic, hydrostatically stressed background. It should be noted that this heuristic theory is based on symmetry arguments alone and provides no further information about the four scalars it identifies. One could therefore just regard them as free parameters of the theory, to be fitted experimentally.

However, it is *not* clear that they actually represent four degrees of freedom. They could well be found to depend on some smaller (or larger) set of material-dependent parameters if constitutive behaviour were considered.

The theories of Dahlen (1972b), Tromp & Trampert (2018) and indeed Dahlen & Tromp (1998, eq.3.135) can all be seen as special cases of eq.(3.14). Each theory corresponds to choosing

$$\begin{aligned} c &= -2a \\ d &= -2b, \end{aligned} \tag{3.20}$$

and they are then distinguished by their values of a and b. In Dahlen & Tromp (1998, eq.3.135) a and b are regarded as free parameters, yielding the expression

$$\begin{aligned} \Xi_{ijkl} = &\left(\kappa - \frac{2}{3}\mu\right)\delta_{ij}\delta_{kl} + \mu(\delta_{ik}\delta_{jl} + \delta_{il}\delta_{jk}) \\ &+ a\big(\delta_{ij}\Delta T^0_{kl} + \delta_{kl}\Delta T^0_{ij}\big) + b\big(\delta_{ik}\Delta T^0_{jl} + \delta_{il}\Delta T^0_{jk} + \delta_{jk}\Delta T^0_{il} + \delta_{jl}\Delta T^0_{ik}\big)\,. \end{aligned} \tag{3.21}$$

The authors subsequently arrive at Dahlen's original expression (e.g. Dahlen & Tromp, 1998, eq.3.139)

$$\begin{aligned} \Xi_{ijkl} = &\left(\kappa - \frac{2}{3}\mu\right)\delta_{ij}\delta_{kl} + \mu(\delta_{ik}\delta_{jl} + \delta_{il}\delta_{jk}) \\ &+ \frac{1}{2}\big(\delta_{ij}\Delta T^0_{kl} + \delta_{kl}\Delta T^0_{ij}\big) - \frac{1}{2}\big(\delta_{ik}\Delta T^0_{jl} + \delta_{il}\Delta T^0_{jk} + \delta_{jk}\Delta T^0_{il} + \delta_{jl}\Delta T^0_{ik}\big) \end{aligned} \tag{3.22}$$

by making the "convenient" choice

$$a = -b = \frac{1}{2}. \tag{3.23}$$

Given eq.(3.20) this is the unique choice of a and b that ensures the aforementioned characteristic features of Dahlen's theory: that seismic wave speeds have no explicit pressure-dependence, and that P-wave speeds are unaffected by deviatoric stress to first order in perturbation theory. Tromp & Trampert, on the other hand, set

$$\begin{aligned} a &= \frac{1}{2} + \frac{1}{3}\mu' - \frac{1}{2}\kappa' \\ b &= -\frac{1}{2} - \frac{1}{2}\mu', \end{aligned} \tag{3.24}$$

with κ' and μ' denoting the pressure-derivatives of the elastic moduli. Their elastic tensor is thus (Tromp & Trampert, 2018, eq.44)

$$\begin{aligned} \Xi_{ijkl} = &\left(\kappa - \frac{2}{3}\mu\right)\delta_{ij}\delta_{kl} + \mu(\delta_{ik}\delta_{jl} + \delta_{il}\delta_{jk}) \\ &+ \frac{1}{2}\left(1 - \kappa' + \frac{2}{3}\mu'\right)\big(\delta_{ij}\Delta T^0_{kl} + \delta_{kl}\Delta T^0_{ij}\big) \\ &- \frac{1}{2}\big(1 + \mu'\big)\big(\delta_{ik}\Delta T^0_{jl} + \delta_{il}\Delta T^0_{jk} + \delta_{jk}\Delta T^0_{il} + \delta_{jl}\Delta T^0_{ik}\big)\,. \end{aligned} \tag{3.25}$$

The motivation behind this particular combination of a and b is that it leads to the wave speeds

$$\begin{aligned}\rho c_p^2 &= \left(\kappa + \kappa' \Delta p^0\right) + \frac{4}{3}\left(\mu + \mu' \Delta p^0\right) \\ \rho c_s^2 &= \left(\mu + \mu' \Delta p^0\right)\end{aligned} \tag{3.26}$$

when an incremental hydrostatic stress Δp^0 is induced in an isotropic medium of density ρ. The authors argue that this is desirable on the grounds that these are the classical expressions for isotropic wave speeds, but with elastic constants that are *explicitly* corrected for an incremental pressure.

3.1.1.3 Anisotropic materials

The theory just discussed depended on the assumption that the body was isotropic. It would be rendered inconsistent if $\mathbf{\Gamma}$ were taken to be anything other than an isotropic tensor, as we did throughout Section 3.1.1.2. This is a consequence of the fact that the theory is based on eq.(3.14); a more general form of $\mathbf{\Pi}$ must be used if materials of lower symmetry are to be considered.

The work of Tromp et al. (2019), mentioned earlier, has partially resolved this issue. They generalise the results of Tromp & Trampert (2018) to obtain an elastic tensor that depends on the stress linearly, but does *not* implicitly assume that the material under study is isotropic. They take the tensor $\mathbf{\Gamma}$ to have components (Tromp et al., 2019, eq.8)

$$\Gamma_{ijkl} = \left(\kappa - \frac{2}{3}\mu\right)\delta_{ij}\delta_{kl} + \mu(\delta_{ik}\delta_{jl} + \delta_{il}\delta_{jk}) + \gamma_{ijkl}, \tag{3.27}$$

where $\boldsymbol{\gamma}$ satisfies the classical elastic symmetries but is *not* an isotropic tensor. Their elastic tensor $\mathbf{\Xi}$ can be derived from our eq.(3.6) by demanding that $\mathbf{\Pi}$ possess the symmetries

$$\Pi_{ijklmn} = \Pi_{ijmnkl} = \Pi_{klmnij} = \Pi_{mnijkl} = \Pi_{mnklij} \tag{3.28}$$

in addition to those stated in eq.(3.11). By doing this, eq.(3.9) can be solved uniquely to give *all* of $\mathbf{\Pi}$'s components in terms of those of $\mathbf{\Xi}'$:

$$\begin{aligned}\Pi_{ijklmn} = -\frac{1}{8}\big(&\delta_{in}\Xi'_{mjkl} + \delta_{im}\Xi'_{njkl} + \delta_{jn}\Xi'_{imkl} + \delta_{jm}\Xi'_{inkl} \\ &+\delta_{kn}\Xi'_{ijml} + \delta_{km}\Xi'_{ijnl} + \delta_{ln}\Xi'_{ijkm} + \delta_{lm}\Xi'_{ijkn}\big)\,.\end{aligned} \tag{3.29}$$

The elastic tensor's dependence on incremental stress is thus parametrised by pressure-derivatives alone, analogously to the isotropic case (cf. eq.3.20). Under this theory $\mathbf{\Pi}$ is described by 21 independent components at most.

3.1.2 Aims of this chapter

This completes our initial survey of the elastic tensor's linearised stress dependence. Working on the basis of symmetry arguments alone we have established that the previous approaches to the problem might not be sufficiently general. In particular, equations (3.20) and (3.29) seem to

imply that the stress dependence of the elastic tensor should be parametrisable solely in terms of the pressure dependence of the elastic moduli, a physical result that is not obvious to the present author. Nevertheless, recall that Tromp et al. (2019) tested the validity of their theory by carrying out *ab initio* calculations. They found good, but not perfect, agreement between theory and experiment. Given the nature of such calculations it is difficult to make precise statements about the significance of the discrepancies, but the general agreement does provide clear support for their parametrisation. It is also worth noting that the approach of Section 3.1.1 brings one to a usable theory rather quickly. The issue, however, is that it gives no clear sense of how $\mathbf{\Pi}$ is determined from the underlying constitutive relation. As the theory stands there appears to be no way to obtain $\mathbf{\Pi}$'s components besides by performing experiments. Such experiments are already challenging for the cubic materials considered by Tromp et al. (2019), wherein three parameters were to be found, and they might become very difficult for more anisotropic materials. One might wonder if $\mathbf{\Pi}$ emerges from a more "fundamental" source than its definition in eq.(3.6).

The present work thus has two main aims. The first is to better understand the previous theoretical work on the elastic tensor's linearised stress dependence. Having established the general characteristics of that theory in Section 3.1.1 we now wish to ask whether the components of $\mathbf{\Pi}$ can be obtained more readily in some other way. A secondary aim is to construct a nonlinear theory of the elastic tensor's stress dependence. This is not purely academic, despite the fact that deviatoric stresses within the present-day Earth are presumably rather small. Methodologically speaking, I feel that it is clearer to derive as much as possible without approximating any physical behaviour because it provides a firm foundation for subsequent, physically-motivated linearisation. In formulating a nonlinear theory we hope to gain greater insight into the linear theory.

In order to make progress I take a new approach rooted firmly in the theories of finite elasticity and constitutive behaviour. I present that argument in Section 3.3, having first reviewed the necessary ideas in Section 3.2. After deriving the main result I give some examples, both numerical and analytical, in Section 3.4, and discuss the implications of the theory in Sections 3.5 and 3.6. In this introduction I have used as far as possible the notation of Dahlen & Tromp (1998) in order to make close contact with previous work. Our theoretical developments owe a lot to Marsden & Hughes (1994), so from Section 3.2 onwards I switch to (approximately) their notation, which will allow the interested reader of Sections 3.2 and 3.3 to "cross-reference" easily. The content of Sections 3.2–3.4 is necessarily quite technical, so the reader who is primarily interested in my results might wish to proceed straight to Section 3.5. I have therefore restated some of the chapter's important results therein using the notation of Dahlen & Tromp, as well as including a complete "translation table" between the two notation systems in Appendix B.1.4.

3.2 A review of elasticity

In this section I summarise the aspects of elasticity pertinent to this chapter. For more details see, for example, Marsden & Hughes (1994), Dahlen & Tromp (1998) or Truesdell & Noll (2004). In order to make reference to formulae within the solid mechanics literature we will now follow the notation of Marsden & Hughes (henceforward MH) fairly closely. A modest innovation on my part is to use sans-serif bold font for fourth-rank tensors so as to contrast them with

second-rank tensors. This allows us to distinguish between the second elastic tensor $\mathbf{C}$ and the right Cauchy-Green deformation tensor $\mathbf{C}$ without having to resort to index notation. I also refer the reader to Appendix B.1: Section B.1.1 lists some standard results from group theory that I will refer to; B.1.2 defines some non-standard notations and operators that I have found helpful; and B.1.3 finally illustrates the usage of these operators while presenting a calculation that is salient to the present work.

3.2.1 Basic definitions and results

3.2.1.1 Equations of motion

The deformation of an elastic body is described relative to a fixed *reference configuration*, with each particle labelled by its position within the associated *reference body* $\mathcal{B} \subseteq \mathbb{R}^3$, which is assumed to be connected, bounded, and have an open interior. At a time t, the position in physical space of the particle at $\mathbf{x} \in \mathcal{B}$ is written $\boldsymbol{\varphi}(\mathbf{x}, t)$. In this manner, we define a mapping

$$\boldsymbol{\varphi} : \mathcal{B} \times \mathbb{R} \to \mathbb{R}^3, \tag{3.30}$$

which is called the *motion* of the body relative to the reference configuration. For a fixed time, t, the image of the mapping $\boldsymbol{\varphi}(\cdot, t)$ is written $\mathcal{B}_t$ and represents the region of physical space the body instantaneously occupies. It will be assumed that for each fixed time the mapping $\boldsymbol{\varphi}(\cdot, t) : \mathcal{B} \to \mathcal{B}_t$ is smooth with a smooth inverse. A fundamental object derived from the motion is its *deformation gradient*,

$$\mathbf{F} = D_{\mathbf{x}}\boldsymbol{\varphi}, \tag{3.31}$$

where $D_{\mathbf{x}}$ denotes partial differentiation with respect to position as defined through

$$\boldsymbol{\varphi}(\mathbf{x} + \delta\mathbf{x}, t) = \boldsymbol{\varphi}(\mathbf{x}, t) + (D_{\mathbf{x}}\boldsymbol{\varphi})(\mathbf{x}, t) \cdot \delta\mathbf{x} + \mathcal{O}\big(\|\delta\mathbf{x}\|^2\big)\,. \tag{3.32}$$

(We will generally neglect the subscript on D where it is unambiguous which variable we are differentiating with respect to.) Equivalently, the Cartesian components of the deformation gradient are

$$F_{ij} = \frac{\partial \varphi_i}{\partial x_j}. \tag{3.33}$$

The *Jacobian* is then defined as

$$J = \det \mathbf{F}. \tag{3.34}$$

Due to our assumption that $\boldsymbol{\varphi}(\cdot, t) : \mathcal{B} \to \mathcal{B}_t$ has a smooth inverse, it follows from the inverse function theorem (MH, p.31) that the deformation gradient takes values in the general linear group $\mathbf{GL}(3)$ (Appendix B.1.1). We assume without loss of generality that J is everywhere positive, meaning that the motion is orientation preserving.

The *density* at time t at the point $\mathbf{y} \in \mathcal{B}_t$ in physical space is written $\varrho(\mathbf{y}, t)$. From conservation

of mass, we are led to define the *referential density*,

$$\rho(\mathbf{x}) = J(\mathbf{x},t)\varrho[\boldsymbol{\varphi}(\mathbf{x},t),t]\,, \tag{3.35}$$

a time-*independent* function within the reference body (MH, p.87, Theorem 5.7). Cauchy's theorem implies that the traction $\mathbf{T}$ acting on a surface-element within $\mathcal{B}_t$ is related linearly to the unit-normal $\hat{\mathbf{N}}$ of the corresponding reference surface element within $\mathcal{B}$ (MH, p.127). We can therefore define the *first Piola-Kirchhoff stress tensor* $\mathbf{P}$ through (MH, p.7)

$$\mathbf{T} = \mathbf{P}\cdot\hat{\mathbf{N}}. \tag{3.36}$$

This expression is equivalent to eq.(2.41) of Dahlen & Tromp (1998) but, as discussed in Appendix B.1.4, we place our indices according to a different convention. From Newton's second law we obtain the momentum equation

$$\rho\ddot{\boldsymbol{\varphi}} - \mathrm{Div}\mathbf{P} = \mathbf{f}, \tag{3.37}$$

where dots are used to represent time differentiation, the divergence of a tensor field is given by

$$(\mathrm{Div}\mathbf{P})_i = \partial_j P_{ij}, \tag{3.38}$$

and $\mathbf{f}$ denotes the body forces acting on $\mathcal{B}$.

3.2.1.2 Constitutive relations

To complete the equations of motion we need to relate $\mathbf{P}$ and $\boldsymbol{\varphi}$ through a suitable constitutive relation. We follow Dahlen (1972a) by restricting attention to *hyperelastic materials*, in which case the first Piola-Kirchhoff stress depends on the motion through the expression

$$\mathbf{P}(\mathbf{x},t) = (D_{\mathbf{F}}W)[\mathbf{x},\mathbf{F}(\mathbf{x},t)]\,, \tag{3.39}$$

where $W : \mathcal{B}\times\mathbf{GL}(3)\to\mathbb{R}$ is the *strain-energy function* and $D_{\mathbf{F}}W$ denotes its partial derivative with respect to $\mathbf{F}$ (MH, p.190, Theorem 2.4).

The form of the strain-energy function is constrained by the *principle of material-frame indifference*. Discussed at length by Marsden & Hughes (1994) and Truesdell & Noll (2004), it requires that

$$W(\mathbf{x},\mathbf{RF}) = W(\mathbf{x},\mathbf{F}) \tag{3.40}$$

for all rotation matrices $\mathbf{R}\in\mathbf{SO}(3)$ and $\mathbf{F}\in\mathbf{GL}(3)$ (see Appendix B.1.1). It can be shown using the polar decomposition theorem (MH, p.8) that this condition holds if and only if for some auxiliary strain-energy function V we can write

$$W(\mathbf{x},\mathbf{F}) = V(\mathbf{x},\mathbf{C})\,, \tag{3.41}$$

with the symmetric *right Cauchy–Green deformation tensor* defined to be

$$\mathbf{C} = \mathbf{F}^T\mathbf{F}. \tag{3.42}$$

Applying the chain rule to differentiate eq.(3.41), we arrive at an alternative expression for the first Piola-Kirchhoff stress in terms of V. It is readily established (see Appendix B.1.3) that

$$D_{\mathbf{F}}W(\mathbf{x},\mathbf{F}) = 2\mathbf{F}D_{\mathbf{C}}V(\mathbf{x},\mathbf{C})\,. \tag{3.43}$$

From this expression we are led to define the symmetric *second Piola-Kirchhoff stress tensor* (MH, p.196, Theorem 2.11)

$$\mathbf{S}(\mathbf{x},t) = 2D_{\mathbf{C}}V[\mathbf{x},\mathbf{C}(\mathbf{x},t)]\,. \tag{3.44}$$

Hence we obtain the identity

$$\mathbf{P} = \mathbf{F}\mathbf{S}. \tag{3.45}$$

A third useful stress tensor is the *Cauchy stress*, $\boldsymbol{\sigma}$. It relates the traction on a surface element at $\mathbf{y} \in \mathcal{B}_t$ to the surface's instantaneous unit-normal $\hat{\mathbf{n}}$. From this definition it can be shown (MH, p.135) that

$$\mathbf{P} = J(\boldsymbol{\sigma}\circ\boldsymbol{\varphi})\,\mathbf{F}^{-T}. \tag{3.46}$$

Although it is perhaps not obvious from this expression, the Cauchy stress is symmetric. Using eq.(3.45) we obtain (MH, p.136, Definition 2.8)

$$\boldsymbol{\sigma}\circ\boldsymbol{\varphi} = \frac{1}{J}\mathbf{F}\mathbf{S}\mathbf{F}^T, \tag{3.47}$$

and the symmetry of $\boldsymbol{\sigma}$ follows from that of $\mathbf{S}$.

3.2.1.3 Linearisation of the equations of motion

For seismological purposes it is generally sufficient to study linearised elastodynamics. We define an *equilibrium configuration* $\boldsymbol{\varphi}_e : \mathcal{B} \to \mathbb{R}^3$ to be a time-independent solution of the equations of motion subject to a time-independent body force $\mathbf{f}_e$ and surface traction $\mathbf{T}_e$. The resulting equilibrium first Piola-Kirchhoff stress is given by

$$\mathbf{P}_e(\mathbf{x}) = D_{\mathbf{F}}W[\mathbf{x},\mathbf{F}_e(\mathbf{x})]\,, \tag{3.48}$$

where $\mathbf{F}_e = D_{\mathbf{x}}\boldsymbol{\varphi}_e$. Using eq.(3.45) and (3.47), the three equilibrium stress tensors are then related by

$$\mathbf{P}_e = \mathbf{F}_e\mathbf{S}_e = J_e(\boldsymbol{\sigma}_e\circ\boldsymbol{\varphi}_e)\,\mathbf{F}_e^{-T}. \tag{3.49}$$

If such a body is subject to a small disturbance from equilibrium, we can look for solutions of the form

$$\boldsymbol{\varphi}(\mathbf{x},t) = \boldsymbol{\varphi}_e(\mathbf{x}) + \epsilon\,\mathbf{u}(\mathbf{x},t) + \mathcal{O}\big(\epsilon^2\big)\,, \tag{3.50}$$

where $\mathbf{u}$ is the displacement vector and ϵ a dimensionless perturbation parameter. Under this ansatz the deformation gradient becomes

$$\mathbf{F}(\mathbf{x},t) = \mathbf{F}_e(\mathbf{x}) + \epsilon\,D_{\mathbf{x}}\mathbf{u}(\mathbf{x},t) + \mathcal{O}\big(\epsilon^2\big)\,, \tag{3.51}$$

while the first Piola-Kirchhoff stress expands to

$$\mathbf{P}(\mathbf{x},t) = \mathbf{P}_e(\mathbf{x}) + \epsilon\,\mathbf{A}(\mathbf{x}) \cdot D_{\mathbf{x}}\mathbf{u}(\mathbf{x},t) + \mathcal{O}(\epsilon^2), \tag{3.52}$$

where we have defined the *first elastic tensor* (MH, p.209, Proposition 4.4b)

$$\mathbf{A}(\mathbf{x}) = D^2_{\mathbf{F}} W[\mathbf{x}, \mathbf{F}_e(\mathbf{x})]\,. \tag{3.53}$$

Note that the first elastic tensor possesses the so-called hyperelastic symmetry,

$$\mathbf{A}^T = \mathbf{A}, \tag{3.54}$$

due to the equality of mixed partial derivatives. In index notation this relationship takes the familiar form $\mathsf{A}_{ijkl} = \mathsf{A}_{klij}$. We will henceforward follow standard seismological terminology and refer to $\mathbf{A}$ simply as "the elastic tensor" unless that is likely to cause confusion.

As shown by eq.(4.248), the elastic tensor completely describes the linearised constitutive behaviour of the body. In particular, at a point $\mathbf{x} \in \mathcal{B}$ there will be three possible elastic wave speeds in the direction of the unit vector $\hat{\mathbf{p}}$. These wave speeds, c, are determined through the eigenvalue problem (e.g. Dahlen & Tromp, 1998, Section 3.6.3)

$$\mathbf{B}(\mathbf{x}, \hat{\mathbf{p}}) \cdot \mathbf{a} = c^2 \mathbf{a}, \tag{3.55}$$

where $\mathbf{a}$ is the corresponding polarisation vector, and the Christoffel matrix has components

$$B_{ik}(\mathbf{x}, \hat{\mathbf{p}}) = \frac{1}{\rho(\mathbf{x})} \mathsf{A}_{ijkl}(\mathbf{x}) \hat{p}_j \hat{p}_l. \tag{3.56}$$

This matrix is symmetric due to eq.(3.54), hence the c^2 are real. Within an elastic solid it is conventionally assumed that these squared wave speeds are positive, a necessary condition for well-posedness of the linearised equations of motion (e.g. Marsden & Hughes, 1994). As the propagation direction $\hat{\mathbf{p}}$ varies over the unit two-sphere, the three positive wave-speeds define the so-called *slowness surface* at $\mathbf{x}$. In general, this surface will be comprised of three distinct sheets, though they can sometimes touch due to degenerate eigenvalues within eq.(3.55).

Finally, it is useful to express the elastic tensor in terms of the auxiliary strain-energy function

V. We define the equilibrium second Piola-Kirchhoff stress as

$$\mathbf{S}_e(\mathbf{x}) = 2D_{\mathbf{C}}V[\mathbf{x}, \mathbf{C}_e(\mathbf{x})]\,, \tag{3.57}$$

and introduce the *second elastic tensor* (MH, p.209, Proposition 4.4a)

$$\mathbf{C}(\mathbf{x}) = 4D^2_{\mathbf{C}}V[\mathbf{x}, \mathbf{C}_e(\mathbf{x})]\,. \tag{3.58}$$

Suppressing all spatial arguments to avoid clutter, it then follows from the results of Appendix B.1.3 (see also MH, p.209, Proposition 4.5) that

$$\mathsf{A} = \mathsf{L}_{\mathbf{F}_e}\mathsf{C}\,\mathsf{L}^T_{\mathbf{F}_e} + \mathsf{R}_{\mathbf{S}_e}. \tag{3.59}$$

It is worth emphasising that the tensor C has the full set of classical elastic symmetries,

$$\mathsf{C}_{ijkl} = \mathsf{C}_{jikl} = \mathsf{C}_{ijlk} = \mathsf{C}_{klij}, \tag{3.60}$$

due to the symmetry of $\mathbf{C}_e$, and so possesses at most 21 independent components.

3.2.2 Transformation of the reference configuration

The motion of an elastic body has been described relative to a fixed reference configuration involving material parameters ρ and W. The same body can, of course, be described using a different choice of reference configuration, and it is natural to ask how the two points of view are related. This question was discussed by Al-Attar & Crawford (2016) and Al-Attar et al. (2018); here we simply recall the results relevant to this work.

3.2.2.1 Particle-relabelling

Let $\boldsymbol{\varphi} : \mathcal{B}\times\mathbb{R} \to \mathbb{R}$ denote the motion of an elastic body relative to a given reference configuration. The same motion relative to a different reference configuration will be written $\tilde{\boldsymbol{\varphi}} : \tilde{\mathcal{B}} \times \mathbb{R} \to \mathbb{R}$, where $\tilde{\mathcal{B}}$ is the associated reference body that will not, in general, be equal to $\mathcal{B}$. At a time t, the particle labelled by $\mathbf{x} \in \mathcal{B}$ lies at the point $\boldsymbol{\varphi}(\mathbf{x}, t)$ in physical space. Relative to the second description of the motion, there must be a unique point $\tilde{\mathbf{x}} \in \tilde{\mathcal{B}}$ such that

$$\boldsymbol{\varphi}(\mathbf{x}, t) = \tilde{\boldsymbol{\varphi}}(\tilde{\mathbf{x}}, t). \tag{3.61}$$

This correspondence between $\mathbf{x}$ and $\tilde{\mathbf{x}}$ holds for all times, defining a mapping $\boldsymbol{\xi} : \tilde{\mathcal{B}} \to \mathcal{B}$ that relates the two motions through

$$\boldsymbol{\varphi}(\mathbf{x}, t) = \tilde{\boldsymbol{\varphi}}[\boldsymbol{\xi}(\tilde{\mathbf{x}}), t]. \tag{3.62}$$

It is assumed for simplicity that $\boldsymbol{\xi}$ is smooth and has a smooth inverse. Under such a *particle relabelling transformation* the form of the equations of motion is clearly left unchanged, while it was shown by Al-Attar & Crawford (2016) that the material parameters $\tilde{\rho}$ and $\tilde{W}$ relative to the

second reference configuration can be obtained from those in the first by

$$\tilde{\rho}(\tilde{\mathbf{x}}) = J_{\boldsymbol{\xi}}(\tilde{\mathbf{x}})\, \rho[\boldsymbol{\xi}(\tilde{\mathbf{x}})], \tag{3.63}$$

$$\tilde{W}(\tilde{\mathbf{x}}, \tilde{\mathbf{F}}) = J_{\boldsymbol{\xi}}(\tilde{\mathbf{x}})\, W[\boldsymbol{\xi}(\tilde{\mathbf{x}})\,, \tilde{\mathbf{F}}\, \mathbf{F}_{\boldsymbol{\xi}}(\tilde{\mathbf{x}})^{-1}], \tag{3.64}$$

where $\mathbf{F}_{\boldsymbol{\xi}} = D\boldsymbol{\xi}$ and $J_{\boldsymbol{\xi}} = \det \mathbf{F}_{\boldsymbol{\xi}}$.

3.2.2.2 Natural reference configurations

When considering linearised motions of an elastic body it is conventional to select the reference configuration so that the equilibrium configuration takes the simple form

$$\boldsymbol{\varphi}_e(\mathbf{x}) = \mathbf{x}. \tag{3.65}$$

In this manner, the label for each particle is simply its position in physical space at equilibrium. In the terminology of Al-Attar & Crawford (2016), such a reference configuration is said to be *natural*. The equilibrium deformation gradient then satisfies

$$\mathbf{F}_e(\mathbf{x}) = \mathbf{1}, \tag{3.66}$$

while its Jacobian is everywhere equal to one. Given this choice, the equilibrium first Piola-Kirchhoff stress is obtained by evaluating the first derivative of the strain-energy at the identity:

$$\mathbf{P}_e = D_{\mathbf{F}} W(\cdot, \mathbf{1})\,. \tag{3.67}$$

An attractive feature of natural reference configurations is that the distinction between the different equilibrium stress-tensors vanishes. It is trivial to verify that equation (3.49) now reads

$$\mathbf{P}_e = \mathbf{S}_e = \boldsymbol{\sigma}_e. \tag{3.68}$$

In particular, it follows that

$$\boldsymbol{\sigma}_e = D_{\mathbf{F}} W(\cdot, \mathbf{1}) = 2 D_{\mathbf{C}} V(\cdot, \mathbf{1})\,, \tag{3.69}$$

an expression we will dissect in Section 3.3.

In the same manner, the elastic tensor takes the simpler form

$$\mathsf{a} = D^2_{\mathbf{F}} W(\cdot, \mathbf{1})\,, \tag{3.70}$$

which, from eq.(B.50), can be written equivalently as

$$\mathsf{a} = \mathsf{c} + \mathsf{R}_{\boldsymbol{\sigma}_e}. \tag{3.71}$$

Note that we have denoted the first and second elastic tensors by lower-case a and c. This is a notational convention used by Marsden & Hughes, the aim of which is to emphasise that these

elastic tensors are defined with respect to (what is here termed) a natural reference configuration. As noted above, the tensor

$$\mathsf{c} = 4D^2_{\mathbf{C}}V(\cdot, \mathbf{1}) \tag{3.72}$$

possesses all the classical elastic symmetries. In contrast, the second term in eq.(3.71) has components

$$[\mathsf{R}_{\boldsymbol{\sigma}_e}]_{ijkl} = \delta_{ik}[\boldsymbol{\sigma}_e]_{jl} \tag{3.73}$$

which, for general $\boldsymbol{\sigma}_e \neq \mathbf{0}$, are not invariant under the interchange of either $i \leftrightarrow j$ or $k \leftrightarrow l$ (although the symmetry of $\boldsymbol{\sigma}_e$ ensures that $\mathsf{R}_{\boldsymbol{\sigma}_e}$ possesses the hyperelastic symmetry). We therefore see that a inherits the full complement of classical symmetries *only with respect to a stress-free natural reference configuration.* Moreover, it is only with respect to a natural reference configuration that the propagation directions $\hat{\mathbf{p}}$ within eq.(3.55) can be equated with directions in physical space, allowing the slowness surface to be interpreted in a straightforward manner. Eq.(3.71) is precisely equivalent to eq.(3.2), though it is important to note that this equivalence only holds with respect to a natural reference configuration.

3.2.3 Material symmetries

We end our review of finite elasticity theory by discussing material symmetries. These results can be found in MH (Chapter 3, Section 3.5) and Gurtin et al. (2010, Chapter 50), though we place additional emphasis on certain points.

Relative to a fixed reference configuration, the *material symmetry group* of a strain-energy function W at a point $\mathbf{x} \in \mathcal{B}$ is

$$\mathrm{Sym}(W, \mathbf{x}) = \{\mathbf{Q} \in \mathbf{SL}(3) \,|\, W(\mathbf{x}, \mathbf{FQ}) = W(\mathbf{x}, \mathbf{F}),\ \forall \mathbf{F} \in \mathbf{GL}(3)\}\,, \tag{3.74}$$

where $\mathbf{SL}(3)$ denotes the special linear group on $\mathbb{R}^3$ whose definition is recalled in Appendix B.1.1. Physically, the symmetry group reflects the invariance of the strain-energy with respect to orientation of stretching. Following Noll (1974), the body is said to be fluid at a point if the symmetry group is equal to $\mathbf{SL}(3)$, and solid if it is a proper subgroup thereof.

Under a change of reference configuration, the symmetry group is not generally invariant. To see this, let $\boldsymbol{\xi} : \tilde{\mathcal{B}} \to \mathcal{B}$ be a particle relabelling transformation, and suppose that $\boldsymbol{\xi}(\tilde{\mathbf{x}}) = \mathbf{x}$. If $\tilde{\mathbf{Q}} \in \mathrm{Sym}(\tilde{W}, \tilde{\mathbf{x}})$ then from eq.(3.64) we obtain

$$W[\mathbf{x}, \tilde{\mathbf{F}}\tilde{\mathbf{Q}}\mathbf{F}_{\boldsymbol{\xi}}(\tilde{\mathbf{x}})^{-1}] = W[\mathbf{x}, \tilde{\mathbf{F}}\mathbf{F}_{\boldsymbol{\xi}}(\tilde{\mathbf{x}})^{-1}] \tag{3.75}$$

for all $\tilde{\mathbf{F}} \in \mathbf{GL}(3)$. Hence for a unique $\mathbf{Q} \in \mathrm{Sym}(W, \mathbf{x})$ we have

$$\tilde{\mathbf{Q}}\mathbf{F}_{\boldsymbol{\xi}}(\tilde{\mathbf{x}})^{-1} = \mathbf{F}_{\boldsymbol{\xi}}(\tilde{\mathbf{x}})^{-1}\mathbf{Q}. \tag{3.76}$$

This establishes a group isomorphism between $\mathrm{Sym}(W, \mathbf{x})$ and $\mathrm{Sym}(\tilde{W}, \tilde{\mathbf{x}})$, which is given con-

cretely through matrix conjugation:

$$\mathrm{Sym}(W, \mathbf{x}) \ni \mathbf{Q} \mapsto \mathbf{F}_{\boldsymbol{\xi}}(\tilde{\mathbf{x}})^{-1}\mathbf{Q}\mathbf{F}_{\boldsymbol{\xi}}(\tilde{\mathbf{x}}) \in \mathrm{Sym}(\tilde{W}, \tilde{\mathbf{x}}). \tag{3.77}$$

This mapping leaves $\mathbf{SL}(3)$ invariant, hence our definitions of the material symmetry group itself and of an elastic fluid are sound. Noll (1965) showed that, up to this isomorphism, the largest proper subgroup of $\mathbf{SL}(3)$ is equal to the special orthogonal group $\mathbf{SO}(3)$. We can, therefore, define an elastic solid to be *isotropic* at a point if its symmetry group relative to an arbitrary reference configuration is isomorphic under matrix conjugation to $\mathbf{SO}(3)$. Equivalently, it is isotropic if for *some* reference configuration its symmetry group is equal to $\mathbf{SO}(3)$. If the symmetry group is isomorphic to a proper subgroup of $\mathbf{SO}(3)$ we say the solid is *anisotropic*, with the extreme case being when this group consists of the identity matrix alone. In between these two end-members can be found, for example, *transversely-isotropic* materials, whose symmetry group is isomorphic under matrix conjugation to $\mathbf{SO}(2)$. This corresponds physically to the strain-energy being invariant under rotations about a certain fixed axis.

Importantly, the preceding discussion is independent of any particular choice of reference configuration. It corrects a mistake of Al-Attar & Crawford (2016), who implied that material symmetries can be lost or gained through particle relabelling transformations. Such transformations simply represent a change in our description of the body's deformation. They cannot entail any physical consequences.

As a final concept that we will need later, consider a natural reference configuration for a *stress-free* elastic body in equilibrium. Such a configuration is defined by $DV(\mathbf{C}^*) = \mathbf{0}$ with $\mathbf{C}^* = \mathbf{1}$. From eq.(3.74), the material symmetry group acts on $\mathbf{C}$ according to $\mathbf{C} \mapsto \mathbf{Q}^T\mathbf{C}\mathbf{Q}$, so by definition we have

$$V\big(\mathbf{Q}^T\mathbf{C}^*\mathbf{Q}\big) = V(\mathbf{C}^*)\,, \tag{3.78}$$

from which

$$V\big(\mathbf{Q}^T\mathbf{Q}\big) = V(\mathbf{1})\,. \tag{3.79}$$

For the equilibrium to be stable, $\mathbf{C}^* = \mathbf{1}$ must lie at a strict local minimum of the strain-energy function. This allows us to equate the arguments of the left and right hand sides of eq.(3.79). The elements of the symmetry group then satisfy

$$\mathbf{Q}^T\mathbf{Q} = \mathbf{1}, \tag{3.80}$$

from which it is clear that $\mathbf{Q} \in \mathbf{SO}(3)$. The symmetry group of a stress-free elastic body, described with respect to a natural reference configuration, is therefore *equal* to a subgroup of $\mathbf{SO}(3)$ rather than just isomorphic thereto. For example, in the stress-free case an isotropic body in a natural reference configuration has a material symmetry group equal to the whole of $\mathbf{SO}(3)$, while that of a transversely-isotropic material is equal to $\mathbf{SO}(2)$, having fixed the orientation of the symmetry-axis.

3.3 Functional dependence of the elastic tensor on equilibrium stress

Having recalled the necessary results and notations from the theory of elasticity, we now turn to our main question. Namely, we seek to determine the functional dependence of the elastic tensor on the equilibrium Cauchy stress.

3.3.1 Parametrised dependence on the equilibrium configuration

For an equilibrium body $\mathcal{B}$, the equilibrium Cauchy stress and elastic tensor take the form

$$\boldsymbol{\sigma}(\mathbf{x}) = DW(\mathbf{x}, \mathbf{1}) \tag{3.81a}$$

$$\mathbf{a}(\mathbf{x}) = D^2W(\mathbf{x}, \mathbf{1})\,, \tag{3.81b}$$

where W is the strain-energy function with respect to a natural reference configuration, and for notational simplicity we have dropped the subscript from $\boldsymbol{\sigma}_e$. Our hope is to express the elastic tensor as a function of the equilibrium stress. Variations in $\boldsymbol{\sigma}$ arise, of course, though changes to the equilibrium configuration, but the dependence of eqs.(3.81) thereon is masked by the use of a natural reference configuration. As a first step, we must reformulate eqs.(3.81) in a way that makes fully explicit the dependence of the two equations on the equilibrium configuration.

We consider an arbitrary fixed reference configuration with the associated reference body denoted by $\tilde{\mathcal{B}}$, and with strain-energy function $\tilde{W}$. The correspondence between this reference configuration and the natural reference configuration $\mathcal{B}$ is given by a mapping

$$\boldsymbol{\Phi} : \tilde{\mathcal{B}} \to \mathcal{B}. \tag{3.82}$$

This is just the equilibrium configuration of the body relative to our newly introduced reference configuration (see Fig. 3.3). Regarding the inverse mapping $\boldsymbol{\Phi}^{-1}$ as a particle relabelling transformation, we can use eq.(3.64) to relate W to $\tilde{W}$:

$$W\big[\boldsymbol{\Phi}(\tilde{\mathbf{x}}), \mathbf{F}'\big] = J_{\mathbf{F}}(\tilde{\mathbf{x}})^{-1}\tilde{W}\big[\tilde{\mathbf{x}}, \mathbf{F}'\mathbf{F}(\tilde{\mathbf{x}})\big]\,. \tag{3.83}$$

To avoid cluttered notations here and in what follows, we write $\mathbf{F}$ for the equilibrium deformation gradient $D\boldsymbol{\Phi}$ and $J_{\mathbf{F}} = \det \mathbf{F}$, while $\mathbf{F}'$ represents an arbitrary element of $\mathbf{GL}(3)$. From eq.(3.83) we see that $W[\boldsymbol{\Phi}(\tilde{\mathbf{x}}), \cdot]$ depends only on $\tilde{W}$ at the fixed point $\tilde{\mathbf{x}} \in \tilde{\mathcal{B}}$. Furthermore, the relationship is parametrised by $\mathbf{F}$ *evaluated at* $\tilde{\mathbf{x}}$. All in all, the two functions are related in a local manner; no generality is lost by focusing on a single, arbitrary point in $\mathcal{B}$ and its pre-image in $\tilde{\mathcal{B}}$. We do this from now on, dropping all spatial arguments to arrive at the simpler relations

$$\boldsymbol{\sigma} = DW(\mathbf{1}) \tag{3.84a}$$

$$\mathbf{a} = D^2W(\mathbf{1}) \tag{3.84b}$$

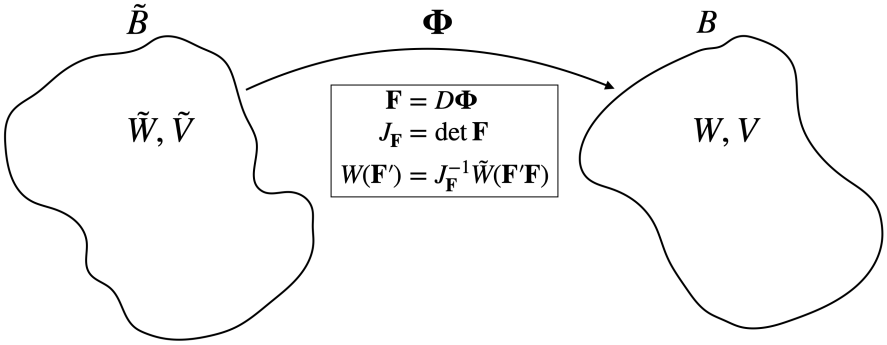

Figure 3.3: The setup of our problem. The reference body $\tilde{\mathcal{B}}$, with fixed elastic properties, is considered to be a reference configuration for the equilibrium body $\mathcal{B}$. The two bodies are related by the equilibrium-mapping $\mathbf{\Phi}$, permitting us to use particle-relabelling transformations to write the strain-energy function W in terms of $\tilde{W}$.

and

$$W\big(\mathbf{F}'\big) = J_{\mathbf{F}}^{-1}\tilde{W}\big(\mathbf{F}'\mathbf{F}\big)\,. \tag{3.85}$$

To complete the reformulation of eqs.(3.84) we apply the chain rule to eq.(3.85) so as to write $\boldsymbol{\sigma}$ and $\mathbf{a}$ explicitly in terms of $\tilde{W}$ and $\mathbf{F}$. It is in fact preferable to work not with W, but rather with the auxiliary strain-energy function V that encodes material-frame indifference automatically. Defining $\mathbf{C}' = (\mathbf{F}')^T\mathbf{F}'$, we recall that V will satisfy

$$W\big(\mathbf{F}'\big) = V\big(\mathbf{C}'\big)\,, \tag{3.86}$$

and from eqs. (3.85) and (3.86) we see that the relationship between V in $\mathcal{B}$ and its counterpart $\tilde{V}$ in $\tilde{\mathcal{B}}$ is given by

$$V(\mathbf{C}') = J_{\mathbf{F}}^{-1}\tilde{V}(\mathsf{T}_{\mathbf{F}}^T \cdot \mathbf{C}'), \tag{3.87}$$

where the operator $\mathsf{T}_{\mathbf{F}}$ is defined in eq.(B.20). From Appendix B.1.3 we have

$$DW(\mathbf{F}') = 2\mathsf{L}_{\mathbf{F}'} \cdot DV(\mathbf{C}') \tag{3.88}$$

$$D^2W\big(\mathbf{F}'\big) = 2\mathsf{R}_{DV(\mathbf{C}')} + 4\mathsf{L}_{\mathbf{F}'}D^2V\big(\mathbf{C}'\big)\ \mathsf{L}_{\mathbf{F}'}^T, \tag{3.89}$$

and it is readily shown from eq.(3.87) that

$$DV\big(\mathbf{C}'\big) = \mathsf{T}_{\mathbf{F}} \cdot D\tilde{V}(\mathsf{T}_{\mathbf{F}}^T \cdot \mathbf{C}') \tag{3.90}$$

$$D^2V\big(\mathbf{C}'\big) = \mathsf{T}_{\mathbf{F}}D^2\tilde{V}(\mathsf{T}_{\mathbf{F}}^T \cdot \mathbf{C}')\mathsf{T}_{\mathbf{F}}^T. \tag{3.91}$$

Evaluating these results at $\mathbf{C}' = \mathbf{1}$ – and noting that $\mathsf{T}_{\mathbf{F}}^T \cdot \mathbf{1} = \mathbf{C}$ – we obtain the first of our

desired expressions,

$$\boldsymbol{\sigma} = 2J_{\mathbf{F}}^{-1}\mathbf{T}_{\mathbf{F}} \cdot D\tilde{V}(\mathbf{C}). \tag{3.92}$$

Note that it is equivalent to eq.(3.47) but has been restated in a different notation. By considering the second derivative we then obtain the expression

$$\mathbf{a} = 4J_{\mathbf{F}}^{-1}\mathbf{T}_{\mathbf{F}} D^2\tilde{V}(\mathbf{C})\, \mathbf{T}_{\mathbf{F}}^T + \mathbf{R}_{\boldsymbol{\sigma}}, \tag{3.93}$$

which is equivalent to the expression of MH (p.217, Box 4.1). We have thus expressed both the equilibrium Cauchy stress and the elastic tensor as explicit functions of $\mathbf{F}$, the equilibrium deformation gradient relative to the fixed reference configuration $\tilde{\mathcal{B}}$. To emphasise this point we introduce the notation

$$\boldsymbol{\sigma} = \hat{\boldsymbol{\sigma}}(\mathbf{F}) \equiv 2J_{\mathbf{F}}^{-1}\mathbf{T}_{\mathbf{F}} \cdot D\tilde{V}(\mathbf{C}) \tag{3.94a}$$

$$\mathbf{a} = \hat{\mathbf{a}}(\mathbf{F}) \equiv 4J_{\mathbf{F}}^{-1}\mathbf{T}_{\mathbf{F}} D^2\tilde{V}(\mathbf{C})\, \mathbf{T}_{\mathbf{F}}^T + \mathbf{R}_{\hat{\boldsymbol{\sigma}}(\mathbf{F})}, \tag{3.94b}$$

with $\hat{\boldsymbol{\sigma}}$ (resp. $\hat{\mathbf{a}}$) the function that takes an equilibrium deformation gradient to the corresponding equilibrium Cauchy stress (resp. elastic tensor). It is worth observing that both of these relations are nonlinear for any non-trivial choice of strain-energy function $\tilde{V}$.

Through eqs.(3.94) one can consider a wide variety of problems where a body's elastic properties change as a result of changing its equilibrium configuration. Tromp et al. (2019, Section 4) studied just such a problem when they performed their *ab initio* calculations: the (unstrained) sample was subjected to a known strain, and this induced both an incremental Cauchy stress and a change in the elastic tensor. On a more seismological level (e.g. Tromp & Trampert, 2018) one might wish to understand how a given deformation of one of the Earth's regions affects seismic wave propagation and stresses therein. Such a deformation could result from small-scale phenomena such as a cave-in within a gas field, or from large-scale effects like tidal loading. The important feature common to all these problems is that there is a known initial state $\tilde{\mathcal{B}}$ that is deformed in a prescribed way. This produces a new state $\mathcal{B}$ whose elastic properties are fully determined in terms of those of $\tilde{\mathcal{B}}$ by eqs.(3.94). As long as $\tilde{V}$ and its derivatives are well-behaved the computations necessitated by these problems can in principle be performed readily. Note that to solve these problems there is in fact no need to find the stress dependence of the elastic tensor.

3.3.2 Parametrised dependence on equilibrium stress

Seismic inverse theory leads one to a subtly different problem. Say that we wish to study the equilibrium elastic properties of a certain region within the deep Earth as the equilibrium configuration evolves, and that we would particularly like to know about the equilibrium stress. We measure that region's properties using seismic data: we make surface observations of (small-amplitude, high-frequency) seismic waves that have passed through the region's neighbourhood, construct seismograms, and then use those seismograms to invert for the elastic tensor $\mathbf{a}$ of

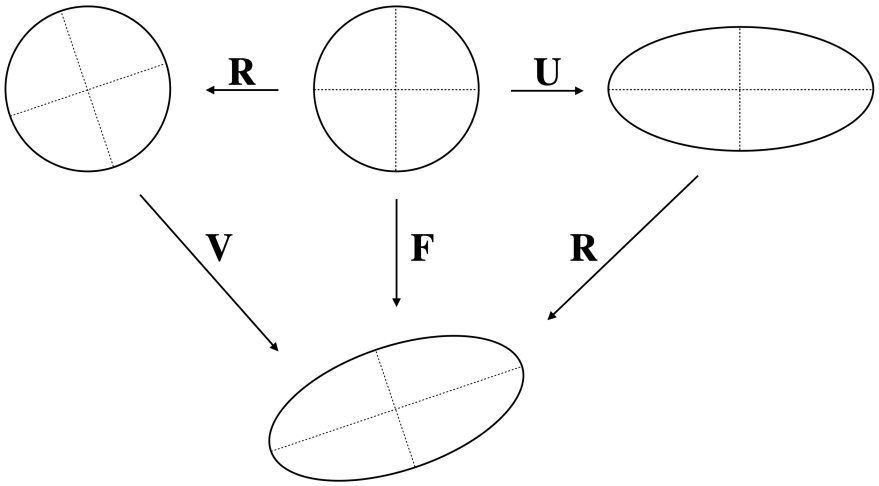

Figure 3.4: The polar decomposition theorem. An arbitrary element $\mathbf{F}$ of $\mathbf{GL}(3)$ can be decomposed as $\mathbf{RU}$, corresponding to a stretch followed by a rotation, or vice versa as $\mathbf{VR}$. Note that $\mathbf{U}$ and $\mathbf{V}$ represent stretches along different principal axes.

the region. Importantly, the equilibrium stress $\boldsymbol{\sigma}$ cannot be measured "directly" in this way. However, if we knew the stress dependence of the elastic tensor, we would be able to invert *changes* in $\mathbf{a}$ for *changes* in $\boldsymbol{\sigma}$ as the equilibrium configuration evolves. Our task is therefore to find $\mathbf{a}$ as an explicit function of $\boldsymbol{\sigma}$. Eqs.(3.94) provide the necessary link between $\mathbf{a}$ and $\boldsymbol{\sigma}$, but it is not yet in a useful form, parametrised as it is by $\mathbf{F}$. Unlike in the previous problem, $\mathbf{F}$ cannot be regarded as a known quantity because it could only ever be "measured" by inverting seismic data for $\mathbf{a}$ and then using eq.(3.94b) to invert for $\mathbf{F}$. Given this, we will eliminate $\mathbf{F}$ from eqs.(3.94) and ask only how $\mathbf{a}$ varies upon varying $\boldsymbol{\sigma}$. The mathematical problem we are trying to solve can be couched most succinctly (with reference to Figure 3.3) as follows: if we observe a given $\boldsymbol{\sigma}$ in $\mathcal{B}$, assume that $\boldsymbol{\sigma}$ was induced by elastically deforming $\tilde{\mathcal{B}}$, and parametrise the properties of $\tilde{\mathcal{B}}$ by choosing a specific form of $\tilde{V}$, what elastic tensor $\mathbf{a}$ will be observed in $\mathcal{B}$?

The ideal approach to this second problem appears to be to find $\mathbf{F}$ as a function of $\boldsymbol{\sigma}$ from eq.(3.94a), and then substitute the result into eq.(3.94b) to give $\mathbf{a}$ as a function of $\boldsymbol{\sigma}$. However, a given equilibrium Cauchy stress can be produced by many different deformation gradients, so there is rather a conspicuous mathematical problem. The function $\hat{\boldsymbol{\sigma}}$ maps elements in the nine-dimensional group $\mathbf{GL}(3)$ into the six-dimensional vector space of symmetric matrices on $\mathbb{R}^3$, which means that the equation $\hat{\boldsymbol{\sigma}}(\mathbf{F}) = \boldsymbol{\sigma}$ for $\mathbf{F}$ is underdetermined. How might we "invert" $\hat{\boldsymbol{\sigma}}$ for $\mathbf{F}$ when $\boldsymbol{\sigma}$ only provides us with six numbers? What does this underdetermination imply for the elastic tensor? A way into the problem is to recall the *polar decomposition theorem* (MH, p.3; see also Fig. 3.4), which shows that any $\mathbf{F} \in \mathbf{GL}(3)$ can be written as

$$\mathbf{F} = \mathbf{RU} = \mathbf{VR}, \tag{3.95}$$

for unique $\mathbf{R} \in \mathbf{SO}(3)$ and where $\mathbf{U}$ and $\mathbf{V}$ are unique, symmetric, positive-definite matrices. The theorem is a rigorous demonstration that any deformation gradient can be considered as "stretch followed by rotation" (the first equality) or "rotation followed by stretch" (the second). It

thus provides a natural way of factoring the deformation gradient into the product of a rotation matrix and a symmetric matrix. Crucially, $\mathbf{U}$ and $\boldsymbol{\sigma}$ have the same dimensions. Our goal now becomes to investigate how far $\mathbf{R}$ and $\mathbf{U}$ "interact" and whether or not $\hat{\boldsymbol{\sigma}}$ can in some sense be inverted for $\mathbf{U}$. To fully resolve the issue we must examine carefully how the principle of material-frame indifference and material symmetries manifest within eqs.(3.94).

Material-frame indifference concerns the behaviour of the strain-energy function and related quantities under transformations of the deformation gradient of the form $\mathbf{F} \mapsto \mathbf{RF}$ with $\mathbf{R} \in \mathbf{SO}(3)$. Recalling that the value of the right Cauchy–Green deformation tensor is invariant under such a transformation, and using eq.(B.23), we see immediately from eqs.(3.94) that

$$\hat{\boldsymbol{\sigma}}(\mathbf{RF}) = \mathsf{T}_{\mathbf{R}} \cdot \hat{\boldsymbol{\sigma}}(\mathbf{F}) \tag{3.96a}$$

$$\hat{\mathbf{a}}(\mathbf{RF}) = \mathsf{T}_{\mathbf{R}} \hat{\mathbf{a}}(\mathbf{F})\, \mathsf{T}_{\mathbf{R}}^{T} \tag{3.96b}$$

for all $\mathbf{R} \in \mathbf{SO}(3)$. Substituting the polar decomposition $\mathbf{F} = \mathbf{RU}$ into eqs.(3.94) and making use of eqs.(3.96) we then obtain

$$\hat{\boldsymbol{\sigma}}(\mathbf{F}) = \mathsf{T}_{\mathbf{R}} \cdot \hat{\boldsymbol{\Sigma}}(\mathbf{U}) \tag{3.97a}$$

$$\hat{\mathbf{a}}(\mathbf{F}) = \mathsf{T}_{\mathbf{R}} \hat{\mathbf{A}}(\mathbf{U})\, \mathsf{T}_{\mathbf{R}}^{T}, \tag{3.97b}$$

where we have defined the functions

$$\hat{\boldsymbol{\Sigma}}(\mathbf{U}) = 2J_{\mathbf{U}}^{-1} \mathsf{T}_{\mathbf{U}} \cdot D\tilde{V}\big(\mathbf{U}^2\big) \tag{3.98a}$$

$$\hat{\mathbf{A}}(\mathbf{U}) = 4J_{\mathbf{U}}^{-1} \mathsf{T}_{\mathbf{U}} D^2\tilde{V}\big(\mathbf{U}^2\big)\, \mathsf{T}_{\mathbf{U}} + \mathsf{R}_{\hat{\boldsymbol{\Sigma}}(\mathbf{U})}, \tag{3.98b}$$

whose arguments are *required* to be symmetric, positive-definite matrices. Importantly, the function $\hat{\boldsymbol{\Sigma}}$ maps symmetric matrices into symmetric matrices. As a result, there is no dimensional obstruction to its being invertible. We will assume that a unique inverse $\hat{\boldsymbol{\Sigma}}^{-1}$ exists wherever required, an assumption that is natural as long as the stress is not too large (see Appendix B.2).

We can now examine solutions of the equation $\hat{\boldsymbol{\sigma}}(\mathbf{F}) = \boldsymbol{\sigma}$ for given $\boldsymbol{\sigma}$. We write $\mathbf{F} = \mathbf{RU}$ as above, but now suppose that the value of $\mathbf{R} \in \mathbf{SO}(3)$ has been fixed arbitrarily. Using eq.(3.97a) we then trivially obtain

$$\mathbf{U} = \hat{\boldsymbol{\Sigma}}^{-1}\big(\mathsf{T}_{\mathbf{R}}^{T} \cdot \boldsymbol{\sigma}\big)\,, \tag{3.99}$$

whence it follows that the equilibrium deformation gradient is given by

$$\mathbf{F} = \hat{\mathbf{F}}(\boldsymbol{\sigma}, \mathbf{R}) \equiv \mathsf{L}_{\mathbf{R}} \cdot \hat{\boldsymbol{\Sigma}}^{-1}\big(\mathsf{T}_{\mathbf{R}}^{T} \cdot \boldsymbol{\sigma}\big)\,. \tag{3.100}$$

Here we see concretely where the missing three degrees of freedom enter into the inversion of $\hat{\boldsymbol{\sigma}}$. While eq.(3.100) constitutes *one* solution of the given equation, it is not unique. Letting $\mathbf{R}$ vary over $\mathbf{SO}(3)$ generates a three-parameter family of solutions, and the uniqueness of the polar decomposition means that every $\mathbf{R}$ must correspond to a different $\mathbf{F}$. Moreover, *any* $\mathbf{F}$ that solves $\hat{\boldsymbol{\sigma}}(\mathbf{F}) = \boldsymbol{\sigma}$ can be polar-decomposed and written in terms of $\boldsymbol{\sigma}$ using eq.(3.100), so we

have clearly obtained *all* solutions of the equation. Crucially, the non-uniqueness carries over into the elastic tensor. Substitution of eq.(3.100) into eq.(3.94b) yields

$$\mathsf{a} = \hat{\mathsf{a}}\Big[\hat{\mathbf{F}}(\boldsymbol{\sigma}, \mathbf{R})\Big] \equiv \bar{\mathsf{a}}(\boldsymbol{\sigma}, \mathbf{R})\,, \tag{3.101}$$

where the function $\bar{\mathsf{a}}$ can be written more expansively as

$$\bar{\mathsf{a}}(\boldsymbol{\sigma}, \mathbf{R}) = \mathsf{T}_{\mathbf{R}}\Big[\Big(\hat{\mathsf{A}} \circ \hat{\boldsymbol{\Sigma}}^{-1}\Big)\big(\mathsf{T}_{\mathbf{R}}^T \cdot \boldsymbol{\sigma}\big)\Big]\,\mathsf{T}_{\mathbf{R}}^T. \tag{3.102}$$

It follows that we cannot expect to write the elastic tensor as a function of the equilibrium Cauchy stress alone. A definite value for a depends on the arbitrary choice of an element of $\mathbf{SO}(3)$.

We can add some nuance to this result by considering material symmetries. Let $\mathrm{Sym}(\tilde{W})$ denote the material symmetry group (which could be trivial) at the point of interest, whose elements $\mathbf{Q}$ act on the deformation gradient on the right through $\mathbf{F} \mapsto \mathbf{FQ}$. In terms of the right Cauchy–Green deformation tensor such a transformation takes the form $\mathbf{C} \mapsto \mathbf{Q}^T\mathbf{C}\mathbf{Q} = \mathsf{T}_{\mathbf{Q}}^T \cdot \mathbf{C}$, and by definition we have

$$\tilde{V}(\mathsf{T}_{\mathbf{Q}}^T \cdot \mathbf{C}) = \tilde{V}(\mathbf{C}) \tag{3.103}$$

for all $\mathbf{Q} \in \mathrm{Sym}(\tilde{W})$. Differentiating this relation in the now standard manner yields

$$D\tilde{V}(\mathbf{C}) = \mathsf{T}_{\mathbf{Q}} \cdot D\tilde{V}\big(\mathsf{T}_{\mathbf{Q}}^T \cdot \mathbf{C}\big) \tag{3.104}$$

$$D^2\tilde{V}(\mathbf{C}) = \mathsf{T}_{\mathbf{Q}} D^2\tilde{V}\big(\mathsf{T}_{\mathbf{Q}}^T \cdot \mathbf{C}\big)\,\mathsf{T}_{\mathbf{Q}}^T. \tag{3.105}$$

Using the properties of $\mathsf{T}_{\mathbf{F}}$ we then find from eqs.(3.94) that

$$\hat{\boldsymbol{\sigma}}(\mathbf{FQ}) = 2J_{\mathbf{F}}^{-1}\mathsf{T}_{\mathbf{F}} \cdot \Big[\mathsf{T}_{\mathbf{Q}} \cdot D\tilde{V}\big(\mathsf{T}_{\mathbf{Q}}^T \cdot \mathbf{C}\big)\Big] \tag{3.106a}$$

$$\hat{\mathsf{a}}(\mathbf{FQ}) = 4J_{\mathbf{F}}^{-1}\mathsf{T}_{\mathbf{F}}\Big[\mathsf{T}_{\mathbf{Q}} D^2\tilde{V}\big(\mathsf{T}_{\mathbf{Q}}^T \cdot \mathbf{C}\big)\,\mathsf{T}_{\mathbf{Q}}^T\Big]\,\mathsf{T}_{\mathbf{F}}^T + \mathsf{R}_{\hat{\boldsymbol{\sigma}}(\mathbf{FQ})}, \tag{3.106b}$$

from which it readily follows that

$$\hat{\boldsymbol{\sigma}}(\mathbf{FQ}) = \hat{\boldsymbol{\sigma}}(\mathbf{F}) \tag{3.107a}$$

$$\hat{\mathsf{a}}(\mathbf{FQ}) = \hat{\mathsf{a}}(\mathbf{F}) \tag{3.107b}$$

for any $\mathbf{Q} \in \mathrm{Sym}(\tilde{W})$.

We can now understand $\bar{\mathsf{a}}$'s non-unique stress dependence by studying how the structure implied by eqs.(3.107) manifests within $\hat{\boldsymbol{\Sigma}}^{-1}$. To that end, it is simplest if we consider $\tilde{\mathcal{B}}$ to constitute a natural reference configuration for an equilibrium body that is stress-free. What follows is therefore based on the assumption that there exists *some* stress-free reference-configuration with respect to which we can describe $\mathcal{B}$. This way we can take $\mathrm{Sym}(\tilde{W})$ to be *equal*, rather than just isomorphic, to a subgroup of $\mathbf{SO}(3)$. Because all $\mathbf{Q} \in \mathrm{Sym}(\tilde{W})$ are then rotations, the material symmetry group acts through $(\mathbf{R}, \mathbf{U}) \mapsto (\mathbf{RQ}, \mathbf{Q}^T\mathbf{U}\mathbf{Q})$ on the level of the polar

decomposition. Therefore, using eq.(3.97a) we find that eq.(3.107a) requires

$$\hat{\boldsymbol{\Sigma}}(\mathsf{T}_{\mathbf{Q}} \cdot \mathbf{U}) = \mathsf{T}_{\mathbf{Q}} \cdot \hat{\boldsymbol{\Sigma}}(\mathbf{U}) \tag{3.108}$$

for arbitrary $\mathbf{Q} \in \mathrm{Sym}(\tilde{W})$. This equation expresses the intuitive notion that a stretch $\mathbf{U}$ and rotation $\mathbf{Q}$ will together induce the same stress no matter the order in which they are imposed – as long as $\mathbf{Q}$ is in the material symmetry group. In any case, by acting the inverse function $\hat{\boldsymbol{\Sigma}}^{-1}$ on this expression we obtain the analogous result

$$\hat{\boldsymbol{\Sigma}}^{-1}(\mathsf{T}_{\mathbf{Q}} \cdot \boldsymbol{\Sigma}) = \mathsf{T}_{\mathbf{Q}} \cdot \hat{\boldsymbol{\Sigma}}^{-1}(\boldsymbol{\Sigma}) \tag{3.109}$$

for arbitrary symmetric $\boldsymbol{\Sigma}$, which we may substitute into eq.(3.100) to conclude that

$$\begin{aligned}
\hat{\mathbf{F}}(\boldsymbol{\sigma}, \mathbf{RQ}) &= \mathsf{L}_{\mathbf{RQ}} \cdot \hat{\boldsymbol{\Sigma}}^{-1}(\mathsf{T}^T_{\mathbf{RQ}} \cdot \boldsymbol{\sigma}) \\
&= (\mathsf{L}_{\mathbf{R}}\mathsf{L}_{\mathbf{Q}}) \cdot \hat{\boldsymbol{\Sigma}}^{-1}[\mathsf{T}^T_{\mathbf{Q}} \cdot (\mathsf{T}^T_{\mathbf{R}} \cdot \boldsymbol{\sigma})] \\
&= (\mathsf{L}_{\mathbf{R}}\mathsf{L}_{\mathbf{Q}}\mathsf{T}^T_{\mathbf{Q}}) \cdot \hat{\boldsymbol{\Sigma}}^{-1}(\mathsf{T}^T_{\mathbf{R}} \cdot \boldsymbol{\sigma}) \\
&= \hat{\mathbf{F}}(\boldsymbol{\sigma}, \mathbf{R})\, \mathbf{Q}.
\end{aligned} \tag{3.110}$$

This relationship does not allow us to determine $\mathbf{F}$ any more precisely – it will *always* be known only up to an element of $\mathbf{SO}(3)$ – but we may trivially write

$$\hat{\mathbf{a}}\Big[\hat{\mathbf{F}}(\boldsymbol{\sigma}, \mathbf{RQ})\Big] = \hat{\mathbf{a}}\Big[\hat{\mathbf{F}}(\boldsymbol{\sigma}, \mathbf{R})\, \mathbf{Q}\Big]. \tag{3.111}$$

It follows immediately from eq.(3.107b) that

$$\hat{\mathbf{a}}\Big[\hat{\mathbf{F}}(\boldsymbol{\sigma}, \mathbf{RQ})\Big] = \hat{\mathbf{a}}\Big[\hat{\mathbf{F}}(\boldsymbol{\sigma}, \mathbf{R})\Big]. \tag{3.112}$$

Hence, using the notation of eq.(3.101), we have obtained the key identity

$$\bar{\mathbf{a}}(\boldsymbol{\sigma}, \mathbf{RQ}) = \bar{\mathbf{a}}(\boldsymbol{\sigma}, \mathbf{R}) \quad \forall \mathbf{Q} \in \mathrm{Sym}(\tilde{W}). \tag{3.113}$$

Eq.(3.113) implies that two distinct rotation matrices $\mathbf{R}, \mathbf{R}' \in \mathbf{SO}(3)$ will lead to the same elastic tensor via eq.(3.101) if $\mathbf{R}^T\mathbf{R}' \in \mathrm{Sym}(\tilde{W})$. It is readily verified that this defines an equivalence relation, meaning that $\mathbf{SO}(3)$ can be partitioned into distinct equivalence classes, with the resulting *quotient space* denoted by $\mathbf{SO}(3)/\mathrm{Sym}(\tilde{W})$. The function $\bar{\mathbf{a}}(\boldsymbol{\sigma}, \cdot)$ therefore depends not on the rotation matrix $\mathbf{R}$ directly, but only on the equivalence class in $\mathbf{SO}(3)/\mathrm{Sym}(\tilde{W})$ to which it belongs. In this manner the number of additional parameters required to fix a definite value of the elastic tensor can be reduced.

In summary, we have shown that it is possible to express the elastic tensor as a function of equilibrium stress, but only at the cost of introducing extra arbitrary parameters. Given our initial comments about the form of $\hat{\boldsymbol{\sigma}}$, the presence of these parameters is not surprising. After all, we were essentially trying to fix nine numbers knowing only six. What is pleasing is that we have been able to exploit material-frame indifference to 'package' these extra degrees of

freedom into a rotation matrix and write down a solution that is still well-defined. In addition, although our argument appeared at first to suggest that the rotation matrix was wholly arbitrary, we have shown that the presence of material symmetries can reduce the number of arbitrary parameters to be specified. On a physical level, we have shown formally that if one observes a given Cauchy stress in an arbitrary (hyperelastic) material, and assumes the material to have reached its present state by some elastic deformation from a prior state with known properties, it is generally impossible to "disentangle" the effects of the rotation- and stretch-components of the elastic deformation. As a consequence, one cannot in general construct the elastic tensor unambiguously.

3.3.3 Linearisation

In a geophysical context it will often be convenient to regard the total equilibrium Cauchy stress in the body $\mathcal{B}$ as some small perturbation to the equilibrium Cauchy stress of the reference-body $\tilde{\mathcal{B}}$. It is therefore useful to linearise expression (3.101), the calculations for which are laid out in Appendix B.3. We assume that there exists a zeroth-order equilibrium configuration $\tilde{\mathcal{B}}$ possessing Cauchy stress $\boldsymbol{\sigma}^0$ and elastic tensor $\mathsf{a}^0 = \mathsf{c}^0 + \mathsf{R}_{\boldsymbol{\sigma}^0}$. We can set $\mathbf{R}^0$ to the identity without loss of generality because this zeroth-order state is taken to be known.

We linearise the system about a small perturbing stress. With ϵ a small parameter, the stress is set to

$$\boldsymbol{\sigma} = \boldsymbol{\sigma}^0 + \epsilon\,\boldsymbol{\sigma}^1. \tag{3.114}$$

We must also linearise the rotation matrix of eq.(3.101). It is set to the identity at zeroth-order, so its perturbation satisfies

$$\mathbf{R} = \mathbf{1} + \epsilon\,\boldsymbol{\omega}^1 + \mathcal{O}\big(\epsilon^2\big)\,, \tag{3.115}$$

with $\boldsymbol{\omega}^1$ an antisymmetric matrix. Substituting these into eq.(3.101) and Taylor expanding, we may write

$$\mathsf{a} = \mathsf{a}^0 + \epsilon\,\mathsf{a}^1 + \mathcal{O}\big(\epsilon^2\big)\,. \tag{3.116}$$

The perturbed elastic tensor a^1 is decomposed as

$$\mathsf{a}^1 = \mathsf{c}^1 + \mathsf{R}_{\boldsymbol{\sigma}^1}, \tag{3.117}$$

consistent with eq.(3.71). Under these definitions, we show in Appendix B.3.1 that c^1 is given by

$$\mathsf{c}^1 = \mathsf{X}_{\mathbf{u}^1+\boldsymbol{\omega}^1}\mathsf{c}^0 + \mathsf{c}^0\mathsf{X}_{\mathbf{u}^1-\boldsymbol{\omega}^1} - \mathsf{c}^0\mathrm{tr}\big(\mathbf{u}^1\big) + 8D^3\tilde{V}(\mathbf{1})\cdot\mathbf{u}^1, \tag{3.118a}$$

where $\mathbf{u}^1$ is a symmetric matrix which satisfies a generalised linear stress-strain relationship

$$\boldsymbol{\sigma}^1 - \mathsf{X}_{\boldsymbol{\omega}^1}\cdot\boldsymbol{\sigma}^0 = \big(\mathsf{c}^0 + \overline{\mathsf{X}}_{\boldsymbol{\sigma}^0} - \boldsymbol{\sigma}^0\otimes\mathbf{1}\big)\cdot\mathbf{u}^1. \tag{3.118b}$$

In these expressions we have introduced the tensor product on matrices (eq.B.19) and the

notations $\mathbf{X}$ (eq.B.25) and $\overline{\mathbf{X}}$ (eq.B.32). Thus, in order to fully specify the perturbation to the elastic tensor we must provide:

(1). the perturbation to the stress, $\boldsymbol{\sigma}^1$;

(2). $\boldsymbol{\sigma}^0$ and $\mathbf{c}^0$, which encode information about the zeroth-order equilibrium body;

(3). further information about the zeroth-order equilibrium body, via the third derivatives of its strain-energy function at equilibrium;

(4). an arbitrary antisymmetric matrix $\boldsymbol{\omega}^1$.

Eqs.(3.118) is a general result whose derivation makes no particular demands on the form of the zeroth-order equilibrium configuration, but we can already make several observations. Firstly, no matter its functional form, $\mathbf{c}^1$ can be shown to possess all the classical elastic symmetries, as required by eq.(3.71). Secondly, given that it is explicitly linear in the stress-perturbation, this theory is superficially rather close to those of Dahlen (1972a), Dahlen & Tromp (1998), Tromp & Trampert (2018) and Tromp et al. (2019), discussed in Section 3.1. There are some important differences, though. For one, our linearised theory makes explicit reference to third derivatives of the strain-energy function at equilibrium. In fact, those third derivatives can be seen as parametrising the theory. Moreover, eqs.(3.118) are parametrised further by the arbitrary degrees of freedom associated with $\boldsymbol{\omega}^1$. One might imagine that terms in $\boldsymbol{\omega}^1$ would drop out when we compute, say, the Christoffel operator, so that it would have no effect on observable phenomena, but we show later, for the particular case of a transversely-isotropic material, that this does not happen. Lastly, it is trivial to show that the strain-energy function's third derivatives are fully specified by at most 56 numbers, so our parametrisation requires up to 59 (=56+3) numbers, more than Tromp et al.'s 21 but fewer than the 126 derived heuristically in Section 3.1. The relationship between the existing theories and this new linearised theory will become clearer as we consider some more concrete examples.

3.4 Examples

We now illustrate how the preceding results apply to a few different physical situations. We will consider both large and small stresses, making use of eqs.(3.118) for the latter. The examples discussed here are intended simply to illustrate the general behaviour implied by our theoretical results. For that reason we have used standard, simple strain-energy functions, and all physical quantities are presented suitably nondimensionalised. Henceforward, we will refer to the body $\mathcal{B}$ of the previous section simply as 'the equilibrium body'. We will describe the fixed reference body $\tilde{\mathcal{B}}$ as the *background body*, and similarly for all its associated quantities such as strain-energy function and material symmetry group. All calculations for the following examples were carried out in Mathematica 12. The scenarios involving large stress required numerical inversion of the nonlinear function $\hat{\boldsymbol{\Sigma}}$, for which we used Mathematica's inbuilt 'FindRoot' function.

3.4.1 Isotropic materials

We begin by considering isotropic, stress-free background bodies. In the isotropic special case $\boldsymbol{\sigma}$ alone provides a unique specification of $\mathbf{a}$. To see this, it is sufficient to return to the identity

$$\bar{\mathbf{a}}(\boldsymbol{\sigma}, \mathbf{R}) = \bar{\mathbf{a}}(\boldsymbol{\sigma}, \mathbf{RQ}) \,, \tag{3.119}$$

for some $\mathbf{R}$ and $\mathbf{Q}$ both in $\mathbf{SO}(3)$. By the standard group axioms we may write

$$\mathbf{Q} = \mathbf{R}^T \mathbf{R}', \tag{3.120}$$

where $\mathbf{R}'$ is another arbitrary element of $\mathbf{SO}(3)$, whence

$$\bar{\mathbf{a}}(\boldsymbol{\sigma}, \mathbf{R}) = \bar{\mathbf{a}}\big(\boldsymbol{\sigma}, \mathbf{R}'\big) \,. \tag{3.121}$$

The matrices $\mathbf{R}$ and $\mathbf{R}'$ are both arbitrary, so $\bar{\mathbf{a}}(\boldsymbol{\sigma}, \cdot)$ is independent of the choice of rotation matrix. When evaluating $\bar{\mathbf{a}}$ we may therefore set $\mathbf{R} = \mathbf{1}$ without loss of generality. The elastic tensor is then given conveniently by

$$\mathbf{a} = \bar{\mathbf{a}}(\boldsymbol{\sigma}, \mathbf{1}) \,. \tag{3.122}$$

This argument shows that all rotations are equivalent up to right multiplication by $\mathbf{SO}(3)$; in other words, the quotient space

$$\mathbf{SO}(3)/\mathrm{Sym}(\tilde{W}) = \mathbf{SO}(3)/\mathbf{SO}(3) \tag{3.123}$$

is a set which contains just one element. With these preliminaries we are in position to investigate the behaviour of isotropic materials under induced stress.

3.4.1.1 Exact response to deviatoric stress

The nonlinearity of expression (3.101) implies that a general material's response to induced stress is influenced by derivatives of the strain-energy function higher than second-order. We demonstrate this in Fig. 3.5, contrasting the slowness surfaces of two different isotropic materials under the same induced stress. The strain-energy functions describing the background bodies are (e.g. Holzapfel, 2000) *modified Saint-Venant Kirchhoff*,

$$\tilde{W}_{\mathrm{MSVK}}(\mathbf{F}) = \frac{\lambda}{2} \log^2 J + \frac{\mu}{4} \mathrm{tr}\Big([\mathbf{C} - \mathbf{1}]^2 \Big) \,, \tag{3.124}$$

and *neo-Hookean*,

$$\tilde{W}_{\mathrm{NH}}(\mathbf{F}) = \frac{\mu}{2} \left[\mathrm{tr}(\mathbf{C}) - 3 + \frac{2\mu}{\lambda} (J^{-\frac{\lambda}{\mu}} - 1) \right] , \tag{3.125}$$

where λ and μ are constants. The limit of vanishing induced stress is obtained in both cases by evaluating the background strain-energy functions and their derivatives at $\mathbf{F} = \mathbf{1}$. In that case

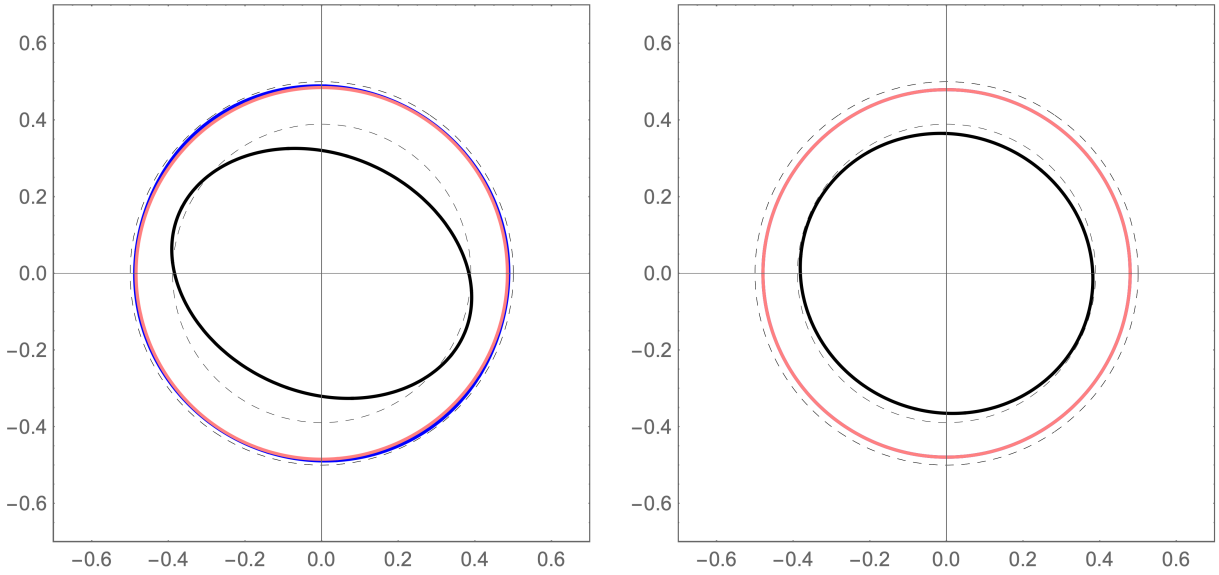

Figure 3.5: The behaviour of two different isotropic materials subject to the same induced stress. The left panel shows how a material governed by a modified Saint-Venant Kirchhoff strain-energy function reacts when a certain deviatoric stress of magnitude $\|\boldsymbol{\sigma}\| \sim \mu$ is induced. We plot the $x-y$ slowness surface, with the zero-stress slowness surface shown faintly for reference. P-waves and S-waves are both affected by the stress. We show the same on the right, but for a material governed by a neo-Hookean constitutive relation. Shear-waves are not noticeably split here and the P-wave response is muted. Thus, the two materials behave differently under stress, despite being indistinguishable in its absence.

the materials are indistinguishable, each possessing the classical isotropic elastic tensor

$$\mathsf{a}_{ijkl} = \mathsf{c}_{ijkl} = \lambda\delta_{ij}\delta_{kl} + \mu(\delta_{ik}\delta_{jl} + \delta_{il}\delta_{jk})\,. \tag{3.126}$$

Indeed, any strain-energy function that purports to describe an isotropic solid must give this result in the relevant limit. It is also apparent that λ and μ should be interpreted as the standard Lamé parameters. Under large induced stress, though, the strain-energy functions are evaluated away from the identity, meaning that third- and higher-order derivatives become relevant. As shown in Fig.3.5, where we have induced a deviatoric stress of magnitude $\|\boldsymbol{\sigma}\| \sim \mu$, the materials then display distinct behaviour.

3.4.1.2 Exact response to hydrostatic stress

When a hydrostatic pressure is induced in a stress-free, isotropic solid, its only effect on the elastic tensor is to change the elastic moduli. Here we derive exact expressions for λ and μ as functions of pressure. We return to eqs.(3.98) and write

$$\mathbf{U} = \phi\mathbf{1}, \tag{3.127}$$

for some positive scalar ϕ. Given that the system is isotropic and the induced stress hydrostatic, it follows from symmetry considerations and eq.(3.108) that $\mathbf{U}$ cannot take any other form. The deformation gradient itself can only ever be known up to an arbitrary rotation matrix, so it is

given by

$$\mathbf{F} = \mathbf{R}\mathbf{U} = \phi\mathbf{R}, \tag{3.128}$$

with $\mathbf{R} \in \mathbf{SO}(3)$, while the right Cauchy–Green deformation tensor is

$$\mathbf{C} = \phi^2\mathbf{1}. \tag{3.129}$$

This deformation gradient corresponds physically to a local compression or dilation of the background-body with a rotation superimposed; $\phi < 1$ effects a compression and vice versa. If the resulting equilibrium pressure in $\mathcal{B}$ is p, the Cauchy stress is $\boldsymbol{\sigma} = -p\mathbf{1}$, so from eqs. (3.94), (3.97) and (3.98)

$$-p\mathbf{1} = \frac{2}{\phi} D\tilde{V}\big(\phi^2\mathbf{1}\big) \tag{3.130a}$$

$$\mathsf{a} = 4\phi D^2\tilde{V}\big(\phi^2\mathbf{1}\big) + \mathsf{R}_{\boldsymbol{\sigma}}. \tag{3.130b}$$

We can set $\mathbf{R}$ to the identity in these expressions because the background material is isotropic (see eq.3.122).

Now, for the stress-free isotropic medium represented by $\tilde{\mathcal{B}}$, the strain-energy function $\tilde{V}$ is a function of the three *scalar invariants* of $\mathbf{C}$ (Holzapfel, 2000). Defining the scalar invariants as

$$I_i(\mathbf{C}) \equiv \mathrm{tr}\big(\mathbf{C}^i\big)\,, \quad i = 1, 2, 3, \tag{3.131}$$

we can write the strain-energy function as

$$\tilde{V}(\mathbf{C}) \equiv V\big[I_1(\mathbf{C})\,, I_2(\mathbf{C})\,, I_3(\mathbf{C})\big]\,. \tag{3.132}$$

From the chain rule, its first and second derivatives are

$$D\tilde{V} = \sum_i V_i\, DI_i \tag{3.133}$$

$$D^2\tilde{V} = \sum_{ij} V_{ij}\, DI_i \otimes DI_j + \sum_i V_i\, D^2 I_i, \tag{3.134}$$

where we have written the derivatives of V with respect to its arguments in an obvious way. When the derivatives are evaluated at $\mathbf{C} = \phi^2\mathbf{1}$, we will write e.g.

$$v_{13} = V_{13}\big[I_1\big(\phi^2\mathbf{1}\big),\, I_2\big(\phi^2\mathbf{1}\big),\, I_3\big(\phi^2\mathbf{1}\big)\big]\,, \tag{3.135}$$

and similarly for the other derivatives. With this, one finds after a little algebra that

$$-p\mathbf{1} = \frac{2}{\phi}\big(v_1 + 2v_2\phi^2 + 3v_3\phi^4\big)\,\mathbf{1} \tag{3.136a}$$

$$\begin{aligned}\mathsf{a} = 4\phi\big[&\big(v_{11} + 4v_{12}\phi^2 + (4v_{22} + 6v_{13})\,\phi^4 + 12v_{23}\phi^6 + 9v_{33}\phi^8\big)\,\mathbf{1}\otimes\mathbf{1} \\ &+ \big(2v_2 + 6v_3\phi^2\big)\,\overline{\mathsf{id}}\big] + \mathsf{R}_{\boldsymbol{\sigma}}.\end{aligned} \tag{3.136b}$$

where the operator $\overline{\mathbf{id}}$ has been defined in eq.(B.33) and has components

$$(\overline{\mathbf{id}})_{ijkl} = \frac{1}{2}(\delta_{ik}\delta_{jl} + \delta_{il}\delta_{jk})\,. \tag{3.137}$$

We identify the coefficients of the first two operators in the expression for $\mathbf{a}$ as the Lamé parameters, given as functions of ϕ, so we reach the equations

$$\lambda = 4\phi\big[v_{11} + 4v_{12}\phi^2 + (4v_{22} + 6v_{13})\,\phi^4 + 12v_{23}\phi^6 + 9v_{33}\phi^8\big] \tag{3.138a}$$

$$\mu = 4\phi\big(v_2 + 3v_3\phi^2\big)\,. \tag{3.138b}$$

ϕ is obtained as a function of p by inverting the relation

$$-p = \frac{2}{\phi}\big(v_1 + 2v_2\phi^2 + 3v_3\phi^4\big)\,, \tag{3.138c}$$

which would be performed numerically for a general strain-energy function. The Lamé parameters are then given as explicit functions of the equilibrium pressure, parametrised by the derivatives of V.

It is also useful to note that the form of $\mathbf{U}$ considered here, despite producing a stressed configuration from an unstressed one, does not alter the material symmetry group, $\mathrm{Sym}(\tilde{W}) = \mathbf{SO}(3)$. Material symmetry groups transform under a particle-relabelling transformation according to eq.(3.77), and with $\mathbf{F} = \phi\mathbf{R}$

$$\begin{aligned}\mathrm{Sym}(W) &= \Big\{\mathbf{F}^{-1}\mathbf{Q}\mathbf{F}, \mathbf{Q} \in \mathrm{Sym}(\tilde{W})\Big\}\\ &= \Big\{\mathbf{R}^T\mathbf{Q}\mathbf{R}, \mathbf{Q} \in \mathrm{Sym}(\tilde{W})\Big\}\\ &= \mathrm{Sym}(\tilde{W}).\end{aligned} \tag{3.139}$$

As expected on physical grounds, inducing a pressure in an isotropic body does not break the isotropy. All our conclusions from Section 3.3 therefore apply to an isotropic body even under hydrostatic stress. In particular, we can linearise about a hydrostatically stressed equilibrium given by $\mathbf{U} = \mathbf{1}$ (Appendix B.3.1) without having to refer the system back to some unstressed state.

3.4.1.3 Linearised response to small stress

Eqs.(3.118) simplify dramatically when we consider a small stress induced in a hydrostatically pre-stressed equilibrium. The total stress is written as

$$\boldsymbol{\sigma} = -p^0\mathbf{1} - p^1\mathbf{1} + \boldsymbol{\tau}^1, \tag{3.140}$$

with

$$\begin{aligned} p^1 &\ll p^0\\ \|\boldsymbol{\tau}^1\| &\ll p^0\\ \mathrm{tr}\big(\boldsymbol{\tau}^1\big) &= 0,\end{aligned} \tag{3.141}$$

and the complete elastic tensor is (Appendix B.3.2)

$$\mathsf{a}_{ijkl} = \left(\kappa - \frac{2}{3}\mu + p^1 c\right)\delta_{ij}\delta_{kl} + \big(\mu + p^1 d\big)\big(\delta_{ik}\delta_{jl} + \delta_{il}\delta_{jk}\big) - \big(p^0 + p^1\big)\,\delta_{ik}\delta_{jl} \\ + a\big(\delta_{ij}\tau^1_{kl} + \delta_{kl}\tau^1_{ij}\big) + b\big(\delta_{ik}\tau^1_{jl} + \delta_{jl}\tau^1_{ik} + \delta_{il}\tau^1_{jk} + \delta_{jk}\tau^1_{il}\big) + \delta_{ik}\tau^1_{jl}. \tag{3.142}$$

The constants a, b, c and d are defined to be

$$a = \frac{\kappa - \frac{2}{3}\mu + \frac{1}{2}\zeta_2}{\mu - p^0} \tag{3.143a}$$

$$b = \frac{\mu + \frac{1}{4}\zeta_3}{\mu - p^0} \tag{3.143b}$$

$$c = -\frac{\kappa - \frac{2}{3}\mu + 3\zeta_1 + 2\zeta_2}{3\kappa + p^0} \tag{3.143c}$$

$$d = -\frac{\mu + \frac{3}{2}\zeta_2 + \zeta_3}{3\kappa + p^0}, \tag{3.143d}$$

with ζ_1, ζ_2 and ζ_3 the *Murnaghan constants* (Murnaghan, 1937) which offer a complete characterisation of the third derivatives of an isotropic strain-energy function about equilibrium. Up to third-order accuracy in the deformation gradient, specification of p^0, κ, μ, ζ_1, ζ_2 and ζ_3 is sufficient to fix all the elastic properties of the background body. In light of Section 3.4.1.2, it should be emphasised that κ, μ, ζ_1, ζ_2 and ζ_3 are constants defined relative to the hydrostatically stressed background. It should be noted that these results first appeared in the geophysics literature (up to notation) in the nearly forgotten work of Walton (1974, Section 5), which was in part a response to Dahlen's (1972a; 1972b) papers. Similar expressions were also derived by Hughes & Kelly (1953).

Eq.(3.142) is precisely equivalent to eq.(3.19). In particular, the four independent components of $\mathbf{\Pi}$ that we identified by symmetry arguments in Section 3.1.1.2 have simply dropped out of the linearisation procedure. Moreover, our consideration of constitutive theory has led to a more precise definition of those constants. All four are explicitly determined by the constitutive relation used to describe the background body, emerging from the theory as dimensionless combinations of the equilibrium pressure, shear and bulk moduli, and the three Murnaghan constants. This shows explicitly that they represent just three degrees of freedom. These results reduce to those of Dahlen (1972b) and Tromp & Trampert (2018) for certain values of the elastic moduli and Murnaghan constants; we present a detailed comparison between this theory and previous work in Appendix B.4.

3.4.2 Transversely-isotropic materials

Whilst an isotropic material's response to a given induced stress is determined solely by its background strain-energy function, we also need to account for eq.(3.101)'s non-unique stress-dependence when considering materials with smaller symmetry groups. For example, we stated above that the symmetry group of a stress-free, transversely-isotropic material is $\mathbf{SO}(2)$. A definite value of $\mathbf{a}$ therefore depends upon the choice of an arbitrary element of the quotient space

$\mathbf{SO}(3)/\mathbf{SO}(2)$. This reflects the fact that $\bar{\mathbf{a}}(\boldsymbol{\sigma}, \cdot)$ cannot distinguish between matrices that only differ in how much rotation they cause about the symmetry axis. Therefore to evaluate $\bar{\mathbf{a}}(\boldsymbol{\sigma}, \mathbf{R})$ we should only choose arbitrarily between rotation matrices whose own axes of rotation lie in the plane perpendicular to the symmetry axis. In order to pick such a matrix we must choose a direction for its rotation-axis – a direction in $\mathbb{R}^2$ described by an angle ϕ – and then specify an angle of rotation θ about that axis. Careful consideration of the possibility of double-counting shows that

$$\begin{aligned} &\theta \in [0, \pi) \\ &\phi \in [0, 2\pi) \end{aligned} \tag{3.144}$$

(or vice versa). It is clear that we have effectively specified a point on $\mathbb{S}^2$, the unit 2-sphere, or equivalently a direction in $\mathbb{R}^3$. Indeed, it may be established by rigorous methods that $\mathbf{SO}(3)/\mathbf{SO}(2) \cong \mathbb{S}^2$.

3.4.2.1 Exact response to deviatoric stress

The effect of $\mathbf{a}$'s non-unique stress dependence is illustrated by Fig. 3.6, which shows slowness surfaces of a material described by the transversely-isotropic strain-energy function

$$\tilde{W}_{\mathrm{TI}}(\mathbf{F}) = \tilde{W}_{\mathrm{MSVK}}(\mathbf{F}) + [\alpha + 2\beta \log J + \gamma(I_4 - 1)](I_4 - 1) - \frac{\alpha}{2}(I_5 - 1)\,. \tag{3.145}$$

In this equation α, β and γ are extra material constants required to describe a transversely-isotropic material, while I_4 and I_5 are the two further scalar invariants in terms of which a transversely-isotropic strain energy function is parametrised (Holzapfel, 2000). They are defined as

$$I_4 = \langle \boldsymbol{\nu}, \mathbf{C} \cdot \boldsymbol{\nu} \rangle \tag{3.146}$$

$$I_5 = \left\langle \boldsymbol{\nu}, \mathbf{C}^2 \cdot \boldsymbol{\nu} \right\rangle, \tag{3.147}$$

with the unit-vector $\boldsymbol{\nu}$ pointing along the material's symmetry-axis. This strain-energy function is adapted from Bonet & Burton (1998), although our definition of β differs from theirs by a factor of two and we have defined the 'isotropic part' of the function differently. The equilibrium configuration is unstressed, with elastic tensor

$$\begin{aligned} \mathsf{a}_{ijkl} = \mathsf{c}_{ijkl} = {} & \lambda \delta_{ij}\delta_{kl} + \mu(\delta_{ik}\delta_{jl} + \delta_{il}\delta_{jk}) + 8\gamma \nu_i \nu_j \nu_k \nu_l \\ & + 4\beta(\nu_i \nu_j \delta_{kl} + \delta_{ij}\nu_k \nu_l) - \alpha(\nu_i \nu_k \delta_{jl} + \nu_j \nu_k \delta_{il} + \nu_j \nu_l \delta_{ik} + \nu_i \nu_l \delta_{jk})\,, \end{aligned} \tag{3.148}$$

which can be written alternatively as

$$\mathsf{a} = \mathsf{c} = \lambda \mathbf{1} \otimes \mathbf{1} + 2\mu \overline{\mathsf{id}} + 8\gamma \mathbf{N} \otimes \mathbf{N} + 4\beta(\mathbf{1} \otimes \mathbf{N} + \mathbf{N} \otimes \mathbf{1}) - 2\alpha \overline{\mathbf{X}}_{\mathbf{N}} \tag{3.149}$$

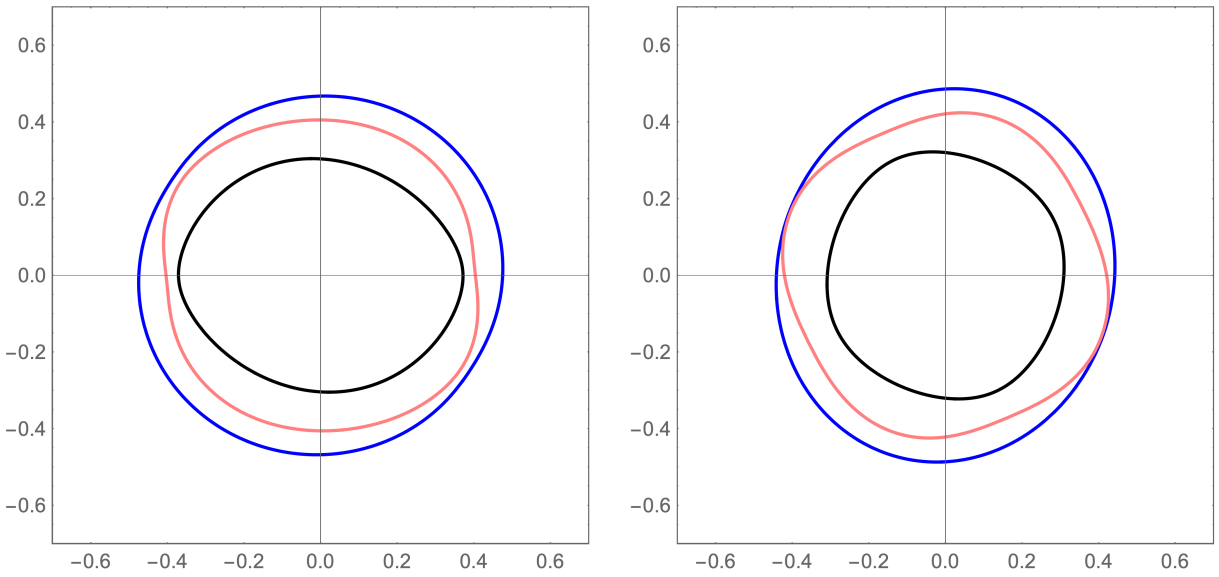

Figure 3.6: Two x–y slowness surfaces of an initially transversely-isotropic material in which *the same* large deviatoric stress has been induced, but with different choices of the arbitrary parameters θ and ϕ. The slow- and fast-directions of P-waves are different, as are the shear-wave splitting patterns. The distinct physical behaviour implied in the two panels is a result of changing the arbitrary parameters in $\bar{\mathbf{a}}(\boldsymbol{\sigma}, \mathbf{R})$. This reflects our assumed ignorance of the orientation of the material before the stress was induced.

if we define $\mathbf{N}$ as

$$\mathbf{N} \equiv \boldsymbol{\nu} \otimes \boldsymbol{\nu}. \tag{3.150}$$

We have induced the same stress in the material in both panels of the figure, but selected different (θ, ϕ) pairs, producing slowness surfaces *of different shapes*. It should be emphasised that the material is described by the same strain-energy function in both panels; that the two slowness surfaces demonstrate distinct physical behaviour is due solely to $\mathbf{a}$'s non-unique dependence on $\boldsymbol{\sigma}$ (eq.3.101).

3.4.2.2 Linearised response to deviatoric stress

Finally, we consider how a transversely-isotropic material responds to a small induced stress. This is the simplest nontrivial example in which one can show analytically how the arbitrary rotation matrix of eq.(3.101) manifests in the linearised elastic tensor.

In an isotropic material we took the background (zeroth-order) state to be hydrostatic, but in the transversely-isotropic case we should consider a more general zeroth-order stress of the form

$$\boldsymbol{\sigma}^0 = -\left(p^0 + \frac{q^0}{3}\right)\mathbf{1} + q^0 \boldsymbol{\nu} \otimes \boldsymbol{\nu}. \tag{3.151}$$

The pressure is p^0 as before, but the stress now possesses in addition a background deviatoric component consistent with the $\mathbf{SO}(2)$ symmetry. We then induce a small stress $\boldsymbol{\sigma}^1$, and a tedious

calculation laid out in Appendix B.3.3 leads to the linearised elastic tensor

$$\begin{aligned}\mathbf{c}^1 = {}& \eta_1\mathbf{1}\otimes\mathbf{1} + \eta_2\overline{\mathbf{id}} + \eta_3\mathbf{N}\otimes\mathbf{N} + \eta_4(\mathbf{1}\otimes\mathbf{N} + \mathbf{N}\otimes\mathbf{1}) + \eta_5\overline{\mathbf{X}}_{\mathbf{N}} \\ & + \eta_6\overline{\mathbf{X}}_{\boldsymbol{\sigma}^1} + \eta_7\big(\mathbf{1}\otimes\boldsymbol{\sigma}^1 + \boldsymbol{\sigma}^1\otimes\mathbf{1}\big) + \eta_8\big(\mathbf{N}\otimes\boldsymbol{\sigma}^1 + \boldsymbol{\sigma}^1\otimes\mathbf{N}\big) \\ & + \eta_9\big[\mathbf{1}\otimes\big(\mathbf{X}_{\mathbf{N}}\cdot\boldsymbol{\sigma}^1\big) + \big(\mathbf{X}_{\mathbf{N}}\cdot\boldsymbol{\sigma}^1\big)\otimes\mathbf{1}\big] + \eta_{10}\big[\mathbf{N}\otimes\big(\mathbf{X}_{\mathbf{N}}\cdot\boldsymbol{\sigma}^1\big) + \big(\mathbf{X}_{\mathbf{N}}\cdot\boldsymbol{\sigma}^1\big)\otimes\mathbf{N}\big] \\ & + \eta_{11}\overline{\mathbf{X}}_{(\mathbf{X}_{\mathbf{N}}\cdot\boldsymbol{\sigma}^1)} + \eta_{12}\big(\overline{\mathbf{X}}_{\boldsymbol{\sigma}^1}\overline{\mathbf{X}}_{\mathbf{N}} + \overline{\mathbf{X}}_{\mathbf{N}}\overline{\mathbf{X}}_{\boldsymbol{\sigma}^1}\big) \\ & + \eta_{13}\overline{\mathbf{X}}_{\boldsymbol{\omega}} + \eta_{14}[\mathbf{1}\otimes(\mathbf{X}_{\boldsymbol{\omega}}\cdot\mathbf{N}) + (\mathbf{X}_{\boldsymbol{\omega}}\cdot\mathbf{N})\otimes\mathbf{1}] \\ & + \eta_{15}[\mathbf{N}\otimes(\mathbf{X}_{\boldsymbol{\omega}}\cdot\mathbf{N}) + (\mathbf{X}_{\boldsymbol{\omega}}\cdot\mathbf{N})\otimes\mathbf{N}] + \eta_{16}\big(\overline{\mathbf{X}}_{\boldsymbol{\omega}}\overline{\mathbf{X}}_{\mathbf{N}} - \overline{\mathbf{X}}_{\mathbf{N}}\overline{\mathbf{X}}_{\boldsymbol{\omega}}\big)\,, \end{aligned} \tag{3.152}$$

with the constants $\{\eta_i\}$ defined in eqs.(B.154). The antisymmetric matrix $\boldsymbol{\omega}$ defines a vector pointing in an arbitrary direction in the plane perpendicular to the unperturbed material symmetry axis. Its components are

$$\omega_i = -\epsilon_{ijk}\omega_{jk}, \tag{3.153}$$

where ϵ_{ijk} are the components of the Levi-Civita tensor, and its direction and magnitude are precisely the two arbitrary constants that must be fixed. On the other hand the $\{\eta_i\}$ are unique, scalar-valued functions of:

(1). the constants p^0 and q^0 which parametrise the zeroth-order equilibrium stress;

(2). the transversely-isotropic constants λ, μ, α, β and γ (which are implicitly functions of p^0, q^0 and their respective stress-free values);

(3). $\mathrm{tr}\big(\boldsymbol{\sigma}^1\big)$ and $\big\langle\boldsymbol{\nu},\boldsymbol{\sigma}^1\cdot\boldsymbol{\nu}\big\rangle$;

(4). the nine constants $\{\zeta_i\}$ defined in eq.(B.144) which, analogously to the Murnaghan constants, parametrise the third derivatives of a transversely-isotropic strain-energy function.

The precise functional forms of the $\{\eta_i\}$ are not nearly as important as the fact that they depend on the nine further degrees of freedom represented by the $\{\zeta_i\}$, not to mention the two arbitrary parameters contained within $\boldsymbol{\omega}^1$. In contrast, when Tromp et al.'s (2019) result is specialised to the transversely-isotropic case it has just five free parameters, namely the pressure derivatives of the elastic moduli (the independent components of their tensor $\boldsymbol{\Gamma}'$). I also believe that the term in η_{11} within eq.(3.152) is not present in Tromp et al.'s expression.

As a last point, let us consider the perturbation to the Christoffel operator associated with terms in $\boldsymbol{\omega}^1$. Continuing to ignore spatial arguments, one can show that definition (3.56) is equivalent to

$$\langle\mathbf{a},\rho\mathbf{B}(\mathbf{p})\cdot\mathbf{a}\rangle = \langle\mathbf{a}\otimes\mathbf{p},\mathbf{a}\cdot(\mathbf{a}\otimes\mathbf{p})\rangle \tag{3.154}$$

for arbitrary $\mathbf{a}$ and where ρ is the density in the deformed state. From this it is a matter of

algebra to show that the contribution to $\rho\mathbf{B}$ of the terms in $\boldsymbol{\omega}^1$ is

$$\begin{aligned}\rho\mathbf{B} =&(\eta_{14}+\eta_{16})\langle\boldsymbol{\nu},\mathbf{p}\rangle\big[\mathbf{p}\otimes\big(\boldsymbol{\omega}^1\times\boldsymbol{\nu}\big)+\big(\boldsymbol{\omega}^1\times\boldsymbol{\nu}\big)\otimes\mathbf{p}\big]\\&+\left(\eta_{14}+\frac{1}{2}\eta_{16}\right)\big\langle\boldsymbol{\omega}^1\times\boldsymbol{\nu},\mathbf{p}\big\rangle(\mathbf{p}\otimes\boldsymbol{\nu}+\boldsymbol{\nu}\otimes\mathbf{p})\\&+\Big(\eta_{15}\langle\boldsymbol{\nu},\mathbf{p}\rangle^2+\eta_{16}\|\mathbf{p}\|^2\Big)\big[\boldsymbol{\nu}\otimes\big(\boldsymbol{\omega}^1\times\boldsymbol{\nu}\big)+\big(\boldsymbol{\omega}^1\times\boldsymbol{\nu}\big)\otimes\boldsymbol{\nu}\big]\\&+\langle\boldsymbol{\nu},\mathbf{p}\rangle\big\langle\boldsymbol{\omega}^1\times\boldsymbol{\nu},\mathbf{p}\big\rangle(\eta_{15}\boldsymbol{\nu}\otimes\boldsymbol{\nu}+\eta_{16}\mathbf{1})\,.\end{aligned}\tag{3.155}$$

Each of the coefficients η_{14}, η_{15} and η_{16} depends on a different combination of the $\{\zeta_i\}$. But the $\{\zeta_i\}$ parametrise the third-derivatives of the strain energy and can be specified independently both of the other elastic constants and of each other. It is therefore clear that $\boldsymbol{\omega}^1$ will generally contribute nonzero terms to the Christoffel operator.

3.5 Discussion

Working under the theory of finite elasticity, we have investigated how changes of equilibrium, changes in stress and changes in the elastic tensor are interrelated within hyperelastic bodies. Central to the discussion are eqs.(3.94), which we can restate in the notation of Dahlen & Tromp (1998, Sections 2.10 & 3.6) as

$$T^0_{ij} = \frac{\rho^0}{\det\mathbf{F}}F_{ip}F_{jq}\frac{\partial U^L}{\partial E^L_{pq}}\tag{3.156a}$$

$$\Xi_{ijkl} = \frac{\rho^0}{\det\mathbf{F}}F_{ip}F_{jq}F_{kr}F_{ls}\frac{\partial^2 U^L}{\partial E^L_{pq}\partial E^L_{rs}}.\tag{3.156b}$$

These equations tell us how a hyperelastic body's equilibrium Cauchy stress and elastic tensor change when the body is deformed by a motion with deformation gradient $\mathbf{F}$, assuming that the body is described by a given constitutive function U^L. They can be used to approach both forward- and inverse-problems within geophysics, which we now illustrate by considering briefly the problem of *monsoon loading*, an example that also allows us to contextualise our main results.

In regions that experience heavy monsoons, the rainwater accumulating on the Earth's surface causes the crust to be loaded nontrivially by different amounts at different times of the year (e.g. Fu et al., 2013). This load causes the crust to deform, and induces associated stresses within it. Given that the deformation occurs over a timescale of months – a timescale significantly greater than that associated with seismic wave propagation – we model the deformations to be quasi-static. That is, we take seismic waves propagating through the Earth at a given time to 'see' a static equilibrium Earth that does not interact with them *dynamically*. Nevertheless, the deformation of the crust does affect the propagation of the seismic waves because the equilibrium configuration changes, and through eq.(3.156b) there is a consequent change in the elastic tensor. To take a simple example, if we start with a reference state that is isotropic, the change in equilibrium will almost certainly induce seismic anisotropy. The results of the present chapter give us a number of ways of thinking about how the elastic tensor changes.

A first approach makes direct use of eqs.(3.156) from the perspective of forward-modelling.

For concreteness, say that we know the constitutive relation governing the Earth. We then model the rainfall-induced deformation by solving a quasi-static mapping problem, from which we obtain the change in equilibrium configuration. The resultant mapping has a deformation gradient $\mathbf{F}$, and we can use eqs.(3.156) to compute the associated change in both the equilibrium Cauchy stress and the elastic tensor. Hence, we can directly compute the expected seismic anisotropy.

The procedure just outlined is appealing, but it rests on the assumption that we know the rainfall loading sufficiently well to predict the change in configuration. Although this might be realistic in some cases, it is unlikely to be true in general. If anything, it is perhaps more pragmatic to pose the inverse-problem instead: given that an equilibrium deformation leads to seismic anisotropy, and given that we can observe seismic waves readily, what can seismic data tell us about $\mathbf{F}$, and hence about the change in the equilibrium configuration and the water load? For this problem we do not even need eq.(3.156a); we need only collect seismic data and use (3.156b) to invert for the nine components of $\mathbf{F}$ (taking account of the condition that $\mathbf{F}$ be the gradient of a mapping). The equilibrium mapping could then be (partially) reconstructed, or we could just bypass it and invert directly for the water load.

At this point we could, if we wished, use eq.(3.156a) to compute the change in equilibrium stress. That would amount to performing a (rather roundabout) inversion of seismic observations for equilibrium stress. But what if we were less interested in learning about the surface water load than about the stresses within the Earth? In that case it would be desirable, from the perspective of inversion, to bypass $\mathbf{F}$ and just invert for $\mathbf{T}^0$ directly, not least because the Cauchy stress has fewer components than $\mathbf{F}$. For that we would need to consider the stress dependence of the elastic tensor; that is, find an explicit expression for $\boldsymbol{\Xi}$ as a function of $\mathbf{T}^0$. In searching for such an expression we are effectively asking if it is possible to parametrise an equilibrium configuration, not in terms of the deformation gradient that gave rise to it, but rather in terms of its present Cauchy stress. We are thus led to address the following problem: if we observe a *given* Cauchy stress and assume that it arose due to *some* elastic deformation of a state with *given* constitutive properties, what elastic tensor would we measure?

As discussed at length in Section 3.3, in order to find $\boldsymbol{\Xi}$ as a function of $\mathbf{T}^0$ we must eliminate $\mathbf{F}$ from eqs.(3.156). We solve (3.156a) in order to find $\mathbf{F}$ as a function of $\mathbf{T}^0$, and substitute the result into (3.156b). Physically, (3.156a) describes how a deformation alters an elastic body's equilibrium Cauchy stress. But because many different values of $\mathbf{F}$ can lead to the same change in $\mathbf{T}^0$, the mathematical problem of inverting (3.156a) to find $\mathbf{F}$ in terms of $\mathbf{T}^0$ is naturally underdetermined. It turns out that $\mathbf{F}$ depends not only on $\mathbf{T}^0$, but also on an arbitrary rotation matrix. One can then show that the elastic tensor itself is given as a function of both the Cauchy stress and an arbitrary rotation. As emphasised in Section 3.3, the presence of these arbitrary parameters shows that measurement of the Cauchy stress *alone* is not sufficient to constrain the elastic tensor fully. However, we also found that the more symmetric the initial, reference state, the fewer the arbitrary parameters. In fact, for an isotropic reference state one can ignore the rotation matrix entirely; in that case the Cauchy stress does provide enough information to fix the elastic tensor.

Having derived an expression for the nonlinear dependence of $\boldsymbol{\Xi}$ on $\mathbf{T}^0$, we proceeded to

linearise it. From the point of view of performing inversions this step is not strictly necessary, but it is useful for two reasons. Firstly, the changes in the Earth's equilibrium stress due to quasi-static deformation are likely to be small because the deformations we consider will almost always be small. This will certainly be the case with monsoon loading; and I also refer the reader to Tromp & Trampert (2018, Section 8.2) for a discussion of the effects of equilibrium stress on seismic waveforms in the Groningen gas field. On balance, the change in the elastic tensor should be well described by a linearised theory, and such a theory should be quicker to implement computationally. Secondly, the theories discussed in Section 3.1 are all linear in the stress, so we must linearise our theory in order to carry out a comparison.

Linearising within a general anisotropic material, the elastic tensor depends not only on $\Delta\mathbf{T}^0$ but also on a small, arbitrary, antisymmetric matrix $\boldsymbol{\omega}^1$ that results from linearising the rotation matrix of eq.(3.101). Our general linearised expression (3.118) can be expanded and rewritten in the notation of Section 3.1 to give

$$\Delta\Xi_{ijkl} = \Pi_{ijklmn}\Delta T^0_{mn} + \Pi'_{ijklmn}\omega^1_{mn}, \tag{3.157}$$

where $\boldsymbol{\Pi}$ is the tensor relating changes in $\boldsymbol{\Xi}$ to $\Delta\mathbf{T}^0$, just as before, while we have defined another tensor $\boldsymbol{\Pi}'$ that relates changes in $\boldsymbol{\Xi}$ to $\boldsymbol{\omega}^1$. The components of $\boldsymbol{\Pi}$ and $\boldsymbol{\Pi}'$ are expressed in terms of the third derivative of the strain-energy function evaluated in the background state, and the components of the background elastic tensor $\boldsymbol{\Gamma}$; it can be shown that they therefore possess up to 56 independent components besides the elastic moduli. These rather complicated expressions are given in Appendix B.1.4, while here I make two general points. Firstly, $\boldsymbol{\Pi}'$ will not usually vanish, which indicates that even linearised stress dependence will generally involve some level of arbitrariness. Inspection of Appendix B.3.1 will show that the neglect of $\boldsymbol{\Pi}'$ is equivalent to assuming that $\Delta\mathbf{T}^0$ was induced by a *symmetric* deformation gradient, *i.e.* a pure stretch. Secondly, we have shown that $\boldsymbol{\Pi}$ need not possess the further symmetries,

$$\Pi_{ijklmn} = \Pi_{ijmnkl} = \Pi_{klmnij} = \Pi_{mnijkl} = \Pi_{mnklij}, \tag{3.158}$$

imposed in eq.(3.28). In short, our theory is parametrised differently from that of Tromp et al. (2019); we require up to 59 (=56+3) numbers, while Tromp et al. need a maximum of 21. The respective theories are therefore unlikely to give the same results when used to perform inversions.

This statement can be substantiated a little further by applying our general linearised expression to a transversely-isotropic material. We found that nine material-dependent parameters and two arbitrary constants (besides the five elastic moduli) were needed to specify the elastic tensor's linearised stress dependence. Our results cannot be equivalent to those of Tromp et al. because their expression requires just five further constants, parametrised as it is by pressure-derivatives of the elastic moduli. (I have not presented here the complete expression for transversely-isotropic $\boldsymbol{\Pi}$; I trust that the reader who has worked through Appendix B.3.3 will forgive me.)

We have performed the most complete comparison with Tromp et al.'s work in the linearised isotropic case – which is presumably the case of most practical importance. Our expression for the elastic tensor takes precisely the form derived in Section 3.1.1 featuring the four constants a,

b, c and d (eq.3.19). Furthermore, we have shown by considering constitutive behaviour that those constants are functions of the *Murnaghan constants* $\zeta_{1,2,3}$ (Murnaghan, 1937):

$$a = \frac{\kappa - \frac{2}{3}\mu + \frac{1}{2}\zeta_2}{\mu - p^0} \tag{3.159a}$$

$$b = \frac{\mu + \frac{1}{4}\zeta_3}{\mu - p^0} \tag{3.159b}$$

$$c = -\frac{\kappa - \frac{2}{3}\mu + 3\zeta_1 + 2\zeta_2}{3\kappa + p^0} \tag{3.159c}$$

$$d = -\frac{\mu + \frac{3}{2}\zeta_2 + \zeta_3}{3\kappa + p^0}. \tag{3.159d}$$

As a result they represent three degrees of freedom. Up to notation, these four expressions first appeared in the work of Walton (1974, eqs.31–34). Taking into account different definitions of the elastic moduli, we have also established in Appendix B.4 that the expressions of Dahlen (1972b) and Tromp & Trampert (2018) are consistent with this theory for certain parameter choices. Those theories thus apply to a subset of isotropic materials. If one wished to invert seismic data for equilibrium stress using Tromp & Trampert's theory, one would need to specify (or invert for) two parameters, the pressure-derivatives of κ and μ. Our theory would require three such parameters. Finally, it is interesting that we have found expressions for the pressure-derivatives of the elastic moduli (c and d; see Appendix B.4) in terms of the Murnaghan constants. To our knowledge, this result has not appeared in the literature since Walton's work.

Our linearised results would probably be more taxing to apply to observational seismology than those of Tromp et al. because we require the measurement and fitting of more parameters. Moreover, the strain-energy function's third-derivatives are at present measured less readily than the moduli's pressure-derivatives. It is also evident from Tromp et al.'s *ab initio* calculations (carried out for a material with cubic symmetry) that the extra effects we have derived are not particularly large. We would be keen to see if further such calculations can clarify this apparent "unreasonable effectiveness" of pressure-derivatives. Nevertheless, our theory should be practical for isotropic reference states: the Murnaghan constants of various materials have been measured in the past (e.g. Hughes & Kelly, 1953; Egle & Bray, 1976; Payan et al., 2009) and in the isotropic case our theory just requires one more parameter than Tromp et al.'s.

There are a number of potential geophysical applications of this work, but I must first mention two caveats. Firstly, the Earth is not elastic over geological time-scales, hence it is not reasonable to regard its equilibrium as having arisen through a finite deformation of an elastic material away from some hypothetical stress-free state. Within future work it would therefore be interesting to extend our methods to account for viscoelastic effects; that would also complement the work in the applied mathematics and engineering literature (e.g. Ogden & Singh, 2011; Destrade & Ogden, 2012; Gower et al., 2017) that accounts for initial stresses that cannot be related to a deformation gradient. Nevertheless, our framework should give valid descriptions of phenomena that occur over time-scales sufficiently short for the Earth to respond in an elastic – or only slightly anelastic – manner. For example, one might consider the effect on elastic wave speeds of processes that are fast relative to viscoelastic relaxation times but

slow compared to those of seismic wave propagation, such as body tides, seasonal loading in the hydrosphere, or anthropogenic activity. A second caveat is that inverting seismic data for equilibrium stress is already rendered challenging by the fact that the equilibrium stress is not an entirely free parameter, but is constrained to satisfy the equilibrium equations (Backus, 1967; Al-Attar & Woodhouse, 2010). Our results make clear that it is also necessary to either provide or simultaneously invert for additional parameters related to third derivatives of the strain-energy function and, in some cases, infinitesimal rotations. Finally, given the importance of symmetry groups to this work, I would also be interested to see how our results mesh with the theory of *homogenisation* (e.g. Cupillard & Capdeville, 2018; Capdeville & Métivier, 2018) which describes how small-scale structures are 'smeared out' to produce effective media with *different symmetry properties* (recall for instance Backus's (1962) point that long-wavelength seismic waves passing through a layered isotropic medium 'see' a transversely-isotropic *effective* medium).

3.6 Conclusions

We have derived an expression for the elastic tensor as an explicit function of equilibrium Cauchy stress. Our results differ from previous treatments in two main ways: they show that the elastic tensor's dependence on equilibrium stress is generally both nonlinear and non-unique. On account of the nonlinearity alone, knowledge of a material's background elastic-tensor is not sufficient to determine the material's response to an induced stress; we require the information contained within higher-order derivatives of the background strain-energy function. Furthermore, the elastic tensor is a function not only of the equilibrium stress, but also of an arbitrary rotation matrix. As such, even with a definite strain-energy function in hand, the change in the elastic tensor due to an induced stress depends on the non-unique choice of this matrix. The non-uniqueness arises from the fact that the stress is considered to have been induced by an unspecified elastic deformation. However, we have also shown that the degree of non-uniqueness is reduced if the material under study has a nontrivial background material symmetry group.

In the linearised case, our approach shows that the characterisation of a material's response to a small induced stress depends on more parameters than have been made explicit in previous studies (Tromp & Trampert, 2018; Tromp et al., 2019). We have shown moreover that the previous expressions for the elastic tensor's stress dependence can be obtained as special cases of our linearised results. Our expressions should be seen to extend the work of the previous authors by including some extra terms that were not captured by their derivation. The approach of first deriving a nonlinear expression, and only then linearising, has also allowed us to suggest a different interpretation of the parametrisation of the elastic tensor's linearised stress dependence. Whilst Tromp et al. suggest that the relevant parameters are the pressure-derivatives of the elastic moduli, I propose the use of a larger set of parameters: the third-derivatives of the strain-energy function, and, for anisotropic materials, infinitesimal rotations. That said, I would like to emphasise once again that the expressions of Tromp et al. are able to fit experimental data rather well for the case of a cubic material. So whilst it seems theoretically necessary to account for more parameters, on a practical level it might not be required. This is a curious result that is not obvious to the present author, and I would be keen to see it investigated further.

CHAPTER 4

On the elastodynamics of rotating, solid planets

4.1 Introduction

The Earth's gravest seismic free oscillation ${}_0S_2$ has a period of about an hour (Dahlen & Tromp, 1998), whilst the characteristic timescales of Earth's rotational behaviour are $\sim$24 hours and $\sim$400 days (Munk & McDonald, 1960). This great separation of timescales suggests a division of sorts between the physics of the Earth's rotational and elastic behaviours, and indeed, most approaches to the normal modes of rotating Earth models fall approximately into two categories (see Dehant & Mathews, 2015, Chapter 7). One such approach is to prioritise rotation over elasticity. On a physical level, we essentially model the Earth as three rigid bodies (representing the inner core, outer core and mantle) each of which is described by an Euler equation and whose respective motions are coupled by gravity and boundary torques. The normal modes associated with the angular velocity are found by solving these Euler equations, with the outer core's fluidity and the mantle's elasticity treated as perturbations that can be accounted for through *transfer functions* (e.g. Dehant & Mathews, 2015, Ch. 2). Although this procedure does not provide us with the seismic modes of the corresponding non-rigid model, it is very useful if one is most interested in the Earth's nutation and wobble. Transfer functions are only applicable to axially symmetric, ellipsoidal Earth models, but this drawback's severity will be determined by the problem at hand. Recent numerical work in this vein has been carried by Triana et al. (2019) and Rekier et al. (2020).

A second approach, initiated by Smith (1974) and expanded upon by Dahlen & Smith (1975) and Smith (1977) among others, gives precedence instead to the equations of elastic motion. No Euler equation is written down: one accounts for the Earth's rotation by posing the elastodynamic PDEs with respect to a frame that rotates with the *uniform* angular velocity of the *equilibrium* Earth and whose origin coincides with the equilibrium Earth's CoM. One then linearises these equations and solves for a small displacement field. The whole motion of the body – both its elastic and rotational characteristics – is bound up in that displacement field. This approach is arguably more physically complete, but one must use slightly *ad hoc* methods to accommodate

secular modes such as the axial spin mode (e.g. Dahlen & Smith, 1975, pp. 614-616). Moreover, the rotational 'component' of the motion is bound up with the elastic component in a somewhat unclear manner. Nevertheless, Wahr (1981a,b,c) was able to use this framework to great effect in determining the body tides and nutations of an elliptical, rotating, elastic and oceanless earth. Wahr's theoretical work was recently extended by Lau et al. (2015) using ideas from more recent work on theoretical seismology. The work of Lau et al. (2015, 2016, 2017) is arguably the most advanced example of this second approach to a rotating Earth's elastodynamics, even though it cannot describe nutations fully.

So should the Earth's dynamics be described by a suitably modified Euler equation or a suitably modified momentum equation? The premise of this chapter is that both are relevant. This is not an original idea. In his spectacular study of Earth's oceans' effect on the Chandler wobble, for example, Dahlen (1976) began by explicitly considering a linearised Euler equation and a linearised momentum equation. He coupled them together through the angular velocity and the moment of inertia tensor, and only then exploited the separation of the rotational and elastic timescales to absorb the momentum equation into the Euler equation. His procedure, which is in principle exact, showed that seismic motion affects rotation through nothing more than a modified inertia tensor.

To my knowledge Dahlen's 1976 study contains the most complete formulation of the rotational dynamics of deformable bodies, but even there it is not made clear how the angular velocity, the elastic motion *and their respective governing equations* all emerge from the exact equations of continuum mechanics. In this connection it is worth quoting at length from Smith (1977):

> An additional, and equally important, objective of this study is to approach systematically the theoretical study of free wobble from a unified point of view. Virtually all theoretical studies of the Earth's free wobbles disjoin wobble conceptually from all other elastic-gravitational normal modes of the rotating Earth and make ad hoc accommodation for that portion of the Earth's motion which is rigid rotation. (The only exception known to me is the Appendix of Hough (1895).) This separation is unnecessary and somewhat artificial (although not erroneous) and it complicates our understanding of the behaviour of the rotating Earth by leaving the implication that certain of the Earth's free motions cannot be understood by solely studying the continuum equations of motion but instead require that we resort to 'extra' physical principles such as Euler's equations.

The present author feels that Smith's comments are equally relevant to the situation of today, where the physical unity of Earth's rotation and elastodynamics is still not fully reflected in the literature. Not only does this lead to a lack of physical clarity, but it also obscures potential avenues for approximation and numerical solution. Our goal in this chapter is to unite the best aspects of Smith's approach with the best of Dehant, Mathews, Wahr et al., and in so doing to obtain equations that are as well-suited as possible to the analysis of a rotating Earth model's long-period dynamics. We take seriously Smith's desire to see rotational behaviour embraced by the exact equations of continuum mechanics, while also taking seriously the utility of working with Euler equations. This leads us to ask if one can exactly reformulate the equations of

continuum mechanics in such a way that both the elastic and rotational aspects of the dynamics are seen to emerge naturally.

To make progress we will synthesise concepts from both finite elasticity and geometric mechanics, and derive a set of equations that brings us as close to rigid-body motion as possible (in a sense that we will make precise below) while still incorporating elastic motion exactly. Importantly, those equations will place rotation and elasticity on an 'equal footing', and we will have given a precise definition of the elastic body's angular velocity. The latter point is of some importance because there is no unique way to define a deformable body's angular velocity (e.g. Munk & McDonald, 1960; Lambeck, 2005). Our discussion also deviates from the classic papers of Dahlen and Smith in that we do not at any point work within a frame of reference that rotates uniformly with the equilibrium Earth's angular velocity. Instead, our derivation will lead to equations of motion that describe elastodynamics within a reference frame that rotates *variably*, with its orientation chosen so that the elastic motion carries no net linear or angular momentum at any time. In the pursuit of physical clarity our derivations will not approximate any motions as 'small', although we will linearise the equations of motion in due course. This chapter concerns itself almost exclusively with solid, hyperelastic bodies, but we will discuss qualitatively the necessary extensions to fluid-solid bodies in Section 4.7.

We present the necessary background on Hamilton's principle in Section 4.2. Section 4.3 then shows how Hamilton's principle provides an elegant formulation of rigid body dynamics, both exact and linearised. Following that, we review finite elasticity in Section 4.4, and we build on all the preceding ideas in Section 4.5 to derive the exact equations of motion of a rotating, self-gravitating elastic body. Section 4.5 follows the template laid out in Section 4.3. We then linearise those equations and discuss how their numerical solution could be carried out, after which we show that these ideas can readily be extended to $N \geq 2$ bodies all interacting through gravity. Throughout this chapter we restrict attention to a body that is either wholly fluid or wholly solid.

Regarding notation, we have also found it easier to introduce new notations 'on the fly', rather than consigning them to an appendix as we did in Chapter 3. We continue to notate differentiation with a 'D' on the whole, although we use ∇ to represent differentiation with respect to a position in $\mathbb{R}^3$, and ∂_t for time-derivatives.

4.2 Review of Hamilton's principle

This chapter revolves around the derivation of both exact and linearised equations of motion from variational principles. Here we will briefly discuss a simple illustrative example: the dynamics of a single, real scalar field

$$\psi : \mathcal{B} \times \mathcal{I} \mapsto \mathbb{R} \tag{4.1}$$

with $\mathcal{B} \subset \mathbb{R}^3$ the field's spatial domain and $\mathcal{I}$ the time-interval of interest. Outlining our approach, particularly our approach to linearisation, in this simple scenario will save a lot of space in later sections; the results shown here are easily extended to the case of multiple vector-valued fields.

We also aim to show that Hamilton's principle provides an elegant approach to linearising the equations – and particularly to deriving the sort of linearised *weak forms* that will be important in our planned future numerical work.

4.2.1 The action

Hamilton's principle of least action (e.g. Marsden & Hughes, 1994) states that a dynamical system will behave in such a way that its *action* is extremized subject to fixed endpoint conditions, the action $\mathcal{S}$ being a functional of the motion defined as

$$\mathcal{S} = \int_{\mathcal{I}} L(t)\,\mathrm{d}t, \tag{4.2}$$

where L is the *Lagrangian*. The Lagrangian is a functional of the motion equal to the difference between the system's kinetic and potential energies. For our single scalar field we take the Lagrangian to be a local functional of ψ given by

$$L(t) = \int_{\mathcal{B}} \mathcal{L}\Big[\psi(\mathbf{x},t), \dot{\psi}(\mathbf{x},t), \nabla\psi(\mathbf{x},t)\Big]\,\mathrm{d}V, \tag{4.3}$$

where $\mathcal{L} : \mathbb{R}\times\mathbb{R}\times\mathbb{R}^3 \mapsto \mathbb{R}$ is the *Lagrangian density*. All in all, the action is the functional $\hat{\mathcal{S}}$ of ψ given by

$$\mathcal{S} = \hat{\mathcal{S}}[\psi] \equiv \int_{\mathcal{I}}\int_{\mathcal{B}} \mathcal{L}\Big(\psi, \dot{\psi}, \nabla\psi\Big)\,\mathrm{d}V\,\mathrm{d}t. \tag{4.4}$$

For example, in the simple case of a Sine–Gordon field of mass m the Lagrangian density (suitably nondimensionalised) would be

$$\mathcal{L}\Big(\psi, \dot{\psi}, \nabla\psi\Big) = \frac{1}{2}\dot{\psi}^2 - \frac{1}{2}\|\nabla\psi\|^2 + m^2(\cos\psi - 1)\,. \tag{4.5}$$

4.2.2 Exact Euler–Lagrange equations

The *Euler–Lagrange equations* are derived by extremizing the action with respect to ψ, subject to the endpoint conditions that the variation $\delta\psi$ vanish at the initial and final times. $\delta\mathcal{S}$, the first variation of the action, is the term in $\hat{\mathcal{S}}[\psi+\delta\psi]$ linear in $\delta\psi$:

$$\mathcal{S} + \delta\mathcal{S} = \hat{\mathcal{S}}[\psi+\delta\psi] + \mathcal{O}\big(\delta\psi^2\big)\,. \tag{4.6}$$

We can express $\delta\mathcal{S}$ conveniently through the partial derivatives of $\mathcal{L}$ with respect to its arguments:

$$\begin{aligned}\hat{\mathcal{S}}[\psi+\delta\psi] &= \int_{\mathcal{I}}\int_{\mathcal{B}} \mathcal{L}\Big(\psi+\delta\psi, \dot{\psi}+\partial_t\delta\psi, \nabla\psi+\nabla\delta\psi\Big)\,\mathrm{d}V\,\mathrm{d}t \\ &= \hat{\mathcal{S}}[\psi] + \int_{\mathcal{I}}\int_{\mathcal{B}}\Big[D_{\psi}\mathcal{L}(\psi,\dot{\psi},\nabla\psi)\delta\psi + D_{\dot{\psi}}\mathcal{L}(\psi,\dot{\psi},\nabla\psi)\partial_t\delta\psi \\ &\qquad\qquad + \Big\langle D_{\nabla\psi}\mathcal{L}(\psi,\dot{\psi},\nabla\psi), \nabla\delta\psi\Big\rangle\Big]\,\mathrm{d}V\,\mathrm{d}t + \mathcal{O}\big(\delta\psi^2\big) \\ &= \hat{\mathcal{S}}[\psi] + \int_{\mathcal{I}}\int_{\mathcal{B}}\Big[D_{\psi}\mathcal{L}(\psi,\dot{\psi},\nabla\psi) - \partial_t D_{\dot{\psi}}\mathcal{L}(\psi,\dot{\psi},\nabla\psi) - \nabla\cdot D_{\nabla\psi}\mathcal{L}(\psi,\dot{\psi},\nabla\psi)\Big]\,\delta\psi\,\mathrm{d}V\,\mathrm{d}t \\ &\qquad + \int_{\mathcal{I}}\int_{\partial\mathcal{B}}\Big\langle D_{\nabla\psi}\mathcal{L}(\psi,\dot{\psi},\nabla\psi), \hat{\mathbf{n}}\Big\rangle\,\delta\psi\,\mathrm{d}S\,\mathrm{d}t + \mathcal{O}\big(\delta\psi^2\big)\,, \end{aligned} \tag{4.7}$$

where in the second line we have defined the partial derivatives $D_{\psi}\mathcal{L}$, $D_{\dot{\psi}}\mathcal{L}$ and $D_{\nabla\psi}\mathcal{L}$, and in the third we have integrated by parts in both space and time and made use of the endpoint conditions on $\delta\psi$. From this we have

$$\begin{aligned}\delta\mathcal{S} = &\int_{\mathcal{I}}\int_{\mathcal{B}}\Big[D_{\psi}\mathcal{L}(\psi,\dot{\psi},\nabla\psi) - \partial_t D_{\dot{\psi}}\mathcal{L}(\psi,\dot{\psi},\nabla\psi) - \nabla\cdot D_{\nabla\psi}\mathcal{L}(\psi,\dot{\psi},\nabla\psi)\Big]\,\delta\psi\,\mathrm{d}V\,\mathrm{d}t \\ &+ \int_{\mathcal{I}}\int_{\partial\mathcal{B}}\Big\langle D_{\nabla\psi}\mathcal{L}(\psi,\dot{\psi},\nabla\psi), \hat{\mathbf{n}}\Big\rangle\,\delta\psi\,\mathrm{d}S\,\mathrm{d}t, \end{aligned} \tag{4.8}$$

and by demanding that this vanish for arbitrary $\delta\psi$ we obtain the Euler–Lagrange equations

$$D_{\psi}\mathcal{L}(\psi,\dot{\psi},\nabla\psi) - \partial_t D_{\dot{\psi}}\mathcal{L}(\psi,\dot{\psi},\nabla\psi) - \nabla\cdot D_{\nabla\psi}\mathcal{L}(\psi,\dot{\psi},\nabla\psi) = 0, \tag{4.9}$$

which are subject to the boundary condition

$$\Big\langle D_{\nabla\psi}\mathcal{L}(\psi,\dot{\psi},\nabla\psi), \hat{\mathbf{n}}\Big\rangle = 0 \tag{4.10}$$

on $\partial\mathcal{B}$. For the Sine–Gordon field mentioned earlier we have

$$\ddot{\psi} - \nabla^2\psi + m^2\sin\psi = 0,\ \mathbf{x}\in\mathcal{B} \tag{4.11a}$$

$$\langle\hat{\mathbf{n}}, \nabla\psi\rangle\,,\ \mathbf{x}\in\partial\mathcal{B}. \tag{4.11b}$$

4.2.3 Linearised action and Euler–Lagrange equations

The action we have just discussed depended only on ψ and its derivatives. But we will often find ourselves studying actions that also depend on a small parameter ϵ and take the schematic form

$$\mathcal{S} = \int_{\mathcal{I}}\int_{\mathcal{B}}\Big[\mathcal{L}^{(0)}\Big(\psi,\dot{\psi},\nabla\psi\Big) + \epsilon\mathcal{L}^{(1)}\Big(\psi,\dot{\psi},\nabla\psi\Big)\Big]\,\mathrm{d}V\,\mathrm{d}t \equiv \hat{\mathcal{S}}^{(0)}[\psi] + \epsilon\hat{\mathcal{S}}^{(1)}[\psi]. \tag{4.12}$$

Let us make the *ansatz* that the motion may be written as a Taylor-series in ϵ,

$$\psi = \sum_i \epsilon^i\psi^{(i)}. \tag{4.13}$$

Substituting this into eq.(4.12) and expanding the action as a series in ϵ we find that

$$\mathcal{S} = \mathcal{S}^{(0)}\Big[\psi^{(0)} + \epsilon\psi^{(1)} + \epsilon^2\psi^{(2)}\Big] + \epsilon\mathcal{S}^{(1)}\Big[\psi^{(0)} + \epsilon\psi^{(1)}\Big] + \mathcal{O}\big(\epsilon^3\big)\,. \tag{4.14}$$

For notational convenience we define the shorthands

$$D\mathcal{L}(\psi,\dot\psi,\nabla\psi)\cdot\psi' \equiv D_\psi\mathcal{L}(\psi,\dot\psi,\nabla\psi)\psi' + D_{\dot\psi}\mathcal{L}(\psi,\dot\psi,\nabla\psi)\dot\psi' + \Big\langle D_{\nabla\psi}\mathcal{L}(\psi,\dot\psi,\nabla\psi), \nabla\psi'\Big\rangle \tag{4.15}$$

$$\begin{aligned}\psi''\cdot D^2\mathcal{L}(\psi,\dot\psi,\nabla\psi)\cdot\psi' \equiv{}& D^2_{\psi\psi}\mathcal{L}(\psi,\dot\psi,\nabla\psi)\psi'\psi'' + D^2_{\psi\dot\psi}\mathcal{L}(\psi,\dot\psi,\nabla\psi)\Big(\psi'\dot\psi'' + \psi''\dot\psi'\Big)\\ &+(\text{all other partial derivative terms})\end{aligned} \tag{4.16}$$

for $\mathcal{L}^{(0)}$'s and $\mathcal{L}^{(1)}$'s first and second partial derivatives. Using this notation we can write the action succinctly as

$$\begin{aligned}\mathcal{S} = {}& \mathcal{S}^{(0)}\Big[\psi^{(0)}\Big]\\ &+\epsilon\Big\{\mathcal{S}^{(1)}\Big[\psi^{(0)}\Big] + \int_{\mathcal{I}}\int_{\mathcal{B}} D\mathcal{L}^{(0)}\cdot\psi^{(1)}\,\mathrm{d}V\,\mathrm{d}t\Big\}\\ &+\epsilon^2\Big\{\frac{1}{2}\int_{\mathcal{I}}\int_{\mathcal{B}}\psi^{(1)}\cdot D^2\mathcal{L}^{(0)}\cdot\psi^{(1)}\,\mathrm{d}V\,\mathrm{d}t + \int_{\mathcal{I}}\int_{\mathcal{B}} D\mathcal{L}^{(1)}\cdot\psi^{(1)}\,\mathrm{d}V\,\mathrm{d}t\\ &\qquad + \int_{\mathcal{I}}\int_{\mathcal{B}} D\mathcal{L}^{(0)}\cdot\psi^{(2)}\,\mathrm{d}V\,\mathrm{d}t\Big\}\,,\end{aligned} \tag{4.17}$$

where it is understood that the derivatives are evaluated at the zeroth-order field configuration. Now, the terms in $D\mathcal{L}^{(0)}$ vanish *if we choose $\psi^{(0)}$ to be the solution to the zeroth-order equations of motion,* as is standard in perturbation theory. We can then neglect $\hat{\mathcal{S}}^{(0)}[\psi^{(0)}]$ and $\hat{\mathcal{S}}^{(1)}[\psi^{(0)}]$ as well because they are known constants. All in all, the action can be written as

$$\mathcal{S} = \epsilon^2\mathcal{S}^{(2)} + \mathcal{O}\big(\epsilon^3\big)\,, \tag{4.18}$$

where the *effective second-order action* $\mathcal{S}^{(2)}$ is given by

$$\mathcal{S}^{(2)} \equiv \frac{1}{2}\int_{\mathcal{I}}\int_{\mathcal{B}}\psi^{(1)}\cdot D^2\mathcal{L}^{(0)}\cdot\psi^{(1)}\,\mathrm{d}V\,\mathrm{d}t + \int_{\mathcal{I}}\int_{\mathcal{B}} D\mathcal{L}^{(1)}\cdot\psi^{(1)}\,\mathrm{d}V\,\mathrm{d}t. \tag{4.19}$$

The linearised Euler–Lagrange equations governing $\psi^{(1)}$ are obtained by demanding that $\mathcal{S}^{(2)}$ be extremized by $\psi^{(1)}$. The variation is

$$\delta\mathcal{S}^{(2)} = \int_{\mathcal{I}}\int_{\mathcal{B}}\Big[\psi^{(1)}\cdot D^2\mathcal{L}^{(0)}\cdot\delta\psi^{(1)} + D\mathcal{L}^{(1)}\cdot\delta\psi^{(1)}\Big]\,\mathrm{d}V\,\mathrm{d}t. \tag{4.20}$$

If we now substitute an arbitrary test-function ψ' for $\delta\psi$ (with ψ' obeying the same endpoint conditions as $\delta\psi$) we obtain

$$\int_{\mathcal{I}}\int_{\mathcal{B}}\psi'\cdot D^2\mathcal{L}^{(0)}\cdot\psi^{(1)}\,\mathrm{d}V\,\mathrm{d}t = -\int_{\mathcal{I}}\int_{\mathcal{B}} D\mathcal{L}^{(1)}\cdot\psi'\,\mathrm{d}V\,\mathrm{d}t. \tag{4.21}$$

Let us now return to our Sine–Gordon field once more and take the zeroth-order solution to be just $\psi^{(0)} = 0$; this simplifies the rest of the argument. In that case eq.(4.21) reduces to

$$\int_{\mathcal{I}}\int_{\mathcal{B}}\Big(\dot{\psi}'\dot{\psi}^{(1)} - \Big\langle\nabla\psi', \nabla\psi^{(1)}\Big\rangle - m^2\psi'\psi^{(1)}\Big)\,\mathrm{d}V\,\mathrm{d}t = -\int_{\mathcal{I}}\int_{\mathcal{B}} D\mathcal{L}^{(1)}\cdot\psi'\,\mathrm{d}V\,\mathrm{d}t. \tag{4.22}$$

If we perform some simple integrations by parts we arrive at

$$\begin{aligned}\int_{\mathcal{I}}\int_{\mathcal{B}}\psi'\Big[\ddot{\psi}^{(1)} - \nabla^2\psi^{(1)} + m^2\psi^{(1)} - \Big(D_{\psi}\mathcal{L}^{(1)} - \partial_t D_{\dot{\psi}}\mathcal{L}^{(1)} - \nabla\cdot D_{\nabla\psi}\mathcal{L}^{(1)}\Big)\Big]\,\mathrm{d}V\,\mathrm{d}t \\ + \int_{\mathcal{I}}\int_{\partial\mathcal{B}}\psi'\Big\langle\hat{\mathbf{n}}, \nabla\psi^{(1)} - D_{\nabla\psi}\mathcal{L}^{(1)}\Big\rangle\,\mathrm{d}S\,\mathrm{d}t = 0.\end{aligned} \tag{4.23}$$

Given that ψ' is arbitrary and that none of its time-derivatives occur in this expression, this is equivalent to

$$\begin{aligned}\int_{\mathcal{B}}\psi'\Big[\ddot{\psi}^{(1)} - \nabla^2\psi^{(1)} + m^2\psi^{(1)} - \Big(D_{\psi}\mathcal{L}^{(1)} - \partial_t D_{\dot{\psi}}\mathcal{L}^{(1)} - \nabla\cdot D_{\nabla\psi}\mathcal{L}^{(1)}\Big)\Big]\,\mathrm{d}V \\ + \int_{\partial\mathcal{B}}\psi'\Big\langle\hat{\mathbf{n}}, \nabla\psi^{(1)} - D_{\nabla\psi}\mathcal{L}^{(1)}\Big\rangle\,\mathrm{d}S = 0\end{aligned} \tag{4.24}$$

for all $t \in \mathcal{I}$, where we now interpret ψ' as a time-*independent* test-function. These are the linearised Euler–Lagrange equations in *weak form*. It is the weak form that is the important ingredient in the sort of Galerkin-expansion-based numerical solutions that we will discuss later and that we described in Chapter 2. Incidentally, we have obtained a forced *Klein–Gordon* equation. This is as expected given that we started with a Sine–Gordon Lagrangian.

The moral here is that we can linearise equations of motion about a given zeroth-order solution by expanding the action to *second-order* in a small parameter, but using only *first-order* fields. We can ignore terms in $\psi^{(2)}$ by choosing $\psi^{(0)}$ to satisfy the zeroth-order EoMs. We remark that these linearised equations of motion, along with their boundary conditions, could have been derived by first writing down the exact Euler–Lagrange equations associated with action (4.12) and then just linearising those equations directly. Nevertheless, deriving a quadratic effective action and then writing down the weak form is sometimes simpler, and it is certainly better suited to our ultimate numerical purposes. Weak forms are also useful because they contain the boundary conditions implicitly. Throughout this chapter we will present exact EoMs in strong form and linearised EoMs (generally) in weak form.

4.3 Rigid-body motion: a variational approach

We begin our study of rotating planets' elastodynamics by discussing the motion of a *rigid* body in an arbitrary potential field. Having first set out the necessary kinematics, we will see how Hamiltonian's principle can be used to derive the exact equations of motion. We then derive linearised equations and study the normal modes of a uniformly rotating rigid body. This is a simple model for the Earth that we will build on in Section 4.5. We finish by extending these ideas to $N \geq 2$ bodies interacting gravitationally.

This section has two main aims. First, it gives a self-contained overview of exact and linearised

rigid body motion. More importantly, though, it is a 'warm-up' for Section 4.5. This section runs through Section 4.5's derivations, developing the necessary ideas, but without the added complication of deformability.

4.3.1 Kinematics

The motion of a rigid body is described relative to a fixed *reference configuration*, with each particle labelled by its position within the associated *reference body* $\mathcal{B} \subseteq \mathbb{R}^3$, which is assumed to be connected, bounded, and have an open interior. At a time t, the position in physical space of the particle at $\mathbf{x} \in \mathcal{B}$ is written $\boldsymbol{\varphi}(\mathbf{x}, t)$. In this manner, we define a mapping

$$\boldsymbol{\varphi} : \mathcal{B} \times \mathbb{R} \mapsto \mathbb{R}^3, \tag{4.25}$$

which is called the *motion* of the body relative to the reference configuration. For a fixed time, t, the image of the mapping $\boldsymbol{\varphi}(\cdot, t)$ is written $\mathcal{B}_t$ and represents the region of physical space the body instantaneously occupies. It will be assumed that for each fixed time the mapping $\boldsymbol{\varphi}(\cdot, t) : \mathcal{B} \mapsto \mathcal{B}_t$ is smooth with a smooth inverse. For a rigid body it is conventional to take the reference configuration to be equal to the body's true configuration at $t = 0$, that is

$$\mathcal{B} = \mathcal{B}_0. \tag{4.26}$$

We are free to choose coordinates for the reference body such that $\mathcal{B}$'s centre-of-mass (CoM) lies at the origin. This means that

$$\int_{\mathcal{B}} \rho(\mathbf{x})\mathbf{x} \, \mathrm{d}V = 0, \tag{4.27}$$

where the *density* $\rho(\mathbf{x})$ denotes the mass per unit volume at the point $\mathbf{x} \in \mathcal{B}$. This choice of coordinates will give several simplifications in the following derivations.

The defining feature of rigid-body motion is that the distance between any two referential points $\mathbf{x}_1$ and $\mathbf{x}_2$ is constant throughout the motion:

$$\|\boldsymbol{\varphi}(\mathbf{x}_2, t) - \boldsymbol{\varphi}(\mathbf{x}_1, t)\| = \|\mathbf{x}_2 - \mathbf{x}_1\| \tag{4.28}$$

for all t. One can show that the most general motion for which this holds takes the form

$$\boldsymbol{\varphi}(\mathbf{x}, t) = \boldsymbol{\Phi}(t) + \mathbf{R}(t) \cdot \mathbf{x} \tag{4.29}$$

with

$$\boldsymbol{\Phi} : \mathcal{I} \mapsto \mathbb{R}^3 \tag{4.30}$$

$$\mathbf{R} : \mathcal{I} \mapsto \mathbf{SO}(3) \tag{4.31}$$

and where $\mathbf{SO}(3)$ is the *three-dimensional special orthogonal group*. $\boldsymbol{\Phi}$ represents the motion of

the CoM, as can be seen by substituting eq.(4.29) into the definition of the CoM:

$$CoM \equiv \frac{1}{m}\int_{\mathcal{B}} \rho(\mathbf{x})\boldsymbol{\varphi}(\mathbf{x},t)\,\mathrm{d}V = \boldsymbol{\Phi}(t) + \frac{1}{m}\mathbf{R}(t)\cdot\int_{\mathcal{B}} \rho(\mathbf{x})\mathbf{x}\,\mathrm{d}V. \tag{4.32}$$

The second term vanishes thanks to our choice of reference frame (4.27), so

$$\boldsymbol{\Phi}(t) = CoM. \tag{4.33}$$

The elements of $\mathbf{SO}(3)$ are rotation matrices, so the overall motion represented by eq.(4.29) is the sum of the motion *of* the CoM and an overall rotation *about* the CoM. This pleasant interpretation only holds because we chose to place the coordinate system's origin at the CoM.

4.3.2 An important tangent: matrix Lie groups, antisymmetric matrices and cross products

$\mathbf{SO}(3)$ is a *matrix Lie group* (e.g. Iserles, 2009) whose elements satisfy

$$\mathbf{R}^{-1} = \mathbf{R}^T \tag{4.34}$$

$$\det \mathbf{R} = 1. \tag{4.35}$$

If we differentiate the relation $\mathbf{R}^T\mathbf{R} = \mathbf{1}$ with respect to time we find that

$$\dot{\mathbf{R}}^T\mathbf{R} + \mathbf{R}^T\dot{\mathbf{R}} = 0, \tag{4.36}$$

which can be rearranged to give

$$\mathbf{R}^T\dot{\mathbf{R}} = -\left(\mathbf{R}^T\dot{\mathbf{R}}\right)^T. \tag{4.37}$$

This shows that $\mathbf{R}^T\dot{\mathbf{R}}$ is *antisymmetric*, that is,

$$\dot{\mathbf{R}} = \mathbf{R}\boldsymbol{\Omega} \tag{4.38}$$

for an antisymmetric matrix $\boldsymbol{\Omega}$ that is known in the context of rigid body motion as the *body angular velocity*. If $\mathbf{R} = \mathbf{1}$, then $\dot{\mathbf{R}}$ itself is antisymmetric. This shows that $\mathbf{SO}(3)$'s tangent space at the identity consists of all antisymmetric (3×3) matrices. This space – which is a *vector space* – is defined to be $\mathfrak{so}(3)$, the *Lie algebra* of $\mathbf{SO}(3)$.

$\mathfrak{so}(3)$ is *spanned* by the three (3×3) antisymmetric matrices $\mathbf{J}_{1,2,3}$ known as the *generators* of $\mathbf{SO}(3)$. These matrices have components

$$[\mathbf{J}_\alpha]_{ij} = -\varepsilon_{\alpha ij}, \tag{4.39}$$

taking the explicit forms

$$\mathbf{J}_1 = \begin{pmatrix} 0 & 0 & 0 \\ 0 & 0 & -1 \\ 0 & 1 & 0 \end{pmatrix} \tag{4.40a}$$

$$\mathbf{J}_2 = \begin{pmatrix} 0 & 0 & 1 \\ 0 & 0 & 0 \\ -1 & 0 & 0 \end{pmatrix} \tag{4.40b}$$

$$\mathbf{J}_3 = \begin{pmatrix} 0 & -1 & 0 \\ 1 & 0 & 0 \\ 0 & 0 & 0 \end{pmatrix}. \tag{4.40c}$$

It follows that they satisfy the commutation relations

$$[\mathbf{J}_\alpha, \mathbf{J}_\beta] = \varepsilon_{\alpha\beta\gamma}\delta^{\gamma\mu}\mathbf{J}_\mu \tag{4.41}$$

and that their inner product is

$$g_{\alpha\beta} \equiv \langle \mathbf{J}_\alpha, \mathbf{J}_\beta \rangle_{\mathfrak{so}(3)} = 2\delta_{\alpha\beta}, \tag{4.42}$$

where we have defined the $\mathfrak{so}(3)$ *inner product* as

$$\big\langle \mathbf{\Omega}, \mathbf{\Omega}' \big\rangle_{\mathfrak{so}(3)} = -\mathrm{tr}\big(\mathbf{\Omega}\mathbf{\Omega}'\big) \tag{4.43}$$

(*c.f.* Appendix B.1.2, eq. B.16). In the preceding expressions ε_{ijk} is the *Levi–Civita symbol*, which we define with the sign convention

$$\varepsilon_{123} = +1. \tag{4.44}$$

The $\{\mathbf{J}_\alpha\}$ are referred to as the generators of $\mathbf{SO}(3)$ because any linear combination of them can be exponentiated to give a rotation matrix, that is, all $\mathbf{R} \in \mathbf{SO}(3)$ can be written as

$$\mathbf{R} = \exp\left(\theta \sum_i n_i \mathbf{J}_i\right), \tag{4.45}$$

where the angle of rotation is $\theta \in [0, 2\pi)$, and the unit vector $\mathbf{n} \in \mathbb{S}^2$ gives the axis of rotation. It is clear from this expression that a rotation matrix represents three degrees of freedom. We define rotations (by an angle θ) about the x-, y- and z-axes respectively as

$$\mathbf{R}_x(\theta) = \exp(\theta \mathbf{J}_1) \tag{4.46a}$$

$$\mathbf{R}_y(\theta) = \exp(\theta \mathbf{J}_2) \tag{4.46b}$$

$$\mathbf{R}_z(\theta) = \exp(\theta \mathbf{J}_3). \tag{4.46c}$$

It is also helpful to define the *adjoint representations* of $\mathbf{SO}(3)$. An element of $\mathbf{SO}(3)$ can operate

on an element of $\mathfrak{so}(3)$ to produce another element of $\mathfrak{so}(3)$ through the so-called *big adjoint* operator

$$\mathsf{Ad} : \mathfrak{so}(3) \times \mathbf{SO}(3) \mapsto \mathfrak{so}(3), \tag{4.47}$$

defined so that it actively rotates the element of $\mathfrak{so}(3)$ by the rotation matrix:

$$\mathsf{Ad}_{\mathbf{R}} \cdot \boldsymbol{\Omega}' \equiv \mathbf{R}\boldsymbol{\Omega}'\mathbf{R}^T. \tag{4.48}$$

The *little adjoint* operator, on the other hand, is the derivative of $\mathsf{Ad}_{\mathbf{R}}$ with respect to $\mathbf{R}$. Expanding $\mathbf{R}$ about the identity as $\mathbf{R} = \mathbf{1} + \boldsymbol{\Omega}$,

$$\begin{aligned}\mathsf{Ad}_{\mathbf{R}} \cdot \boldsymbol{\Omega}' &= (\mathbf{1} + \boldsymbol{\Omega})\,\boldsymbol{\Omega}'(\mathbf{1} - \boldsymbol{\Omega}) \\ &= \boldsymbol{\Omega}' + \left[\boldsymbol{\Omega}, \boldsymbol{\Omega}'\right] + \dots \\ &\equiv \boldsymbol{\Omega}' + \mathsf{ad}_{\boldsymbol{\Omega}} \cdot \boldsymbol{\Omega}' + \dots .\end{aligned} \tag{4.49}$$

ad therefore satisfies

$$\mathsf{ad} : \mathfrak{so}(3) \times \mathfrak{so}(3) \mapsto \mathfrak{so}(3), \tag{4.50}$$

with its action defined as the *commutator* of two antisymmetric matrices:

$$\mathsf{ad}_{\boldsymbol{\Omega}} \cdot \boldsymbol{\Omega}' \equiv \left[\boldsymbol{\Omega}, \boldsymbol{\Omega}'\right]. \tag{4.51}$$

The $\{\mathbf{J}_\alpha\}$ form a basis for the space of antisymmetric matrices. That is, we may write any $\boldsymbol{\Omega} \in \mathfrak{so}(3)$ as

$$\boldsymbol{\Omega} = \Omega^\alpha \mathbf{J}_\alpha \tag{4.52}$$

for some set of components $\Omega^{1,2,3}$. This basis is orthogonal, but it is *not* normalised, so when we write expressions in component form we must include a metric and distinguish between co- and contravariant indices as we did in eq.(4.41). The covariant components of the metric were defined in eq.(4.42) to be

$$g_{\alpha\beta} = 2\delta_{\alpha\beta}, \tag{4.53}$$

and thus its contravariant components are trivially

$$g^{\alpha\beta} = \frac{1}{2}\delta^{\alpha\beta}. \tag{4.54}$$

Throughout this chapter we will write such component-form expressions using 'up and down' Greek indices. On the other hand, we will sometimes need to view the $\{\mathbf{J}_\alpha\}$, not as basis vectors, but as matrices that act on elements of $\mathbb{R}^3$ such as Cartesian position vectors. In those situations we will denote the components of the matrices and vectors by 'downstairs' Roman indices (as in

eqs. 4.39 and 4.70). We use the summation convention unless stated otherwise.

This might all seem a little excessive. After all, we could easily produce an orthonormal basis for $\mathfrak{so}(3)$ if we just multiplied each generator by $1/\sqrt{2}$. But the resulting basis vectors would *not* then obey the commutation relations (4.41), and it is desirable that they should because in that case $\boldsymbol{\Omega}$ has a ready physical interpretation. Specifically, its contravariant components $\{\Omega^\alpha\}$ will be equal to the *Cartesian* components of the standard body angular velocity vector discussed in the physical rigid body literature (e.g. Landau & Lifshitz, 1976; Rajeev, 2013). It therefore seems preferable to do as little damage as possible to the commutation relations and accept a little extra complication when performing calculations in component-form.

As an example, let us calculate $[\mathsf{ad}_{\boldsymbol{\Omega}}]_\alpha{}^\beta$, the *mixed* components of $\mathsf{ad}_{\boldsymbol{\Omega}}$ with respect to the generator basis. If we also expand $\boldsymbol{\Omega}$ as $\Omega^\gamma \mathbf{J}_\gamma$, then

$$\begin{aligned}
[\mathsf{ad}_{\boldsymbol{\Omega}}]_\alpha{}^\beta &= [\mathsf{ad}_{\boldsymbol{\Omega}}]_{\alpha\mu}\, g^{\mu\beta} \\
&= \langle \mathbf{J}_\alpha, \mathsf{ad}_{\boldsymbol{\Omega}} \cdot \mathbf{J}_\mu \rangle_{\mathfrak{so}(3)}\, g^{\mu\beta} \\
&= \Omega^\gamma \langle \mathbf{J}_\alpha, [\mathbf{J}_\gamma, \mathbf{J}_\mu] \rangle_{\mathfrak{so}(3)}\, g^{\mu\beta}.
\end{aligned} \tag{4.55}$$

Now we use the commutation relation (4.41) to write

$$[\mathbf{J}_\gamma, \mathbf{J}_\mu] = \varepsilon_{\gamma\mu\nu}\delta^{\nu\rho}\mathbf{J}_\rho. \tag{4.56}$$

With this,

$$\begin{aligned}
[\mathsf{ad}_{\boldsymbol{\Omega}}]_\alpha{}^\beta &= \Omega^\gamma \varepsilon_{\gamma\mu\nu}\delta^{\nu\rho} g_{\alpha\rho} g^{\mu\beta} \\
&= \Omega^\gamma \varepsilon_{\nu\gamma\mu}\delta^{\nu\rho}(2\delta_{\alpha\rho})\left(\frac{1}{2}\delta^{\mu\beta}\right) \\
&= \Omega^\gamma \varepsilon_{\alpha\gamma\mu}\delta^{\mu\beta},
\end{aligned} \tag{4.57}$$

where in the second line we have used the metric's definition (4.42) and contracted some indices. $\mathsf{ad}_{\boldsymbol{\Omega}}$'s components can thus be rewritten in matrix form as

$$[\mathsf{ad}_{\boldsymbol{\Omega}}]_\alpha{}^\beta = \begin{bmatrix} 0 & -\Omega^3 & \Omega^2 \\ \Omega^3 & 0 & -\Omega^1 \\ -\Omega^2 & \Omega^1 & 0 \end{bmatrix}. \tag{4.58}$$

This matrix is the representation of an operator on $\mathfrak{so}(3)$, so we have written it with square brackets to distinguish it from 'true' matrices such as the elements of $\mathbf{SO}(3)$ and $\mathfrak{so}(3)$.

The little adjoint operator acts on $\mathfrak{so}(3)$ analogously to how the cross product acts on $\mathbb{R}^3$. Just as $\mathbf{a} \times \mathbf{a} = 0$, so $\mathsf{ad}_{\boldsymbol{\Omega}} \cdot \boldsymbol{\Omega} = 0$. And we can further the analogy by looking at $\mathsf{ad}_{\boldsymbol{\Omega}} \cdot \boldsymbol{\omega}$, with

$\boldsymbol{\omega} = \omega^\alpha \mathbf{J}_\alpha$. The operator is expanded on the $\mathbf{J}_\alpha$-basis as

$$\begin{aligned}\mathsf{ad}_{\boldsymbol{\Omega}} \cdot \boldsymbol{\omega} &= \Omega^\alpha \omega^\beta [\mathbf{J}_\alpha, \mathbf{J}_\beta] \\ &= \left(\varepsilon_{\gamma\alpha\beta}\Omega^\alpha\omega^\beta\right)\delta^{\gamma\mu}\mathbf{J}_\mu \\ &\equiv (\mathsf{ad}_{\boldsymbol{\Omega}} \cdot \boldsymbol{\omega})^\mu \, \mathbf{J}_\mu. \end{aligned} \tag{4.59}$$

If we choose to view $\{\Omega^\alpha\}$ and $\{\omega^\alpha\}$ as the components of *Cartesian* vectors $\tilde{\boldsymbol{\Omega}}$ and $\tilde{\boldsymbol{\omega}}$, then it is clear that the $\mathbf{J}_\alpha$-components of $\mathsf{ad}_{\boldsymbol{\Omega}} \cdot \boldsymbol{\omega}$ are just the Cartesian components of $\tilde{\boldsymbol{\Omega}} \times \tilde{\boldsymbol{\omega}}$.

Finally, let us ask how torques map from $\mathbb{R}^3$ into $\mathfrak{so}(3)$. Torques commonly take the form

$$\tilde{\mathbf{L}} = \mathbf{x} \times \mathbf{f}, \tag{4.60}$$

for some position vector $\mathbf{x}$ and force $\mathbf{f}$. We may write the corresponding antisymmetric matrix $\mathbf{L} \in \mathfrak{so}(3)$ as

$$\mathbf{L} = \mathbf{x} \wedge \mathbf{f}, \tag{4.61}$$

after defining the *skew-symmetric product* $\wedge : \mathbb{R}^3 \times \mathbb{R}^3 \mapsto \mathfrak{so}(3)$, whose action on two arbitrary vectors $\mathbf{a}$ and $\mathbf{b}$ is given by

$$\mathbf{a} \wedge \mathbf{b} = \frac{1}{2}(\mathbf{b} \otimes \mathbf{a} - \mathbf{a} \otimes \mathbf{b}) \tag{4.62}$$

(e.g. Stone & Goldbart, 2009). Note that our definition of $\wedge$ contains an extra minus sign compared to that of Stone & Goldbart; this is to ensure that $\mathbf{L}$'s covariant components are the same as the components of $\tilde{\mathbf{L}}$:

$$\begin{aligned} L_\alpha &= \langle \mathbf{J}_\alpha, \mathbf{x} \wedge \mathbf{f} \rangle_{\mathfrak{so}(3)} \\ &= \frac{1}{2}\mathrm{tr}[\mathbf{J}_\alpha(\mathbf{x} \otimes \mathbf{f} - \mathbf{f} \otimes \mathbf{x})] \\ &= -\frac{1}{2}\varepsilon_{\alpha ij}(x_j f_i - x_i f_j) \\ &= \varepsilon_{\alpha ij} x_i f_j \\ &= \tilde{L}_\alpha. \end{aligned} \tag{4.63}$$

The wedge product of two vectors also obeys the relation

$$\mathsf{Ad}_{\mathbf{R}} \cdot (\mathbf{a} \wedge \mathbf{b}) = (\mathbf{R} \cdot \mathbf{a}) \wedge (\mathbf{R} \cdot \mathbf{b}), \tag{4.64}$$

which is analogous to the standard result

$$\mathbf{R} \cdot (\mathbf{a} \times \mathbf{b}) = (\mathbf{R} \cdot \mathbf{a}) \times (\mathbf{R} \cdot \mathbf{b}). \tag{4.65}$$

The little adjoint, meanwhile, acts according to

$$\mathsf{ad}_{\boldsymbol{\Omega}} \cdot (\mathbf{a} \wedge \mathbf{b}) = (\boldsymbol{\Omega} \cdot \mathbf{a}) \wedge \mathbf{b} + \mathbf{a} \wedge (\boldsymbol{\Omega} \cdot \mathbf{b}) \,. \tag{4.66}$$

We will make no further mention of cross products henceforward, working exclusively with their skew-symmetric cousins.

4.3.3 Back to kinematics

The antisymmetric matrix $\boldsymbol{\Omega}$ defined above by

$$\boldsymbol{\Omega} \equiv \mathbf{R}^T \dot{\mathbf{R}} \tag{4.67}$$

is the *body angular velocity*. (We remark that one can also define the *spatial angular velocity* by $\boldsymbol{\omega} \equiv \mathsf{Ad}_{\mathbf{R}} \cdot \boldsymbol{\Omega}$, but it is not a quantity that we will use in this chapter.) Using $\boldsymbol{\Omega}$ we can express the rigid body's velocity as

$$\dot{\boldsymbol{\varphi}} = \dot{\boldsymbol{\Phi}} + \mathbf{R}\boldsymbol{\Omega} \cdot \mathbf{x}. \tag{4.68}$$

Using this, and recalling constraint (4.27), we can express the body's *kinetic energy* in terms of $\boldsymbol{\Phi}$ and $\boldsymbol{\Omega}$ as

$$\begin{aligned} \mathcal{T} &\equiv \int_{\mathcal{B}} \frac{1}{2} \rho(\mathbf{x}) \|\dot{\boldsymbol{\varphi}}(\mathbf{x}, t)\|^2 \, \mathrm{d}V \\ &= \frac{1}{2} m \|\dot{\boldsymbol{\Phi}}\|^2 + \frac{1}{2} \int_{\mathcal{B}} \rho \langle \boldsymbol{\Omega} \cdot \mathbf{x}, \boldsymbol{\Omega} \cdot \mathbf{x} \rangle \, \mathrm{d}V. \end{aligned} \tag{4.69}$$

We then expand $\boldsymbol{\Omega}$ on the basis provided by $\{\mathbf{J}_\alpha\}$ and use their definitions (4.39) to rewrite the rotational kinetic energy as

$$\begin{aligned} \frac{1}{2} \int_{\mathcal{B}} \rho \langle \boldsymbol{\Omega} \cdot \mathbf{x}, \boldsymbol{\Omega} \cdot \mathbf{x} \rangle \, \mathrm{d}V &= \frac{1}{2} \Omega^\alpha \Omega^\beta \int_{\mathcal{B}} \rho \langle \mathbf{J}_\alpha \cdot \mathbf{x}, \mathbf{J}_\beta \cdot \mathbf{x} \rangle \, \mathrm{d}V \\ &= \frac{1}{2} \Omega^\alpha \Omega^\beta \int_{\mathcal{B}} \rho \varepsilon_{\alpha i p} x_p \epsilon_{\beta i q} x_q \, \mathrm{d}V \\ &= \frac{1}{2} \Omega^\alpha \Omega^\beta \int_{\mathcal{B}} \rho \Big(\|\mathbf{x}\|^2 \, \delta_{\alpha\beta} - x_\alpha x_\beta \Big) \, \mathrm{d}V \\ &\equiv \frac{1}{2} \langle \boldsymbol{\Omega}, \mathbb{I} \cdot \boldsymbol{\Omega} \rangle_{\mathfrak{so}(3)} \,, \end{aligned} \tag{4.70}$$

where in the final line we have introduced the *body moment of inertia* operator $\mathbb{I} : \mathfrak{so}(3) \mapsto \mathfrak{so}(3)$. $\mathbb{I}$ is a symmetric operator, with covariant $\mathbf{J}_\alpha$-components

$$I_{\alpha\beta} = \int_{\mathcal{B}} \rho \Big(\|\mathbf{x}\|^2 \, \delta_{\alpha\beta} - x_\alpha x_\beta \Big) \, \mathrm{d}V. \tag{4.71}$$

With this the kinetic energy assumes its final form

$$\mathcal{T} = \frac{1}{2} m \|\dot{\boldsymbol{\Phi}}\|^2 + \frac{1}{2} \langle \boldsymbol{\Omega}, \mathbb{I} \cdot \boldsymbol{\Omega} \rangle_{\mathfrak{so}(3)} \,. \tag{4.72}$$

The kinetic energy has thus been partitioned neatly into energy associated with the CoM's linear motion, and energy due to rotation about the centre of mass. Again (and at the risk of labouring the point) this clean division would not have emerged had we chosen to work in a coordinate system in which eq.(4.27) did not hold: $\mathbf{\Phi}$ would not represent the body's centre of mass, and $\mathcal{T}$ would contain a cross-term between $\mathbf{\Phi}$ and $\mathbf{R}$. The resulting system would of course describe the same dynamics, but without such a straightforward interpretation.

4.3.4 Variational principle

The action for our rigid body is

$$\mathcal{S} = \int_{\mathcal{I}} (\mathcal{T} - \mathcal{V}) \, \mathrm{d}t. \tag{4.73}$$

We have already derived the form of $\mathcal{T}$ for an isolated rigid body. As for $\mathcal{V}$, in this section we will consider an arbitrary external potential

$$\mathcal{V} : \mathbb{R}^3 \times \mathbf{SO}(3) \mapsto \mathbb{R}. \tag{4.74}$$

For the sorts of problems we have in mind $\mathcal{V}$ might take the form

$$\mathcal{V}(\mathbf{\Phi}, \mathbf{R}) = m^* \int_{\mathcal{B}} \rho(\mathbf{x}) \Gamma(\mathbf{\Phi} + \mathbf{R} \cdot \mathbf{x}) \, \mathrm{d}V, \tag{4.75}$$

where

$$\Gamma(\mathbf{y}) = -\frac{G}{\|\mathbf{y}\|} \tag{4.76}$$

with G Newton's gravitational constant; this represents the rigid body's gravitational potential energy due to point mass m^* at the origin. The sum of several such terms could be used to model the effect of tidal forces due to the Moon, Sun and other bodies. For now, though, we will keep the potential general.

With these preliminaries we find that the rigid body action is

$$\mathcal{S} = \int_{\mathcal{I}} \left(\frac{1}{2} m \|\dot{\mathbf{\Phi}}\|^2 + \frac{1}{2} \langle \mathbf{\Omega}, \mathbb{I} \cdot \mathbf{\Omega} \rangle_{\mathfrak{so}(3)} - \mathcal{V}(\mathbf{\Phi}, \mathbf{R}) \right) \mathrm{d}t. \tag{4.77}$$

This is not the full story, though. The action as written appears to be a functional of three independent functions: $\mathbf{\Phi}$, $\mathbf{R}$ and $\mathbf{\Omega}$. But $\mathbf{R}$ and $\mathbf{\Omega}$ *are not independent*, linked as they are by definition (4.67); in order to obtain the correct dynamics we must include that definition. One approach would be to impose (4.67) only when the action is varied. In other words, $\mathbf{\Omega}$ would be subject not to wholly arbitrary variation, but only to variations that satisfy (4.67). Such an approach brings one to the EoMs quickly, but it is not clear to this author how it can be used to find the linearised EoMs (see Section 4.3.6 and later). We will therefore use a different method whereby constraint (4.67) is implicitly imposed on the action through a Lagrange multiplier. Not only will this offer a systematic way of deriving linearised EoMs, but it also introduces a

principal theme of this chapter, namely that Lagrange multipliers provide a convenient method of imposing complicated constraints on a system. We proceed by defining the Lagrange multiplier

$$\mathbf{\Lambda} : \mathcal{I} \mapsto \mathfrak{so}(3) \tag{4.78}$$

and rewriting the rigid-body action as

$$\mathcal{S} = \hat{\mathcal{S}}[\mathbf{\Phi}, \mathbf{R}, \mathbf{\Omega}, \mathbf{\Lambda}] = \int_{\mathcal{I}} \left(\frac{1}{2} m \|\dot{\mathbf{\Phi}}\|^2 + \frac{1}{2} \langle \mathbf{\Omega}, \mathbb{I} \cdot \mathbf{\Omega} \rangle_{\mathfrak{so}(3)} + \left\langle \mathbf{\Lambda}, \mathbf{R}^T \dot{\mathbf{R}} - \mathbf{\Omega} \right\rangle_{\mathfrak{so}(3)} - \mathcal{V}(\mathbf{\Phi}, \mathbf{R}) \right) \mathrm{d}t. \tag{4.79}$$

With the inclusion of the Lagrange multiplier term $\mathbf{R}$, $\mathbf{\Omega}$ and $\mathbf{\Lambda}$ can all be considered mutually independent.

4.3.5 Euler–Lagrange equations

We now vary $\mathcal{S}$ with respect to $\mathbf{\Phi}$, $\mathbf{R}$, $\mathbf{\Omega}$ and $\mathbf{\Lambda}$, subject to fixed endpoint conditions. Given that $\mathbf{\Phi}$, $\mathbf{\Omega}$ and $\mathbf{\Lambda}$ are all vector-valued functions, they can be varied just by adding a small element of the relevant vector space:

$$\mathbf{\Phi} \to \mathbf{\Phi} + \delta\mathbf{\Phi} \tag{4.80a}$$

$$\mathbf{\Omega} \to \mathbf{\Omega} + \delta\mathbf{\Omega} \tag{4.80b}$$

$$\mathbf{\Lambda} \to \mathbf{\Lambda} + \delta\mathbf{\Lambda}, \tag{4.80c}$$

with $\delta\mathbf{\Phi} \in \mathbb{R}^3$ and $\delta\mathbf{\Omega}, \delta\mathbf{\Lambda}, \in \mathfrak{so}(3)$. We cannot do this with $\mathbf{R}$, however, because $\mathbf{SO}(3)$ is not a vector space. Instead we write a small change in $\mathbf{R}$ as

$$\mathbf{R} \to \mathbf{R} \mathrm{e}^{\delta\boldsymbol{\theta}} \tag{4.81}$$

for arbitrary small $\delta\boldsymbol{\theta} \in \mathfrak{so}(3)$; this way the group structure is respected and the right hand side is guaranteed to be an element of $\mathbf{SO}(3)$. The exponential is then Taylor-expanded to give

$$\mathbf{R} \to \mathbf{R} + \mathbf{R}\delta\boldsymbol{\theta}. \tag{4.82}$$

Substituting these expressions into $\mathcal{S}$, neglecting all cross terms between small quantities, and defining the *net external force and torque* as

$$\mathbf{f} = -D_{\mathbf{\Phi}} \mathcal{V} \tag{4.83}$$

$$\mathbf{L} = -\mathbf{R}^T D_{\mathbf{R}} \mathcal{V}, \tag{4.84}$$

the action varies to $\mathcal{S} \to \mathcal{S} + \delta\mathcal{S}$, with $\delta\mathcal{S}$ given by

$$\delta\mathcal{S} = \int_{\mathcal{I}} \Big(m\Big\langle \dot{\boldsymbol{\Phi}}, \delta\dot{\boldsymbol{\Phi}} \Big\rangle + \langle \delta\boldsymbol{\Omega}, \mathbb{I}\cdot\boldsymbol{\Omega} \rangle_{\mathfrak{so}(3)} + \Big\langle \boldsymbol{\Lambda}, (\mathbf{R}\delta\boldsymbol{\theta})^T \dot{\mathbf{R}} + \mathbf{R}^T \partial_t (\mathbf{R}\delta\boldsymbol{\theta}) - \delta\boldsymbol{\Omega} \Big\rangle_{\mathfrak{so}(3)} + \Big\langle \delta\boldsymbol{\Lambda}, \mathbf{R}^T\dot{\mathbf{R}} - \boldsymbol{\Omega} \Big\rangle_{\mathfrak{so}(3)} + \langle \mathbf{f}, \delta\boldsymbol{\Phi} \rangle + \langle \mathbf{L}, \delta\boldsymbol{\theta} \rangle_{\mathfrak{so}(3)} \Big)\, \mathrm{d}t. \tag{4.85}$$

We can simplify the term in $\boldsymbol{\Lambda}$ by substituting the relationship $\mathbf{R}^T\dot{\mathbf{R}} = \boldsymbol{\Omega}$ directly into the action *except where it is enforced by the Lagrange multiplier*; recalling the definition (4.51) of the little adjoint operator that term becomes

$$\langle \boldsymbol{\Lambda}, \partial_t\delta\boldsymbol{\theta} + [\boldsymbol{\Omega}, \delta\boldsymbol{\theta}] - \delta\boldsymbol{\Omega} \rangle_{\mathfrak{so}(3)} = \langle \boldsymbol{\Lambda}, (\partial_t + \mathsf{ad}_{\boldsymbol{\Omega}})\cdot\boldsymbol{\theta} - \delta\boldsymbol{\Omega} \rangle_{\mathfrak{so}(3)}\,. \tag{4.86}$$

Performing a few other easy rearrangements we arrive at

$$\delta\mathcal{S} = \int_{\mathcal{I}} \Big(\Big\langle \delta\boldsymbol{\Phi}, -m\ddot{\boldsymbol{\Phi}} + \mathbf{f} \Big\rangle + \langle \delta\boldsymbol{\Omega}, \mathbb{I}\cdot\boldsymbol{\Omega} - \boldsymbol{\Lambda} \rangle_{\mathfrak{so}(3)} + \langle \boldsymbol{\Lambda}, (\partial_t + \mathsf{ad}_{\boldsymbol{\Omega}})\cdot\delta\boldsymbol{\theta} \rangle_{\mathfrak{so}(3)} + \Big\langle \delta\boldsymbol{\Lambda}, \mathbf{R}^T\dot{\mathbf{R}} - \boldsymbol{\Omega} \Big\rangle_{\mathfrak{so}(3)} + \langle \delta\boldsymbol{\theta}, \mathbf{L} \rangle_{\mathfrak{so}(3)} \Big)\, \mathrm{d}t. \tag{4.87}$$

Given that $\delta\boldsymbol{\theta}$ vanishes at the start- and end-times, one can show that

$$\langle \boldsymbol{\Lambda}, (\partial_t + \mathsf{ad}_{\boldsymbol{\Omega}})\cdot\delta\boldsymbol{\theta} \rangle_{\mathfrak{so}(3)} = -\langle\!\langle (\partial_t + \mathsf{ad}_{\boldsymbol{\Omega}})\cdot\boldsymbol{\Lambda}, \delta\boldsymbol{\theta} \rangle_{\mathfrak{so}(3)}\,, \tag{4.88}$$

so we may finally write $\delta\mathcal{S}$ as

$$\delta\mathcal{S} = \int_{\mathcal{I}} \Big(\Big\langle \delta\boldsymbol{\Phi}, -m\ddot{\boldsymbol{\Phi}} + \mathbf{f} \Big\rangle + \langle \delta\boldsymbol{\Omega}, \mathbb{I}\cdot\boldsymbol{\Omega} - \boldsymbol{\Lambda} \rangle - \langle \delta\boldsymbol{\theta}, (\partial_t + \mathsf{ad}_{\boldsymbol{\Omega}})\cdot\boldsymbol{\Lambda} - \mathbf{L} \rangle + \Big\langle \delta\boldsymbol{\Lambda}, \mathbf{R}^T\dot{\mathbf{R}} - \boldsymbol{\Omega} \Big\rangle_{\mathfrak{so}(3)} \Big)\, \mathrm{d}t. \tag{4.89}$$

The Euler–Lagrange equations are thus seen to be:

$$m\ddot{\boldsymbol{\Phi}} = \mathbf{f}(\boldsymbol{\Phi}, \mathbf{R}) \tag{4.90a}$$

$$(\partial_t + \mathsf{ad}_{\boldsymbol{\Omega}})\,\mathbb{I}\cdot\boldsymbol{\Omega} = \mathbf{L}(\boldsymbol{\Phi}, \mathbf{R}) \tag{4.90b}$$

$$\dot{\mathbf{R}} = \mathbf{R}\boldsymbol{\Omega} \tag{4.90c}$$

We have recovered Newton's Second Law for the body's CoM, while $\boldsymbol{\Omega}$ obeys the *Euler equations*. The kinematic identity (4.90c) that completes the system is the so-called *reconstruction equation*.

For the point mass potential (4.75) the force and torque take the following forms. Differentiation with respect to $\boldsymbol{\Phi}$ proceeds readily to give

$$\mathbf{f} = -D_{\boldsymbol{\Phi}}\mathcal{V}(\boldsymbol{\Phi}, \mathbf{R}) = -m^* \int_{\mathcal{B}} \rho\nabla\Gamma(\boldsymbol{\Phi} + \mathbf{R}\cdot\mathbf{x})\, \mathrm{d}V. \tag{4.91}$$

Computing the torque requires the derivative of $\mathcal{V}$ with respect to $\mathbf{R}$, which is perhaps not so

familiar. One way to calculate it is to use the definition

$$\mathcal{V}(\mathbf{\Phi}, \mathbf{R} + \delta\mathbf{R}) = \mathcal{V}(\mathbf{\Phi}, \mathbf{R}) + \langle D_{\mathbf{R}}\mathcal{V}(\mathbf{\Phi}, \mathbf{R}), \delta\mathbf{R}\rangle + \mathcal{O}\big(|\mathbf{R}|^2\big)\,, \tag{4.92}$$

so that we can keep things in terms of scalars. For the point mass potential we find

$$\begin{aligned}\langle D_{\mathbf{R}}\mathcal{V}, \delta\mathbf{R}\rangle &= m^* \int_{\mathcal{B}} \rho\langle \nabla\Gamma, \delta\mathbf{R}\cdot\mathbf{x}\rangle \,\mathrm{d}V \\ &= m^* \int_{\mathcal{B}} \rho\big\langle \mathbf{R}^T\cdot\nabla\Gamma, \mathbf{R}^T\delta\mathbf{R}\cdot\mathbf{x}\big\rangle \,\mathrm{d}V.\end{aligned} \tag{4.93}$$

Given that $\mathbf{R}^T\delta\mathbf{R}$ is antisymmetric, this equals

$$m^* \int_{\mathcal{B}} \rho\big\langle \mathbf{x}\wedge\big(\mathbf{R}^T\cdot\nabla\Gamma\big)\,, \mathbf{R}^T\delta\mathbf{R}\big\rangle_{\mathfrak{so}(3)} \,\mathrm{d}V, \tag{4.94}$$

where we have used definition (4.62) of the wedge product, which we recall has an 'extra' minus sign. We may finally flip the $\mathbf{R}^T$ over to the other side of the inner product to give

$$\langle D_{\mathbf{R}}\mathcal{V}, \delta\mathbf{R}\rangle = \left\langle \mathbf{R}\left[m^* \int_{\mathcal{B}} \rho\mathbf{x}\wedge\big(\mathbf{R}^T\cdot\nabla\Gamma\big)\,\mathrm{d}V\right], \delta\mathbf{R}\right\rangle. \tag{4.95}$$

This is true for arbitrary $\delta\mathbf{R}$, so $\mathcal{V}$'s $\mathbf{R}$-derivative is

$$D_{\mathbf{R}}\mathcal{V}(\mathbf{\Phi}, \mathbf{R}) = \mathbf{R}\left[m^* \int_{\mathcal{B}} \rho\mathbf{x}\wedge\big(\mathbf{R}^T\cdot\nabla\Gamma(\mathbf{\Phi} + \mathbf{R}\cdot\mathbf{x})\big)\,\mathrm{d}V\right]. \tag{4.96}$$

It follows that the torque is

$$\mathbf{L} = m^* \int_{\mathcal{B}} \rho\mathbf{x}\wedge\big\{\mathbf{R}^T\cdot[-\nabla\Gamma(\mathbf{\Phi} + \mathbf{R}\cdot\mathbf{x})]\big\}\,\mathrm{d}V. \tag{4.97}$$

Recalling from Section 4.3.2 that the wedge product of two vectors is analogous to their cross product, we see that this torque is exactly what should be expected on physical grounds. The term in $-\nabla\Gamma$ gives the force acting at the referential point $\mathbf{x}$, the factor of $\mathbf{R}^T$ 'translates' that force into the body-frame, and we then form the force's moment by taking the wedge product with $\mathbf{x}$ before integrating over the body.

Lastly, we remark that one can write the Euler equations in component-form by expanding $\mathbf{\Omega}$, $\mathbb{I}$ and $\mathbf{L}$ on the basis of the $\{\mathbf{J}_\alpha\}$:

$$I_{\alpha\gamma}\dot{\Omega}^\gamma + [\mathsf{ad}_{\mathbf{\Omega}}]_\alpha{}^\beta I_{\beta\gamma}\Omega^\gamma = L_\alpha, \tag{4.98}$$

which can be written as

$$I_{\alpha\gamma}\dot{\Omega}^\gamma + \Omega^\beta\epsilon_{\alpha\beta\mu}\delta^{\mu\nu}I_{\nu\gamma}\Omega^\gamma = L_\alpha \tag{4.99}$$

using (4.57). If we interpret $\{\Omega^\alpha\}$, $\{I_{\alpha\beta}\}$ and $\{L_\alpha\}$ as the components of Cartesian tensors and

recall eq. (4.63), then we can rewrite this in the more usual form

$$\mathbb{I}\cdot\dot{\boldsymbol{\Omega}}+\boldsymbol{\Omega}\times(\mathbb{I}\cdot\boldsymbol{\Omega})=m^*\int_{\mathcal{B}}\rho\mathbf{x}\times\left\{\mathbf{R}^T\cdot[-\nabla\Gamma(\boldsymbol{\Phi}+\mathbf{R}\cdot\mathbf{x})]\right\}\,\mathrm{d}V. \tag{4.100}$$

Indeed, these are just the standard Euler equations of e.g. Landau & Lifshitz (1976). We will stick to a representation in terms of antisymmetric matrices for the rest of this chapter.

4.3.6 Equilibria and linearisation

Equations (4.90) show that the linear and rotational motions of a rigid body are generally coupled together. This runs against the intuition that one might develop from observing bodies moving near the Earth's surface: in such cases the potential $\mathcal{V}$ is simply

$$\mathcal{V}(\boldsymbol{\Phi},\mathbf{R})=\int_{\mathcal{B}}\rho g\langle\mathbf{z},\boldsymbol{\Phi}+\mathbf{R}\cdot\mathbf{x}\rangle\,\mathrm{d}V=mg\Phi_z, \tag{4.101}$$

as a result of which $\mathbf{L}$ vanishes and $\mathbf{f}$ depends only on $\boldsymbol{\Phi}$. There is thus a complete decoupling of linear and rotational motion. That this decoupling does not usually happen makes the analysis of rigid-body motion rather complicated in general – and it is worth noting that even in the torque-free case an analytic solution to the Euler equations only exists in terms of *Jacobi elliptic functions* (e.g. Landau & Lifshitz, 1976). Fortunately we can take a different approach to realistic problems of planetary physics.

Taking a closer look at the point-mass potential

$$\mathcal{V}(\boldsymbol{\Phi},\mathbf{R})=m^*\int_{\mathcal{B}}\rho(\mathbf{x})\Gamma(\boldsymbol{\Phi}+\mathbf{R}\cdot\mathbf{x})\,\mathrm{d}V \tag{4.102}$$

we see that $\|\boldsymbol{\Phi}\|\gg\|\mathbf{x}\|$ in general. This leads us to expand $\mathcal{V}$ in a Taylor-series about $\boldsymbol{\Phi}$, which gives to second order

$$\mathcal{V}(\boldsymbol{\Phi},\mathbf{R})\approx m^*\int_{\mathcal{B}}\rho\Gamma(\boldsymbol{\Phi})\,\mathrm{d}V+\frac{1}{2!}\epsilon\,m^*\int_{\mathcal{B}}\rho\langle\mathbf{R}\cdot\mathbf{x},\nabla\nabla\Gamma(\boldsymbol{\Phi})\,\mathbf{R}\cdot\mathbf{x}\rangle\,\mathrm{d}V, \tag{4.103}$$

with the term linear in $\mathbf{x}$ vanishing due to the constraint on the coordinate system, and where we have inserted a dimensionless bookkeeping perturbation parameter ϵ. Observe that $\nabla\nabla\Gamma(\boldsymbol{\Phi})$ has Cartesian components

$$[\nabla\nabla\Gamma(\boldsymbol{\Phi})]_{ij}=\frac{G}{\|\boldsymbol{\Phi}\|^5}\Big(\|\boldsymbol{\Phi}\|^2\,\delta_{ij}-3\Phi_i\Phi_j\Big), \tag{4.104}$$

somewhat reminiscent of the moment of inertia. Indeed, if we define the *reduced moment of inertia tensor* $\mathbb{J}:\mathbb{R}^3\mapsto\mathbb{R}^3$, whose Cartesian components are

$$J_{ij}=I_{ij}-\frac{1}{3}I_{kk}\delta_{ij}, \tag{4.105}$$

then after some simple algebra we can write the potential as

$$\mathcal{V} = \mathcal{V}^{(0)}(\mathbf{\Phi}) + \epsilon\, \mathcal{V}^{(1)}(\mathbf{\Phi}, \mathbf{R}), \tag{4.106}$$

with

$$\begin{aligned} \mathcal{V}^{(0)}(\mathbf{\Phi}) &= -\frac{Gm^* m}{\|\mathbf{\Phi}\|} \\ \mathcal{V}^{(1)}(\mathbf{\Phi}, \mathbf{R}) &= \frac{3}{2}\frac{Gm^*}{\|\mathbf{\Phi}\|^5}\left\langle \mathbf{\Phi}, \mathbf{R}\mathbb{J}\mathbf{R}^T \cdot \mathbf{\Phi} \right\rangle . \end{aligned} \tag{4.107}$$

As discussed in Section 4.2, we can seek zeroth-order equilibrium solutions to a system with potential $\mathcal{V}^{(0)}$, then linearise to find the perturbations caused by $\mathcal{V}^{(1)}$. For the remainder of this subsection we will work with an arbitrary potential of the form of eq.(4.106).

At zeroth-order the torque vanishes identically and there is no coupling between $\mathbf{\Phi}^{(0)}$ and $\mathbf{R}^{(0)}$:

$$m\ddot{\mathbf{\Phi}}^{(0)} = \mathbf{f}^{(0)}\left(\mathbf{\Phi}^{(0)}\right) \equiv -D_{\mathbf{\Phi}}\mathcal{V}^{(0)}\left(\mathbf{\Phi}^{(0)}, \mathbf{R}^{(0)}\right) \tag{4.108a}$$

$$(\partial_t + \mathsf{ad}_{\mathbf{\Omega}^{(0)}})\, \mathbb{I} \cdot \mathbf{\Omega}^{(0)} = 0 \tag{4.108b}$$

$$\dot{\mathbf{R}}^{(0)} = \mathbf{R}^{(0)}\mathbf{\Omega}^{(0)}. \tag{4.108c}$$

The body's CoM could execute some complicated motion depending on $\mathcal{V}^{(0)}$, but that motion will have no effect on the zeroth-order rotational motion which is governed by a *free* Euler equation. We can therefore take the zeroth-order angular velocity to be constant in time, satisfying

$$\mathsf{ad}_{\mathbf{\Omega}^{(0)}}\mathbb{I} \cdot \mathbf{\Omega}^{(0)} = 0. \tag{4.109}$$

For this to hold it is sufficient that the eigenvalue equation

$$\mathbb{I} \cdot \mathbf{\Omega}^{(0)} = \lambda \mathbf{\Omega}^{(0)} \tag{4.110}$$

be satisfied. In component form eq.(4.110) reads

$$g^{\alpha\mu} I_{\mu\beta}\left[\mathbf{\Omega}^{(0)}\right]^{\beta} = \lambda\left[\mathbf{\Omega}^{(0)}\right]^{\alpha}, \tag{4.111}$$

which is trivially equivalent to

$$\delta^{\alpha\mu} I_{\mu\beta}\left[\mathbf{\Omega}^{(0)}\right]^{\beta} = 2\lambda\left[\mathbf{\Omega}^{(0)}\right]^{\alpha} \tag{4.112}$$

given eq.(4.54). Now and for the rest of this section we will work in a coordinate system orientated so that

$$I_{\alpha\beta} = \begin{bmatrix} A & 0 & 0 \\ 0 & B & 0 \\ 0 & 0 & C \end{bmatrix} \tag{4.113}$$

with $C > B > A$. The unique *secularly stable* solution to eq.(4.110) is well known to be a *uniform* rotation about the body's axis of greatest inertia. For this we take

$$\boldsymbol{\Omega}^{(0)} = \Omega^{(0)}\mathbf{J}_3 \tag{4.114a}$$

$$\lambda = C/2 \tag{4.114b}$$

for some constant $\Omega^{(0)}$. The corresponding zeroth-order rotation matrix $\mathbf{R}^{(0)}$ can be found trivially by integrating the reconstruction equation to give

$$\mathbf{R}^{(0)}(t) = \mathbf{R}_0^{(0)} \exp(\boldsymbol{\Omega}^{(0)} t), \tag{4.115}$$

for the initial condition $\mathbf{R}^{(0)}\big|_{t=0} = \mathbf{R}_0^{(0)}$. For the rest of this chapter we will take the zeroth-order body and spatial coordinate systems to have the same orientation at $t = 0$, which can be arranged by setting $\mathbf{R}_0^{(0)} = \mathbf{1}$. The secularly stable equilibrium solution is then

$$\boldsymbol{\Omega}^{(0)}(t) = \Omega^{(0)}\mathbf{J}_3 \tag{4.116a}$$

$$\mathbf{R}^{(0)}(t) = \exp(\boldsymbol{\Omega}^{(0)} t) = \begin{pmatrix} \cos(\Omega^{(0)}t) & -\sin(\Omega^{(0)}t) & 0 \\ \sin(\Omega^{(0)}t) & \cos(\Omega^{(0)}t) & 0 \\ 0 & 0 & 1 \end{pmatrix}, \tag{4.116b}$$

describing a body in constant rotation about its Z-axis at constant angular velocity $\Omega^{(0)}$ – and with the body Z-axis aligned with the spatial z-axis.

We now perturb the body from this equilibrium by subjecting it to the potential

$$\mathcal{V}(\boldsymbol{\Phi}, \mathbf{R}) = \mathcal{V}^{(0)}(\boldsymbol{\Phi}) + \epsilon\, \mathcal{V}^{(1)}(\boldsymbol{\Phi}, \mathbf{R}). \tag{4.117}$$

As discussed in Section 4.2 our approach is to write the fields as truncated series in ϵ,

$$\boldsymbol{\Phi} = \boldsymbol{\Phi}^{(0)} + \epsilon\boldsymbol{\Phi}^{(1)} \tag{4.118a}$$

$$\boldsymbol{\Omega} = \boldsymbol{\Omega}^{(0)} + \epsilon\boldsymbol{\Omega}^{(1)} \tag{4.118b}$$

$$\boldsymbol{\Lambda} = \boldsymbol{\Lambda}^{(0)} + \epsilon\boldsymbol{\Lambda}^{(1)} \tag{4.118c}$$

$$\mathbf{R} = \mathbf{R}^{(0)} \exp\Big[\epsilon\boldsymbol{\theta}^{(1)}\Big], \tag{4.118d}$$

then substitute them into the action (4.79) and extract the part *quadratic* in ϵ. We are only interested in cross-terms between first-order fields, *and will systematically neglect all other terms.*

Let us work term-by-term. Expanding the CoM's kinetic energy is easy:

$$\frac{1}{2}m\|\dot{\boldsymbol{\Phi}}\|^2 = \epsilon^2 \frac{1}{2}m\|\dot{\boldsymbol{\Phi}}^{(1)}\|^2. \tag{4.119}$$

The same goes for the rotational kinetic energy:

$$\frac{1}{2}\langle \boldsymbol{\Omega}, \mathbb{I}\cdot\boldsymbol{\Omega}\rangle_{\mathfrak{so}(3)} = \epsilon^2 \frac{1}{2}\Big\langle \boldsymbol{\Omega}^{(1)}, \mathbb{I}\cdot\boldsymbol{\Omega}^{(1)}\Big\rangle_{\mathfrak{so}(3)}. \tag{4.120}$$

As for the potential term, if we define

$$\mathbf{f}^{(1)} = -D_{\mathbf{\Phi}}\mathcal{V}^{(1)}(\mathbf{\Phi}^{(0)}, \mathbf{R}^{(0)}) \tag{4.121}$$

$$\mathbf{L}^{(1)} = -\Big(\mathbf{R}^{(0)}\Big)^T D_{\mathbf{R}}\mathcal{V}^{(1)}(\mathbf{\Phi}^{(0)}, \mathbf{R}^{(0)}) \tag{4.122}$$

$$\boldsymbol{\tau}^{(0)} = -D^2_{\mathbf{\Phi}}\mathcal{V}^{(0)}(\mathbf{\Phi}^{(0)}), \tag{4.123}$$

then $\mathcal{V}$ expands as

$$\mathcal{V}(\mathbf{\Phi}, \mathbf{R}) = -\epsilon^2\left\{\Big\langle \mathbf{f}^{(1)}, \mathbf{\Phi}^{(1)}\Big\rangle + \Big\langle \mathbf{L}^{(1)}, \boldsymbol{\theta}^{(1)}\Big\rangle_{\mathfrak{so}(3)} + \frac{1}{2}\Big\langle \mathbf{\Phi}^{(1)}, \boldsymbol{\tau}^{(0)} \cdot \mathbf{\Phi}^{(1)}\Big\rangle\right\}. \tag{4.124}$$

The fiddly term is the one with the Lagrange multipler: $\Big\langle \mathbf{\Lambda}, \mathbf{R}^T\dot{\mathbf{R}} - \mathbf{\Omega}\Big\rangle_{\mathfrak{so}(3)}$. To proceed we expand (4.118d) for $\mathbf{R}$ to give

$$\mathbf{R} = \mathbf{R}^{(0)}\left(\mathbf{1} + \epsilon\boldsymbol{\theta}^{(1)} + \frac{1}{2}\epsilon^2\boldsymbol{\theta}^{(1)}\boldsymbol{\theta}^{(1)}\right). \tag{4.125}$$

Then we recall that the zeroth-order reconstruction states that $(\mathbf{R}^{(0)})^T\dot{\mathbf{R}}^{(0)} = \mathbf{\Omega}^{(0)}$. If we also define

$$\Delta_t^{(0)} = \partial_t + \mathsf{ad}_{\mathbf{\Omega}^{(0)}}, \tag{4.126}$$

after a little algebra we find that

$$\mathbf{R}^T\dot{\mathbf{R}} = \mathbf{\Omega}^{(0)} + \epsilon\Delta_t^{(0)} \cdot \boldsymbol{\theta}^{(1)} - \frac{1}{2}\epsilon^2\mathsf{ad}_{\boldsymbol{\theta}^{(1)}} \cdot \Big(\Delta_t^{(0)} \cdot \boldsymbol{\theta}^{(1)}\Big). \tag{4.127}$$

The full Lagrange-multiplier term thus expands as

$$\begin{aligned}\Big\langle \mathbf{\Lambda}, \mathbf{R}^T\dot{\mathbf{R}} - \mathbf{\Omega}\Big\rangle_{\mathfrak{so}(3)} &= \left\langle \mathbf{\Lambda}^{(0)} + \epsilon\mathbf{\Lambda}^{(1)}, \epsilon\Big(\Delta_t^{(0)} \cdot \boldsymbol{\theta}^{(1)} - \mathbf{\Omega}^{(1)}\Big) - \frac{1}{2}\epsilon^2\mathsf{ad}_{\boldsymbol{\theta}^{(1)}}\Delta_t^{(0)} \cdot \boldsymbol{\theta}^{(1)}\right\rangle_{\mathfrak{so}(3)} \\ &= \epsilon^2\left\{\Big\langle \mathbf{\Lambda}^{(1)}, \Delta_t^{(0)} \cdot \boldsymbol{\theta}^{(1)} - \mathbf{\Omega}^{(1)}\Big\rangle_{\mathfrak{so}(3)} - \frac{1}{2}\Big\langle \mathbf{\Lambda}^{(0)}, \mathsf{ad}_{\boldsymbol{\theta}^{(1)}}\Delta_t^{(0)} \cdot \boldsymbol{\theta}^{(1)}\Big\rangle_{\mathfrak{so}(3)}\right\}.\end{aligned} \tag{4.128}$$

It is clear that $\mathbf{\Lambda}^{(1)}$ will act to constrain the kinematic identity

$$\mathbf{\Omega}^{(1)} = \Delta_t^{(0)} \cdot \boldsymbol{\theta}^{(1)}, \tag{4.129}$$

so we can substitute this identity directly into the action *except in the Lagrange multiplier term.* That gives

$$\Big\langle \mathbf{\Lambda}, \mathbf{R}^T\dot{\mathbf{R}} - \mathbf{\Omega}\Big\rangle_{\mathfrak{so}(3)} = \epsilon^2\left\{\Big\langle \mathbf{\Lambda}^{(1)}, \Delta_t^{(0)} \cdot \boldsymbol{\theta}^{(1)} - \mathbf{\Omega}^{(1)}\Big\rangle_{\mathfrak{so}(3)} - \frac{1}{2}\Big\langle \mathbf{\Lambda}^{(0)}, \mathsf{ad}_{\boldsymbol{\theta}^{(1)}} \cdot \mathbf{\Omega}^{(1)}\Big\rangle_{\mathfrak{so}(3)}\right\}, \tag{4.130}$$

and we can finally write down the quadratic action

$$\mathcal{S}^{(2)} = \int_{\mathcal{I}} \Big\{ \frac{1}{2}\Big\langle \boldsymbol{\Omega}^{(1)}, \mathbb{I}\cdot\boldsymbol{\Omega}^{(1)}\Big\rangle_{\mathfrak{so}(3)} + \Big\langle \boldsymbol{\Lambda}^{(1)}, \Delta_t^{(0)}\cdot\boldsymbol{\theta}^{(1)} - \boldsymbol{\Omega}^{(1)}\Big\rangle_{\mathfrak{so}(3)} + \frac{1}{2}\Big\langle \boldsymbol{\theta}^{(1)}, \mathsf{ad}_{\boldsymbol{\Lambda}^{(0)}}\cdot\boldsymbol{\Omega}^{(1)}\Big\rangle_{\mathfrak{so}(3)} + \Big\langle \mathbf{L}^{(1)}, \boldsymbol{\theta}^{(1)}\Big\rangle_{\mathfrak{so}(3)} + \frac{1}{2}m\Big\langle \dot{\boldsymbol{\Phi}}^{(1)}, \dot{\boldsymbol{\Phi}}^{(1)}\Big\rangle + \Big\langle \mathbf{f}^{(1)}, \boldsymbol{\Phi}^{(1)}\Big\rangle + \frac{1}{2}\Big\langle \boldsymbol{\Phi}^{(1)}, \boldsymbol{\tau}^{(0)}\cdot\boldsymbol{\Phi}^{(1)}\Big\rangle \Big\}\,\mathrm{d}t. \tag{4.131}$$

Varying this with respect to $\boldsymbol{\Phi}^{(1)}$, $\boldsymbol{\Omega}^{(1)}$, $\boldsymbol{\theta}^{(1)}$ and $\boldsymbol{\Lambda}^{(1)}$ will give the linearised EoMs.

It is quickly verified that the Euler–Lagrange equations are initially given by

$$m\ddot{\boldsymbol{\Phi}}^{(1)} = \mathbf{f}^{(1)} + \boldsymbol{\tau}^{(0)}\cdot\boldsymbol{\Phi}^{(1)} \tag{4.132a}$$

$$\Delta_t^{(0)}\cdot\boldsymbol{\Lambda}^{(1)} = \frac{1}{2}\mathsf{ad}_{\boldsymbol{\Lambda}^{(0)}}\cdot\boldsymbol{\Omega}^{(1)} + \mathbf{L}^{(1)} \tag{4.132b}$$

$$\boldsymbol{\Lambda}^{(1)} = \mathbb{I}\cdot\boldsymbol{\Omega}^{(1)} - \frac{1}{2}\mathsf{ad}_{\boldsymbol{\Lambda}^{(0)}}\cdot\boldsymbol{\theta}^{(1)} \tag{4.132c}$$

$$\Delta_t^{(0)}\cdot\boldsymbol{\theta}^{(1)} = \boldsymbol{\Omega}^{(1)}, \tag{4.132d}$$

and we recall that $\boldsymbol{\Lambda}^{(0)} = \mathbb{I}\cdot\boldsymbol{\Omega}^{(0)} = \lambda\boldsymbol{\Omega}^{(0)}$ at zeroth-order. The dynamics of the system enter in the first two equations, whilst the second pair are purely kinematic relations. In fact, eq.(4.132d) is just the first-order reconstruction equation. We can find something that looks more like a linearised Euler equation by substituting (4.132c) into (4.132b) to give

$$\Delta_t^{(0)}\cdot\Big(\mathbb{I}\cdot\boldsymbol{\Omega}^{(1)}\Big) - \frac{1}{2}\Big[\Delta_t^{(0)}\cdot\Big(\mathsf{ad}_{\boldsymbol{\Lambda}^{(0)}}\cdot\boldsymbol{\theta}^{(1)}\Big) + \mathsf{ad}_{\boldsymbol{\Lambda}^{(0)}}\cdot\boldsymbol{\Omega}^{(1)}\Big] = \mathbf{L}^{(1)}. \tag{4.133}$$

It is readily shown that $\Delta_t^{(0)}$ commutes with $\mathsf{ad}_{\boldsymbol{\Lambda}^{(0)}}$, so we can use (4.132d) to write

$$\Delta_t^{(0)}\cdot\Big(\mathbb{I}\cdot\boldsymbol{\Omega}^{(1)}\Big) - \mathsf{ad}_{\boldsymbol{\Lambda}^{(0)}}\cdot\boldsymbol{\Omega}^{(1)} = \mathbf{L}^{(1)}. \tag{4.134}$$

We make some final simplifications by expanding the definitions of $\Delta_t^{(0)}$ and $\boldsymbol{\Lambda}^{(0)}$. The first-order equations are ultimately summarised as

$$m\ddot{\boldsymbol{\Phi}}^{(1)} = \mathbf{f}^{(1)} + \boldsymbol{\tau}^{(0)}\cdot\boldsymbol{\Phi}^{(1)} \tag{4.135a}$$

$$[\mathbb{I}\partial_t + \mathsf{ad}_{\boldsymbol{\Omega}^{(0)}}(\mathbb{I}-\lambda)]\cdot\boldsymbol{\Omega}^{(1)} = \mathbf{L}^{(1)} \tag{4.135b}$$

$$(\partial_t + \mathsf{ad}_{\boldsymbol{\Omega}^{(0)}})\cdot\boldsymbol{\theta}^{(1)} = \boldsymbol{\Omega}^{(1)}. \tag{4.135c}$$

4.3.7 Analytic solution

At this point we can profit from a change of notation. We drop all superscript zeroes and ones, and to avoid ambiguity between the zeroth- and first-order angular velocities we notate the latter by $\mathbf{m}$.

In many cases the first-order torque $\mathbf{L}$ will be a linear combination of terms with discrete

angular frequencies:

$$\mathbf{L} = \sum_{\alpha} \mathbf{L}_{\alpha} \mathrm{e}^{\mathrm{i}\nu_{\alpha} t}, \tag{4.136}$$

for some set of antisymmetric matrices $\{\mathbf{L}_{\alpha}\}$ and scalars $\{\nu_{\alpha}\}$. This will hold to a very good approximation for the point-mass potential we discussed earlier, for in that case

$$\mathbf{L} = 3\frac{Gm^*}{\|\mathbf{\Phi}\|^5}\big(\mathbf{R}^T \cdot \mathbf{\Phi}\big) \wedge \big(\mathbb{J}\mathbf{R}^T \cdot \mathbf{\Phi}\big)\,. \tag{4.137}$$

The $\{\nu_{\alpha}\}$ then arise from the body's zeroth-order angular frequency $\Omega^{(0)}$ (which we will just notate as Ω from now on) and frequencies associated with the zeroth-order *orbit*. For a circular orbit there would only be one such frequency while for eccentric orbits there would be other frequencies. As long as the orbit is not too eccentric (and for the Earth and Moon that is a very good approximation) an expression of the form (4.136) should work well. For torques of this form we can seek a *steady-state* solution of the form

$$\mathbf{m} = \sum_{\alpha} \mathbf{m}_{\alpha} \mathrm{e}^{\mathrm{i}\nu_{\alpha} t} \tag{4.138a}$$

$$\boldsymbol{\theta} = \sum_{\alpha} \boldsymbol{\theta}_{\alpha} \mathrm{e}^{\mathrm{i}\nu_{\alpha} t} \tag{4.138b}$$

for some $\{\mathbf{m}_{\alpha}\}$ and $\{\boldsymbol{\theta}_{\alpha}\}$. Substituting (4.138a) into eq.(4.135b) and exploiting linearity then leads to the equations

$$[\mathrm{i}\nu_{\alpha}\mathbb{I} + \mathsf{ad}_{\mathbf{\Omega}}(\mathbb{I} - \lambda)] \cdot \mathbf{m}_{\alpha} = \mathbf{L}_{\alpha}, \tag{4.139}$$

which can be solved separately for each frequency to give

$$\mathbf{m}_{\alpha} = [\mathrm{i}\nu_{\alpha}\mathbb{I} + \mathsf{ad}_{\mathbf{\Omega}}(\mathbb{I} - \lambda)]^{-1} \cdot \mathbf{L}_{\alpha}. \tag{4.140}$$

The linearised reconstruction equation then gives

$$\boldsymbol{\theta}_{\alpha} = [\mathrm{i}\nu_{\alpha} + \mathsf{ad}_{\mathbf{\Omega}}]^{-1} \cdot \mathbf{m}_{\alpha}. \tag{4.141}$$

If we define the operators

$$\mathsf{D}(\nu) \equiv \mathrm{i}\nu\mathbb{I} + \mathsf{ad}_{\mathbf{\Omega}}(\mathbb{I} - \lambda) \tag{4.142a}$$

$$\mathsf{\Delta}(\nu) \equiv \mathrm{i}\nu + \mathsf{ad}_{\mathbf{\Omega}}, \tag{4.142b}$$

then $\mathbf{m}$ and $\boldsymbol{\theta}$ can be written succinctly as

$$\mathbf{m}(t) = \sum_{\alpha} \mathsf{D}(\nu_{\alpha})^{-1} \cdot \mathbf{L}_{\alpha} \mathrm{e}^{\mathrm{i}\nu_{\alpha} t} \tag{4.143a}$$

$$\boldsymbol{\theta}(t) = \sum_{\alpha} \mathsf{\Delta}(\nu_{\alpha})^{-1} \mathsf{D}(\nu_{\alpha})^{-1} \cdot \mathbf{L}_{\alpha} \mathrm{e}^{\mathrm{i}\nu_{\alpha} t}. \tag{4.143b}$$

Of course, this procedure will fail if any of the $\{\nu_\alpha\}$ are *eigenfrequencies* of D and/or $\mathsf{\Delta}$, that is, values of ν for which $\det \mathsf{D}(\nu)$ and/or $\det \mathsf{\Delta}(\nu)$ vanish. This is due to resonance, a phenomenon that is well documented in the tidal literature in the context of the Nearly Diurnal Free Wobble (e.g. Agnew, 2015). The approach commonly adopted within tidal theory is to approximate the sum (4.136) by an expansion in terms of the resonant frequencies (ibid. eq. 20). Alternatively, one can seek a *transient solution* to eqs. (4.135b) and (4.135c) besides the steady state one.

In order to find the transient solution it is useful to introduce the *Fourier–Laplace transform* (e.g. Friedlander et al., 1998). The Fourier–Laplace transform of a function $f : \mathbb{R}^+ \mapsto \mathbb{R}$ is defined to be the function $\tilde{f} : \mathbb{C} \mapsto \mathbb{C}$ given by

$$\tilde{f}(\nu) \equiv \int_0^\infty f(t) \mathrm{e}^{-\mathrm{i}\nu t} \mathrm{d}t. \tag{4.144}$$

Note that the forward transform has $t = 0$ as its lower limit rather than $t = -\infty$: it is not a Fourier transform! The inverse transform is realised by

$$f(t) = \frac{1}{2\pi} \int_{-\infty - \mathrm{i}\varepsilon}^{\infty - \mathrm{i}\varepsilon} \tilde{f}(\nu) \mathrm{e}^{\mathrm{i}\nu t} \mathrm{d}\nu, \tag{4.145}$$

with ε chosen so that all the integrand's singularities lie above the line $z = -\mathrm{i}\varepsilon$.

Fourier–Laplace transforming eqs.(4.135) gives

$$\mathsf{D}(\nu) \cdot \mathbf{m}(\nu) = \mathbf{L}^{(1)}(\nu) + \mathbb{I} \cdot \overline{\mathbf{m}} \tag{4.146a}$$

$$\mathsf{\Delta}(\nu) \cdot \boldsymbol{\theta}(\nu) = \mathbf{m}(\nu) + \overline{\boldsymbol{\theta}} \tag{4.146b}$$

after a brief calculation, where

$$\overline{\mathbf{m}} \equiv \mathbf{m}_{|t=0} \tag{4.147a}$$

$$\overline{\boldsymbol{\theta}} \equiv \boldsymbol{\theta}_{|t=0}. \tag{4.147b}$$

Note that these initial conditions enter the frequency domain problem as (frequency-independent) effective forcing terms. The frequency-domain problem is solved by inverting D and $\mathsf{\Delta}$ to give

$$\mathbf{m}(\nu) = \mathsf{D}(\nu)^{-1} \cdot (\mathbf{L}(\nu) + \mathbb{I} \cdot \overline{\mathbf{m}}) \tag{4.148a}$$

$$\boldsymbol{\theta}(\nu) = \mathsf{\Delta}(\nu)^{-1} \cdot \big(\mathbf{m}(\nu) + \overline{\boldsymbol{\theta}}\big) = \mathsf{\Delta}(\nu)^{-1} \cdot \overline{\boldsymbol{\theta}} + \mathsf{\Delta}(\nu)^{-1} \mathsf{D}(\nu)^{-1} \cdot (\mathbf{L}(\nu) + \mathbb{I} \cdot \overline{\mathbf{m}}) \,. \tag{4.148b}$$

We then obtain the time-domain solution by inverse Fourier–Laplace transforming:

$$\mathbf{m}(t) = \frac{1}{2\pi} \int_{-\infty - \mathrm{i}\varepsilon}^{\infty - \mathrm{i}\varepsilon} \mathbf{m}(\nu) \mathrm{e}^{\mathrm{i}\nu t} \mathrm{d}\nu \tag{4.149a}$$

$$\boldsymbol{\theta}^{(1)}(t) = \frac{1}{2\pi} \int_{-\infty - \mathrm{i}\varepsilon}^{\infty - \mathrm{i}\varepsilon} \boldsymbol{\theta}^{(1)}(\nu) \mathrm{e}^{\mathrm{i}\nu t} \mathrm{d}\nu. \tag{4.149b}$$

To carry out the transformation it will be convenient to identify the singularities of $\mathbf{m}(\nu)$ and $\boldsymbol{\theta}(\nu)$. It seems reasonable to assume that $\mathbf{L}(t)$ has compact support, which implies that $\mathbf{L}(\nu)$ is

an entire function. Therefore the singularities can only arise from $\Delta(\nu)^{-1}$ and $\mathsf{D}(\nu)^{-1}$.

At this point it is simplest to calculate component-wise with respect to the $\mathbf{J}_\alpha$-basis. Eqs. (4.146) are written in component-form as

$$D_{\alpha\beta}m^\beta = L_\alpha + I_{\alpha\beta}\overline{m}^\beta \tag{4.150a}$$
$$\Delta^\alpha{}_\beta\,\theta^\beta = m^\alpha + \overline{\theta}^\alpha, \tag{4.150b}$$

with the components of Δ and D given explicitly by

$$D_{\alpha\beta} = \mathrm{i}\nu I_{\alpha\beta} + [\mathsf{ad}_{\mathbf{\Omega}}]_\alpha{}^\gamma\left(I_{\gamma\beta} - \frac{C}{2}g_{\gamma\beta}\right) \tag{4.151a}$$
$$\Delta^\alpha{}_\beta = \mathrm{i}\nu g^\alpha{}_\beta + [\mathsf{ad}_{\mathbf{\Omega}}]^\alpha{}_\beta\,, \tag{4.151b}$$

where we have recalled that the zeroth-order solution (4.114) has $\lambda = C/2$. We now shuffle some indices to give

$$[\mathsf{ad}_{\mathbf{\Omega}}]^\alpha{}_\beta = g^{\alpha\mu}[\mathsf{ad}_{\mathbf{\Omega}}]_\mu{}^\nu\, g_{\nu\beta}, \tag{4.152}$$

then note that $g_{\alpha\beta} = 2\delta_{\alpha\beta}$ (eq. 4.42) and that $g^\alpha{}_\beta = \delta^\alpha{}_\beta$ by definition. It follows that

$$D_{\alpha\beta} = \mathrm{i}\nu I_{\alpha\beta} + [\mathsf{ad}_{\mathbf{\Omega}}]_\alpha{}^\gamma(I_{\gamma\beta} - C\delta_{\gamma\beta}) \tag{4.153a}$$
$$\Delta^\alpha{}_\beta = \mathrm{i}\nu\delta^\alpha{}_\beta + \delta^{\alpha\mu}[\mathsf{ad}_{\mathbf{\Omega}}]_\mu{}^\nu\,\delta_{\nu\beta}. \tag{4.153b}$$

Now, we showed in eq.(4.57) that

$$[\mathsf{ad}_{\mathbf{\Omega}}]_\alpha{}^\beta = \Omega^\gamma\varepsilon_{\alpha\gamma\mu}\delta^{\mu\beta}, \tag{4.154}$$

for any $\mathbf{\Omega}$. In the present case $\mathbf{\Omega}$ has only a $\mathbf{J}_3$-component (with magnitude Ω), so

$$[\mathsf{ad}_{\mathbf{\Omega}}]_\alpha{}^\beta = \begin{bmatrix} 0 & -\Omega & 0 \\ \Omega & 0 & 0 \\ 0 & 0 & 0 \end{bmatrix}. \tag{4.155}$$

Given that $I_{\alpha\beta} = \mathrm{diag}[A, B, C]$ (eq. 4.113), we may finally write D and Δ with respect to the $\mathbf{J}_\alpha$-basis as

$$\mathsf{D} = \begin{bmatrix} \mathrm{i}\nu A & (C-B)\Omega & 0 \\ (A-C)\Omega & \mathrm{i}\nu B & 0 \\ 0 & 0 & \mathrm{i}\nu C \end{bmatrix} \tag{4.156a}$$

$$\Delta = \begin{bmatrix} \mathrm{i}\nu & -\Omega & 0 \\ \Omega & \mathrm{i}\nu & 0 \\ 0 & 0 & \mathrm{i}\nu \end{bmatrix}. \tag{4.156b}$$

We no longer attempt to distinguish between the operator and its components, but that should not lead to confusion.

We must now invert these matrices and investigate their singularities as functions of ν. If we introduce the dimensionless factor

$$\sigma_{\mathrm{CW}} = \sqrt{\frac{(A-C)(B-C)}{AB}}, \tag{4.157}$$

and define the *Chandler wobble eigenfrequency*

$$\Omega_{\mathrm{CW}} = \sigma_{\mathrm{CW}}\Omega, \tag{4.158}$$

D and $\mathsf{\Delta}$ can readily be inverted to give

$$\mathsf{D}^{-1} = \frac{\mathrm{i}}{\nu(\nu^2 - \Omega_{\mathrm{CW}}^2)}(ABC)^{-1}\,\mathrm{adj}\mathsf{D} \tag{4.159a}$$

$$\mathsf{\Delta}^{-1} = \frac{\mathrm{i}}{\nu(\nu^2 - \Omega^2)}\mathrm{adj}\mathsf{\Delta}, \tag{4.159b}$$

with the *adjugate matrices* given by

$$\mathrm{adj}\mathsf{D} = \begin{bmatrix} -\nu^2 BC & +\mathrm{i}\nu\Omega(B-C)\,C & 0 \\ -\mathrm{i}\nu\Omega(A-C)\,C & -\nu^2 AC & 0 \\ 0 & 0 & \left(\Omega_{\mathrm{CW}}^2 - \nu^2\right)AB \end{bmatrix} \tag{4.160a}$$

$$\mathrm{adj}\mathsf{\Delta} = \begin{bmatrix} -\nu^2 & +\mathrm{i}\nu\Omega & 0 \\ -\mathrm{i}\nu\Omega & -\nu^2 & 0 \\ 0 & 0 & \Omega^2 - \nu^2 \end{bmatrix}. \tag{4.160b}$$

Importantly, the adjugate matrices are *analytic* functions of ν and cannot display any singular behaviour. The singular behaviour comes exclusively from the prefactors; the values of ν for which the prefactors are singular are of course the respective operators' *eigenvalues*. From the prefactors' form it is clear that D^{-1} and $\mathsf{\Delta}^{-1}$ – and consequently $\mathbf{m}(\nu)$ and $\boldsymbol{\theta}(\nu)$ – are *meromorphic* functions whose poles all lie above the integration contour $z = -\mathrm{i}\varepsilon$ of eqs.(4.149). We may therefore use *Jordan's lemma* to close the integration contour in the upper half-plane, and then use the *residue theorem* to write

$$\mathbf{m}(t) = \mathrm{i}\sum_{\nu_\alpha} \operatorname*{Res}_{\nu=\nu_\alpha}\left[\mathbf{m}(\nu)\mathrm{e}^{\mathrm{i}\nu t}\right] \tag{4.161a}$$

$$\boldsymbol{\theta}(t) = \mathrm{i}\sum_{\nu_\alpha} \operatorname*{Res}_{\nu=\nu_\alpha}\left[\boldsymbol{\theta}(\nu)\mathrm{e}^{\mathrm{i}\nu t}\right], \tag{4.161b}$$

where the $\{\nu_\alpha\}$ are the values of ν for which the respective functions are singular (e.g. Stone & Goldbart, 2009). Substituting from eqs.(4.148) the explicit forms of $\mathbf{m}(\nu)$ and $\boldsymbol{\theta}(\nu)$ we can

finally write the time-domain solutions as

$$\mathbf{m}(t) = -\sum_{\nu_\alpha} \operatorname*{Res}_{\nu=\nu_\alpha} \left[\frac{\mathrm{e}^{\mathrm{i}\nu t}}{\nu\big(\nu^2 - \Omega_{\mathrm{CW}}^2\big)} \right] (ABC)^{-1} \operatorname{adj}\mathsf{D}(\nu_\alpha) \cdot (\mathbf{L}(\nu_\alpha) + \mathbb{I} \cdot \overline{\mathbf{m}}) \tag{4.162a}$$

$$\begin{aligned} \boldsymbol{\theta}(t) = &-\sum_{\nu_\alpha} \operatorname*{Res}_{\nu=\nu_\alpha} \left[\frac{\mathrm{e}^{\mathrm{i}\nu t}}{\nu(\nu^2 - \Omega^2)} \right] \operatorname{adj}\boldsymbol{\Delta}(\nu_\alpha) \cdot \overline{\boldsymbol{\theta}} \\ &- \mathrm{i} \sum_{\nu_\alpha} \operatorname*{Res}_{\nu=\nu_\alpha} \left[\frac{\mathrm{e}^{\mathrm{i}\nu t}}{\nu^2(\nu^2 - \Omega^2)\big(\nu^2 - \Omega_{\mathrm{CW}}^2\big)} \right] (ABC)^{-1} \operatorname{adj}\mathsf{D}(\nu_\alpha) \operatorname{adj}\boldsymbol{\Delta}(\nu_\alpha) \cdot (\mathbf{L}(\nu_\alpha) + \mathbb{I} \cdot \overline{\mathbf{m}}) \,. \end{aligned} \tag{4.162b}$$

Without evaluating these expressions we can already see several of the solutions' features. $\mathbf{m}(t)$ exhibits two main types of behaviour. Due to the poles at $\nu = \pm\Omega_{\mathrm{CW}}$ it will oscillate with angular frequency Ω_{CW}. This motion is the *Eulerian free precession*, usually referred to in geophysical contexts as the *Chandler wobble*. Besides this there will be a constant shift in the angular velocity as a result of the pole at $\nu = 0$: the *axial spin mode*. These motions are mirrored by $\boldsymbol{\theta}$, but in $\boldsymbol{\theta}$ there also emerges an oscillatory mode with angular velocity Ω. For reasons that will become apparent shortly, this is called the *tilt-over mode*.

Evaluating the sums requires tedious but straightforward algebra. After defining the quantities

$$L_{1,\mathrm{CW}} = L_1(\Omega_{\mathrm{CW}}) + A\overline{m_1} \tag{4.163a}$$

$$L_{2,\mathrm{CW}} = L_2(\Omega_{\mathrm{CW}}) + B\overline{m_2} \tag{4.163b}$$

$$m_{1,\mathrm{CW}} = A^{-1} \left[L_{1,\mathrm{CW}} - \mathrm{i}\sqrt{\frac{A(B-C)}{B(A-C)}} L_{2,\mathrm{CW}} \right] \tag{4.163c}$$

$$m_{2,\mathrm{CW}} = B^{-1} \left[L_{2,\mathrm{CW}} + \mathrm{i}\sqrt{\frac{B(A-C)}{A(B-C)}} L_{1,\mathrm{CW}} \right] \tag{4.163d}$$

$$\theta'_{1,\mathrm{CW}} = -C^{-1}\Omega_{\mathrm{CW}}^{-1} \frac{A-C}{A} \left[L_{1,\mathrm{CW}} - \mathrm{i}\frac{B-C}{B} L_{2,\mathrm{CW}} \right] \tag{4.163e}$$

$$\theta'_{2,\mathrm{CW}} = -C^{-1}\Omega_{\mathrm{CW}}^{-1} \frac{B-C}{B} \left[L_{2,\mathrm{CW}} + \mathrm{i}\frac{A-C}{A} L_{1,\mathrm{CW}} \right] \tag{4.163f}$$

$$\theta_{\mathrm{TOM}} = \big[\overline{\theta_1} + \mathrm{i}\overline{\theta_2}\big] + \Omega^{-1}C^{-1}\{[L_2(\Omega) + B\overline{m_2}] - \mathrm{i}[L_1(\Omega) + A\overline{m_1}]\} \tag{4.163g}$$

$$\theta_{\mathrm{ASM}} = \overline{\theta_3} + \big[\overline{m_3} + C^{-1}L_3(0)\big]\, t, \tag{4.163h}$$

we reach the expressions

$$\mathbf{m}(t) = \big[\theta_{\mathrm{ASM}} - \overline{\theta_3}\big]\, \mathbf{J}_3 + \Re\big[\mathrm{e}^{\mathrm{i}\Omega_{\mathrm{CW}}t}(m_{1,\mathrm{CW}}\mathbf{J}_1 + m_{2,\mathrm{CW}}\mathbf{J}_2)\big] \tag{4.164a}$$

$$\boldsymbol{\theta}(t) = \theta_{\mathrm{ASM}}\mathbf{J}_3 + \Re\big\{\mathrm{e}^{\mathrm{i}\Omega t}\theta_{\mathrm{TOM}}(\mathbf{J}_1 + \mathrm{i}\mathbf{J}_2)\big\} + \Im\big\{\mathrm{e}^{\mathrm{i}\Omega_{\mathrm{CW}}t}\big(\theta'_{1,\mathrm{CW}}\mathbf{J}_1 + \theta'_{2,\mathrm{CW}}\mathbf{J}_2\big)\big\}\,, \tag{4.164b}$$

which give clear illustrations of the behaviour we just discussed. $\Re$ and $\Im$ indicate respectively

an expression's real and imaginary parts. Now recall that the full solutions for $\boldsymbol{\Omega}$ and $\mathbf{R}$ are

$$\boldsymbol{\Omega}(t) = \boldsymbol{\Omega}^{(0)}(t) + \epsilon\mathbf{m}(t) \tag{4.165a}$$

$$\mathbf{R}(t) = \mathbf{R}^{(0)}(t)[\mathbf{1} + \epsilon\boldsymbol{\theta}(t)] \tag{4.165b}$$

correct to $\mathcal{O}(\epsilon)$. It is clear how $\boldsymbol{\Omega}^{(0)}$ and $\mathbf{m}$ will combine to produce $\boldsymbol{\Omega}$. But it is perhaps not so obvious what behaviour $\mathbf{R}$ will exhibit. To see what happens multiply eq.(4.165b) on the right by $[\mathbf{R}^{(0)}]^T\mathbf{R}^{(0)} = \mathbf{1}$, so that

$$\mathbf{R} = (\mathbf{1} + \epsilon\mathsf{Ad}_{\mathbf{R}^{(0)}} \cdot \boldsymbol{\theta})\,\mathbf{R}^{(0)}. \tag{4.166}$$

$\mathbf{J}_3$ can be shown to be an eigenvector of $\mathsf{Ad}_{\mathbf{R}^{(0)}}$ with eigenvalue 1, while $\mathbf{J}_1 \pm \mathrm{i}\mathbf{J}_2$ are eigenvectors with eigenvalues $\mathrm{e}^{\mp\mathrm{i}\Omega t}$. It follows that

$$\begin{aligned}\mathbf{R}(t) = \Re\Big\{\mathbf{1} + \epsilon[&\theta_{\mathrm{ASM}}\mathbf{J}_3 + \theta_{\mathrm{TOM}}(\mathbf{J}_1 + \mathrm{i}\mathbf{J}_2) \\ &-\mathrm{i}\mathrm{e}^{\mathrm{i}(\Omega_{\mathrm{CW}}-\Omega)t}\theta^{+}_{\mathrm{CW}}(\mathbf{J}_1 + \mathrm{i}\mathbf{J}_2) - \mathrm{i}\mathrm{e}^{\mathrm{i}(\Omega_{\mathrm{CW}}+\Omega)t}\theta^{-}_{\mathrm{CW}}(\mathbf{J}_1 - \mathrm{i}\mathbf{J}_2)\Big]\Big\}\mathbf{R}^{(0)}(t),\end{aligned} \tag{4.167}$$

for some coefficients $\theta^{\pm}_{\mathrm{CW}} = \left(\theta'_{1,\mathrm{CW}} \mp \mathrm{i}\theta'_{2,\mathrm{CW}}\right)/2$. Finally, upon defining

$$\boldsymbol{\Theta}_{\mathrm{TOM}} = \Re[\theta_{\mathrm{TOM}}(\mathbf{J}_1 + \mathrm{i}\mathbf{J}_2)] \tag{4.168a}$$

$$\theta_{\mathrm{CW},1} = \Im\big\{\mathrm{e}^{\mathrm{i}\Omega_{\mathrm{CW}}t}\big[\theta'_{1,\mathrm{CW}}\cos(\Omega t) - \theta'_{2,\mathrm{CW}}\sin(\Omega t)\big]\big\} \tag{4.168b}$$

$$\theta_{\mathrm{CW},2} = \Im\big\{\mathrm{e}^{\mathrm{i}\Omega_{\mathrm{CW}}t}\big[\theta'_{1,\mathrm{CW}}\sin(\Omega t) + \theta'_{2,\mathrm{CW}}\cos(\Omega t)\big]\big\} \tag{4.168c}$$

and exploiting the commutativity of the infinitesimal rotations, we can write $\mathbf{R}$ correct to $\mathcal{O}(\epsilon)$ as

$$\mathbf{R}(t) = [\mathbf{1} + \epsilon\boldsymbol{\Theta}_{\mathrm{TOM}}]\,\mathbf{R}_x[\epsilon\theta_{\mathrm{CW},1}]\,\mathbf{R}_y[\epsilon\theta_{\mathrm{CW},2}]\,\mathbf{R}_z[\Omega t + \epsilon\theta_{\mathrm{ASM}}]\,. \tag{4.169}$$

We see that the tilt-over mode is aptly named: a nonzero value of θ_{TOM} literally causes the body to tilt over by a small angle that is constant in time: the (retrograde) diurnal oscillation of eq.(4.164b) has essentially been aliased from the equilibrium body frame into the spatial frame (see Smith, 1977). This expression shows further that the Chandler wobble manifests complexly in the spatial frame. It causes the body's *geographical north pole* to approximately precess in the x–y plane. The fact that $\theta'_{1,\mathrm{CW}} \neq \theta'_{2,\mathrm{CW}}$ means that this motion will generally be elliptically polarised. Moreover, the prefactor of $\mathrm{e}^{\mathrm{i}\Omega_{\mathrm{CW}}t}$ causes the precessional amplitude to be modulated at the Chandler wobble frequency. Throughout all of this the body continues to rotate about its polar axis with angular frequency $\Omega + \overline{m_3} + C^{-1}L_3(0)$, with the small angular offset $\overline{\theta_3}$.

In summary, we can compute the normal modes of a uniformly rotating rigid body in two different ways. One method is to Fourier–Laplace transform the linearised Euler and reconstruction equations, locate their singularities in the frequency-domain, and then compute the inverse transformation by explicitly evaluating a residue sum. This method revolves around finding the system's eigenvalues. A second approach, which is valid when the body is forced at

discrete frequencies that are *distinct* from its eigenfrequencies, is simply to invert D and Δ at each of the forcing frequencies (the inverse is guaranteed to exist) and then perform a discrete sum over each frequency. This 'direct-solution' approach has the advantage that *we do not need to find the eigenfrequencies*. For that reason it generalises much more readily than the first approach to the very large matrices we will encounter in Section 4.5. It can in fact be seen as a precursor to the *direct numerical solution* method of Al-Attar et al. (2012) that we discuss in Section 4.5.5.

4.3.8 Extension to two bodies

4.3.8.1 Towards the Keplerian two-body problem: exact action and Euler–Lagrange equations

Hamilton's principle provides a convenient framework for coupling the dynamics of multiple bodies. Let us consider two rigid bodies whose respective motions are given by

$$\boldsymbol{\varphi}_i(\mathbf{x}, t) = \boldsymbol{\Phi}_i(t) + \mathbf{R}_i \cdot \mathbf{x}, \tag{4.170}$$

with respect to reference bodies $\mathcal{B}_i$, with $i = 1, 2$. All the kinematic identities we derived earlier for one body are taken to hold for each body individually. We can therefore define each body's free action as

$$\mathcal{S}_i = \int_{\mathcal{I}} \left[\frac{1}{2} m \|\dot{\boldsymbol{\Phi}}_i\|^2 + \frac{1}{2} \langle \boldsymbol{\Omega}_i, \mathbb{I}_i \cdot \boldsymbol{\Omega}_i \rangle_{\mathfrak{so}(3)} + \left\langle \boldsymbol{\Lambda}_i, \mathbf{R}_i^T \dot{\mathbf{R}}_i - \boldsymbol{\Omega}_i \right\rangle_{\mathfrak{so}(3)} \right] \mathrm{d}t, \tag{4.171}$$

where

$$\boldsymbol{\Omega}_i = \mathbf{R}_i^T \dot{\mathbf{R}}_i \tag{4.172}$$

and $\mathbb{I}_i : \mathfrak{so}(3) \mapsto \mathfrak{so}(3)$ has covariant $\mathbf{J}_\alpha$-components

$$[\mathbb{I}_i]_{\alpha\beta} = \int_{\mathcal{B}_i} \rho_i (\|\mathbf{x}\| \, \delta_{\alpha\beta} - x_\alpha x_\beta) \, \mathrm{d}V. \tag{4.173}$$

It will also be useful to define the *reduced moment of inertia* $\mathbb{J}_i : \mathbb{R}^3 \mapsto \mathbb{R}^3$, whose Cartesian components are

$$[\mathbb{J}_i]_{mn} = [\mathbb{I}_i]_{mn} - \frac{1}{3} (\mathbb{I}_i)_{kk} \, \delta_{mn}. \tag{4.174}$$

In terms of these free actions, the overall action for a system of two non-interacting, free rigid bodies is (somewhat trivially)

$$\mathcal{S} = \mathcal{S}_1 + \mathcal{S}_2. \tag{4.175}$$

Now, the only difference between gravitationally isolated and interacting bodies is their gravitational binding energy, which for our two rigid bodies is given by

$$\mathcal{V}_g(\mathbf{\Phi}_1, \mathbf{R}_1, \mathbf{\Phi}_2, \mathbf{R}_2) = \int_{\mathcal{B}_1} \mathrm{d}V \rho_1(\mathbf{x}) \int_{\mathcal{B}_2} \mathrm{d}V' \rho_2(\mathbf{x}') \Gamma\left\{\left[\mathbf{\Phi}_1 + \mathbf{R}_1 \cdot \mathbf{x}\right] - \left[\mathbf{\Phi}_2 + \mathbf{R}_2 \cdot \mathbf{x}'\right]\right\}. \tag{4.176}$$

The action describing the interacting rigid bodies follows readily:

$$\mathcal{S} = \int_{\mathcal{I}} \left\{ \sum_{i=1}^{2} \left[\frac{1}{2} m_i \|\dot{\mathbf{\Phi}}_i\|^2 + \frac{1}{2} \langle \mathbf{\Omega}_i, \mathbb{I}_i \cdot \mathbf{\Omega}_i \rangle_{\mathfrak{so}(3)} + \left\langle \mathbf{\Lambda}_i, \mathbf{R}_i^T \dot{\mathbf{R}}_i - \mathbf{\Omega}_i \right\rangle_{\mathfrak{so}(3)} \right] - \mathcal{V}_g(\mathbf{\Phi}_1, \mathbf{R}_1, \mathbf{\Phi}_2, \mathbf{R}_2) \right\} \mathrm{d}t. \tag{4.177}$$

Before proceeding to the Euler–Lagrange equations we can apply some intuition learned from the Keplerian two-body problem. It is well known that the motion of two interacting point masses with displacements $\mathbf{\Phi}_{1,2}(t)$ is analysed most readily after defining the *total mass*

$$M = m_1 + m_2, \tag{4.178}$$

the *reduced mass*

$$\mu = \frac{m_1 m_2}{m_1 + m_2}, \tag{4.179}$$

and changing variables according to

$$\begin{aligned} \mathbf{r}(t) &= \mathbf{\Phi}_1(t) - \mathbf{\Phi}_2(t) \\ \mathbf{d}(t) &= \frac{1}{M}[m_1 \mathbf{\Phi}_1(t) + m_2 \mathbf{\Phi}_2(t)]. \end{aligned} \tag{4.180}$$

$\mathbf{d}$ is referred to as the *barycentre*. Applying this transformation to the rigid-body action gives

$$\begin{aligned} \mathcal{S} = \int_{\mathcal{I}} \Bigg\{ & \frac{1}{2} M \left\|\dot{\mathbf{d}}\right\|^2 + \frac{1}{2} \mu \|\dot{\mathbf{r}}\|^2 \\ & + \sum_{i=1}^{2} \left[\frac{1}{2} \langle \mathbf{\Omega}_i, \mathbb{I}_i \cdot \mathbf{\Omega}_i \rangle_{\mathfrak{so}(3)} + \left\langle \mathbf{\Lambda}_i, \mathbf{R}_i^T \dot{\mathbf{R}}_i - \mathbf{\Omega}_i \right\rangle_{\mathfrak{so}(3)} \right] - \mathcal{V}_g(\mathbf{r}, \mathbf{R}_1, \mathbf{R}_2) \Bigg\} \mathrm{d}t, \end{aligned} \tag{4.181}$$

where we have redefined

$$\mathcal{V}_g(\mathbf{r}, \mathbf{R}_1, \mathbf{R}_2) = \int_{\mathcal{B}_1} \mathrm{d}V \rho_1(\mathbf{x}) \int_{\mathcal{B}_2} \mathrm{d}V' \rho_2(\mathbf{x}') \Gamma\left[\mathbf{r} + \mathbf{R}_1(t) \cdot \mathbf{x} - \mathbf{R}_2(t) \cdot \mathbf{x}'\right]. \tag{4.182}$$

All the hard work to derive the Euler–Lagrange equations has already been done. We can dispense with the barycentre motion quickly: the action contains no terms in $\mathbf{d}$, but only a kinetic term in $\dot{\mathbf{d}}$, so $\mathbf{d}$ is a *cyclic variable* obeying

$$\ddot{\mathbf{d}} = 0. \tag{4.183}$$

Regarding $\mathbf{r}$, a comparison of actions (4.181) and (4.79) shows that we can vary $\mathbf{r}$ *precisely* as

we varied $\mathbf{\Phi}$ in Section 4.3.5[†]. If we define the force (*c.f.* eq. 4.83)

$$\mathbf{f}_K = -D_{\mathbf{r}}\mathcal{V}_g, \tag{4.184}$$

then $\mathbf{r}$ must satisfy

$$\mu\ddot{\mathbf{r}} = \mathbf{f}_K(\mathbf{r}, \mathbf{R}_1, \mathbf{R}_2)\,. \tag{4.185}$$

The very same logic applies to the rotational variables, so we are led to define the net torque on the i'th body (*c.f.* eq. 4.84)

$$\mathbf{L}_i^K = -\mathbf{R}_i^T D_{\mathbf{R}_i}\mathcal{V}_g \tag{4.186}$$

and write down the equations

$$(\partial_t + \mathsf{ad}_{\mathbf{\Omega}_i})\,\mathbb{I}_i \cdot \mathbf{\Omega}_i = \mathbf{L}_i^K(\mathbf{r}, \mathbf{R}_1, \mathbf{R}_2) \tag{4.187}$$

$$\dot{\mathbf{R}}_i = \mathbf{R}_i\mathbf{\Omega}_i. \tag{4.188}$$

The net force and torque take the explicit forms

$$\mathbf{f}_K(\mathbf{r}, \mathbf{R}_1, \mathbf{R}_2) = -\int_{\mathcal{B}_1} \mathrm{d}V\rho_1 \int_{\mathcal{B}_2} \mathrm{d}V'\rho_2'\nabla\Gamma\big(\mathbf{r} + \mathbf{R}_1\cdot\mathbf{x} - \mathbf{R}_2\cdot\mathbf{x}'\big) \tag{4.189}$$

$$\mathbf{L}_i^K(\mathbf{r}, \mathbf{R}_1, \mathbf{R}_2) = (-1)^i \int_{\mathcal{B}_1} \mathrm{d}V\rho_1 \int_{\mathcal{B}_2} \mathrm{d}V'\rho_2'\mathbf{x}\wedge\nabla\Gamma\big(\mathbf{r} + \mathbf{R}_1\cdot\mathbf{x} - \mathbf{R}_2\cdot\mathbf{x}'\big)\,, \tag{4.190}$$

and in summary, the equations of motion of two rigid bodies interacting under gravity are

$$\ddot{\mathbf{d}} = 0 \tag{4.191a}$$

$$\mu\ddot{\mathbf{r}} = \mathbf{f}_K(\mathbf{r}, \mathbf{R}_1, \mathbf{R}_2) \tag{4.191b}$$

$$(\partial_t + \mathsf{ad}_{\mathbf{\Omega}_i})\,\mathbb{I}_i \cdot \mathbf{\Omega}_i = \mathbf{L}_i^K(\mathbf{r}, \mathbf{R}_1, \mathbf{R}_2) \tag{4.191c}$$

$$\dot{\mathbf{R}}_i = \mathbf{R}_i\mathbf{\Omega}_i. \tag{4.191d}$$

with $i = 1, 2$. This completes the derivation.

These equations of motion are extremely complicated! But if the bodies are very far apart, that is $\|\mathbf{r}\| \gg \|\mathbf{R}_1\cdot\mathbf{x} - \mathbf{R}_2\cdot\mathbf{x}'\|$, then $\mathbf{f}_K$ and $\mathbf{L}_i^K$ are to leading order

$$\mathbf{f}_K = -G\frac{m_1 m_2}{\|\mathbf{r}\|^3}\mathbf{r} \tag{4.192}$$

$$\mathbf{L}_i^K = 0, \tag{4.193}$$

where we have used the definition of Γ and recalled that $\int_{\mathcal{B}_i}\rho_i\mathbf{x}\,\mathrm{d}V$ vanishes. Under this

[†]Indeed, it was in anticipation of calculations such as these that we developed the one-body EoMs with an arbitrary potential.

approximation the equations of motion simplify to

$$\ddot{\mathbf{d}} = 0 \tag{4.194a}$$

$$\ddot{\mathbf{r}} = -\frac{GM}{\|\mathbf{r}\|^3}\mathbf{r} \tag{4.194b}$$

$$(\partial_t + \mathsf{ad}_{\mathbf{\Omega}_i})\,\mathbb{I}_i \cdot \mathbf{\Omega}_i = 0 \tag{4.194c}$$

$$\dot{\mathbf{R}}_i = \mathbf{R}_i\mathbf{\Omega}_i. \tag{4.194d}$$

The CoM and rotational motions have decoupled and we have thus recovered free rigid-body motion on the one hand, and the standard Kepler problem on the other. Indeed, one expects on physical grounds that if the bodies are sufficiently far apart then each 'sees' the other as a point mass. It follows that they orbit each other like point particles, while each one performs free rigid-body motion. In particular, there is nothing to stop us taking each body to be in a state of uniform rotation about its 3-axis as before:

$$\mathbf{\Omega}_i = \Omega_i\mathbf{J}_3. \tag{4.195}$$

This together with an arbitrary, given solution to

$$\ddot{\mathbf{r}} = -G\frac{M}{\|\mathbf{r}\|^3}\mathbf{r} \tag{4.196}$$

will form the zeroth-order solution about which we linearise next. To be concrete, we define the zeroth-order *potential*

$$\mathcal{V}_g^{(0)}(\mathbf{r}) = -G\frac{m_1m_2}{\|\mathbf{r}\|}, \tag{4.197}$$

and the zeroth-order *solutions*

$$\ddot{\mathbf{r}}^{(0)} = -\frac{GM}{\left\|\mathbf{r}^{(0)}\right\|^3}\mathbf{r}^{(0)} \tag{4.198a}$$

$$\mathbf{\Omega}_i^{(0)} = \Omega_i^{(0)}\mathbf{J}_3 \tag{4.198b}$$

$$\dot{\mathbf{R}}_i^{(0)} = \mathbf{R}_i^{(0)}\mathbf{\Omega}_i^{(0)}. \tag{4.198c}$$

We can now consider small perturbations about these solutions. (The barycentre will be ignored henceforth.)

4.3.8.2 The perturbed Kepler problem: linearised action and Euler–Lagrange equations

The gravitational binding energy of the two-body system can be Taylor-expanded to second-order as

$$\begin{aligned}\mathcal{V}_g &= \int_{\mathcal{B}_1} \mathrm{d}V\rho_1 \int_{\mathcal{B}_2} \mathrm{d}V'\rho_2'\Gamma\big(\mathbf{r}+\mathbf{R}_1\cdot\mathbf{x}-\mathbf{R}_2\cdot\mathbf{x}'\big)\\ &= \int_{\mathcal{B}_1} \mathrm{d}V\rho_1 \int_{\mathcal{B}_2} \mathrm{d}V'\rho_2'\Gamma(\mathbf{r}) + \int_{\mathcal{B}_1} \mathrm{d}V\rho_1 \int_{\mathcal{B}_2} \mathrm{d}V'\rho_2'\big\langle\nabla\Gamma(\mathbf{r})\,,\mathbf{R}_1\cdot\mathbf{x}-\mathbf{R}_2\cdot\mathbf{x}'\big\rangle\\ &\quad + \frac{1}{2!}\int_{\mathcal{B}_1} \mathrm{d}V\rho_1 \int_{\mathcal{B}_2} \mathrm{d}V'\rho_2'\big\langle\nabla\nabla\Gamma(\mathbf{r})\cdot\big(\mathbf{R}_1\cdot\mathbf{x}-\mathbf{R}_2\cdot\mathbf{x}'\big)\,,\mathbf{R}_1\cdot\mathbf{x}-\mathbf{R}_2\cdot\mathbf{x}'\big\rangle+\dots. \end{aligned} \tag{4.199}$$

The terms linear in $\mathbf{x}$, $\mathbf{x}'$ and $\mathbf{x}\otimes\mathbf{x}'$ all vanish because $\int_{\mathcal{B}_i}\rho_i\mathbf{x}\,\mathrm{d}V=0$, leaving

$$\mathcal{V}_g = \mathcal{V}_g^{(0)} + \frac{1}{2}m_2\int_{\mathcal{B}_1}\big\langle\mathbf{x},\mathbf{R}_1^T\nabla\nabla\Gamma(\mathbf{r})\mathbf{R}_1\cdot\mathbf{x}\big\rangle\,\mathrm{d}V + \frac{1}{2}m_1\int_{\mathcal{B}_2}\big\langle\mathbf{x}',\mathbf{R}_2^T\nabla\nabla\Gamma(\mathbf{r})\mathbf{R}_2\cdot\mathbf{x}'\big\rangle\,\mathrm{d}V \tag{4.200}$$

at second order. It then follows with a little algebra that

$$\mathcal{V}_g = \mathcal{V}_g^{(0)} + \epsilon\frac{3}{2}\frac{G}{\|\mathbf{r}\|^5}\big\langle\mathbf{r},\big(m_2\mathbf{R}_1\mathbb{J}_1\mathbf{R}_1^T+m_1\mathbf{R}_2\mathbb{J}_2\mathbf{R}_2^T\big)\cdot\mathbf{r}\big\rangle\,, \tag{4.201}$$

where we have inserted the bookkeeping small parameter ϵ. We are led to define

$$\mathcal{V}_g^{(1)}(\mathbf{r},\mathbf{R}_1,\mathbf{R}_2) = \frac{3}{2}\frac{G}{\|\mathbf{r}\|^5}\big\langle\mathbf{r},\big(m_2\mathbf{R}_1\mathbb{J}_1\mathbf{R}_1^T+m_1\mathbf{R}_2\mathbb{J}_2\mathbf{R}_2^T\big)\cdot\mathbf{r}\big\rangle\,, \tag{4.202}$$

so that the potential is given by

$$\mathcal{V}_g = \mathcal{V}_g^{(0)} + \epsilon\mathcal{V}_g^{(1)}. \tag{4.203}$$

We can now directly apply the results of Section 4.3.6 to write down the linearised equations of motion.

By analogy with eqs. (4.121), (4.122) and (4.123) of Section 4.3.6 we define the zeroth- and first-order forcings as

$$\mathbf{f}^{(0)} = -D_{\mathbf{r}}\mathcal{V}_g^{(0)}(\mathbf{r}^{(0)}) \tag{4.204}$$

$$\mathbf{f}^{(1)} = -D_{\mathbf{r}}\mathcal{V}_g^{(1)}(\mathbf{r}^{(0)},\mathbf{R}_1^{(0)},\mathbf{R}_2^{(0)}) \tag{4.205}$$

$$\mathbf{L}_i^{(1)} = -\Big(\mathbf{R}_i^{(0)}\Big)^T D_{\mathbf{R}_i}\mathcal{V}_g^{(1)}(\mathbf{r}^{(0)},\mathbf{R}_1^{(0)},\mathbf{R}_2^{(0)}) \tag{4.206}$$

$$\boldsymbol{\tau}^{(0)} = -D_{\mathbf{r}}^2\mathcal{V}_g^{(0)}(\mathbf{r}^{(0)}), \tag{4.207}$$

and by analogy with eq.(4.135) we write down the equations of motion

$$\mu\ddot{\mathbf{r}}^{(1)} = \mathbf{f}^{(1)} + \boldsymbol{\tau}^{(0)} \cdot \mathbf{r}^{(1)} \tag{4.208a}$$

$$\left[\mathbb{I}_i\partial_t + \mathsf{ad}_{\boldsymbol{\Omega}_i^{(0)}}(\mathbb{I}_i - C_i/2)\right] \cdot \boldsymbol{\Omega}_i^{(1)} = \mathbf{L}_i^{(1)} \tag{4.208b}$$

$$\left(\partial_t + \mathsf{ad}_{\boldsymbol{\Omega}_i^{(0)}}\right) \cdot \boldsymbol{\theta}_i^{(1)} = \boldsymbol{\Omega}_i^{(1)}. \tag{4.208c}$$

This strikes the present author as a surprisingly tractable set of equations. A key point is that $\boldsymbol{\Omega}_i^{(1)}$ and $\mathbf{r}^{(1)}$ do not directly interact. Both the linearised Kepler and Euler equations can be integrated *separately* once the zeroth-order system has been solved, so spin-orbit coupling only manifests through interactions between first- and zeroth-order quantities. Numerical solution is consequently quite easy, at least in principle. In particular, $\mathbf{L}_i$ takes the form

$$\mathbf{L}_i = \frac{G}{\|\mathbf{r}\|^5} \begin{cases} m_2\left(\mathbf{R}_1^T \cdot \mathbf{r}\right) \wedge \left(\mathbb{J}_1\mathbf{R}_1^T \cdot \mathbf{r}\right), \, i = 1 \\ m_1\left(\mathbf{R}_2^T \cdot \mathbf{r}\right) \wedge \left(\mathbb{J}_2\mathbf{R}_2^T \cdot \mathbf{r}\right), \, i = 2. \end{cases} \tag{4.209}$$

This is represented in frequency space by a series of discrete peaks, so the direct-solution approach of Section 4.3.7 should be sufficient to compute $\boldsymbol{\Omega}_i^{(1)}$ and $\boldsymbol{\theta}_i^{(1)}$. The frequency content of $\mathbf{L}_i^{(1)}$ is derived from: each body's equilibrium uniform rotation, the main orbital frequency, and further 'overtones' associated with nonzero eccentricity. Calculating $\mathbf{r}^{(1)}$, on the other hand, is really the domain of *orbital perturbation theory* (e.g. Kopeikin et al., 2011; Poisson & Will, 2014), discussion of which we defer to later work. For now we just remark that $\boldsymbol{\tau}^{(0)}$ represents a *dipole field*:

$$\boldsymbol{\tau}^{(0)}(\mathbf{r}) = \frac{Gm_1m_2}{\|\mathbf{r}\|^5}\left(\|\mathbf{r}\|^2\,\mathbf{1} - 3\mathbf{r}\otimes\mathbf{r}\right). \tag{4.210}$$

It represents the tidal forces experienced by the bodies as they are perturbed from the zeroth-order orbit and sample variations in the $1/r$ potential field. Finally, $\mathbf{f}^{(1)}$ takes the form

$$\mathbf{f}^{(1)} = -\frac{3G}{\|\mathbf{r}\|^7}\left(\|\mathbf{r}\|^2\,\mathbf{1} - \frac{5}{2}\mathbf{r}\otimes\mathbf{r}\right)\left(m_2\mathbf{R}_1\mathbb{J}_1\mathbf{R}_1^T + m_1\mathbf{R}_2\mathbb{J}_2\mathbf{R}_2^T\right)\cdot\mathbf{r}. \tag{4.211}$$

Given that it contains $\mathbf{R}_1^{(0)}$ and $\mathbf{R}_2^{(0)}$, which most likely vary much more quickly than $\mathbf{r}^{(0)}$, we speculate that *multiple timescale analysis* (e.g. Bender & Orszag, 2013) could simplify eq. (4.208a)'s numerical solution considerably.

4.3.9 Extension to N bodies

By analogy with eq.(4.176) the gravitational binding energy of N rigid bodies is

$$\mathcal{V}_g(\boldsymbol{\Phi}_1,\mathbf{R}_1;\boldsymbol{\Phi}_2,\mathbf{R}_2;\ldots;\boldsymbol{\Phi}_N,\mathbf{R}_N) = \frac{1}{2}\sum_{i\neq j}^{N}\int_{\mathcal{B}_i}\int_{\mathcal{B}_j}\rho_i\rho_j'\Gamma\left(\boldsymbol{\Phi}_i - \boldsymbol{\Phi}_j + \mathbf{R}_i\cdot\mathbf{x} - \mathbf{R}_j\cdot\mathbf{x}'\right)\,\mathrm{d}V'\,\mathrm{d}V, \tag{4.212}$$

where we sum over both i and j from 1 to N, excluding terms with $i = j$ and including a factor of $1/2$ to avoid double-counting. With this, the N body action is

$$\begin{aligned}\mathcal{S} &= \hat{\mathcal{S}}[\boldsymbol{\Phi}_1, \mathbf{R}_1; \boldsymbol{\Phi}_2, \mathbf{R}_2; \ldots; \boldsymbol{\Phi}_N, \mathbf{R}_N] \\ &= \int_{\mathcal{I}} \left\{ \sum_{i=1}^{N} \left[\frac{1}{2} m_i \left\| \dot{\boldsymbol{\Phi}}_i \right\|^2 + \frac{1}{2} \langle \boldsymbol{\Omega}_i, \mathbb{I}_i \cdot \boldsymbol{\Omega}_i \rangle + \left\langle \boldsymbol{\Lambda}_i, \mathbf{R}_i^T \dot{\mathbf{R}}_i - \boldsymbol{\Omega}_i \right\rangle \right] \right. \\ &\qquad \left. - \mathcal{V}_g(\boldsymbol{\Phi}_1, \mathbf{R}_1; \boldsymbol{\Phi}_2, \mathbf{R}_2; \ldots; \boldsymbol{\Phi}_N, \mathbf{R}_N) \right\} \mathrm{d}t. \end{aligned} \tag{4.213}$$

In light of the preceding sections it then follows that the equations of motion are

$$m_i \ddot{\boldsymbol{\Phi}}_i = \mathbf{f}_i \tag{4.214a}$$

$$(\partial_t + \mathsf{ad}_{\boldsymbol{\Omega}_i})\, \mathbb{I}_i \cdot \boldsymbol{\Omega}_i = \mathbf{L}_i \tag{4.214b}$$

$$\dot{\mathbf{R}}_i = \mathbf{R}_i \boldsymbol{\Omega}_i, \tag{4.214c}$$

with the net force and torque defined to be

$$\mathbf{f}_i = -D_{\boldsymbol{\Phi}_i} \mathcal{V}_g = -\sum_{j \neq i} \int_{\mathcal{B}_i} \int_{\mathcal{B}_j} \rho_i \rho_j' \nabla \Gamma\big(\boldsymbol{\Phi}_i - \boldsymbol{\Phi}_j + \mathbf{R}_i \cdot \mathbf{x} - \mathbf{R}_j \cdot \mathbf{x}'\big)\, \mathrm{d}V'\, \mathrm{d}V \tag{4.215}$$

$$\mathbf{L}_i = -\mathbf{R}_i^T D_{\mathbf{R}_i} \mathcal{V}_g = -\sum_{j \neq i} \int_{\mathcal{B}_i} \int_{\mathcal{B}_j} \rho_i \rho_j' \mathbf{x} \wedge \big[\mathbf{R}_i^T \cdot \nabla \Gamma\big(\boldsymbol{\Phi}_i - \boldsymbol{\Phi}_j + \mathbf{R}_i \cdot \mathbf{x} - \mathbf{R}_j \cdot \mathbf{x}'\big)\big]\, \mathrm{d}V'\, \mathrm{d}V. \tag{4.216}$$

Just as for the two-body problem, if all N bodies are taken to be very far apart then their Euler equations cease to interact, but now the $\{\boldsymbol{\Phi}_i\}$ will obey the *N-body problem*

$$\ddot{\boldsymbol{\Phi}}_i = \sum_{j \neq i} \frac{G m_j}{\|\boldsymbol{\Phi}_j - \boldsymbol{\Phi}_i\|^3} (\boldsymbol{\Phi}_j - \boldsymbol{\Phi}_i)\,. \tag{4.217}$$

This chaotic system is infamously difficult to integrate numerically over long times. Nevertheless, if it could be done then we would in principle obtain N first-order torques $\{\mathbf{L}_i^{(1)}\}$ represented as a sum over discrete frequencies. We could therefore compute $\boldsymbol{\Omega}^{(1)}$ and $\boldsymbol{\theta}^{(1)}$ to some desired level of accuracy using the direct-solution method of Section 4.3.7. However, the chaotic nature of the N-body problem would likely produce extremely complicated frequency-domain structure in the $\{\mathbf{L}_i^{(1)}\}$, so performing the necessary computations could be quite time-consuming. Fortunately, these sorts of problems are probably of limited relevance to the geosciences.

4.3.10 Summary

We have derived the exact and linearised equations of motion of $N \geq 1$ rigid bodies interacting through Newtonian gravity. Our treatment was based on Hamilton's principle, and we showed that the correct equations of motion can be derived by using Lagrange multipliers to constrain the angular velocity to behave correctly. Most importantly from a geophysical perspective, we have also given a detailed discussion of the normal modes of a uniformly rotating rigid body. Up to (possibly considerable) numerical difficulties, this section's results also provide an exact

framework for studying the coupled orbital and rotational dynamics of systems of N rigid bodies, as well as computing the first-order effect of N-body gravitational interactions on each rigid body's rotation. We will now extend these ideas to bodies that can deform elastically.

4.4 Interlude: a review of finite elasticity

Here we review the elastodynamics of a single body. Much of the following can be found in Al-Attar et al. (2018) (hereafter AAA18) and references therein, so we have included here only what is necessary to ensure that this chapter is self-contained on a notational level. We also direct the reader to Marsden & Hughes (1994) and Dahlen & Tromp (1998) for alternative treatments of the material.

4.4.1 Kinematics

The deformation of an elastic body is described relative to a fixed *reference configuration*, with each particle labelled by its position within the associated *reference body* $\mathcal{B} \subseteq \mathbb{R}^3$, which is assumed to be connected, bounded, and have an open interior. At a time t, the position in physical space of the particle at $\mathbf{x} \in \mathcal{B}$ is written $\boldsymbol{\varphi}(\mathbf{x}, t)$. In this manner, we define a mapping

$$\boldsymbol{\varphi} : \mathcal{B} \times \mathbb{R} \mapsto \mathbb{R}^3, \tag{4.218}$$

which is called the *motion* of the body relative to the reference configuration. For a fixed time, t, the image of the mapping $\boldsymbol{\varphi}(\cdot, t)$ is written $\mathcal{B}_t$ and represents the region of physical space the body instantaneously occupies. It will be assumed that for each fixed time the mapping $\boldsymbol{\varphi}(\cdot, t) : \mathcal{B} \mapsto \mathcal{B}_t$ is smooth with a smooth inverse. Two fundamental objects derived from the motion are its *velocity* and *deformation gradient*. The former is defined as

$$\mathbf{v}(\mathbf{x}, t) = \dot{\boldsymbol{\varphi}}(\mathbf{x}, t), \tag{4.219}$$

where an overdot denotes *partial* differentiation with respect to time; $\mathbf{v}$ gives the spatial velocity of a particle at the point $\mathbf{y} = \boldsymbol{\varphi}(\mathbf{x}, t)$. The deformation gradient is

$$\mathbf{F} = D_{\mathbf{x}}\boldsymbol{\varphi}, \tag{4.220}$$

where $D_{\mathbf{x}}$ denotes partial differentiation with respect to position as defined through

$$\boldsymbol{\varphi}(\mathbf{x} + \delta\mathbf{x}, t) = \boldsymbol{\varphi}(\mathbf{x}, t) + (D_{\mathbf{x}}\boldsymbol{\varphi})(\mathbf{x}, t) \cdot \delta\mathbf{x} + \mathcal{O}\big(\|\delta\mathbf{x}\|^2\big)\,. \tag{4.221}$$

(We will generally neglect the subscript on D where it is unambiguous which variable we are differentiating with respect to.) Equivalently, the Cartesian components of the deformation gradient are

$$F_{ij} = \frac{\partial \varphi_i}{\partial x_j}. \tag{4.222}$$

The *Jacobian* is then defined as

$$J = \det \mathbf{F}. \tag{4.223}$$

Due to our assumption that $\boldsymbol{\varphi}(\cdot, t) : \mathcal{B} \to \mathcal{B}_t$ has a smooth inverse, it follows from the inverse function theorem (Marsden & Hughes, 1994, p.31) that the deformation gradient takes values in the general linear group $\mathbf{GL}(3)$ (Appendix B.1.1). We assume without loss of generality that J is everywhere positive, meaning that the motion is orientation preserving. The *density* at time t at the point $\mathbf{y} \in \mathcal{B}_t$ in physical space is written $\varrho(\mathbf{y}, t)$. From conservation of mass, we are led to define the *referential density*,

$$\rho(\mathbf{x}) = J(\mathbf{x}, t)\varrho[\boldsymbol{\varphi}(\mathbf{x}, t), t]\,, \tag{4.224}$$

a time-*independent* function within the reference body (Marsden & Hughes, 1994, p.87, Theorem 5.7). Meanwhile, the *kinetic energy* is given in terms of referential quantities as

$$\mathcal{T} = \int_{\mathcal{B}} \frac{1}{2}\rho\|\mathbf{v}\|^2 \, \mathrm{d}V. \tag{4.225}$$

4.4.2 Variational principle

The action is the integrated difference of the body's kinetic and potential energies:

$$\mathcal{S} = \int_{\mathcal{I}} (\mathcal{T} - \mathcal{V}) \, \mathrm{d}t. \tag{4.226}$$

The body's potential energy is composed of two parts, *elastic* and *gravitational*.

The elastic potential energy is related to the motion $\boldsymbol{\varphi}$ through a *constitutive relation*. For hyperelastic materials the elastic energy density is given by a *strain-energy function*

$$W : \mathcal{B} \times \mathbf{GL}(3) \to \mathbb{R}. \tag{4.227}$$

The total elastic potential energy associated with the body's deformation is then given in terms of W by

$$\mathcal{V}_E = \int_{\mathcal{B}} W[\mathbf{x}, \mathbf{F}(\mathbf{x}, t)] \, \mathrm{d}V. \tag{4.228}$$

The form of W is constrained by the *principle of material-frame indifference* (e.g. Marsden & Hughes, 1994; Truesdell & Noll, 2004), which requires that

$$W(\mathbf{x}, \mathbf{RF}) = W(\mathbf{x}, \mathbf{F}) \tag{4.229}$$

for all rotation matrices $\mathbf{R} \in \mathbf{SO}(3)$ and $\mathbf{F} \in \mathbf{GL}(3)$ (see Appendix B.1.1).

Turning to gravity, if we recall our earlier definition

$$\Gamma(\mathbf{y}) = -\frac{G}{\|\mathbf{y}\|}, \tag{4.230}$$

with G Newton's gravitational constant, then the *gravitational potential* at a point $\mathbf{y} \in \mathcal{B}_t$ is written as

$$\phi(\mathbf{y}) = \int_{\mathcal{B}_t} \varrho(\mathbf{y}')\Gamma(\mathbf{y} - \mathbf{y}')\,\mathrm{d}V'. \tag{4.231}$$

For our present purposes it is most useful to employ a referential description of gravity, that is to write the potential as a function defined on the reference body. We can achieve this by setting $\mathbf{y} = \boldsymbol{\varphi}(\mathbf{x}, t)$, $\mathbf{y}' = \boldsymbol{\varphi}(\mathbf{x}', t)$ and making use of eq.(4.224). The resulting *referential potential* ζ is

$$\zeta(\mathbf{x}, t) = \int_{\mathcal{B}} \rho(\mathbf{x}')\Gamma\big[\boldsymbol{\varphi}(\mathbf{x}, t) - \boldsymbol{\varphi}(\mathbf{x}', t)\big]\,\mathrm{d}V'. \tag{4.232}$$

We can make ζ's functional dependence on $\boldsymbol{\varphi}$ clear by defining the functional $\hat{\zeta}$ and writing

$$\zeta(\mathbf{x}, t) = \hat{\zeta}[\boldsymbol{\varphi}(\cdot, t), \mathbf{x}] \equiv \int_{\mathcal{B}} \rho(\mathbf{x}')\Gamma\big[\boldsymbol{\varphi}(\mathbf{x}, t) - \boldsymbol{\varphi}(\mathbf{x}', t)\big]\,\mathrm{d}V', \tag{4.233}$$

but in general we will just use ζ and leave the functional dependence implicit. The total gravitational potential energy of the body is then given in terms of ρ and $\boldsymbol{\varphi}$ by

$$\begin{aligned}
\mathcal{V}_G &= \frac{1}{2}\int_{\mathcal{B}_t} \varrho(\mathbf{y})\phi(\mathbf{y})\,\mathrm{d}V \\
&= \frac{1}{2}\int_{\mathcal{B}} \rho(\mathbf{x}) \int_{\mathcal{B}} \rho(\mathbf{x}')\Gamma\big[\boldsymbol{\varphi}(\mathbf{x}, t) - \boldsymbol{\varphi}(\mathbf{x}', t)\big]\,\mathrm{d}V'\,\mathrm{d}V \\
&= \frac{1}{2}\int_{\mathcal{B}} \rho(\mathbf{x})\zeta(\mathbf{x}, t)\,\mathrm{d}V,
\end{aligned} \tag{4.234}$$

with the factor of $1/2$ entering because both integrals are taken over the same body and therefore double-count each particle.

Similarly to the rigid body case we also define an arbitrary external potential $\mathcal{U} : \mathbb{R}^3 \mapsto \mathbb{R}$, whose contribution to the body's potential energy at time t is

$$\mathcal{V}_{\text{ext}}(t) = \int_{\mathcal{B}} \mathcal{U}[\boldsymbol{\varphi}(\mathbf{x}, t)]\,\mathrm{d}V. \tag{4.235}$$

With this, the action describing the body is finally written as

$$\mathcal{S} = \hat{\mathcal{S}}[\boldsymbol{\varphi}] = \int_{\mathcal{I}} (\mathcal{T} - \mathcal{V}_E - \mathcal{V}_G - \mathcal{V}_{\text{ext}})\,\mathrm{d}t = \int_{\mathcal{I}}\int_{\mathcal{B}} \left(\frac{1}{2}\rho\|\mathbf{v}\|^2 - W(\cdot, \mathbf{F}) - \frac{1}{2}\rho\zeta - \mathcal{U}(\boldsymbol{\varphi})\right)\mathrm{d}V\,\mathrm{d}t. \tag{4.236}$$

We have used the notation $\hat{\mathcal{S}}$ to emphasise that $\mathcal{S}$ is a functional of $\boldsymbol{\varphi}$.

4.4.3 Euler–Lagrange equations

Variation of the action (see Al-Attar & Crawford, 2016) leads to the equations of motion

$$\rho\partial_t\mathbf{v} - \mathrm{Div}\mathbf{P} - \rho\boldsymbol{\gamma} = \mathbf{b}, \tag{4.237}$$

where the divergence of a tensor field is given by

$$(\mathrm{Div}\mathbf{P})_i = \partial_j P_{ij}, \tag{4.238}$$

and we have defined the *gravitational acceleration*

$$\boldsymbol{\gamma} = -\int_{\mathcal{B}} \rho'(\nabla\Gamma)\big[\boldsymbol{\varphi} - \boldsymbol{\varphi}'\big]\,\mathrm{d}V' \tag{4.239}$$

and the *external body force*

$$\mathbf{b} = -D_{\boldsymbol{\varphi}}\mathcal{U}. \tag{4.240}$$

These equations of motion are subject to the boundary condition

$$\mathbf{t}(\mathbf{x},t) \equiv \mathbf{P}(\mathbf{x},t)\cdot\hat{\mathbf{n}}(\mathbf{x}) = 0 \tag{4.241}$$

on $\partial\mathcal{B}$. The tensor $\mathbf{P}$ that appears in these expressions is the *first Piola–Kirchhoff stress*, related to W by

$$\mathbf{P}(\mathbf{x},t) = (D_{\mathbf{F}}W)[\mathbf{x},\mathbf{F}(\mathbf{x},t)]\,, \tag{4.242}$$

where $D_{\mathbf{F}}W$ denotes the partial derivative of W with respect to $\mathbf{F}$. As implied by eq.(4.241) the first Piola–Kirchoff stress provides the linear relation between the traction $\mathbf{t}$ acting on a surface-element within $\mathcal{B}_t$, and the unit-normal $\hat{\mathbf{n}}$ of the corresponding reference surface element within $\mathcal{B}$.

4.4.4 Linearisation

For most geophysical purposes it is sufficient to study linearised elastodynamics. We define an *equilibrium configuration* $\boldsymbol{\varphi}^{(0)} : \mathcal{B} \to \mathbb{R}^3$ to be a time-independent solution of the equations of motion subject to a time-independent body force $\mathbf{b}^{(0)}$. That is

$$\mathrm{Div}\mathbf{P}^{(0)} + \rho\boldsymbol{\gamma}^{(0)} + \mathbf{b}^{(0)} = 0, \tag{4.243}$$

where

$$\boldsymbol{\gamma}^{(0)}(\mathbf{x}) = -\int_{\mathcal{B}} \rho(\mathbf{x}')(\nabla\Gamma)\Big[\boldsymbol{\varphi}^{(0)}(\mathbf{x}) - \boldsymbol{\varphi}^{(0)}(\mathbf{x}')\Big]\,\mathrm{d}V' \tag{4.244}$$

and where the equilibrium first Piola-Kirchhoff stress is given by

$$\mathbf{P}^{(0)}(\mathbf{x}) = D_{\mathbf{F}} W\Big[\mathbf{x}, \mathbf{F}^{(0)}(\mathbf{x})\Big], \tag{4.245}$$

with $\mathbf{F}^{(0)} = D\boldsymbol{\varphi}^{(0)}$.

If such a body is subject to a small disturbance from equilibrium, we can look for solutions of the form

$$\boldsymbol{\varphi}(\mathbf{x}, t) = \boldsymbol{\varphi}^{(0)}(\mathbf{x}) + \epsilon\, \mathbf{u}(\mathbf{x}, t) + \mathcal{O}\big(\epsilon^2\big), \tag{4.246}$$

where $\mathbf{u}$ is the displacement vector and ϵ a dimensionless perturbation parameter. Under this *ansatz* the deformation gradient becomes

$$\mathbf{F}(\mathbf{x}, t) = \mathbf{F}^{(0)}(\mathbf{x}) + \epsilon\, \mathbf{F}_{\mathbf{u}}(\mathbf{x}, t) + \mathcal{O}\big(\epsilon^2\big), \tag{4.247}$$

while the first Piola-Kirchhoff stress expands to

$$\mathbf{P}(\mathbf{x}, t) = \mathbf{P}^{(0)}(\mathbf{x}) + \epsilon\, \mathbf{A}(\mathbf{x}) \cdot \mathbf{F}_{\mathbf{u}}(\mathbf{x}, t) + \mathcal{O}(\epsilon^2). \tag{4.248}$$

We have defined the first-order deformation gradient

$$\mathbf{F}_{\mathbf{u}}(\mathbf{x}, t) = D_{\mathbf{x}} \mathbf{u}(\mathbf{x}, t) \tag{4.249}$$

and the *first elastic tensor*

$$\mathbf{A}(\mathbf{x}) = D^2_{\mathbf{F}} W\Big[\mathbf{x}, \mathbf{F}^{(0)}(\mathbf{x})\Big]. \tag{4.250}$$

The first elastic tensor possesses the so-called hyperelastic symmetry,

$$\mathbf{A}^T = \mathbf{A}, \tag{4.251}$$

due to the equality of mixed partial derivatives. In index notation this relationship takes the familiar form $\mathsf{A}_{ijkl} = \mathsf{A}_{klij}$. We will follow standard seismological terminology henceforward and refer to $\mathbf{A}$ simply as "the elastic tensor" unless that is likely to cause confusion.

We can conveniently derive the linearised EoMs in weak form by following the method described earlier, whereby the *action* is expanded to $\mathcal{O}\big(\epsilon^2\big)$ and variation then carried out with respect to the first-order fields. Substituting the linearised relations above into the action (4.236) and defining the first order external body force as

$$\mathbf{b}^{(1)}(\boldsymbol{\varphi}^{(0)}) = -D_{\boldsymbol{\varphi}} \mathcal{U}^{(1)}(\boldsymbol{\varphi}^{(0)}), \tag{4.252}$$

we find that the action's quadratic part is

$$\mathcal{S}^{(2)} = \int_{\mathcal{I}} \int_{\mathcal{B}} \left[\frac{1}{2} \langle \dot{\mathbf{u}}, \rho \dot{\mathbf{u}} \rangle - \frac{1}{2} \langle \mathbf{F}_{\mathbf{u}}, \mathbf{A} \cdot \mathbf{F}_{\mathbf{u}} \rangle \right.$$
$$\left. - \frac{1}{4} \rho \int_{\mathcal{B}} \left\langle \mathbf{u} - \mathbf{u}', \rho' \nabla\nabla\Gamma^{(0)} \cdot \big(\mathbf{u} - \mathbf{u}'\big) \right\rangle \, \mathrm{d}V' + \left\langle \mathbf{u}, \mathbf{b}^{(1)} \right\rangle \right] \, \mathrm{d}V \, \mathrm{d}t. \tag{4.253}$$

We have also defined the shorthand

$$\nabla\nabla\Gamma^{(0)}(\mathbf{x}, \mathbf{x}') = \nabla\nabla\Gamma \Big[\boldsymbol{\varphi}^{(0)}(\mathbf{x}) - \boldsymbol{\varphi}^{(0)}(\mathbf{x}') \Big]. \tag{4.254}$$

We may now vary the quadratic action with respect to $\mathbf{u}$, and then replace all instances of $\delta\mathbf{u}$ with the test-function

$$\mathbf{v} : \mathcal{B} \times \mathcal{I} \mapsto \mathbb{R}^3. \tag{4.255}$$

Demanding that the result vanish for all test-functions $\mathbf{v}$ we finally arrive at the linearised equations of self-gravitating elastodynamics, in weak form:

$$\int_{\mathcal{I}} \int_{\mathcal{B}} \left[\langle \dot{\mathbf{v}}, \rho \dot{\mathbf{u}} \rangle - \langle \mathbf{F}_{\mathbf{v}}, \mathbf{A} \cdot \mathbf{F}_{\mathbf{u}} \rangle - \frac{1}{2} \rho \int_{\mathcal{B}} \left\langle \mathbf{v} - \mathbf{v}', \rho' \nabla\nabla\Gamma^{(0)} \cdot \big(\mathbf{u} - \mathbf{u}'\big) \right\rangle \, \mathrm{d}V' + \left\langle \mathbf{v}, \mathbf{b}^{(1)} \right\rangle \right] \, \mathrm{d}V \, \mathrm{d}t = 0. \tag{4.256}$$

A few more manipulations can bring this into the form we want. We time-integrate the first term by parts, then eliminate $\mathbf{v}'$ from the gravitational term, to give

$$\int_{\mathcal{I}} \int_{\mathcal{B}} \left[-\langle \mathbf{v}, \rho \ddot{\mathbf{u}} \rangle - \langle \mathbf{F}_{\mathbf{v}}, \mathbf{A} \cdot \mathbf{F}_{\mathbf{u}} \rangle - \left\langle \mathbf{v}, \rho \int_{\mathcal{B}} \rho' \nabla\nabla\Gamma^{(0)} \cdot \big(\mathbf{u} - \mathbf{u}'\big) \, \mathrm{d}V' \right\rangle + \left\langle \mathbf{v}, \mathbf{b}^{(1)} \right\rangle \right] \, \mathrm{d}V \, \mathrm{d}t = 0. \tag{4.257}$$

Next, as we showed in Section 4.2 we can 'take off' the time-integral and interpret $\mathbf{v}$ as a time-independent test-function. Given that ρ, $\mathbf{A}$ and $\nabla\nabla\Gamma^{(0)}$ are constant in time we can Fourier-transform in time to give

$$\int_{\mathcal{B}} \left[\nu^2 \langle \mathbf{v}, \rho \mathbf{u} \rangle - \langle \mathbf{F}_{\mathbf{v}}, \mathbf{A} \cdot \mathbf{F}_{\mathbf{u}} \rangle - \left\langle \mathbf{v}, \rho \int_{\mathcal{B}} \rho' \nabla\nabla\Gamma^{(0)} \cdot \big(\mathbf{u} - \mathbf{u}'\big) \, \mathrm{d}V' \right\rangle + \left\langle \mathbf{v}, \mathbf{b}^{(1)} \right\rangle \right] \, \mathrm{d}V = 0. \tag{4.258}$$

Finally, we define the *linearised gravitational acceleration* to be

$$\boldsymbol{\gamma}^{(1)} = - \int_{\mathcal{B}} \rho' \nabla\nabla\Gamma^{(0)} \cdot \big(\mathbf{u} - \mathbf{u}'\big) \, \mathrm{d}V', \tag{4.259}$$

upon which the Fourier-transformed weak form becomes

$$\nu^2 \int_{\mathcal{B}} \langle \mathbf{v}, \rho \mathbf{u} \rangle \, \mathrm{d}V - \int_{\mathcal{B}} \langle \mathbf{F}_{\mathbf{v}}, \mathbf{A} \cdot \mathbf{F}_{\mathbf{u}} \rangle \, \mathrm{d}V + \int_{\mathcal{B}} \left\langle \mathbf{v}, \rho \boldsymbol{\gamma}^{(1)} \right\rangle \, \mathrm{d}V + \int_{\mathcal{B}} \left\langle \mathbf{v}, \mathbf{b}^{(1)} \right\rangle \, \mathrm{d}V = 0. \tag{4.260}$$

These equations can be solved numerically by *normal-mode coupling*, as outlined in Chapter 1. We will defer discussion of numerical solution to Section 4.5, after we have presented our method

for 'decoupling' the rotational and elastic motion of rotating planets.

4.5 Coupled rotational and elastic deformation

At this stage we have all the tools we need to study the elastodynamics of rotating solid planets. The following discussion more-or-less mirrors Section 4.3. We start with the kinematics and variational principle of a single solid body; most of the important concepts of this section are introduced there. We move on to derive the Euler–Lagrange equations, linearise them, and then give an overview of how the linearised equations might be solved numerically. Finally, we consider how to extend those ideas to $N \geq 2$ solid bodies interacting under gravity.

4.5.1 Kinematics

Recall from Section 4.4.3 that the motion $\boldsymbol{\varphi}$ of a solid, hyperelastic body extremises the action

$$\mathcal{S} = \int_{\mathcal{I}} \int_{\mathcal{B}} \left[\frac{1}{2}\rho \|\mathbf{v}\|^2 - W(\cdot, \mathbf{F}) - \frac{1}{2}\rho\zeta - \mathcal{U}(\boldsymbol{\varphi}) \right] \mathrm{d}V \, \mathrm{d}t. \tag{4.261}$$

Our goal is to rewrite the EoMs governing $\boldsymbol{\varphi}$ so as to give rise naturally to equations that resemble the standard equations both of elasticity and of rigid body motion. How can we reformulate the problem so that this action 'resembles' Section 4.3's action

$$\mathcal{S} = \int_{\mathcal{I}} \left[\frac{1}{2} m \|\dot{\boldsymbol{\Phi}}\|^2 + \frac{1}{2}\langle \boldsymbol{\Omega}, \mathbb{I} \cdot \boldsymbol{\Omega} \rangle_{\mathfrak{so}(3)} + \left\langle \boldsymbol{\Lambda}, \mathbf{R}^T\dot{\mathbf{R}} - \boldsymbol{\Omega} \right\rangle_{\mathfrak{so}(3)} - \mathcal{V}(\boldsymbol{\Phi}, \mathbf{R}) \right] \mathrm{d}t, \tag{4.262}$$

but without neglecting any of the elastic behaviour?

It seems natural to start by rewriting the motion itself in order to make it resemble a rigid body motion. Recall that the key aspects of the rigid body motion (4.29) were the functions $\boldsymbol{\Phi}(t)$, which we came to interpret as the CoM motion, and the rotation matrix $\mathbf{R}(t)$. With this in mind, we decompose the elastic motion $\boldsymbol{\varphi}$ as

$$\boldsymbol{\varphi}(\mathbf{x}, t) = \boldsymbol{\Phi}(t) + \mathbf{R}(t) \cdot \boldsymbol{\varphi}_r(\mathbf{x}, t) \tag{4.263}$$

where

$$\boldsymbol{\Phi} : \mathcal{I} \mapsto \mathbb{R}^3 \tag{4.264}$$

$$\mathbf{R} : \mathcal{I} \mapsto \mathbf{SO}(3) \tag{4.265}$$

$$\boldsymbol{\varphi}_r : \mathcal{B} \times \mathcal{I} \mapsto \mathbb{R}^3, \tag{4.266}$$

and $\boldsymbol{\varphi}_r$ is subject at all times to the constraints

$$\int_{\mathcal{B}} \rho \boldsymbol{\varphi}_r \, \mathrm{d}V = 0 \tag{4.267}$$

$$\int_{\mathcal{B}} \rho \boldsymbol{\varphi}_r \wedge \dot{\boldsymbol{\varphi}}_r \, \mathrm{d}V = 0. \tag{4.268}$$

Through $\boldsymbol{\varphi}_r$ we account fully for elastic behaviour, but with an overall motion that still 'looks rigid'. A key difference between eq.(4.263) and eq.(4.29) is that what was earlier the *label* $\mathbf{x}$ has now become the *field* $\boldsymbol{\varphi}_r$. $\boldsymbol{\varphi}_r$ must satisfy six scalar constraints at all times because in writing decomposition (4.263) we *introduced* six extra time-dependent functions into the problem: the three components of $\boldsymbol{\Phi}(\cdot)$ and the three independent components of $\mathbf{R}(\cdot)$. We are free to choose any six constraints, but we have found those given to be the most convenient both numerically and interpretatively.

To motivate the first constraint we consider the elastic body's centre of mass. In Section 4.3 we showed that $\boldsymbol{\Phi}$ could be interpreted as the CoM motion iff the coordinate system on the reference body was chosen so that $\int_{\mathcal{B}} \rho \mathbf{x} \, \mathrm{d}V$ vanished. Here, by analogy with eq.(4.32) we integrate $\frac{\rho}{m}$ times eq.(4.263) over $\mathcal{B}$ to give

$$\frac{1}{m}\int_{\mathcal{B}} \rho(\mathbf{x})\boldsymbol{\varphi}(\mathbf{x},t)\,\mathrm{d}V = \boldsymbol{\Phi}(t) + \frac{1}{m}\mathbf{R}(t)\cdot\int_{\mathcal{B}} \rho(\mathbf{x})\boldsymbol{\varphi}_r(\mathbf{x},t)\,\mathrm{d}V. \tag{4.269}$$

Just as above, $\boldsymbol{\Phi}$ will represent the motion of the body's centre of mass iff for all time

$$\int_{\mathcal{B}} \rho(\mathbf{x})\boldsymbol{\varphi}_r(\mathbf{x},t)\,\mathrm{d}V = 0. \tag{4.270}$$

In other words, $\boldsymbol{\varphi}_r$ must have its CoM at the origin and carry no net linear momentum. Note that $\int_{\mathcal{B}} \rho \mathbf{x} \, \mathrm{d}V$ is no longer required to vanish: we have exchanged the constraint on the *coordinate system* for a constraint on *the motion itself*. We take eq.(4.270) to provide the first three constraints.

We can obtain three more constraints by considering the total angular momentum associated with $\boldsymbol{\varphi}$. The velocity field $\dot{\boldsymbol{\varphi}}$ is written as

$$\dot{\boldsymbol{\varphi}}(\mathbf{x},t) = \dot{\boldsymbol{\Phi}}(t) + \mathbf{R}(t)\cdot[\dot{\boldsymbol{\varphi}}_r(t) + \boldsymbol{\Omega}(t)\cdot\boldsymbol{\varphi}_r(\mathbf{x},t)]\,, \tag{4.271}$$

where we define $\boldsymbol{\Omega}$ as above:

$$\boldsymbol{\Omega} = \mathbf{R}^T\dot{\mathbf{R}}. \tag{4.272}$$

The total angular momentum is thus, dropping all arguments,

$$\begin{aligned}\int_{\mathcal{B}} \rho\boldsymbol{\varphi}\wedge\dot{\boldsymbol{\varphi}}\,\mathrm{d}V &= \int_{\mathcal{B}} \rho[\boldsymbol{\Phi}+\mathbf{R}\cdot\boldsymbol{\varphi}_r]\wedge\left[\dot{\boldsymbol{\Phi}}+\mathbf{R}\cdot(\dot{\boldsymbol{\varphi}}_r+\boldsymbol{\Omega}\cdot\boldsymbol{\varphi}_r)\right]\,\mathrm{d}V \\ &= \int_{\mathcal{B}} \rho\boldsymbol{\Phi}\wedge\dot{\boldsymbol{\Phi}}\,\mathrm{d}V + \mathsf{Ad}_{\mathbf{R}}\cdot\int_{\mathcal{B}} \rho\boldsymbol{\varphi}_r\wedge(\dot{\boldsymbol{\varphi}}_r+\boldsymbol{\Omega}\cdot\boldsymbol{\varphi}_r)\,\mathrm{d}V.\end{aligned} \tag{4.273}$$

We have used the centre-of-mass constraint (and its trivial corollary $\int_{\mathcal{B}} \rho\dot{\boldsymbol{\varphi}}_r\,\mathrm{d}V = 0$) to eliminate some terms from the second line. We now define the *instantaneous moment of inertia* $\mathbb{I}_r : \mathfrak{so}(3) \mapsto \mathfrak{so}(3)$ whose $\mathbf{J}_\alpha$-components are

$$[\mathbb{I}_r]_{\alpha\beta} = \langle \mathbf{J}_\alpha, \mathbb{I}_r\cdot\mathbf{J}_\beta\rangle_{\mathfrak{so}(3)} = \int_{\mathcal{B}} \rho\Big(\|\boldsymbol{\varphi}_r\|^2\,\delta_{\alpha\beta} - [\boldsymbol{\varphi}_r]_\alpha[\boldsymbol{\varphi}_r]_\beta\Big)\,\mathrm{d}V. \tag{4.274}$$

We are left with

$$\int_{\mathcal{B}} \rho\boldsymbol{\varphi} \wedge \dot{\boldsymbol{\varphi}}\, \mathrm{d}V = m\boldsymbol{\Phi} \wedge \dot{\boldsymbol{\Phi}} + \mathsf{Ad}_{\mathbf{R}}\mathbb{I}_r \cdot \boldsymbol{\Omega} + \mathsf{Ad}_{\mathbf{R}} \cdot \int_{\mathcal{B}} \rho\boldsymbol{\varphi}_r \wedge \dot{\boldsymbol{\varphi}}_r\, \mathrm{d}V. \tag{4.275}$$

If we now demand as our last three constraints that $\boldsymbol{\varphi}_r$ also carry no net angular momentum, *i.e.*

$$\int_{\mathcal{B}} \rho\boldsymbol{\varphi}_r \wedge \dot{\boldsymbol{\varphi}}_r\, \mathrm{d}V = 0, \tag{4.276}$$

then the total angular momentum associated with $\boldsymbol{\varphi}$ factors neatly into the *orbital* angular momentum of the CoM's linear motion, and *spin* angular momentum associated with rotation about the CoM. Moreover, with $\mathbb{I}_r$ and $\boldsymbol{\Omega}$ as defined, the *form* of the spin angular momentum is the same as for a rigid body, but with an effective, time-dependent moment of inertia that accounts for the body's deformation.

These constraints make precise our earlier statements about writing the motion in a fashion that is "as close to rigid body motion as possible". Specifically, the standard Euler equations follow from the conditions that the CoM is at the origin of the coordinate system on $\mathcal{B}$, and that the angular momentum is just orbital and spin. We can achieve those conditions in the elastic case by imposing the stated constraints, and in so doing we give $\boldsymbol{\Phi}$, $\mathbf{R}$ and $\boldsymbol{\Omega}$ an interpretation that is as close to their pure rigid body interpretation as possible. Intuitively, we can see decomposition (4.263) as describing elastic motion that takes place in a rotating frame whose orientation is given by $\mathbf{R}$ and whose centre of mass is at $\boldsymbol{\Phi}$. We will see shortly how the constraints affect the elastic motion $\boldsymbol{\varphi}_r$.

4.5.2 Variational principle

We obtain the rotating elastic body's action by substituting the decomposed motion

$$\boldsymbol{\varphi} = \boldsymbol{\Phi} + \mathbf{R} \cdot \boldsymbol{\varphi}_r \tag{4.277}$$

into action (4.261) and, crucially, including the constraints (4.270) and (4.276) through the method of *Lagrange multipliers*. From eq.(4.271)

$$\mathbf{v} = \mathbf{v}_c + \mathbf{R} \cdot (\mathbf{v}_r + \boldsymbol{\Omega} \cdot \boldsymbol{\varphi}_r), \tag{4.278}$$

and if we define

$$\mathbf{F}_r = D_{\mathbf{x}}\boldsymbol{\varphi}_r \tag{4.279}$$

it is readily shown that $\boldsymbol{\varphi}$'s deformation gradient is

$$\mathbf{F} = \mathbf{R}\mathbf{F}_r. \tag{4.280}$$

The relations

$$W(\mathbf{x}, \mathbf{F}_r) = W(\mathbf{x}, \mathbf{F}) \tag{4.281}$$

$$\zeta_r(\mathbf{x}, t) \equiv \hat{\zeta}[\boldsymbol{\varphi}_r(\cdot, t), \mathbf{x}] = \hat{\zeta}[\boldsymbol{\varphi}(\cdot, t), \mathbf{x}] \tag{4.282}$$

also hold trivially. We now introduce the Lagrange multiplier functions

$$\boldsymbol{\alpha} : \mathcal{I} \mapsto \mathbb{R}^3 \tag{4.283}$$

$$\boldsymbol{\beta} : \mathcal{I} \mapsto \mathfrak{so}(3) \tag{4.284}$$

and substitute everything into the one-body action (4.261) to give the full, constrained action

$$\begin{aligned}\mathcal{S} = \int_{\mathcal{I}} \int_{\mathcal{B}} \Big[&\frac{1}{2}\rho \|\mathbf{v}_c + \mathbf{R} \cdot (\mathbf{v}_r + \boldsymbol{\Omega} \cdot \boldsymbol{\varphi}_r)\|^2 - W(\mathbf{x}, \mathbf{F}_r) - \frac{1}{2}\rho\zeta_r \\ &+ \langle \boldsymbol{\alpha}, \rho \boldsymbol{\varphi}_r \rangle + \langle \dot{\boldsymbol{\varphi}}_r, \rho \boldsymbol{\beta} \cdot \boldsymbol{\varphi}_r \rangle - \mathcal{U}(\boldsymbol{\Phi}, \mathbf{R}, \boldsymbol{\varphi}_r) \Big] \, \mathrm{d}V \, \mathrm{d}t. \end{aligned} \tag{4.285}$$

We have included an arbitrary potential $\mathcal{U} : \mathbb{R}^3 \times \mathbf{SO}(3) \times \mathbb{R}^3 \mapsto \mathbb{R}$. We can simplify eq.(4.285) by explicitly applying the constraints to the kinetic energy term. Expanding out that term and rearranging,

$$\begin{aligned}\int_{\mathcal{I}} \mathcal{T} \, \mathrm{d}t = &\int_{\mathcal{I}} \int_{\mathcal{B}} \frac{1}{2}\rho \Big(\|\mathbf{v}_c\|^2 + \|\mathbf{v}_r\|^2 + \|\boldsymbol{\Omega} \cdot \boldsymbol{\varphi}_r\|^2 \Big) \, \mathrm{d}V \, \mathrm{d}t \\ &+ \int_{\mathcal{I}} \left[\left\langle \mathbf{v}_c, \mathbf{R} \cdot \int_{\mathcal{B}} \rho \mathbf{v}_r \, \mathrm{d}V \right\rangle + \left\langle \mathbf{v}_c, \mathbf{R}\boldsymbol{\Omega} \cdot \int_{\mathcal{B}} \rho \boldsymbol{\varphi}_r \, \mathrm{d}V \right\rangle + \left\langle \boldsymbol{\Omega}, \int_{\mathcal{B}} \rho \boldsymbol{\varphi}_r \wedge \mathbf{v}_r \, \mathrm{d}V \right\rangle_{\mathfrak{so}(3)} \right] \mathrm{d}t \end{aligned} \tag{4.286}$$

and it is clear that the last three terms can be disregarded. Dropping these terms can alternatively be seen as a redefinition of the Lagrange multipliers. Either way, the action becomes

$$\begin{aligned}\mathcal{S} = \int_{\mathcal{I}} \int_{\mathcal{B}} \Big[&\frac{1}{2}\rho \|\mathbf{v}_c\|^2 + \frac{1}{2}\rho \|\mathbf{v}_r\|^2 + \frac{1}{2}\rho \|\boldsymbol{\Omega} \cdot \boldsymbol{\varphi}_r\|^2 - W(\mathbf{x}, \mathbf{F}_r) - \frac{1}{2}\rho\zeta_r \\ &+ \langle \boldsymbol{\alpha}, \rho \boldsymbol{\varphi}_r \rangle + \langle \dot{\boldsymbol{\varphi}}_r, \rho \boldsymbol{\beta} \cdot \boldsymbol{\varphi}_r \rangle - \mathcal{U}(\boldsymbol{\Phi}, \mathbf{R}, \boldsymbol{\varphi}_r) \Big] \, \mathrm{d}V \, \mathrm{d}t, \end{aligned} \tag{4.287}$$

and we can finally rewrite the terms in $\dot{\boldsymbol{\Phi}}$ and $\boldsymbol{\Omega}$ just as we did for a rigid body to give

$$\begin{aligned}\mathcal{S} = \int_{\mathcal{I}} \Bigg\{ &\frac{1}{2} m \left\| \dot{\boldsymbol{\Phi}} \right\|^2 + \frac{1}{2} \langle \boldsymbol{\Omega}, \mathbb{I}_r \cdot \boldsymbol{\Omega} \rangle_{\mathfrak{so}(3)} + \left\langle \boldsymbol{\Lambda}, \mathbf{R}^T \dot{\mathbf{R}} - \boldsymbol{\Omega} \right\rangle_{\mathfrak{so}(3)} \\ &+ \int_{\mathcal{B}} \left[\frac{1}{2}\rho \|\mathbf{v}_r\|^2 - W(\mathbf{x}, \mathbf{F}_r) - \frac{1}{2}\rho\zeta_r + \langle \boldsymbol{\alpha}, \rho \boldsymbol{\varphi}_r \rangle + \langle \dot{\boldsymbol{\varphi}}_r, \rho \boldsymbol{\beta} \cdot \boldsymbol{\varphi}_r \rangle - \mathcal{U}(\boldsymbol{\Phi}, \mathbf{R}, \boldsymbol{\varphi}_r) \right] \mathrm{d}V \Bigg\} \, \mathrm{d}t, \end{aligned} \tag{4.288}$$

including the constraint on the angular velocity through the term in $\boldsymbol{\Lambda}$.

The action has factored into three separate parts each with a clear physical interpretation. The first two terms above are cosmetically identical to the action of a rigid body. The one subtle difference is that the moment of inertia is no longer constant due to its dependence on $\boldsymbol{\varphi}_r$. The

third term above is just the standard action for a self-gravitating elastic body but including the required constraints.

4.5.3 Euler–Lagrange equations

We now vary the action with respect to $\boldsymbol{\Phi}$, $\mathbf{R}$, $\boldsymbol{\Omega}$, $\boldsymbol{\Lambda}$, $\boldsymbol{\varphi}_r$, $\boldsymbol{\alpha}$ and $\boldsymbol{\beta}$ in order to derive the Euler–Lagrange equations. To begin, we define the net force, net torque and body-force as

$$\mathbf{f} = -\int_{\mathcal{B}} D_{\boldsymbol{\Phi}}\mathcal{U}\,\mathrm{d}V \tag{4.289}$$

$$\mathbf{L} = -\mathbf{R}^T\int_{\mathcal{B}} D_{\mathbf{R}}\mathcal{U}\,\mathrm{d}V \tag{4.290}$$

$$\mathbf{b} = -D_{\boldsymbol{\varphi}_r}\mathcal{U} \tag{4.291}$$

respectively. Varying $\mathcal{S}$ with respect to $\boldsymbol{\Phi}$ then yields

$$m\ddot{\boldsymbol{\Phi}} = \mathbf{f}. \tag{4.292}$$

Next, we can derive $\boldsymbol{\Omega}$'s EoMs very quickly by noting that

$$\begin{aligned}\mathcal{S} = \int_{\mathcal{I}}\Big(\frac{1}{2}\langle\boldsymbol{\Omega},\mathbb{I}_r\cdot\boldsymbol{\Omega}\rangle_{\mathfrak{so}(3)} + \Big\langle\boldsymbol{\Lambda},\mathbf{R}^T\dot{\mathbf{R}}-\boldsymbol{\Omega}\Big\rangle_{\mathfrak{so}(3)} - \int_{\mathcal{B}}\mathcal{U}(\boldsymbol{\Phi},\mathbf{R},\boldsymbol{\varphi}_r)\,\mathrm{d}V \\ +(\text{terms in }\mathbf{v}_c,\,\boldsymbol{\varphi}_r,\mathbf{v}_r\text{ and }\mathbf{F}_r\text{ only}))\,\mathrm{d}t.\end{aligned} \tag{4.293}$$

The derivation of Section 4.3 may therefore be replicated line-for-line to obtain

$$(\partial_t + \mathsf{ad}_{\boldsymbol{\Omega}})\cdot\mathbb{I}_r\cdot\boldsymbol{\Omega} = \mathbf{L} \tag{4.294a}$$

$$\dot{\mathbf{R}} = \mathbf{R}\boldsymbol{\Omega}. \tag{4.294b}$$

The variation of the terms in $\boldsymbol{\varphi}_r$ that were not present in Section 4.4 is

$$\begin{aligned}&\delta\int_{\mathcal{I}}\Big\{\frac{1}{2}\langle\boldsymbol{\Omega},\mathbb{I}_r\cdot\boldsymbol{\Omega}\rangle_{\mathfrak{so}(3)} + \int_{\mathcal{B}}(\langle\boldsymbol{\alpha},\rho\boldsymbol{\varphi}_r\rangle + \langle\dot{\boldsymbol{\varphi}}_r,\rho\boldsymbol{\beta}\cdot\boldsymbol{\varphi}_r\rangle)\,\mathrm{d}V\Big\}\,\mathrm{d}t \\ &= \int_{\mathcal{I}}\int_{\mathcal{B}}\{\rho\langle\boldsymbol{\Omega}\cdot\boldsymbol{\varphi}_r,\boldsymbol{\Omega}\cdot\delta\boldsymbol{\varphi}_r\rangle + \langle\boldsymbol{\alpha},\rho\delta\boldsymbol{\varphi}_r\rangle + \langle\dot{\boldsymbol{\varphi}}_r,\rho\boldsymbol{\beta}\cdot\delta\boldsymbol{\varphi}_r\rangle + \langle\delta\dot{\boldsymbol{\varphi}}_r,\rho\boldsymbol{\beta}\cdot\boldsymbol{\varphi}_r\rangle\}\,\mathrm{d}V\,\mathrm{d}t \\ &= \int_{\mathcal{I}}\int_{\mathcal{B}}\Big\{\rho\Big\langle-\boldsymbol{\Omega}^2\cdot\boldsymbol{\varphi}_r + \boldsymbol{\alpha} - 2\boldsymbol{\beta}\cdot\dot{\boldsymbol{\varphi}}_r - \dot{\boldsymbol{\beta}}\cdot\boldsymbol{\varphi}_r,\delta\boldsymbol{\varphi}_r\Big\rangle\Big\}\,\mathrm{d}V\,\mathrm{d}t.\end{aligned} \tag{4.295}$$

In obtaining the second line we have used the identity (*c.f.* eq. 4.70)

$$\langle\boldsymbol{\Omega},\mathbb{I}_r\cdot\boldsymbol{\Omega}\rangle_{\mathfrak{so}(3)} = \int_{\mathcal{B}}\rho\langle\boldsymbol{\Omega}\cdot\boldsymbol{\varphi}_r,\boldsymbol{\Omega}\cdot\boldsymbol{\varphi}_r\rangle\,\mathrm{d}V, \tag{4.296}$$

and to reach the third we have time-integrated the second line's last term by parts and rearranged some terms. Defining

$$\boldsymbol{\gamma}_r = -\int_{\mathcal{B}}\rho'\nabla\Gamma\big[\boldsymbol{\varphi}_r - \boldsymbol{\varphi}_r'\big]\,\mathrm{d}V', \tag{4.297}$$

the resulting Euler–Lagrange equations are

$$\rho\ddot{\boldsymbol{\varphi}}_r - \mathrm{Div}\mathbf{P}_r - \rho\boldsymbol{\gamma}_r + \rho\Big(\boldsymbol{\Omega}^2\cdot\boldsymbol{\varphi}_r + 2\boldsymbol{\beta}\cdot\dot{\boldsymbol{\varphi}}_r + \dot{\boldsymbol{\beta}}\cdot\boldsymbol{\varphi}_r\Big) - \rho\boldsymbol{\alpha} = \mathbf{b}, \tag{4.298}$$

subject to the boundary condition

$$\mathbf{P}_r\cdot\hat{\mathbf{n}} = 0 \tag{4.299}$$

on $\partial\mathcal{B}$.

We complete the derivation by eliminating the Lagrange multipliers $\boldsymbol{\alpha}$ and $\boldsymbol{\beta}$ from the equations for $\boldsymbol{\varphi}_r$. From the point of view of numerical solution this step is not strictly necessary, but it does provide some physical insight. Eq.(4.298) is a balance of force-densities, so we anticipate that integrating it over the reference body to find the net force will give some simplification. We find that

$$\int_{\mathcal{B}}\Big\{\rho\ddot{\boldsymbol{\varphi}}_r - \mathrm{Div}\mathbf{P}_r - \rho\boldsymbol{\gamma}_r + \rho\Big(\boldsymbol{\Omega}^2\cdot\boldsymbol{\varphi}_r + 2\boldsymbol{\beta}\cdot\dot{\boldsymbol{\varphi}}_r + \dot{\boldsymbol{\beta}}\cdot\boldsymbol{\varphi}_r\Big) - \rho\boldsymbol{\alpha}\Big\}\,\mathrm{d}V = \int_{\mathcal{B}}\mathbf{b}\,\mathrm{d}V. \tag{4.300}$$

The terms describing self-gravity and stress vanish because the body can exert no net gravitational or elastic force upon itself. Furthermore, all the terms in which $\boldsymbol{\varphi}_r$ explicitly occurs vanish trivially due to the CoM constraint. We are left with

$$\boldsymbol{\alpha} = -\frac{1}{m}\int_{\mathcal{B}}\mathbf{b}\,\mathrm{d}V. \tag{4.301}$$

Next we compute the net torque associated with eq.(4.298) by writing

$$\int_{\mathcal{B}}\rho\Big\{\boldsymbol{\varphi}_r\wedge\ddot{\boldsymbol{\varphi}}_r + \boldsymbol{\varphi}_r\wedge\big(\boldsymbol{\Omega}^2\cdot\boldsymbol{\varphi}_r\big) + 2\boldsymbol{\varphi}_r\wedge(\boldsymbol{\beta}\cdot\dot{\boldsymbol{\varphi}}_r) + \boldsymbol{\varphi}_r\wedge\Big(\dot{\boldsymbol{\beta}}\cdot\boldsymbol{\varphi}_r\Big)\Big\}\,\mathrm{d}V = \int_{\mathcal{B}}\boldsymbol{\varphi}_r\wedge\mathbf{b}\,\mathrm{d}V. \tag{4.302}$$

We have ignored the self-gravity and stress terms, as well as the term in $\boldsymbol{\alpha}$, because they cannot produce a net torque either. We can now use the constraint on $\boldsymbol{\varphi}_r$'s angular momentum to show, after a brief calculation, that

$$\partial_t(\mathbb{I}_r\cdot\boldsymbol{\beta}) + \mathsf{ad}_{\boldsymbol{\Omega}}\mathbb{I}_r\cdot\boldsymbol{\Omega} = \int_{\mathcal{B}}\boldsymbol{\varphi}_r\wedge\mathbf{b}\,\mathrm{d}V. \tag{4.303}$$

This we may combine with the Euler equation to yield

$$\partial_t[\mathbb{I}_r\cdot(\boldsymbol{\Omega}-\boldsymbol{\beta})] = \mathbf{L} - \int_{\mathcal{B}}\boldsymbol{\varphi}_r\wedge\mathbf{b}\,\mathrm{d}V. \tag{4.304}$$

Now, all the potentials that we will encounter in this chapter can be written as

$$\mathcal{U}(\boldsymbol{\Phi},\mathbf{R},\boldsymbol{\varphi}_r) = \hat{\mathcal{U}}(\boldsymbol{\Phi}+\mathbf{R}\cdot\boldsymbol{\varphi}_r) \tag{4.305}$$

for some auxiliary potential energy function $\hat{\mathcal{U}}:\mathbb{R}^3\mapsto\mathbb{R}$. For potentials *of this form* it is readily

shown that $\mathbf{L}$ and $\int_{\mathcal{B}} \boldsymbol{\varphi}_r \wedge \mathbf{b}\,\mathrm{d}V$ are *equal*. For eq.(4.304) to hold it is therefore sufficient to set

$$\boldsymbol{\beta} = \boldsymbol{\Omega}, \tag{4.306}$$

and our derivation of the equations of motion is complete.

To summarise, we have obtained equations of motion that describe the deformation of a self-gravitating elastic body in terms of:

1. the motion of its centre of mass, $\boldsymbol{\Phi}$;
2. a rotation about that centre of mass, $\mathbf{R}$;
3. and elastic motion $\boldsymbol{\varphi}_r$ with respect to the rotating frame defined by $\boldsymbol{\Phi}$ and $\mathbf{R}$.

This decomposition of the motion is made unique by supplying six time-dependent constraints, which we *chose* so that $\boldsymbol{\varphi}_r$ should carry no net linear or angular momentum. Altogether, the rotating elastic body's motion obeys

$$m\ddot{\boldsymbol{\Phi}} = \mathbf{f} \tag{4.307a}$$

$$(\partial_t + \mathsf{ad}_{\boldsymbol{\Omega}})\,\mathbb{I}_r \cdot \boldsymbol{\Omega} = \mathbf{L} \tag{4.307b}$$

$$\dot{\mathbf{R}} = \mathbf{R}\boldsymbol{\Omega} \tag{4.307c}$$

$$\ddot{\boldsymbol{\varphi}}_r + \boldsymbol{\Omega}^2 \cdot \boldsymbol{\varphi}_r + 2\boldsymbol{\Omega} \cdot \dot{\boldsymbol{\varphi}}_r + \dot{\boldsymbol{\Omega}} \cdot \boldsymbol{\varphi}_r - \frac{1}{\rho}\mathrm{Div}\mathbf{P}_r - \boldsymbol{\gamma}_r = \mathbf{b} - \frac{1}{m}\int_{\mathcal{B}} \mathbf{b}\,\mathrm{d}V \tag{4.307d}$$

$$\int_{\mathcal{B}} \rho\boldsymbol{\varphi}_r\,\mathrm{d}V = 0 \tag{4.307e}$$

$$\int_{\mathcal{B}} \rho\boldsymbol{\varphi}_r \wedge \dot{\boldsymbol{\varphi}}_r\,\mathrm{d}V = 0 \tag{4.307f}$$

$$\mathbf{P}_r \cdot \hat{\mathbf{n}} = 0,\ \mathbf{x} \in \partial\mathcal{B}. \tag{4.307g}$$

We find that the CoM obeys Newton's Second Law, while the angular velocity obeys a modified Euler equation. The modification is that the moment of inertia depends on time implicitly through $\boldsymbol{\varphi}_r$. $\boldsymbol{\varphi}_r$ obeys a momentum equation reminiscent of the standard equations of global seismology, but with some important differences. Firstly, there is no requirement that the angular velocity in eq.(4.307d) be either small or constant. This equation describes finite elastodynamics in a variably rotating frame. Due to the constraint on the CoM the external body force $\mathbf{b}$ can also exert no *net* force. Using gravitationally-inspired terminology, we could say that $\boldsymbol{\varphi}_r$ only sees the *tidal* forces associated with $\mathcal{U}$.

This system is ostensibly far more complicated than the system we started out with,

$$\partial_t \mathbf{v} - \mathrm{Div}\mathbf{P} - \rho\boldsymbol{\gamma} = 0, \tag{4.308}$$

but we find it preferable for three main reasons. First, it achieves the stated goal of the Introduction: we have shown that something like an Euler equation and something like a momentum equation do indeed both emerge from the exact equations of continuum mechanics as applied to a rotating body. Secondly, the fact that $\boldsymbol{\varphi}_r$ is constrained to possess no linear or

angular momentum means that it should never become too large, which should considerably ease numerical solution. Finally, we feel that equations (4.307) point more clearly to different approximation schemes. For instance, we can reach equations similar to those of Dahlen & Tromp (1998) by simply setting $\boldsymbol{\Omega}$ to be a constant in eq.(4.307), linearising with respect to $\boldsymbol{\varphi}_r$, and ignoring the Euler equation. Conversely, one could ignore the momentum equation, set $\boldsymbol{\varphi}_r$ to be constant, and find oneself with a pure rigid body. Most interestingly, though, from this author's perspective, is that these equations offer a systematic way of thinking about how elastic and rotational motion interact, especially in a linearised sense.

4.5.4 Equilibria and linearisation

It is unlikely that we will often want or need exact solutions of eqs.(4.307). When studying planetary bodies we are most likely to be interested in external potentials that look like

$$\mathcal{U}(\boldsymbol{\Phi}, \mathbf{R}, \boldsymbol{\varphi}_r) = m^* \rho \Gamma(\boldsymbol{\Phi} + \mathbf{R} \cdot \boldsymbol{\varphi}_r), \tag{4.309}$$

which generalise the point-mass potential (4.75) that we discussed in Section 4.3. By analogy with the rigid case, we can Taylor-expand this potential as

$$\mathcal{U}(\boldsymbol{\Phi}, \mathbf{R}, \boldsymbol{\varphi}_r) = m^* \rho \Gamma(\boldsymbol{\Phi}) + \frac{1}{2} m^* \rho \langle \mathbf{R} \cdot \boldsymbol{\varphi}_r, \nabla\nabla\Gamma(\boldsymbol{\Phi}) \mathbf{R} \cdot \boldsymbol{\varphi}_r \rangle + \dots \tag{4.310}$$

and consider the second-order term to be a small perturbation $\mathcal{U}^{(1)}$. This allows us to study small elastic and rotational motions about an equilibrium state that is stationary except for a *uniform rotation*.

Such an equilibrium state can be derived by removing the time-derivatives from the momentum and Euler equations to give the equilibrium equations

$$\mathrm{Div}\mathbf{P}_r = \rho\big(\boldsymbol{\Omega}^2 \cdot \boldsymbol{\varphi}_r - \boldsymbol{\gamma}_r\big) \tag{4.311a}$$

$$\mathsf{ad}_{\boldsymbol{\Omega}} \mathbb{I}_r \cdot \boldsymbol{\Omega} = 0 \tag{4.311b}$$

$$\dot{\mathbf{R}} = \mathbf{R}\boldsymbol{\Omega} \tag{4.311c}$$

$$\int_{\mathcal{B}} \rho \boldsymbol{\varphi}_r \, \mathrm{d}V = 0. \tag{4.311d}$$

(We neglect the constraint on $\boldsymbol{\varphi}_r$'s angular momentum because at equilibrium $\dot{\boldsymbol{\varphi}}_r$ is assumed to vanish, automatically satisfying the constraint.) The secularly stable solution has $\boldsymbol{\Omega}$ aligned along $\mathbb{I}_r$'s axis of greatest inertia. $\mathbb{I}_r$ depends on $\boldsymbol{\varphi}_r$ of course, and $\boldsymbol{\varphi}_r$ in turn must satisfy the equilibrium stress equation, so one might think that finding a valid equilibrium would be difficult. Fortunately, though, for any $\boldsymbol{\varphi}_r$ it is true that

$$\int_{\mathcal{B}} \rho\big(\boldsymbol{\Omega}^2 \cdot \boldsymbol{\varphi}_r - \boldsymbol{\gamma}_r\big) \, \mathrm{d}V = \boldsymbol{\Omega}^2 \cdot \int_{\mathcal{B}} \rho \boldsymbol{\varphi}_r \, \mathrm{d}V - \int_{\mathcal{B}} \rho \boldsymbol{\gamma}_r \, \mathrm{d}V = 0, \tag{4.312}$$

and

$$\int_{\mathcal{B}} \boldsymbol{\varphi}_r \wedge \rho\big(\boldsymbol{\Omega}^2 \cdot \boldsymbol{\varphi}_r - \boldsymbol{\gamma}_r\big)\, \mathrm{d}V = \mathsf{ad}_{\boldsymbol{\Omega}} \cdot \int_{\mathcal{B}} \boldsymbol{\varphi}_r \wedge \rho(\boldsymbol{\Omega} \cdot \boldsymbol{\varphi}_r)\, \mathrm{d}V - \int_{\mathcal{B}} \boldsymbol{\varphi}_r \wedge \boldsymbol{\gamma}_r\, \mathrm{d}V = \mathsf{ad}_{\boldsymbol{\Omega}} \mathbb{I}_r \cdot \boldsymbol{\Omega} = 0. \tag{4.313}$$

This means that $\int_{\mathcal{B}} \mathrm{Div}\mathbf{P}_r\, \mathrm{d}V$ and $\int_{\mathcal{B}} \boldsymbol{\varphi}_r \wedge \mathrm{Div}\mathbf{P}_r\, \mathrm{d}V$ both vanish. Thus it follows from the results of Al-Attar & Woodhouse (2010, eq. 58) that eq. (4.311a) will possess solutions for any choice of $\boldsymbol{\varphi}_r$.

We will take as our concrete equilibrium solution

$$\boldsymbol{\Omega}^{(0)}(t) = \Omega^{(0)} \mathbf{J}_3 \tag{4.314a}$$

$$\mathbf{R}^{(0)}(t) = \exp(\boldsymbol{\Omega}^{(0)} t) = \begin{pmatrix} \cos(\Omega^{(0)} t) & -\sin(\Omega^{(0)} t) & 0 \\ \sin(\Omega^{(0)} t) & \cos(\Omega^{(0)} t) & 0 \\ 0 & 0 & 1 \end{pmatrix} \tag{4.314b}$$

$$\left[\mathbb{I}_r^{(0)}\right]_{\alpha\beta} = \begin{bmatrix} A & 0 & 0 \\ 0 & B & 0 \\ 0 & 0 & C \end{bmatrix}, \tag{4.314c}$$

with $C > B > A$. We now take the potential to be of the form

$$\mathcal{U}(\boldsymbol{\Phi}, \mathbf{R}, \boldsymbol{\varphi}_r) = \mathcal{U}^{(0)}(\boldsymbol{\Phi}, \mathbf{R}, \boldsymbol{\varphi}_r) + \epsilon \mathcal{U}^{(1)}(\boldsymbol{\Phi}, \mathbf{R}, \boldsymbol{\varphi}_r) \tag{4.315}$$

for some small parameter ϵ, and substitute into the action the *ansatz*

$$\boldsymbol{\Phi} = \boldsymbol{\Phi}^{(0)} + \epsilon \boldsymbol{\Phi}^{(1)} \tag{4.316a}$$

$$\boldsymbol{\Omega} = \boldsymbol{\Omega}^{(0)} + \epsilon \boldsymbol{\Omega}^{(1)} \tag{4.316b}$$

$$\boldsymbol{\Lambda} = \boldsymbol{\Lambda}^{(0)} + \epsilon \boldsymbol{\Lambda}^{(1)} \tag{4.316c}$$

$$\mathbf{R} = \mathbf{R}^{(0)} \exp\left[\epsilon \boldsymbol{\theta}^{(1)}\right] \tag{4.316d}$$

$$\boldsymbol{\varphi}_r = \boldsymbol{\varphi}_r^{(0)} + \epsilon \mathbf{u} \tag{4.316e}$$

$$\boldsymbol{\alpha} = \boldsymbol{\alpha}^{(0)} + \epsilon \boldsymbol{\alpha}^{(1)} \tag{4.316f}$$

$$\boldsymbol{\beta} = \boldsymbol{\beta}^{(0)} + \epsilon \boldsymbol{\beta}^{(1)}. \tag{4.316g}$$

We also define the first- and second-order inertia tensors $\mathbb{I}_r^{(1)}, \mathbb{I}_r^{(2)} : \mathfrak{so}(3) \mapsto \mathfrak{so}(3)$ to have $\mathbf{J}_\alpha$-components

$$\left[\mathbb{I}_r^{(1)}\right]_{\alpha\beta} = \int_{\mathcal{B}} \rho\Big(2\Big\langle \boldsymbol{\varphi}^{(0)}, \mathbf{u} \Big\rangle \delta_{\alpha\beta} - \varphi_\alpha^{(0)} u_\beta - \varphi_\alpha^{(0)} u_\beta\Big)\, \mathrm{d}V \tag{4.317}$$

$$\left[\mathbb{I}_r^{(2)}\right]_{\alpha\beta} = \int_{\mathcal{B}} \rho\Big(\|\mathbf{u}\|^2 \delta_{\alpha\beta} - u_\alpha u_\beta\Big)\, \mathrm{d}V, \tag{4.318}$$

and note that the following identities hold:

$$\begin{aligned}\Big\langle \boldsymbol{\Omega}^{(0)}, \mathbb{I}_r^{(2)} \cdot \boldsymbol{\Omega}^{(0)} \Big\rangle_{\mathfrak{so}(3)} &= \int_{\mathcal{B}} \rho \Big\langle \boldsymbol{\Omega}^{(0)} \cdot \mathbf{u}, \boldsymbol{\Omega}^{(0)} \cdot \mathbf{u} \Big\rangle \, \mathrm{d}V \\ &= \int_{\mathcal{B}} \Big\langle \mathbf{u}, -\rho \Big(\boldsymbol{\Omega}^{(0)} \Big)^2 \cdot \mathbf{u} \Big\rangle \, \mathrm{d}V \end{aligned} \tag{4.319}$$

$$\begin{aligned}\Big\langle \boldsymbol{\Omega}^{(1)}, \mathbb{I}_r^{(1)} \cdot \boldsymbol{\Omega}^{(0)} \Big\rangle_{\mathfrak{so}(3)} &= \int_{\mathcal{B}} \rho \Big\langle \boldsymbol{\Omega}^{(1)} \cdot \mathbf{u}, \boldsymbol{\Omega}^{(0)} \cdot \boldsymbol{\varphi}^{(0)} \Big\rangle \, \mathrm{d}V + \int_{\mathcal{B}} \rho \Big\langle \boldsymbol{\Omega}^{(1)} \cdot \boldsymbol{\varphi}^{(0)}, \boldsymbol{\Omega}^{(0)} \cdot \mathbf{u}^{(1)} \Big\rangle \, \mathrm{d}V \\ &= \int_{\mathcal{B}} \Big\langle \mathbf{u}, -\rho \Big(\boldsymbol{\Omega}^{(1)} \boldsymbol{\Omega}^{(0)} + \boldsymbol{\Omega}^{(0)} \boldsymbol{\Omega}^{(1)} \Big) \cdot \boldsymbol{\varphi}^{(0)} \Big\rangle \, \mathrm{d}V \end{aligned} \tag{4.320}$$

Building on the results of Sections 4.3.6 and 4.4.4, it is now readily shown that the component of the action quadratic in ϵ is

$$\begin{aligned}\mathcal{S}^{(2)} = \int_{\mathcal{I}} \Bigg\{ & \frac{1}{2} m \Big\langle \dot{\boldsymbol{\Phi}}^{(1)}, \dot{\boldsymbol{\Phi}}^{(1)} \Big\rangle + \Big\langle \mathbf{f}^{(1)}, \boldsymbol{\Phi}^{(1)} \Big\rangle + \frac{1}{2} \Big\langle \boldsymbol{\Phi}^{(1)}, \boldsymbol{\tau}^{(0)} \cdot \boldsymbol{\Phi}^{(1)} \Big\rangle \\ & + \Big\langle \boldsymbol{\Lambda}^{(1)}, \Delta_t^{(0)} \cdot \boldsymbol{\theta}^{(1)} - \boldsymbol{\Omega}^{(1)} \Big\rangle_{\mathfrak{so}(3)} + \frac{1}{2} \Big\langle \boldsymbol{\theta}^{(1)}, \mathsf{ad}_{\boldsymbol{\Lambda}^{(0)}} \cdot \boldsymbol{\Omega}^{(1)} \Big\rangle_{\mathfrak{so}(3)} + \Big\langle \mathbf{L}^{(1)}, \boldsymbol{\theta}^{(1)} \Big\rangle_{\mathfrak{so}(3)} \\ & + \frac{1}{2} \Big\langle \boldsymbol{\Omega}^{(1)}, \mathbb{I}_r^{(0)} \cdot \boldsymbol{\Omega}^{(1)} \Big\rangle_{\mathfrak{so}(3)} + \Big\langle \boldsymbol{\Omega}^{(1)}, \mathbb{I}_r^{(1)} \cdot \boldsymbol{\Omega}^{(0)} \Big\rangle_{\mathfrak{so}(3)} \\ & + \frac{1}{2} \Big\langle \boldsymbol{\Omega}^{(0)}, \mathbb{I}_r^{(2)} \cdot \boldsymbol{\Omega}^{(0)} \Big\rangle_{\mathfrak{so}(3)} \\ & + \int_{\mathcal{B}} \Bigg(\frac{1}{2} \rho \|\dot{\mathbf{u}}\|^2 - \frac{1}{2} \Big\langle \mathbf{F}^{(1)}, \mathbf{A} \cdot \mathbf{F}^{(1)} \Big\rangle - \frac{1}{4} \rho \int_{\mathcal{B}} \rho' \Big\langle \mathbf{u} - \mathbf{u}', \nabla\nabla\Gamma^{(0)} \cdot \big(\mathbf{u} - \mathbf{u}' \big) \Big\rangle \, \mathrm{d}V' \\ & \qquad + \Big\langle \boldsymbol{\alpha}^{(1)}, \rho \mathbf{u} \Big\rangle + \Big\langle \dot{\mathbf{u}}, \rho \boldsymbol{\beta}^{(0)} \cdot \mathbf{u} \Big\rangle + \Big\langle \dot{\mathbf{u}}, \rho \boldsymbol{\beta}^{(1)} \cdot \boldsymbol{\varphi}^{(0)} \Big\rangle + \Big\langle \mathbf{u}, \mathbf{b}^{(1)} \Big\rangle \Bigg) \, \mathrm{d}V \Bigg\} \, \mathrm{d}t. \end{aligned} \tag{4.321}$$

The forcing terms here are

$$\mathbf{f}^{(1)} = - \int_{\mathcal{B}} D_{\boldsymbol{\Phi}} \mathcal{U}^{(1)} \, \mathrm{d}V \tag{4.322}$$

$$\mathbf{L}^{(1)} = -\mathbf{R}^T \int_{\mathcal{B}} D_{\mathbf{R}} \mathcal{U}^{(1)} \, \mathrm{d}V \tag{4.323}$$

$$\mathbf{b}^{(1)} = -D_{\boldsymbol{\varphi}_r} \mathcal{U}^{(1)}, \tag{4.324}$$

with $\mathcal{U}^{(1)}$'s derivatives evaluated at the zeroth-order field configurations.

As shown in Section 4.2, we obtain the weak form EoMs by writing down the variation of this action and then letting the arbitrary variation be a test function. Before we do this, though, we will modify the action in two ways. Firstly, we will ignore the motion of the CoM and drop the terms in $\boldsymbol{\Phi}^{(1)}$. Given that $\boldsymbol{\Phi}^{(1)}$ is decoupled from the other first-order fields we lose no physical insight, and we would prefer to focus on the coupled elastic and rotational deformation. Secondly, we will deal with the annoying Lagrange multiplier $\boldsymbol{\Lambda}^{(1)}$. We know from earlier that it can be made to drop out by some manipulations of the Euler–Lagrange equations, so let us just eliminate it from the action. We do that by varying the action above with respect to $\boldsymbol{\Omega}^{(1)}$, which

tells us that

$$\boldsymbol{\Lambda}^{(1)} = \mathbb{I}_r^{(0)} \cdot \boldsymbol{\Omega}^{(1)} + \mathbb{I}_r^{(1)} \cdot \boldsymbol{\Omega}^{(0)} - \frac{1}{2}\mathsf{ad}_{\boldsymbol{\Lambda}^{(0)}} \cdot \boldsymbol{\theta}^{(1)}. \tag{4.325}$$

We can then substitute for $\boldsymbol{\Lambda}^{(1)}$ in the action, which gives

$$\begin{aligned}\mathcal{S}^{(2)} = \int_{\mathcal{I}} \Big\{ &\Big\langle \mathbb{I}_r^{(0)} \cdot \boldsymbol{\Omega}^{(1)} + \mathbb{I}_r^{(1)} \cdot \boldsymbol{\Omega}^{(0)} - \frac{1}{2}\mathsf{ad}_{\boldsymbol{\Lambda}^{(0)}}\boldsymbol{\theta}^{(1)}, \Delta_t^{(0)} \cdot \boldsymbol{\theta}^{(1)} \Big\rangle_{\mathfrak{so}(3)} \\ &+ \Big\langle \mathbf{L}^{(1)}, \boldsymbol{\theta}^{(1)} \Big\rangle_{\mathfrak{so}(3)} - \frac{1}{2}\Big\langle \boldsymbol{\Omega}^{(1)}, \mathbb{I}_r^{(0)} \cdot \boldsymbol{\Omega}^{(1)} \Big\rangle_{\mathfrak{so}(3)} \\ &+ \frac{1}{2}\Big\langle \boldsymbol{\Omega}^{(0)}, \mathbb{I}_r^{(2)} \cdot \boldsymbol{\Omega}^{(0)} \Big\rangle_{\mathfrak{so}(3)} \\ &+ \int_{\mathcal{B}} \Big(\frac{1}{2}\rho\|\dot{\mathbf{u}}\|^2 - \frac{1}{2}\Big\langle \mathbf{F}^{(1)}, \mathsf{A} \cdot \mathbf{F}^{(1)} \Big\rangle - \frac{1}{4}\rho \int_{\mathcal{B}} \rho' \Big\langle \mathbf{u} - \mathbf{u}', \nabla\nabla\Gamma^{(0)} \cdot \big(\mathbf{u} - \mathbf{u}'\big) \Big\rangle \, \mathrm{d}V' \\ &\qquad + \Big\langle \boldsymbol{\alpha}^{(1)}, \rho\mathbf{u} \Big\rangle + \Big\langle \dot{\mathbf{u}}, \rho\boldsymbol{\beta}^{(0)} \cdot \mathbf{u} \Big\rangle + \Big\langle \dot{\mathbf{u}}, \rho\boldsymbol{\beta}^{(1)} \cdot \boldsymbol{\varphi}^{(0)} \Big\rangle + \Big\langle \mathbf{u}, \mathbf{b}^{(1)} \Big\rangle \Big) \, \mathrm{d}V \Big\} \, \mathrm{d}t. \end{aligned} \tag{4.326}$$

Let us now vary the action field by field. With respect to $\boldsymbol{\Omega}^{(1)}$ the variation is

$$\delta\mathcal{S}^{(2)} = \int_{\mathcal{I}} \Big\langle \delta\boldsymbol{\Omega}^{(1)}, \mathbb{I}^{(0)} \cdot \Big(\Delta_t^{(0)} \cdot \boldsymbol{\theta}^{(1)} - \boldsymbol{\Omega}^{(1)} \Big) \Big\rangle_{\mathfrak{so}(3)} \, \mathrm{d}t, \tag{4.327}$$

which gives us the reconstruction equation. Varying with respect to $\boldsymbol{\theta}^{(1)}$ gives

$$\begin{aligned}\delta\mathcal{S}^{(2)} &= \int_{\mathcal{I}} \Big\langle \delta\boldsymbol{\theta}^{(1)}, \mathbf{L}^{(1)} - \Delta_t^{(0)} \Big(\mathbb{I}_r^{(0)} \cdot \boldsymbol{\Omega}^{(1)} + \mathbb{I}_r^{(1)} \cdot \boldsymbol{\Omega}^{(0)} - \mathsf{ad}_{\boldsymbol{\Lambda}^{(0)}} \cdot \boldsymbol{\theta}^{(1)} \Big) \Big\rangle_{\mathfrak{so}(3)} \, \mathrm{d}t \\ &= \int_{\mathcal{I}} \Big\langle \delta\boldsymbol{\theta}^{(1)}, \mathbf{L}^{(1)} - \Big[\Big(\Delta_t^{(0)}\mathbb{I}_r^{(0)} - \mathsf{ad}_{\boldsymbol{\Lambda}^{(0)}} \Big) \cdot \boldsymbol{\Omega}^{(1)} + \Delta_t^{(0)}\mathbb{I}_r^{(1)} \cdot \boldsymbol{\Omega}^{(0)} \Big] \Big\rangle_{\mathfrak{so}(3)} \, \mathrm{d}t, \end{aligned} \tag{4.328}$$

where we have used the reconstruction equation and the fact that $\Delta_t^{(0)}$ commutes with $\mathsf{ad}_{\boldsymbol{\Lambda}^{(0)}}$. We then vary with respect to $\mathbf{u}$:

$$\begin{aligned}\delta\mathcal{S}^{(2)} = \int_{\mathcal{I}} \int_{\mathcal{B}} \Big[&-\langle \delta\mathbf{F}_{\mathbf{u}}, \mathsf{A} \cdot \mathbf{F}_{\mathbf{u}} \rangle + \Big\langle \delta\mathbf{u}, \mathbf{b}^{(1)} - \rho\ddot{\mathbf{u}} - \rho\Big(\boldsymbol{\Omega}^{(0)}\Big)^2 \cdot \mathbf{u} - 2\boldsymbol{\Omega}^{(0)} \cdot \dot{\mathbf{u}} + \rho\boldsymbol{\gamma}^{(1)} \\ &\qquad - \rho\Big(\boldsymbol{\Omega}^{(0)}\boldsymbol{\Omega}^{(1)} + \boldsymbol{\Omega}^{(1)}\boldsymbol{\Omega}^{(0)} + \dot{\boldsymbol{\Omega}}^{(1)} \Big) \cdot \boldsymbol{\varphi}^{(0)} \Big\rangle \Big] \, \mathrm{d}V \, \mathrm{d}t. \end{aligned} \tag{4.329}$$

Variation with respect to $\boldsymbol{\alpha}^{(1)}$ and $\boldsymbol{\beta}^{(1)}$ is trivial. Altogether, this gives the weak-form equations

$$\begin{aligned}\delta\mathcal{S}^{(2)} = \int_{\mathcal{I}} \int_{\mathcal{B}} \Big[&-\langle \mathbf{F}_{\mathbf{v}}, \mathsf{A} \cdot \mathbf{F}_{\mathbf{u}} \rangle + \Big\langle \mathbf{v}, \mathbf{b}^{(1)} - \rho\ddot{\mathbf{u}} - \rho\Big(\boldsymbol{\Omega}^{(0)}\Big)^2 \cdot \mathbf{u} - 2\boldsymbol{\Omega}^{(0)} \cdot \dot{\mathbf{u}} + \rho\boldsymbol{\gamma}^{(1)} \\ &\qquad - \rho\Big(\boldsymbol{\Omega}^{(0)}\boldsymbol{\Omega}^{(1)} + \boldsymbol{\Omega}^{(1)}\boldsymbol{\Omega}^{(0)} + \dot{\boldsymbol{\Omega}}^{(1)} \Big) \cdot \boldsymbol{\varphi}^{(0)} \Big\rangle \Big] \, \mathrm{d}V \, \mathrm{d}t. \end{aligned} \tag{4.330}$$

together with the rotational equations

$$\left(\Delta_t^{(0)}\mathbb{I}_r^{(0)} - \mathsf{ad}_{\mathbf{\Lambda}^{(0)}}\right)\cdot\mathbf{\Omega}^{(1)} + \Delta_t^{(0)}\mathbb{I}_r^{(1)}\cdot\mathbf{\Omega}^{(0)} = \mathbf{L}^{(1)} \tag{4.331}$$

$$\Delta_t^{(0)}\cdot\boldsymbol{\theta}^{(1)} = \mathbf{\Omega}^{(1)} \tag{4.332}$$

and the constraints

$$\int_{\mathcal{B}}\rho\mathbf{u}\,\mathrm{d}V = 0 \tag{4.333}$$

$$\int_{\mathcal{B}}\rho\boldsymbol{\varphi}^{(0)}\wedge\mathbf{u}\,\mathrm{d}V = 0. \tag{4.334}$$

We now Fourier-transform in time and introduce the operators $\mathcal{A}$, $\mathcal{B}$ and $\mathcal{C}$, which are defined by

$$\begin{aligned}\int_{\mathcal{B}}\langle\mathbf{v},\mathcal{A}\cdot\mathbf{u}\rangle\,\mathrm{d}V = -\nu^2\int_{\mathcal{B}}\rho\langle\mathbf{v},\mathbf{u}\rangle\,\mathrm{d}V + 2\mathrm{i}\nu\int_{\mathcal{B}}\rho\Big\langle\mathbf{v},\mathbf{\Omega}^{(0)}\cdot\mathbf{u}\Big\rangle\,\mathrm{d}V + \int_{\mathcal{B}}\langle\mathbf{F}_{\mathbf{v}},\mathbf{A}\cdot\mathbf{F}_{\mathbf{u}}\rangle\,\mathrm{d}V \\ - \int_{\mathcal{B}}\rho\Big\langle\mathbf{\Omega}^{(0)}\cdot\mathbf{v},\mathbf{\Omega}^{(0)}\cdot\mathbf{u}\Big\rangle\,\mathrm{d}V - \int_{\mathcal{B}}\rho\Big\langle\mathbf{v},\boldsymbol{\gamma}^{(1)}\Big\rangle\,\mathrm{d}V\end{aligned} \tag{4.335}$$

$$\mathcal{B}\cdot\mathbf{\Omega}^{(1)} = \rho\Big(\mathbf{\Omega}^{(0)}\mathbf{\Omega}^{(1)} + \mathbf{\Omega}^{(1)}\mathbf{\Omega}^{(0)} + \mathrm{i}\nu\mathbf{\Omega}^{(1)}\Big)\cdot\boldsymbol{\varphi}^{(0)} \tag{4.336}$$

$$\mathcal{C}\cdot\mathbf{u} = \Delta\mathbb{I}_r^{(1)}\cdot\mathbf{\Omega}^{(0)}, \tag{4.337}$$

where we recall from Section 4.3.6 that $\Delta = \mathrm{i}\nu + \mathsf{ad}_{\mathbf{\Omega}^{(0)}}$ is the frequency-domain operator associated with the reconstruction equation.

Finally, the equations, including the constraints, are thus written succinctly as

$$\int_{\mathcal{B}}\langle\mathbf{v},\mathcal{A}\cdot\mathbf{u}\rangle\,\mathrm{d}V + \int_{\mathcal{B}}\Big\langle\mathbf{v},\mathcal{B}\cdot\mathbf{\Omega}^{(1)}\Big\rangle\,\mathrm{d}V = \int_{\mathcal{B}}\Big\langle\mathbf{v},\mathbf{b}^{(1)}\Big\rangle\,\mathrm{d}V \tag{4.338a}$$

$$\mathcal{C}\cdot\mathbf{u} + \mathsf{D}\cdot\mathbf{\Omega}^{(1)} = \mathbf{L} \tag{4.338b}$$

$$\Delta\cdot\boldsymbol{\theta}^{(1)} = \mathbf{\Omega}^{(1)} \tag{4.338c}$$

$$\int_{\mathcal{B}}\rho\mathbf{u}\,\mathrm{d}V = 0 \tag{4.338d}$$

$$\int_{\mathcal{B}}\rho\boldsymbol{\varphi}^{(0)}\wedge\mathbf{u}\,\mathrm{d}V = 0 \tag{4.338e}$$

The operator $\mathcal{A}$ describes the linearised elastodynamics of a self-gravitating body rotating at *constant* angular velocity $\mathbf{\Omega}^{(0)}$; it is precisely the operator used in global seismology by e.g. Dahlen & Tromp (1998) and Lau et al. (2015). D, on the other hand, is the very operator that we discussed in Section 4.3.6; it corresponds to a linearised Euler equation. $\mathcal{B}\mathbf{\Omega}_1$ produces in the elastic problem an *effective force* due to small variations of the angular velocity. Meanwhile, $\mathcal{C}\mathbf{u}$ alters the inertia tensor from its rigid value, which could be interpreted as producing an effective torque in the linearised Euler equation. Finally, the constraints on the motion ensure that we can interpret $\mathbf{\Omega}^{(1)}$ as a perturbed angular velocity and $\mathbf{u}$ as a momentum-free elastic displacement. In summary, we can obtain a full description of linearised rotational and elastic deformation by combining the standard equations of global seismology and rigid body dynamics – so long as we also include suitable coupling terms and constraints.

Given that $\boldsymbol{\theta}^{(1)}$ does not appear in the momentum and Euler equations (which is a consequence of the present linearisation scheme) those equations do not couple to the reconstruction equation. For that reason we will simply ignore the reconstruction equation in the following discussions, taking for granted that a full solution can be obtained by integrating eq.(4.338c) after finding $\boldsymbol{\Omega}^{(1)}$.

4.5.5 Towards numerical solution

Whilst the linearised Euler equations of Section 4.3.6 could be solved analytically in the frequency-domain, eq.(4.338) cannot. (One can write down a time-domain solution of the form $\mathbf{u} = \mathrm{e}^{\mathrm{i}\sqrt{\mathcal{A}}t}\cdot\mathbf{u}_0$, but expressions of this form are unlikely to be useful for our present purposes.) Nevertheless, a frequency-domain solution could be performed *numerically*. Here we outline how. We will not focus on the precise details of the discretisation scheme, simply assuming in what follows that eq.(4.338) has been transformed into a linear algebraic system through a Galerkin expansion. Our discussion is thus applicable to normal-mode coupling calculations and to the type of pseudo-spectral/spectral-element scheme discussed in Chapter 2. To carry out the expansion we expand both $\mathbf{u}$ and the test function $\mathbf{v}$ on some finite set of basis functions and project out a linear algebraic system. We also expand $\boldsymbol{\Omega}^{(1)}$ exactly on the $\mathbf{J}_\alpha$-basis. After performing the projections we are left with the linear algebraic system

$$\begin{pmatrix} \mathsf{A} & \mathsf{B} \\ \mathsf{C} & \mathsf{D} \end{pmatrix} \begin{pmatrix} \mathsf{u} \\ \mathsf{w} \end{pmatrix} = \begin{pmatrix} \mathsf{b} \\ \mathsf{L} \end{pmatrix}. \tag{4.339}$$

We have tried to denote the discretised operators by the same letter as in the continuous case, but in sans-serif font. The exception is w, which gives the components of $\boldsymbol{\Omega}^{(1)}$. The matrix A should be understood to incorporate the constraints on the elastic displacement's linear and angular momenta. Assuming that N basis functions were used to discretise $\mathbf{u}$, A has dimension $N \times N$, B is $N \times 3$, C is $3 \times N$ and D is 3×3; all these matrices, as well as b and L, are functions of frequency ν. What can we now do with system?

4.5.5.1 Modified Euler equation after Dahlen (1976)

We could start by assuming that we have *some* way of computing the action of A^{-1} on an N-dimensional column vector. If we do, then we could follow Dahlen (1976) and consider directly computing the effect of deformability on the Chandler Wobble eigenfrequency. To do that we seek nontrivial solutions to the *unforced* problem

$$\begin{pmatrix} \mathsf{A} & \mathsf{B} \\ \mathsf{C} & \mathsf{D} \end{pmatrix} \begin{pmatrix} \mathsf{u} \\ \mathsf{w} \end{pmatrix} = \mathsf{0}. \tag{4.340}$$

Given that A, B, C and D are all functions of ν, this an eigenvalue problem for ν whose solutions include the Chandler Wobble eigenfrequency.

We require that the determinant

$$\begin{vmatrix} \mathsf{A} & \mathsf{B} \\ \mathsf{C} & \mathsf{D} \end{vmatrix} \tag{4.341}$$

vanish, or equivalently

$$\det(\mathsf{A})\det\big(\mathsf{D}-\mathsf{C}\mathsf{A}^{-1}\mathsf{B}\big)=0. \tag{4.342}$$

The CW's observed frequency is far smaller than A's lowest eigenfrequency. As noted by Dahlen, this means that A^{-1} is guaranteed to exist in the frequency range of interest. $\det(\mathsf{A})$ is therefore nonzero, so we simply require that

$$\det\big(\mathsf{D}-\mathsf{C}\mathsf{A}^{-1}\mathsf{B}\big)=0. \tag{4.343}$$

To find the CW eigenfrequency we could solve this numerically by, say, Newton's method, taking as our initial guess the corresponding *rigid* CW frequency obtained by solving $\det(\mathsf{D})=0$. Of course, at every step of the iteration one would have to compute the action of A^{-1} nine times (among other things) but the methodology is at least clear. We find Dahlen's approach particularly elegant because it shows that the (low-frequency) rotational behaviour of an elastic body can incorporate elastic behaviour exactly through little more than a modified inertia tensor. Given the computational power available half a century ago, Dahlen's approach to the numerics was to approximate A by its value at zero-frequency, but that should not be necessary today. In the context of normal-mode-coupling, Al-Attar et al. (2012) have presented a method by which the action of A^{-1} can be computed efficiently.

4.5.5.2 Direct numerical solution after Al-Attar et al. (2012)

We will often be faced with problems where the forcing occurs at a *discrete* set of frequencies, such as we discussed in Section 4.3. Rather than seeking to calculate eigenfrequencies, in such cases it is more pragmatic to use the DNS methods of Al-Attar et al. (2012) and our Section 4.3 to solve equation (4.339) with nonzero forcing. Even when the forcing is over a continuum of frequencies, Al-Attar et al. (hereafter A12) showed that one can still solve the frequency-domain problem at a set of *discrete* frequencies and then use a discrete Fourier-transform to synthesise a time-domain solution of acceptable accuracy. Their work was motivated by mode-coupling calculations, but their approach is equally applicable to pseudo-spectral/spectral-element methods.

Up to the constraints on $\mathbf{u}$, our matrix A is precisely the matrix $\tilde{\mathbf{S}}(\omega)$ of A12 (their eq. 2.7). Those authors developed an efficient way of computing the action of $\tilde{\mathbf{S}}(\omega)^{-1}$ for a given ω, based on the *preconditioned biconjugate gradient method* (BCG). The BCG is an iterative method, and in broad terms it requires the ability to calculate the *exact* action of $\tilde{\mathbf{S}}(\omega)$ on an arbitrary vector, and to calculate the *approximate* action of $\tilde{\mathbf{S}}(\omega)^{-1}$. These operations must be performed at each step of the iteration. Extending that method to eq.(4.339) would require two main adjustments.

First, to solve eq.(4.339) we would need to compute the forward action, not of A, but of

$$\begin{pmatrix} \mathsf{A} & \mathsf{B} \\ \mathsf{C} & \mathsf{D} \end{pmatrix}. \tag{4.344}$$

Here the procedure is little more expensive than for A12: their matrix is $(N \times N)$ and ours is $[(N+3) \times (N+3)]$. For A12's calculations $N \sim 10,000$, so the extra 3 dimensions contribute little to the computational cost. In order to do this, we must of course develop a way of computing the components of B and C, but this should be readily achievable by adapting the results of A12 and Akbarashrafi et al. (2017).

The second extension of A12's method concerns the preconditioning. In our problem, preconditioning at the i'th stage of the iteration essentially requires computing an approximation to the vector

$$\begin{pmatrix} \mathsf{A} & \mathsf{B} \\ \mathsf{C} & \mathsf{D} \end{pmatrix}^{-1} \begin{pmatrix} \mathsf{u}_i \\ \mathsf{w}_i \end{pmatrix} \tag{4.345}$$

for some u_i and w_i. If we define the (3×3) matrix

$$\mathsf{Q} = \mathsf{D} - \mathsf{C}\mathsf{A}^{-1}\mathsf{B} \tag{4.346}$$

and the 3-D vector

$$\mathsf{P}_i = \mathsf{Q}^{-1}\left(\mathsf{w}_i - \mathsf{C}\mathsf{A}^{-1}\mathsf{u}_i\right), \tag{4.347}$$

then

$$\begin{pmatrix} \mathsf{A} & \mathsf{B} \\ \mathsf{C} & \mathsf{D} \end{pmatrix}^{-1} \begin{pmatrix} \mathsf{u}_i \\ \mathsf{w}_i \end{pmatrix} = \begin{pmatrix} \mathsf{A}^{-1}\mathsf{u}_i - \left(\mathsf{A}^{-1}\mathsf{B}\right)\mathsf{P}_i \\ \mathsf{P}_i \end{pmatrix}. \tag{4.348}$$

A12 show how the approximate action of A^{-1} (their matrix $\tilde{\mathbf{G}}_0$) can be calculated efficiently. Extending their approach to this problem requires mostly preprocessing, after which only a little more work is needed at each iteration.

The preprocessing involves calculating an approximation to $\mathsf{A}^{-1}\mathsf{B}$, and thence an approximation to Q. Calculating $\mathsf{A}^{-1}\mathsf{B}$ essentially involves carrying out A12's preconditioning 3 times. This should not be too costly an additional step given that A12's preconditioner's action can be made rather cheap to compute. Computing Q then requires $\mathsf{C}\mathsf{A}^{-1}\mathsf{B}$, which should be a trivial step.

At each stage of the iteration the only expensive matrix-vector computation we require is the approximate action of A^{-1} on u_i. We then compute $\mathsf{C}\mathsf{A}^{-1}\mathsf{u}_i$ and thence P_i. Again, this should proceed very quickly once A12's ideas have been applied to C. The only other required calculations involve three-dimensional matrix-vector operations, which are trivial by comparison.

In summary, the DNS method of A12 can in principle be extended readily, from its original application to the unconstrained elastodynamics of a uniformly rotating Earth model, to the constrained elastic-rotational dynamics as formulated in this chapter. The extended method

would only be a little more computationally costly than the original, and moreover, should not necessitate the writing of lots of new code.

4.5.6 Extension to two planets

4.5.6.1 Exact action and Euler–Lagrange equations: the elastodynamic Kepler problem!

Consider two reference bodies $\mathcal{B}_1$ and $\mathcal{B}_2$ each with an associated elastic motion. Each motion is decomposed by direct analogy with eq.(4.263) as

$$\mathbf{\Phi}_i(t) + \mathbf{R}_i(t) \cdot \boldsymbol{\varphi}_i(\mathbf{x}, t), \tag{4.349}$$

where

$$\mathbf{\Phi}_i : \mathcal{I} \mapsto \mathbb{R}^3 \tag{4.350}$$

$$\mathbf{R}_i : \mathcal{I} \mapsto \mathbf{SO}(3) \tag{4.351}$$

$$\boldsymbol{\varphi}_i : \mathcal{B}_i \times \mathcal{I} \mapsto \mathbb{R}^3. \tag{4.352}$$

(Note that we are no longer adorning the elastic motion in the rotating frame with an 'r' in order to avoid a proliferation of indices.) The same constraints are imposed upon each body *individually*,

$$\int_{\mathcal{B}_i} \rho_i \boldsymbol{\varphi}_i \, \mathrm{d}V = 0 \tag{4.353}$$

$$\int_{\mathcal{B}_i} \rho_i \boldsymbol{\varphi}_i \wedge \mathbf{v}_i \, \mathrm{d}V = 0, \tag{4.354}$$

and each body has an associated angular velocity

$$\mathbf{\Omega}_i = \mathbf{R}_i^T \dot{\mathbf{R}}_i \tag{4.355}$$

and moment of inertia $\mathbb{I}_i : \mathfrak{so}(3) \mapsto \mathfrak{so}(3)$ with components

$$[\mathbb{I}_i]_{\alpha\beta} = \int_{\mathcal{B}_i} \rho_i \Big(\|\boldsymbol{\varphi}_i\|^2 \, \delta_{\alpha\beta} - [\boldsymbol{\varphi}_i]_\alpha [\boldsymbol{\varphi}_i]_\beta \Big) \, \mathrm{d}V. \tag{4.356}$$

This means that all the fields can be interpreted in the now-familiar way: $\mathbf{\Phi}_i$ represents the motion of the i'th body's CoM; $\mathbf{R}_i$ effects a rotation about the i'th body's CoM; and $\boldsymbol{\varphi}_i$ represents elastic motion that carries neither linear nor angular momentum, taking place within a frame whose orientation with respect to inertial space is given by $\mathbf{R}_i$ and whose origin is the i'th body's

CoM. Each body has an associated 'free action'

$$\mathcal{S}_i = \int_{\mathcal{I}} \Big[\frac{1}{2} m_i \Big\| \dot{\mathbf{\Phi}}_i \Big\|^2 + \frac{1}{2} \langle \mathbf{\Omega}_i, \mathbb{I}_i \cdot \mathbf{\Omega}_i \rangle_{\mathfrak{so}(3)} + \Big\langle \mathbf{\Lambda}_i, \mathbf{R}_i^T \dot{\mathbf{R}}_i - \mathbf{\Omega}_i \Big\rangle_{\mathfrak{so}(3)} + \int_{\mathcal{B}_i} \Big(\frac{1}{2} \rho_i \|\mathbf{v}_i\|^2 - W_i(\mathbf{x}, \mathbf{F}_i) - \frac{1}{2} \rho_i \zeta_i(\mathbf{x}) + \langle \boldsymbol{\alpha}_i, \rho_i \boldsymbol{\varphi}_i \rangle + \langle \boldsymbol{\beta}_i, \rho_i \boldsymbol{\varphi}_i \wedge \mathbf{v}_i \rangle_{\mathfrak{so}(3)} \Big) \, \mathrm{d}V \Big] \, \mathrm{d}t. \tag{4.357}$$

Just as with rigid bodies, the key point is that the action of two interacting elastic bodies is just the sum of the free actions augmented by a term that represents their gravitational binding energy. This binding energy takes the form

$$\mathcal{V}_g = \int_{\mathcal{B}_1} \int_{\mathcal{B}_2} \rho_1(\mathbf{x}) \rho_2(\mathbf{x}') \Gamma \big[\mathbf{\Phi}_1(t) + \mathbf{R}_1(t) \cdot \boldsymbol{\varphi}_1(\mathbf{x}) - \mathbf{\Phi}_2(t) - \mathbf{R}_2(t) \cdot \boldsymbol{\varphi}_2(\mathbf{x}') \big] \, \mathrm{d}V' \, \mathrm{d}V. \tag{4.358}$$

We now recall from Section 4.3 the definitions of the *total mass*

$$M = m_1 + m_2, \tag{4.359}$$

the *reduced mass*

$$\mu = \frac{m_1 m_2}{m_1 + m_2}, \tag{4.360}$$

and the Keplerian variables

$$\begin{aligned} \mathbf{r}(t) &= \mathbf{\Phi}_1(t) - \mathbf{\Phi}_2(t) \\ \mathbf{d}(t) &= \frac{\mu}{m_2} \mathbf{\Phi}_1(t) + \frac{\mu}{m_2} \mathbf{\Phi}_2(t), \end{aligned} \tag{4.361}$$

and substitute them into the action. Overall, the two-body action comes out as

$$\mathcal{S} = \int_{\mathcal{I}} \Bigg\{ \frac{1}{2} M \Big\| \dot{\mathbf{d}} \Big\|^2 + \frac{1}{2} \mu \|\dot{\mathbf{r}}\|^2 - \mathcal{V}_g(\mathbf{\Phi}_1, \mathbf{R}_1, \boldsymbol{\varphi}_1, \mathbf{\Phi}_2, \mathbf{R}_2, \boldsymbol{\varphi}_2) + \sum_{i=1}^{2} \Big[\frac{1}{2} \langle \mathbf{\Omega}_i, \mathbb{I}_i \cdot \mathbf{\Omega}_i \rangle_{\mathfrak{so}(3)} + \Big\langle \mathbf{\Lambda}_i, \mathbf{R}_i^T \dot{\mathbf{R}}_i - \mathbf{\Omega}_i \Big\rangle_{\mathfrak{so}(3)} + \int_{\mathcal{B}_i} \Big(\frac{1}{2} \rho_i \|\mathbf{v}_i\|^2 - W_i(\mathbf{x}, \mathbf{F}_i) - \frac{1}{2} \rho_i \zeta_i(\mathbf{x}) + \langle \boldsymbol{\alpha}_i, \rho_i \boldsymbol{\varphi}_i \rangle + \langle \boldsymbol{\beta}_i, \rho_i \boldsymbol{\varphi}_i \wedge \mathbf{v}_i \rangle_{\mathfrak{so}(3)} \Big) \, \mathrm{d}V \Big] \Bigg\} \mathrm{d}t. \tag{4.362}$$

The $\mathbf{r}$-, $\mathbf{R}_i$- and $\boldsymbol{\varphi}_i$-derivatives of $\mathcal{V}_g$ can be expressed conveniently in terms of

$$\mathbf{\Gamma}_{ij} \equiv - \int_{\mathcal{B}_j} \rho_j(\mathbf{x}') \nabla \Gamma \big[\mathbf{\Phi}_i(t) - \mathbf{\Phi}_j(t) + \mathbf{R}_i(t) \cdot \boldsymbol{\varphi}_i(\mathbf{x}) - \mathbf{R}_j(t) \cdot \boldsymbol{\varphi}_j(\mathbf{x}') \big] \, \mathrm{d}V', \tag{4.363}$$

valid for $i \neq j$. We can interpret $\mathbf{\Gamma}_{ij}$ as the gravitational force due to (the whole of) body j acting on the particle at the *referential* point $\mathbf{x} \in \mathcal{B}_i$. in line with Newton's Third Law. Note

that this force is of course written as

$$\int_{\mathcal{B}_i} \rho_i \mathbf{\Gamma}_{ij} \, \mathrm{d}V \approx -G \frac{M\mu}{\|\mathbf{r}\|^3} \mathbf{r} \tag{4.364}$$

to leading order.

The Euler–Lagrange equations now follow readily from this section's earlier results:

$$\ddot{\mathbf{d}} = 0 \tag{4.365a}$$

$$\mu \ddot{\mathbf{r}} = \int_{\mathcal{B}_i} \rho_i \mathbf{\Gamma}_{ij} \, \mathrm{d}V \tag{4.365b}$$

$$(\partial_t + \mathsf{ad}_{\mathbf{\Omega}_i}) \, \mathbb{I}_i \cdot \mathbf{\Omega}_i = \int_{\mathcal{B}_i} \rho_i \boldsymbol{\varphi}_i \wedge \left(\mathbf{R}_i^T \cdot \mathbf{\Gamma}_{ij} \right) \, \mathrm{d}V \tag{4.365c}$$

$$\dot{\mathbf{R}}_i = \mathbf{R}_i \mathbf{\Omega}_i \tag{4.365d}$$

$$\ddot{\boldsymbol{\varphi}}_i + \left(\mathbf{\Omega}_i^2 \cdot \boldsymbol{\varphi}_i + 2\mathbf{\Omega}_i \cdot \mathbf{v}_i + \dot{\mathbf{\Omega}}_i \cdot \boldsymbol{\varphi}_i \right) = \frac{1}{\rho_i} \mathrm{Div} \mathbf{P}_i + \boldsymbol{\gamma}_i + \mathbf{R}_i^T \cdot \left(\mathbf{\Gamma}_{ij} - \frac{1}{m_i} \int_{\mathcal{B}_i} \rho_i \mathbf{\Gamma}_{ij} \, \mathrm{d}V \right) \tag{4.365e}$$

$$\int_{\mathcal{B}_i} \rho_i \boldsymbol{\varphi}_i \, \mathrm{d}V = 0 \tag{4.365f}$$

$$\int_{\mathcal{B}_i} \rho_i \boldsymbol{\varphi}_i \wedge \dot{\boldsymbol{\varphi}}_i \, \mathrm{d}V = 0 \tag{4.365g}$$

$$\mathbf{P}_i \cdot \hat{\mathbf{n}} = 0, \, \mathbf{x} \in \partial \mathcal{B}_i. \tag{4.365h}$$

The equations demonstrate how two planets' orbital, rotational and elastic motions are all coupled together by gravity. We have made no approximations, so this system provides a framework for investigating the effect of large planetary deformations on a two-body system's orbital evolution. Consider the Earth–Moon system's early history, for example. Shortly after the proposed Giant Impact, the Earth and Moon would have been close together and rotating rapidly. The rapid rotation would have led to considerably greater flattening than we see in the Earth and Moon of today, while the bodies' closeness would have produced very large body tides. Equations (4.365) can – at least in principle – account for these exotic effects exactly.

4.5.6.2 Linearisation

We might assemble a simple model of the early Earth–Moon system as follows. Analogously to the case of two rigid bodies (Section 4.3.8.2) we could consider a zeroth-order equilibrium where: the bodies' CoMs perform a standard Keplerian orbit; each of the bodies rotates uniformly (and very quickly!) about a principle axis of inertia; and the equilibrium elastic displacements are such that each body's internal stresses balance centrifugal force, self-gravity, and the (large!) tidal forces due to the other body. We would then linearise equations (4.365) about that equilibrium.

Deriving the precise linearised forms is left to future work, but it is evident that one would obtain a linearised Kepler problem perturbed by each body's elastic and rotational motion,

$$\mu \ddot{\mathbf{r}}^{(1)} + \boldsymbol{\tau}^{(0)} \cdot \mathbf{r}^{(1)} = \left(\text{terms in } \mathbf{R}_i^{(0)}, \, \mathbf{\Omega}_i^{(0)}, \, \boldsymbol{\varphi}_i^{(0)} \right), \tag{4.366}$$

as well as a problem of coupled rotation and elasticity perturbed by orbital motion. To solve the

latter problem we could adapt the ideas of Sections 4.3.8 and 4.5.5. After discretisation each body would satisfy a system of the form

$$\begin{pmatrix} \mathsf{A}_i & \mathsf{B}_i \\ \mathsf{C}_i & \mathsf{D}_i \end{pmatrix} \begin{pmatrix} \mathsf{u}_i \\ \mathsf{w}_i \end{pmatrix} = \begin{pmatrix} \mathsf{b}_i \\ \mathsf{L}_i \end{pmatrix}, \tag{4.367}$$

with b_i and L_i represented in frequency space by a series of *discrete peaks* corresponding to the frequency content of the equilibrium orbital and rotational behaviour (*c.f.* eq. 4.208b). Section 4.5.5's putative extension to A12's DNS method is excellently suited to such a problem. For the orbital motion, it is likely that a method based on orbital perturbation theory and multiple timescale analysis of the sort discussed in Section 4.3.8 would also work well here.

4.5.7 N solid planets

We have no further physical ideas to add here, but feel that it is worth writing down the N-body equations for the sake of completeness. Therefore consider N reference bodies $\{\mathcal{B}_i | i = 1, \ldots, N\}$ each having a motion that is decomposed as

$$\boldsymbol{\Phi}_i(t) + \mathbf{R}_i(t) \cdot \boldsymbol{\varphi}_i(\mathbf{x}, t), \tag{4.368}$$

with all the usual considerations. The action for N elastic bodies is the sum of their individual free actions (defined in eq. 4.377) and a term representing the gravitational binding energy:

$$\mathcal{V}_g = \frac{1}{2} \sum_{i \neq j}^{N} \int_{\mathcal{B}_i} \int_{\mathcal{B}_j} \rho_i(\mathbf{x}) \rho_j(\mathbf{x}') \Gamma \big[\boldsymbol{\Phi}_i(t) + \mathbf{R}_i(t) \cdot \boldsymbol{\varphi}_i(\mathbf{x}) - \boldsymbol{\Phi}_j(t) - \mathbf{R}_j(t) \cdot \boldsymbol{\varphi}_j(\mathbf{x}') \big] \, \mathrm{d}V' \, \mathrm{d}V. \tag{4.369}$$

The overall action for the N-body system is therefore

$$\mathcal{S} = \sum_{i=1}^{N} \mathcal{S}_i - \int_{\mathcal{I}} \mathcal{V}_g \, \mathrm{d}t, \tag{4.370}$$

which leads to the Euler–Lagrange equations

$$m_i \ddot{\mathbf{\Phi}}_i = \sum_{j \neq i} \int_{\mathcal{B}_i} \rho_i \mathbf{\Gamma}_{ij} \, \mathrm{d}V \tag{4.371a}$$

$$(\partial_t + \mathsf{ad}_{\mathbf{\Omega}_i}) \, \mathbb{I}_i \cdot \mathbf{\Omega}_i = \int_{\mathcal{B}_i} \rho_i \boldsymbol{\varphi}_i \wedge \left(\mathbf{R}_i^T \cdot \sum_{j \neq i} \mathbf{\Gamma}_{ij} \right) \, \mathrm{d}V \tag{4.371b}$$

$$\dot{\mathbf{R}}_i = \mathbf{R}_i \mathbf{\Omega}_i \tag{4.371c}$$

$$\ddot{\boldsymbol{\varphi}}_i + \Big(\mathbf{\Omega}_i^2 \cdot \boldsymbol{\varphi}_i + 2\mathbf{\Omega}_i \cdot \mathbf{v}_i + \dot{\mathbf{\Omega}}_i \cdot \boldsymbol{\varphi}_i \Big) = \frac{1}{\rho_i} \mathrm{Div} \mathbf{P}_i + \boldsymbol{\gamma}_i + \mathbf{R}_i^T \cdot \sum_{j \neq i} \left(\mathbf{\Gamma}_{ij} - \frac{1}{m_i} \int_{\mathcal{B}_i} \rho_i \mathbf{\Gamma}_{ij} \, \mathrm{d}V \right) \tag{4.371d}$$

$$\int_{\mathcal{B}_i} \rho_i \boldsymbol{\varphi}_i \, \mathrm{d}V = 0 \tag{4.371e}$$

$$\int_{\mathcal{B}_i} \rho_i \boldsymbol{\varphi}_i \wedge \dot{\boldsymbol{\varphi}}_i \, \mathrm{d}V = 0 \tag{4.371f}$$

$$\mathbf{P}_i \cdot \hat{\mathbf{n}} = 0, \; \mathbf{x} \in \partial \mathcal{B}_i. \tag{4.371g}$$

These equations provide an exact framework for investigating the effect of deformability on the evolution of planetary systems, which could be of interest within studies of solar-system formation. All our earlier comments about the Earth–Moon system apply to this problem too, but in the N-body case any problems are presumably magnified.

4.6 Conclusions

We have derived the exact equations of motion of up to N solid, rotating, self-gravitating elastic planets that interact through gravity. Our derivations are based on a particular method of 'decoupling' rotational behaviour from elastic, which is physically motivated and should be computationally useful. It was prefigured to some extent in Dahlen & Smith (1975), but not fully developed. Dahlen & Smith's eq.(97) bears some resemblance to our eq.(4.263), but their work does not treat the rotation matrix as a dynamical variable, nor does it introduce the constraints on the elastic motion that we do. Essentially, they introduced the rotation matrix into their linearised elastodynamic equations as a way of avoiding some difficulties due to the axial spin mode. Our derivations clarify the interplay between planets' rotational and elastic behaviours. In the linearised case they indicate that the current equations of motion used to study the Earth's low frequency behaviour both correspond to certain limits of the exact equations of motion. We also showed that the numerical solution of the linearised EoMs describing one body could, in principle, be achieved through methods that are only a little more taxing than the full-coupling calculations commonly carried out today by e.g. Al-Attar et al. (2012) and Akbarashrafi et al. (2017). The results of this chapter provide a conceptual framework for modelling, say, the exact effect of lateral density variations on the Eulerian Free Precession of an aspherical, solid planet. And in conjunction with the numerical method of Chapter 2 we could include – for the first time in such calculations – the exact effects of boundary topography.

4.7 Further work

4.7.1 Solid Earth models

The results of this dissertation provide in principle a complete framework for the computation of the long-period deformation of solid bodies. The further work needed to achieve this goal is to implement the extensions of Al-Attar et al.'s (2012) DNS full-coupling numerical method that we outlined in Section 4.5.5, a task that could be undertaken readily with only slight modification to existing codes.

An alternative to mode coupling is offered by a hybrid pseudo-spectral/spectral-element scheme of the sort discussed in Chapter 2. Indeed, the extension of Chapter 2's method to the elastodynamic problem involves little more than bookkeeping, and similar methods in that vein have already been developed by Crawford et al. (2018) and Leng et al. (2016, 2019). These methods' utility lies in the fact that they do not require the computation and storage of a truncated set of the eigenfunctions of a spherical reference model. The desired radial precision is determined by the spectral-element mesh, which allows for great flexibility. Another useful feature is that *all* computations can be performed on a spherical domain, with boundary topography converted to volumetric heterogeneity in an exact manner (Al-Attar & Crawford, 2016; Al-Attar et al., 2018). Furthermore, by using a physically-motivated, approximately block-diagonal preconditioner – as we did in Chapter 2 and as Al-Attar et al. (2012) did in the context of mode-coupling (Section 4.5.5.2) – one can ensure that the numerical solution will converge more quickly the closer the body is to being spherically symmetric. Such methods thus inherit some of the advantages of perturbative approaches while avoiding their drawbacks.

Extensions to viscoelastic rheologies should also be quite easy, especially given that DNS methods can account for viscoelasticity without extra computational cost. An important caveat related to viscoelasticity is that Hamilton's Principle is formally inapplicable to dissipative systems. Nevertheless, Hamilton's Principle leads to equations of motion *of precisely the same form* as do derivations based on force-balance (we aim to show this explicitly in later work). The only difference between the two approaches is that force balance derivations do not require the first Piola–Kirchhoff stress to be derived from a strain-energy function. Instead, the existence of the first Piola–Kirchhoff stress follows from *Cauchy's theorem* (e.g. Marsden & Hughes, 1994, p.127) and constitutive behaviour is imposed by relating the FPK stress to the deformation gradient history (e.g. Coleman & Noll, 1961). On a pragmatic level, all this means is that we *can* use the equations of motion derived herein to model viscoelastic bodies, but we must just remember that the stress is not related to a strain-energy function.

In this connection, it would be interesting to extend our results on the elastic tensor's stress dependence to materials with viscoelastic constitutive relationships, but the utility of this to global seismology is dubious – and it would probably be extremely difficult. In any case, even the hyperelastic results of Chapter 3 have provided useful insight. For instance, Lau et al. (2015, eq. 18) take the elastic tensor to depend on stress as described by Dahlen (1972b), but Chapter 3 indicates that this expression is not as general as it could be. Although it is not yet clear how much this affects the density model of Lau et al. (2017), our results identify laterally-varying

equilibrium stress as another source of error in previous studies of LLSVP density.

4.7.2 Fluid-solid Earth models

Most pressingly, the results of this chapter need to be extended in order to be applicable to layered fluid-solid planets. The necessary method has already been illustrated by Al-Attar et al. (2018) in the context of a uniformly rotating, hyperelastic, fluid-solid planet. They treated the two layers of the planet as separate bodies with respective motions $\boldsymbol{\varphi}_1$ and $\boldsymbol{\varphi}_2$, accounting for the interactions at the internal fluid-solid boundary Σ through a Lagrange multiplier that enforced the tangential-slip constraint. Specifically, they added a term to the action of the form

$$\int_{\mathcal{I}} \int_{\Sigma} \varpi \sigma \circ \boldsymbol{\chi} \, \mathrm{d}S \, \mathrm{d}t, \tag{4.372}$$

where $\varpi : \Sigma \times \mathcal{I} \mapsto \mathbb{R}$ is the Lagrange multiplier, $\sigma : \mathbb{R}^3 \mapsto \mathbb{R}$ is a function *chosen* so that $\sigma(\mathbf{x})$ vanishes iff $\mathbf{x} \in \Sigma$, and where $\boldsymbol{\chi}$ is defined by

$$\boldsymbol{\varphi}_1(\cdot, t) \circ \boldsymbol{\chi} = \boldsymbol{\varphi}_2(\cdot, t). \tag{4.373}$$

This produces the action (their eq. 69)

$$\mathcal{S} = \sum_{i=1}^{2} \int_{\mathcal{I}} \int_{\mathcal{B}_i} \left\{ \frac{1}{2} \rho_i \| \dot{\boldsymbol{\varphi}}_i + \boldsymbol{\Omega} \cdot \boldsymbol{\varphi}_i \| - W_i(\mathbf{x}, \mathbf{F}_i) - \frac{1}{2} \rho_i \zeta_i \right\} \mathrm{d}V \, \mathrm{d}t + \int_{\mathcal{I}} \int_{\Sigma} \varpi \sigma \circ \boldsymbol{\chi} \, \mathrm{d}S \, \mathrm{d}t, \tag{4.374}$$

and Al-Attar et al. show that the resulting equations of motion reduce to those derived by Woodhouse & Dahlen (1978).

It is not hard to show that the N-solid-body action (4.370) that we wrote down in Section 4.5.7 could be 'converted' into the action of an N-layer, hyperelastic, fluid-solid planet in the same way. We would just add a term to constrain the motion at each internal boundary Σ_i:

$$\sum_{i=1}^{N-1} \int_{\mathcal{I}} \int_{\Sigma_i} \varpi_i \sigma_i \circ \boldsymbol{\chi}_i \, \mathrm{d}S \, \mathrm{d}t. \tag{4.375}$$

Importantly, $\boldsymbol{\chi}_i$ would have to be defined as

$$\boldsymbol{\Phi}_i + \mathbf{R}_i \cdot [\boldsymbol{\varphi}_i(\cdot, t) \circ \boldsymbol{\chi}_i] = \boldsymbol{\Phi}_{i+1} + \mathbf{R}_{i+1} \cdot \boldsymbol{\varphi}_{i+1}(\cdot, t) \tag{4.376}$$

in order to respect the decomposed motion that we introduced in Section 4.5. With this, the

action would be

$$\begin{aligned}\mathcal{S} = \sum_{i=1}^{N} \int_{\mathcal{I}} \Bigg[&\frac{1}{2} m_i \left\| \dot{\boldsymbol{\Phi}}_i \right\|^2 + \frac{1}{2} \langle \boldsymbol{\Omega}_i, \mathbb{I}_i \cdot \boldsymbol{\Omega}_i \rangle + \left\langle \boldsymbol{\Lambda}_i, \mathbf{R}_i^T \dot{\mathbf{R}}_i - \boldsymbol{\Omega}_i \right\rangle_{\mathfrak{so}(3)} \\ &- \frac{1}{2} \sum_{i \neq j}^{N} \int_{\mathcal{B}_i} \int_{\mathcal{B}_j} \rho_i(\mathbf{x}) \rho_j(\mathbf{x}') \Gamma \left[\boldsymbol{\Phi}_i(t) + \mathbf{R}_i(t) \cdot \boldsymbol{\varphi}_i(\mathbf{x}) - \boldsymbol{\Phi}_j(t) - \mathbf{R}_j(t) \cdot \boldsymbol{\varphi}_j(\mathbf{x}') \right] \mathrm{d}V' \, \mathrm{d}V \\ &+ \int_{\mathcal{B}_i} \left(\frac{1}{2} \rho_i \| \mathbf{v}_i \|^2 - W_i(\mathbf{x}, \mathbf{F}_i) - \frac{1}{2} \rho_i \zeta_i(\mathbf{x}) + \langle \boldsymbol{\alpha}_i, \rho_i \boldsymbol{\varphi}_i \rangle + \langle \boldsymbol{\beta}_i, \rho_i \boldsymbol{\varphi}_i \wedge \mathbf{v}_i \rangle \right) \mathrm{d}V \Bigg] \, \mathrm{d}t \\ &+ \sum_{i=1}^{N-1} \int_{\mathcal{I}} \int_{\Sigma_i} \varpi_i \sigma_i \circ \boldsymbol{\chi}_i \, \mathrm{d}S \, \mathrm{d}t. \end{aligned} \tag{4.377}$$

Deriving the associated Euler–Lagrange equations would be little more conceptually difficult than it was for Al-Attar et al., but it would certainly be more fiddly. We leave that derivation to later work. Nevertheless, with a little thought we can see that the resulting equations of motion would take the same form of those of Section 4.5.7, but with extra forces and torques to represent interactions at the boundaries. Notably, the *nutational* motions of the inner and outer cores would emerge naturally from such a description as solutions of the Euler and reconstruction equations associated with each layer. This general framework would thus give a clear, complete picture of the motions and interactions of Earth's layers, uniting the 'seismological' and 'geodetic' frameworks described in the Introduction to Chapter 4. It would also provide a foundation for investigating how lateral density heterogeneities affect the nearly-diurnal free wobble, the free core nutation, and perhaps even the free inner-core nutation and Slichter modes.

A major advantage of 'breaking down' the Earth into its constituent layers is that it should aid numerical solution. Importantly, it sidesteps the problems that Lau et al. (2017) encountered. Those authors were unable to study the NDFW because their basis was not flexible enough to represent it. But if one regards the Earth's layers as separate bodies, then it seems natural to assemble a separate spectral-element mesh for each layer individually. Moreover, the meshes could be fine-tuned to resolve fine structure only where required. Under such an approach the NDFW, as well as the free inner core nutation and the Slichter modes, should not present too much difficulty.

That being said, the equations discussed here are not precisely the equations that we would seek to solve. As mentioned in Chapter 1, modelling the outer core as inviscid leads to both considerable numerical difficulties and the possible loss of important physical effects. We would therefore solve the equations of motion of a viscoelastic Earth with a viscous outer core. As for a solid body, those equations of motion would not follow from Hamilton's principle, but they would be of the same *form*. The only two differences would be that the stress would not be derived from a strain-energy function, and that the boundary forces and torques would take a different form because in the viscous case they follow from a no-slip boundary condition. In future work we plan to derive the equations of motion of such an Earth model.

The flexibility offered by pseudo-spectral/spectral-element methods would be particularly important when solving for the motion of a viscous outer core. As discussed in Section 1, the boundary layers at the ICB and CMB are expected to be $\sim$ 10m in width. The radial

spectral-element mesh could be adjusted to be exceptionally fine around those regions, and coarser elsewhere. This is a more attractive prospect than with normal-mode coupling, where one would have to use a truly vast basis in order to obtain such high resolution. However, it is possible that such a fine mesh could be required throughout the outer core, which would lead to prohibitive computational expense. This is unlikely to be an issue at seismic frequencies (Rogister & Valette, 2009), but it could lead to severe difficulties in the study of Earth's rotational dynamics.

APPENDIX A

A NON-PERTURBATIVE METHOD FOR GRAVITATIONAL POTENTIAL CALCULATIONS WITHIN HETEROGENEOUS AND ASPHERICAL PLANETS

A.1 Generalised spherical harmonic expansions

Let (r, θ, φ) denote the usual spherical polar coordinates and $(\hat{\mathbf{r}}, \hat{\boldsymbol{\theta}}, \hat{\boldsymbol{\varphi}})$ the associated unit basis vectors. Following Phinney & Burridge (1973), we define the "canonical basis vectors"

$$\hat{\mathbf{e}}_- = \frac{1}{\sqrt{2}}\left(\hat{\boldsymbol{\theta}} - i\hat{\boldsymbol{\varphi}}\right) \tag{A.1}$$

$$\hat{\mathbf{e}}_0 = \hat{\mathbf{r}} \tag{A.2}$$

$$\hat{\mathbf{e}}_+ = -\frac{1}{\sqrt{2}}\left(\hat{\boldsymbol{\theta}} + i\hat{\boldsymbol{\varphi}}\right) , \tag{A.3}$$

and write the contravariant components of a vector $\mathbf{u}$ with respect to this basis as u^-, u^0 and u^+. Each component can be expanded in the form

$$u^\alpha = \sum_{lm} u^\alpha_{lm} Y^\alpha_{lm} , \tag{A.4}$$

where the Y^α_{lm} are the fully normalized generalized spherical harmonics defined in Appendix C of Dahlen & Tromp (1998) and summation is over integer values for $0 \le l \le \infty$ and $-l \le m \le l$.

A scalar field is expanded in terms of scalar spherical harmonics Y^0_{lm} in the usual fashion,

$$\phi = \sum_{lm} \phi_{lm} Y^0_{lm} , \tag{A.5}$$

but we use generalised spherical harmonics to write the contravariant components of its gradient

(a vector field) as

$$(\nabla\phi)^\alpha \equiv \sum_{lm} \phi_{lm}^{|\alpha} Y_{lm}^\alpha \,, \tag{A.6}$$

where

$$\phi_{lm}^{|0} = \frac{d\phi_{lm}}{dr} \tag{A.7}$$

and

$$\phi_{lm}^{|\pm} = \frac{k}{\sqrt{2}} \frac{\phi_{lm}}{r} \tag{A.8}$$

with

$$k = \sqrt{l(l+1)} \,. \tag{A.9}$$

The expansion of a second-rank tensor looks similar. By analogy, we define the contravariant components of $\mathbf{T}$ by

$$\mathbf{T} = \sum_{\alpha\beta} T^{\alpha\beta} \hat{\mathbf{e}}_\alpha \otimes \hat{\mathbf{e}}_\beta \tag{A.10}$$

and expand each component as

$$T^{\alpha\beta} = \sum_{lm} T_{lm}^{\alpha\beta} Y_{lm}^{\alpha+\beta} \,. \tag{A.11}$$

Thus T^{-+}, T^{+-} and T^{00} are all expanded in terms of the Y_{lm}^0, whilst, for example, T^{++} is expanded on Y_{lm}^2. We note in passing that the covariant components of the metric tensor are

$$g_{\alpha\beta} = \begin{pmatrix} 0 & 0 & -1 \\ 0 & 1 & 0 \\ -1 & 0 & 0 \end{pmatrix} \,. \tag{A.12}$$

A.2 Calculation of a for a radial mapping

When the mapping $\boldsymbol{\xi}$ is radial, *i.e.* of the form

$$\boldsymbol{\xi}(\mathbf{x}) = \mathbf{x} + h(\mathbf{x})\hat{\mathbf{x}} \,, \tag{A.13}$$

we can obtain a simple analytic expression for the components of $\mathbf{a}$ in terms of $(\nabla h)^\alpha$. The deformation gradient takes the form

$$\mathbf{F} = \left(1 + \frac{h}{r}\right) \mathbf{1} + \mathbf{x} \otimes \left(\frac{1}{r}\nabla h - \frac{h}{r^2}\hat{\mathbf{x}}\right) \,, \tag{A.14}$$

whereupon we may use the Sherman-Morrison formula (e.g. Van Loan & Golub, 1983) to write down an exact expression for the inverse:

$$\mathbf{F}^{-1} = \left(1 + \frac{h}{r}\right)^{-1} \left(\mathbf{1} - \frac{\mathbf{x} \otimes \left(\frac{1}{r}\nabla h - \frac{h}{r^2}\hat{\mathbf{x}}\right)}{1 + \partial_r h}\right) . \tag{A.15}$$

The matrix-determinant lemma (e.g. Van Loan & Golub, 1983) yields the Jacobian,

$$J = \left(1 + \frac{h}{r}\right)^2 (1 + \partial_r h) , \tag{A.16}$$

and after a few more lines of algebra we find

$$\mathbf{a} = J\mathbf{C}^{-1} = (1 + \partial_r h)\,\mathbf{1} + 2\frac{h}{r}\hat{\mathbf{r}} \otimes \hat{\mathbf{r}} - (\hat{\mathbf{r}} \otimes \nabla h + \nabla h \otimes \hat{\mathbf{r}}) + \frac{\|\nabla h - \frac{h}{r}\hat{\mathbf{r}}\|^2}{1 + \partial_r h}\,\hat{\mathbf{r}} \otimes \hat{\mathbf{r}} . \tag{A.17}$$

Expanding ∇h in the canonical basis and using the metric eq.(A.12) to evaluate the norm, we arrive at

$$\left[a^{\alpha\beta}\right] = \begin{pmatrix} 0 & -(\nabla h)^- & -(1 + \partial_r h) \\ -(\nabla h)^- & 1 - \partial_r h + 2\frac{h}{r} + \frac{(\partial_r h - h/r)^2 - 2(\nabla h)^-(\nabla h)^+}{1 + \partial_r h} & -(\nabla h)^+ \\ -(1 + \partial_r h) & -(\nabla h)^+ & 0 \end{pmatrix} . \tag{A.18}$$

Only if the mapping is radial can we use the Sherman-Morrison formula and matrix-determinant lemma. The reader may verify that the deformation gradient no longer takes the necessary form of "identity plus tensor-product" when terms in $\hat{\boldsymbol{\theta}}$ and $\hat{\boldsymbol{\varphi}}$ are added to eq.(A.13). It is of course possible to find an analytic expression for $a^{\alpha\beta}$ in more general cases; it is just not as elegant.

APPENDIX B

On the stress dependence of the elastic tensor

B.1 Notations and definitions

B.1.1 Groups

We define $\mathbf{GL}(n)$, *the general linear group of dimension* n, to be the set of invertible $n \times n$ matrices under the operation of matrix multiplication. For a general group $\mathbf{G}$, a *subgroup* $\mathbf{H}$ of $\mathbf{G}$ is a subset of the elements of $\mathbf{G}$ that is itself a group; $\mathbf{H}$ is described as a *proper subgroup* of $\mathbf{G}$ if $\mathbf{H} \neq \mathbf{G}$. With this, we can define $\mathbf{SL}(n)$, *the special linear group* of $n \times n$ matrices with *unit* determinant, which is a proper subgroup of $\mathbf{GL}(n)$. A particularly important proper subgroup of $\mathbf{SL}(n)$ is $\mathbf{SO}(n)$, *the n-dimensional special orthogonal group* whose elements are rotation matrices in n dimensions. For any $\mathbf{R} \in \mathbf{SO}(n)$,

$$\det \mathbf{R} = 1 \tag{B.1}$$

$$\mathbf{R}^{-1} = \mathbf{R}^T. \tag{B.2}$$

B.1.2 Some nonstandard linear operators

We have found it useful to introduce the left- and right-multiplication operators $\mathsf{L}_\mathbf{A}$ and $\mathsf{R}_\mathbf{A}$ which act according to

$$\mathsf{L}_\mathbf{A} \cdot \mathbf{B} = \mathbf{AB} \tag{B.3}$$

$$\mathsf{R}_\mathbf{A} \cdot \mathbf{B} = \mathbf{BA} \tag{B.4}$$

for arbitrary matrices $\mathbf{A}, \mathbf{B} \in \mathbf{GL}(3)$. These operators may be represented by fourth-rank tensors. An operator O acts on a matrix $\mathbf{A}$ according to

$$(\mathsf{O} \cdot \mathbf{A})_{ij} = \mathsf{O}_{ijkl} A_{kl}, \tag{B.5}$$

where we use a dot to represent the action of a linear operator on its operand (as is the case throughout this dissertation). Two such operators are composed by writing

$$\left(\mathsf{O}^1\mathsf{O}^2\right)_{ijkl} = \mathsf{O}^1_{ijpq}\mathsf{O}^2_{pqkl}. \tag{B.6}$$

The left- and right-multiplication operators are expressed in index-notation as

$$(\mathsf{L}_\mathbf{A})_{ijkl} = A_{ik}\delta_{lj} \tag{B.7}$$
$$(\mathsf{R}_\mathbf{A})_{ijkl} = \delta_{ik}A_{lj}, \tag{B.8}$$

and, as an example,

$$\begin{aligned}(\mathsf{L}_\mathbf{A}\cdot\mathbf{B})_{ij} =& (\mathsf{L}_\mathbf{A})_{ijkl}\,B_{kl}\\ =& A_{ik}\delta_{lj}B_{kl}\\ =& A_{ik}B_{kj}\\ =& (\mathbf{AB})_{ij}\,.\end{aligned} \tag{B.9}$$

It is clear that $\mathsf{L}_\mathbf{A}$ and $\mathsf{R}_\mathbf{B}$ commute for any choice of $\mathbf{A}$ and $\mathbf{B}$, and that they satisfy

$$\mathsf{R}_\mathbf{AB} = \mathsf{R}_\mathbf{B}\mathsf{R}_\mathbf{A} \tag{B.10}$$
$$\mathsf{L}_\mathbf{AB} = \mathsf{L}_\mathbf{A}\mathsf{L}_\mathbf{B}, \tag{B.11}$$

while their inverses have the property that

$$\mathsf{L}_\mathbf{A}^{-1} = \mathsf{L}_{\mathbf{A}^{-1}} \tag{B.12}$$
$$\mathsf{R}_\mathbf{A}^{-1} = \mathsf{R}_{\mathbf{A}^{-1}}. \tag{B.13}$$

We also define the operators

$$\mathsf{L}_\mathbf{A}^T = \mathsf{L}_{\mathbf{A}^T} \tag{B.14}$$
$$\mathsf{R}_\mathbf{A}^T = \mathsf{R}_{\mathbf{A}^T}. \tag{B.15}$$

Then, defining the inner-product on matrices by

$$\langle\mathbf{A},\mathbf{B}\rangle = \mathrm{tr}\left(\mathbf{AB}^T\right) \tag{B.16}$$

and introducing $\mathbf{C}\in\mathbf{GL}(3)$, it follows quickly that

$$\langle\mathbf{A},\mathsf{L}_\mathbf{C}\cdot\mathbf{B}\rangle = \left\langle\mathsf{L}_\mathbf{C}^T\cdot\mathbf{A},\mathbf{B}\right\rangle, \tag{B.17}$$

and similarly for $\mathsf{R}_\mathbf{C}$. This is the origin of our suggestive notation for $\mathsf{L}_\mathbf{A}^T$ and $\mathsf{R}_\mathbf{A}^T$: with the inner product as defined, they behave superficially as though they were the respective transpose

operators of $\mathsf{L}_\mathbf{A}$ and $\mathsf{R}_\mathbf{A}$. We also define a *norm* on matrices,

$$\|\mathbf{A}\| = \sqrt{\langle \mathbf{A}, \mathbf{A} \rangle}, \tag{B.18}$$

and *tensor-product*,

$$(\mathbf{A} \otimes \mathbf{B}) \cdot \mathbf{C} = \langle \mathbf{B}, \mathbf{C} \rangle \, \mathbf{A}. \tag{B.19}$$

In order to avoid clutter we have – just as for the inner product – simply used the standard notation for a tensor-product and norm on $\mathbb{R}^3$, trusting that context will make our meaning unambiguous.

A particularly useful operator is

$$\mathsf{T}_\mathbf{A} = \mathsf{L}_\mathbf{A} \mathsf{R}_\mathbf{A}^T. \tag{B.20}$$

From the properties of $\mathsf{L}_\mathbf{A}$ and $\mathsf{R}_\mathbf{A}$ discussed above, we clearly have

$$\mathsf{T}_\mathbf{A}^{-1} = \mathsf{T}_{\mathbf{A}^{-1}} \tag{B.21}$$

$$\mathsf{T}_\mathbf{A}^T = \mathsf{T}_{\mathbf{A}^T}, \tag{B.22}$$

as well as the useful *functoral* property

$$\mathsf{T}_{\mathbf{AB}} = \mathsf{T}_\mathbf{A} \mathsf{T}_\mathbf{B}. \tag{B.23}$$

For $\mathbf{R} \in \mathbf{SO}(3)$,

$$\mathsf{T}_\mathbf{R} \cdot \mathbf{A} = \mathbf{R}\mathbf{A}\mathbf{R}^T \tag{B.24}$$

evidently represents a rotation of $\mathbf{A}$ by $\mathbf{R}$. The related operator

$$\mathsf{X}_\mathbf{A} = \mathsf{L}_\mathbf{A} + \mathsf{R}_\mathbf{A}^T \tag{B.25}$$

is the term in $\mathsf{T}_{\mathbf{1}+\mathbf{A}}$ linear in $\mathbf{A}$, and is particularly useful when we consider linearisation. Furthermore, if $\mathbf{A}$ and $\mathbf{B}$ are both symmetric the operator satisfies

$$\mathsf{X}_\mathbf{A} \cdot \mathbf{B} = \mathsf{X}_\mathbf{B} \cdot \mathbf{A}. \tag{B.26}$$

Finally, we must sometimes be careful when writing these operators in component form. Consider the expression for the quadratic part of an isotropic strain-energy function (e.g. Holzapfel, 2000):

$$V_2(\mathbf{C}) = \frac{\lambda}{8} \mathrm{tr}(\mathbf{C})^2 + \frac{\mu}{4} \mathrm{tr}\big(\mathbf{C}^2\big) \, . \tag{B.27}$$

It is easy to show that the stress vanishes at $\mathbf{C} = \mathbf{1}$. In such a stress-free equilibrium we have

(eq.3.71)

$$\mathbf{a} = 4D^2 V_2(\mathbf{1})\,. \tag{B.28}$$

We can evaluate the derivative by using the definitions above to rewrite V_2 as

$$\begin{aligned} V_2(\mathbf{C}) &= \frac{\lambda}{8}\langle \mathbf{1}, \mathbf{C}\rangle^2 + \frac{\mu}{4}\langle \mathbf{C}, \mathbf{id}\cdot\mathbf{C}\rangle \\ &= \left\langle \mathbf{C}, \left(\frac{\lambda}{8}\mathbf{1}\otimes\mathbf{1} + \frac{\mu}{4}\mathbf{id}\right)\cdot\mathbf{C}\right\rangle, \end{aligned} \tag{B.29}$$

where we further define the *identity operator* $\mathbf{id}$, which has components

$$(\mathbf{id})_{ijkl} = \delta_{ik}\delta_{jl}. \tag{B.30}$$

However, in the present context this is not the correct identity operator to use. When differentiating strain-energy functions that depend on the symmetric matrix $\mathbf{C}$ we find ourselves dealing with operators that naturally act on symmetric matrices. Therefore we must remind ourselves that the component-form expressions for these operators will be symmetric on each pair of indices. We denote this by an overline. In general, the process of symmetrisation is defined as follows. The tensor $\mathbf{M}$ is symmetrised on its p'th pair of indices by

$$M_{i_1 j_1 i_2 j_2 \ldots i_p j_p \ldots i_n j_n} \to M_{i_1 j_1 i_2 j_2 \ldots (i_p j_p) \ldots i_n j_n} \equiv \frac{1}{2}\left(M_{i_1 j_1 i_2 j_2 \ldots i_p j_p \ldots i_n j_n} + M_{i_1 j_1 i_2 j_2 \ldots j_p i_p \ldots i_n j_n}\right). \tag{B.31}$$

A fourth-rank tensor $\mathbf{M}$, for example, is symmetrised on both pairs of indices by writing

$$(\overline{\mathbf{M}})_{ijkl} = \mathsf{M}_{(ij)(kl)} = \frac{1}{4}(\mathsf{M}_{ijkl} + \mathsf{M}_{ijlk} + \mathsf{M}_{jikl} + \mathsf{M}_{jikl})\,. \tag{B.32}$$

The symmetrised identity operator is thus written as

$$(\overline{\mathbf{id}})_{ijkl} = \frac{1}{2}(\delta_{ik}\delta_{jl} + \delta_{il}\delta_{jk})\,. \tag{B.33}$$

Substituting this into eq.(B.29) will yield the correct component-form expression for the elastic tensor. Note that this process confers the *minor* elastic symmetries on a fourth-rank tensor, but not necessarily the hyperelastic symmetry.

B.1.3 Example: Differentiation of the strain-energy functions W and V

All the calculations discussed in Chapter 3 could in principle be performed using index notation. However, we found it to be too cumbersome to carry out the calculations of Appendix B.3. The purpose of this appendix is to explain how the operator-based notation detailed above can be used to carry out the differentiations of strain-energy functions in Sections 3.2 and 3.3. It avoids clutter in the main text and moreover illustrates the manipulation of these operators.

For an arbitrary $\mathbf{F} \in \mathbf{GL}(3)$ and $\mathbf{C} = \mathbf{F}^T\mathbf{F}$ we have

$$W(\mathbf{F}) = V(\mathbf{C}), \tag{B.34}$$

neglecting the spatial argument to avoid clutter. We define small perturbations to $\mathbf{F}$ and $\mathbf{C}$, respectively $\delta\mathbf{F}$ and $\delta\mathbf{C}$, such that

$$W(\mathbf{F} + \delta\mathbf{F}) - W(\mathbf{F}) = \langle DW(\mathbf{F}), \delta\mathbf{F}\rangle + \mathcal{O}(\|\delta\mathbf{F}\|^2) \tag{B.35}$$
$$V(\mathbf{C} + \delta\mathbf{C}) - V(\mathbf{C}) = \langle DV(\mathbf{C}), \delta\mathbf{C}\rangle + \mathcal{O}(\|\delta\mathbf{C}\|^2) \tag{B.36}$$

where $\langle\cdot,\cdot\rangle$ is the inner product for matrices (eq.B.16) and $\|\cdot\|$ is the corresponding norm (eq.B.18). It follows from the definition of $\mathbf{C}$ that

$$\delta\mathbf{C} = \mathbf{F}^T\delta\mathbf{F} + \delta\mathbf{F}^T\mathbf{F} + \mathcal{O}(\|\delta\mathbf{F}\|^2), \tag{B.37}$$

which allows us to write

$$\langle DW(\mathbf{F}), \delta\mathbf{F}\rangle = \big\langle DV(\mathbf{C}), \mathbf{F}^T\delta\mathbf{F} + \delta\mathbf{F}^T\mathbf{F}\big\rangle. \tag{B.38}$$

Now, for any matrices $\mathbf{A}$ and $\mathbf{B}$ our inner product satisfies $\langle\mathbf{A},\mathbf{B}\rangle = \big\langle\mathbf{A}^T,\mathbf{B}^T\big\rangle$. This identity, along with the fact that $DV(\mathbf{C})$ is necessarily symmetric, implies that

$$\big\langle DV(\mathbf{C}), \delta\mathbf{F}^T\mathbf{F}\big\rangle = \big\langle DV(\mathbf{C}), \mathbf{F}^T\delta\mathbf{F}\big\rangle, \tag{B.39}$$

and therefore

$$\langle DW(\mathbf{F}), \delta\mathbf{F}\rangle = 2\big\langle DV(\mathbf{C}), \mathbf{F}^T\delta\mathbf{F}\big\rangle. \tag{B.40}$$

Looking at the right hand side, the left multiplication operator defined in eq.(B.3) lets us write

$$\mathbf{F}^T\delta\mathbf{F} = \mathsf{L}^T_{\mathbf{F}} \cdot \delta\mathbf{F}, \tag{B.41}$$

where we have made use of eq.(B.14). Using this notation we find that

$$\big\langle DV(\mathbf{C}), \mathbf{F}^T\delta\mathbf{F}\big\rangle = \big\langle DV(\mathbf{C}), \mathsf{L}^T_{\mathbf{F}} \cdot \delta\mathbf{F}\big\rangle = \langle \mathsf{L}_{\mathbf{F}} \cdot DV(\mathbf{C}), \delta\mathbf{F}\rangle. \tag{B.42}$$

Therefore we conclude that

$$\langle DW(\mathbf{F}), \delta\mathbf{F}\rangle = \langle 2\mathsf{L}_{\mathbf{F}} \cdot DV(\mathbf{C}), \delta\mathbf{F}\rangle. \tag{B.43}$$

Because the perturbation $\delta\mathbf{F}$ was arbitrary, we have established the identity

$$DW(\mathbf{F}) = 2\mathsf{L}_{\mathbf{F}} \cdot DV(\mathbf{C}). \tag{B.44}$$

The derivation of the second-derivative follows a similar pattern. We take as a starting point

the definitions

$$DW(\mathbf{F}+\delta\mathbf{F}) - DW(\mathbf{F}) = D^2W(\mathbf{F})\cdot\delta\mathbf{F} + \mathcal{O}(\|\delta\mathbf{F}\|^2) \tag{B.45}$$

$$DV(\mathbf{C}+\delta\mathbf{C}) - DV(\mathbf{C}) = D^2V(\mathbf{C})\cdot\delta\mathbf{C} + \mathcal{O}(\|\delta\mathbf{C}\|^2), \tag{B.46}$$

for the previously defined $\delta\mathbf{F}$ and $\delta\mathbf{C}$. Using eq.(B.44) the left hand side of eq.(B.45) can be written

$$2\mathsf{L}_{\mathbf{F}+\delta\mathbf{F}}\cdot DV(\mathbf{C}+\delta\mathbf{C}) - 2\mathsf{L}_{\mathbf{F}}\cdot DV(\mathbf{C}). \tag{B.47}$$

Expanding this out to first-order it follows that

$$D^2W(\mathbf{F})\cdot\delta\mathbf{F} = 2\mathsf{L}_{\delta\mathbf{F}}\cdot DV(\mathbf{C}) + 2\mathsf{L}_{\mathbf{F}}\cdot\left[D^2V(\mathbf{C})\cdot\left(\mathbf{F}^T\delta\mathbf{F} + \delta\mathbf{F}^T\mathbf{F}\right)\right], \tag{B.48}$$

where we have used eqs. (B.37) and (B.46). To proceed, we first note that $\mathsf{L}_{\delta\mathbf{F}}\cdot DV(\mathbf{C}) = \mathsf{R}_{DV(\mathbf{C})}\cdot\delta\mathbf{F}$ by definition of the left and right multiplication operators. Secondly,

$$D^2V(\mathbf{C})\cdot(\mathbf{F}^T\delta\mathbf{F} + \delta\mathbf{F}^T\mathbf{F}) = 2D^2V(\mathbf{C})\cdot(\mathbf{F}^T\delta\mathbf{F}) \tag{B.49}$$

because V is a function on symmetric matrices. Given that $\delta\mathbf{F}$ is arbitrary, this establishes our desired expression for the second-derivative of W:

$$D^2W(\mathbf{F}) = 2\mathsf{R}_{DV(\mathbf{C})} + 4\mathsf{L}_{\mathbf{F}}D^2V(\mathbf{C})\ \mathsf{L}_{\mathbf{F}}^T. \tag{B.50}$$

B.1.4 Mapping between different notation conventions

As stated above, Sections 4.1 and 3.5 are written in a notation close to that of Dahlen & Tromp (1998) whilst for the middle sections we use a notation heavily inspired by Marsden & Hughes (1994). Table B.1 summarises the relationship between the two systems. Besides differing choices of letter for various quantities, the principal difference between the two systems concerns index placement. All second-rank tensors must have their indices switched to go from one convention to the other, and for tensors of higher (even) rank the same applies to each pair of indices individually; this is illustrated schematically in Table B.1's last two lines. Note also that we do not follow MH's convention of using upper- and lower-case indices to distinguish between referential and spatial coordinate-systems because we consider both systems to be implicitly Cartesian. Finally, where a quantity of interest does not appear in MH we have notated it with the same letter as DT, although in Sections 3.2–3.4 we consistently place our indices according to MH's conventions; such quantities do not appear in the table.

To conclude this section we "translate" eqs.(3.118) (reproduced in Table B.1) into the notation of Section 4.1, giving expressions for the components of eq.(3.157)'s tensors $\mathbf{\Pi}$ and $\mathbf{\Pi}'$. Let us first recall the elastic tensor $\boldsymbol{\Upsilon}$ that is defined by Dahlen & Tromp (1998, eq.3.123) to have components

$$\Upsilon_{ijkl} = \Xi_{ijkl} + T^0_{ik}\delta_{jl} + T^0_{jk}\delta_{il} - T^0_{ij}\delta_{kl}. \tag{B.51}$$

We now define the very closely related tensor $\mathbf{Y}$, whose components are

$$Y_{ijkl} = \Gamma_{ijkl} + T^B_{ik}\delta_{jl} + T^B_{jk}\delta_{il} - T^B_{ij}\delta_{kl}, \tag{B.52}$$

and we then symmetrise it to form a new tensor $\overline{\mathbf{Y}}$, which has components

$$\overline{Y}_{ijkl} = Y_{ij(kl)} \tag{B.53}$$

and satisfies the symmetries

$$\overline{Y}_{jikl} = \overline{Y}_{ijkl} = \overline{Y}_{ijlk}. \tag{B.54}$$

The inverse tensor $\overline{\mathbf{Y}}^{-1}$ is then defined by the relation

$$\overline{Y}_{ijab}\overline{Y}^{-1}_{abkl} = \frac{1}{2}(\delta_{ik}\delta_{jl} + \delta_{jk}\delta_{il})\,. \tag{B.55}$$

We can now rewrite the generalised stress-strain relationship (eq.3.118b) as

$$\mathbf{u}^1 = \overline{\mathbf{Y}}^{-1} : \left(\Delta\mathbf{T}^0 - \boldsymbol{\omega}^1 \cdot \mathbf{T}^B - \mathbf{T}^B \cdot \boldsymbol{\omega}^1\right). \tag{B.56}$$

Eq.(3.118a) can be dealt with by defining two final tensors:

$$\Theta_{ijklmn} = \delta_{im}\Gamma_{njkl} + \delta_{jm}\Gamma_{inkl} + \delta_{km}\Gamma_{ijnl} + \delta_{lm}\Gamma_{ijkn} - \Gamma_{ijkl}\delta_{mn} + \rho^0\frac{\partial^3 U^L}{\partial E^L_{ij}\partial E^L_{kl}\partial E^L_{mn}}, \tag{B.57}$$

$$\Psi_{ijklmn} = \delta_{im}\Gamma_{njkl} + \delta_{jm}\Gamma_{inkl} + \delta_{km}\Gamma_{ijnl} + \delta_{lm}\Gamma_{ijkn}. \tag{B.58}$$

The components of $\boldsymbol{\Pi}$ and $\boldsymbol{\Pi}'$ are then given by

$$\Pi_{ijklmn} = \Theta_{ijklpq}\overline{Y}^{-1}_{pqmn}, \tag{B.59}$$

$$\Pi'_{ijklmn} = \Theta_{ijklpq}\left(\overline{Y}^{-1}_{pqrn}T^B_{rm} - \overline{Y}^{-1}_{pqrm}T^B_{rn}\right) + \Psi_{ijklmn}. \tag{B.60}$$

Table B.1: The mapping between the two major notation conventions used in this chapter. See the main text for a discussion of the components of $\boldsymbol{\Pi}$ and $\boldsymbol{\Pi}'$. Note also that the first and second elastic tensors are sometimes represented by A and C; we have listed a and c in the table because, like the elastic tensors of Dahlen & Tromp, they are expressed relative to a natural reference configuration.

Quantity	Dahlen & Tromp	Marsden & Hughes
First elastic tensor	$\boldsymbol{\Lambda}$	a
Second elastic tensor	$\boldsymbol{\Xi}$	c
Background (second) elastic tensor	$\boldsymbol{\Gamma}$	c^0
Incremental second elastic tensor	$\Delta\boldsymbol{\Xi}$	c^1
First Piola-Kirchhoff stress	$\mathbf{T}^{PK}$	$\mathbf{P}$
Second Piola-Kirchhoff stress	$\mathbf{T}^{SK}$	$\mathbf{S}$
Eulerian Cauchy stress	$\mathbf{T}^{E}$	$\boldsymbol{\sigma}$
Equilibrium Cauchy stress	$\mathbf{T}^{0}$	$\boldsymbol{\sigma}_e$ (shortened to $\boldsymbol{\sigma}$ in Sections 3.3 and 3.4)
Background Cauchy stress	$\mathbf{T}^{B}$	$\boldsymbol{\sigma}^0$
Incremental Cauchy stress	$\Delta\mathbf{T}^{0}$	$\boldsymbol{\sigma}^1$
Incremental pressure	Δp^0	p^1
Incremental deviatoric stress	$\Delta\boldsymbol{\tau}^0$	$\boldsymbol{\tau}^1$
Polar decomposition theorem	$\mathbf{F}=\mathbf{QR}=\mathbf{LQ}$	$\mathbf{F}=\mathbf{RU}=\mathbf{VR}$
Central equations (3.94)	$T^0_{ij}=\dfrac{\rho^0}{\det\mathbf{F}}F_{ip}F_{jq}\dfrac{\partial U^L}{\partial E^L_{pq}}$ $\Xi_{ijkl}=\dfrac{\rho^0}{\det\mathbf{F}}F_{ip}F_{jq}F_{kr}F_{ls}\dfrac{\partial^2 U^L}{\partial E^L_{pq}\partial E^L_{rs}}$	$\boldsymbol{\sigma}=2J_{\mathbf{F}}^{-1}\mathsf{T}_{\mathbf{F}}\cdot D\tilde{V}(\mathbf{C})$ $\mathsf{a}=4J_{\mathbf{F}}^{-1}\mathsf{T}_{\mathbf{F}}D^2\tilde{V}(\mathbf{C})\,\mathsf{T}_{\mathbf{F}}^{T}+\mathsf{R}_{\boldsymbol{\sigma}}$
Linearised expressions (3.118)	$\Delta\Xi_{ijkl}=\Pi_{ijklmn}\Delta T^0_{mn}+\Pi'_{ijklmn}\omega^1_{mn}$	$\mathsf{c}^1=\mathsf{X}_{\mathbf{u}^1+\boldsymbol{\omega}^1}\mathsf{c}^0+\mathsf{c}^0\mathsf{X}_{\mathbf{u}^1-\boldsymbol{\omega}^1}-\mathsf{c}^0\mathrm{tr}\big(\mathbf{u}^1\big)+8D^3\tilde{V}(\mathbf{1})\cdot\mathbf{u}^1$ $\mathbf{u}^1=\big(\mathsf{c}^0+\overline{\mathsf{X}}_{\boldsymbol{\sigma}^0}-\boldsymbol{\sigma}^0\otimes\mathbf{1}\big)^{-1}\cdot\big(\boldsymbol{\sigma}^1-\mathsf{X}_{\boldsymbol{\omega}^1}\cdot\boldsymbol{\sigma}^0\big)$
Any second-rank tensor	$[\mathbf{D}\&\mathbf{T}]_{ij}$	$[\mathbf{M}\&\mathbf{H}]_{ji}$
Any fourth-rank tensor	$[\mathbf{D}\&\mathbf{T}]_{ijkl}$	$[\mathbf{M}\&\mathbf{H}]_{jilk}$

B.2 The invertibility of $\hat{\boldsymbol{\Sigma}}$

The existence of the inverse function $\hat{\boldsymbol{\Sigma}}^{-1}$ depends on the specific choice of constitutive relation; without fixing $\tilde{V}$ concretely it is difficult to obtain definite results. However, we can show that the inverse mapping exists at least locally in cases of some physical importance. To proceed, we appeal to the *inverse function theorem* (e.g. Marsden & Hughes, 1994). The theorem tells us that the nonlinear mapping $\hat{\boldsymbol{\Sigma}}$ has a well-defined inverse function in some open neighbourhood of $\hat{\boldsymbol{\Sigma}}(\mathbf{U})$ if $D\hat{\boldsymbol{\Sigma}}(\mathbf{U})$, a linear mapping from the vector-space of symmetric matrices into itself, is invertible.

Let us work in the vicinity of $\mathbf{U} = \mathbf{1}$. We will set $\mathbf{R} = \mathbf{1}$ for clarity, but that does not affect the validity of our argument. In that case we have

$$\hat{\boldsymbol{\Sigma}}(\mathbf{1}) = 2DV(\mathbf{1})\,. \tag{B.61}$$

Making use of eq.(B.26) of Appendix B.1, we can expand $\hat{\boldsymbol{\Sigma}}$ about the identity as

$$\begin{aligned}\hat{\boldsymbol{\Sigma}}(\mathbf{1}+\mathbf{u}) &= 2[1-\mathrm{tr}(\mathbf{u})][\mathbf{id}+\mathbf{X}_{\mathbf{u}}]\cdot\big[DV(\mathbf{1})+2D^2V(\mathbf{1})\cdot\mathbf{u}\big]\\ &= \hat{\boldsymbol{\Sigma}}(\mathbf{1})-\mathrm{tr}(\mathbf{u})\,\hat{\boldsymbol{\Sigma}}(\mathbf{1})+\mathbf{X}_{\mathbf{u}}\cdot\hat{\boldsymbol{\Sigma}}(\mathbf{1})+4D^2V(\mathbf{1})\cdot\mathbf{u}\\ &= \hat{\boldsymbol{\Sigma}}(\mathbf{1})+\Big(4D^2V(\mathbf{1})+\mathbf{X}_{\hat{\boldsymbol{\Sigma}}(\mathbf{1})}-\hat{\boldsymbol{\Sigma}}(\mathbf{1})\otimes\mathbf{1}\Big)\cdot\mathbf{u},\end{aligned} \tag{B.62}$$

with $\mathbf{u}$ a small symmetric matrix. We have shown that

$$D\hat{\boldsymbol{\Sigma}}(\mathbf{1}) = 4D^2V(\mathbf{1})+\overline{\mathbf{X}}_{\hat{\boldsymbol{\Sigma}}(\mathbf{1})}-\hat{\boldsymbol{\Sigma}}(\mathbf{1})\otimes\mathbf{1}, \tag{B.63}$$

where we have written $\mathbf{X}_{\hat{\boldsymbol{\Sigma}}(\mathbf{1})}$ in its explicitly symmetrised form $\overline{\mathbf{X}}_{\hat{\boldsymbol{\Sigma}}(\mathbf{1})}$ (eq.B.32). Inspection of expression (B.63) indicates that the invertibility of $D^2V(\mathbf{1})$ is a sufficient condition for $D\hat{\boldsymbol{\Sigma}}(\mathbf{1})$ to possess a unique inverse locally, in the absence of equilibrium stress. As long as $\hat{\boldsymbol{\Sigma}}(\mathbf{1})$ is not too large, invertibility of $D^2V(\mathbf{1})$ should remain sufficient for the local existence of a unique $\hat{\boldsymbol{\Sigma}}^{-1}$. One can show that $D^2V(\mathbf{1})$ being invertible is equivalent to the condition of *linearised stability* of the equilibrium (e.g. Marsden & Hughes, 1994). It is essential to enforce linearised stability, for otherwise unphysical motions are permitted in which the strain-energy decreases upon deformation.

In summary, we have argued that linearised stability of the equilibrium is a sufficient condition for $\hat{\boldsymbol{\Sigma}}$ to possess a unique inverse in the neighbourhood of $\hat{\boldsymbol{\Sigma}}(\mathbf{1})$, as long as the equilibrium stress is not too large. By no means is this a proof of the global invertibility of $\hat{\boldsymbol{\Sigma}}$, but we believe that it makes it plausible that we should be able to write down a well-defined inverse function $\hat{\boldsymbol{\Sigma}}^{-1}$ when required.

B.3 Calculation of the linearised elastic tensor

B.3.1 General expressions

We assume that the body is initially in a state described by

$$\boldsymbol{\sigma} = \boldsymbol{\sigma}^0 \tag{B.64}$$

$$\mathsf{a} = \mathsf{a}^0. \tag{B.65}$$

Both quantities are considered to be the derivatives of some background strain-energy evaluated at the identity, so that a^0 is given uniquely by

$$\mathsf{a}^0 = \bar{\mathsf{a}}\left(\boldsymbol{\sigma}^0, \mathbf{1}\right). \tag{B.66}$$

Once again, the function $\bar{\mathsf{a}}$ has the form

$$\bar{\mathsf{a}}(\boldsymbol{\sigma}, \mathbf{R}) = \mathsf{T}_{\mathbf{R}}\left[\left(\hat{\mathsf{A}} \circ \hat{\boldsymbol{\Sigma}}^{-1}\right)\left(\mathsf{T}_{\mathbf{R}}^T \cdot \boldsymbol{\sigma}\right)\right] \mathsf{T}_{\mathbf{R}}^T. \tag{B.67}$$

We then introduce a small change in the stress:

$$\boldsymbol{\sigma} = \boldsymbol{\sigma}^0 + \boldsymbol{\sigma}^1 \tag{B.68}$$

for small $\boldsymbol{\sigma}^1$. The system is assumed to be perturbative, so that we may write

$$\mathsf{a} = \mathsf{a}^0 + \mathsf{a}^1 \tag{B.69}$$

for small a^1. For the rest of this section we will neglect all terms higher than first order.

Under the framework of Section 3.3, the change in stress is considered to be induced by some deformation gradient $\mathbf{F}$, so it follows that $\mathbf{F}$ should take the form

$$\mathbf{F} = \mathbf{1} + \mathbf{f}. \tag{B.70}$$

with $\mathbf{f}$ small. Now, the arbitrary rotation matrix $\mathbf{R}$ in eq.(B.67) is a relic of $\mathbf{F}$, having been introduced by the identity

$$\mathbf{F} = \mathbf{R}\mathbf{U}. \tag{B.71}$$

Therefore it too must be considered to be a small perturbation to its background value:

$$\mathbf{R} = \mathbf{1} + \boldsymbol{\omega}, \tag{B.72}$$

with $\boldsymbol{\omega}$ some small antisymmetric matrix. The same is true for $\mathbf{U}$, that is

$$\mathbf{U} = \mathbf{1} + \mathbf{u}, \tag{B.73}$$

but with the small matrix $\mathbf{u}$ of course symmetric. It is clear that the elastic tensor satisfies

$$\mathbf{a}^0 + \mathbf{a}^1 = \bar{\mathbf{a}}\big(\boldsymbol{\sigma}^0 + \boldsymbol{\sigma}^1, \mathbf{1} + \boldsymbol{\omega}\big)\,, \tag{B.74}$$

which we may expand in a Taylor series to find

$$\mathbf{a}^1 = (D_{\boldsymbol{\sigma}}\bar{\mathbf{a}})\big(\boldsymbol{\sigma}^0, \mathbf{1}\big) \cdot \boldsymbol{\sigma}^1 + (D_{\mathbf{R}}\bar{\mathbf{a}})\big(\boldsymbol{\sigma}^0, \mathbf{1}\big) \cdot \boldsymbol{\omega}. \tag{B.75}$$

The $\mathbf{R}$-derivative can conveniently be written in terms of the $\boldsymbol{\sigma}$-derivative. Using the full form of $\bar{\mathbf{a}}$ from eq.(B.67), as well as the operator $\mathbf{id}$ defined in eq.(B.30),

$$\begin{aligned}
\bar{\mathbf{a}}(\boldsymbol{\sigma}, \mathbf{1} + \boldsymbol{\omega}) &= (\mathbf{id} + \mathbf{X}_{\boldsymbol{\omega}})\Big[\Big(\hat{\mathbf{A}} \circ \hat{\boldsymbol{\Sigma}}^{-1}\Big)(\boldsymbol{\sigma} - \mathbf{X}_{\boldsymbol{\omega}} \cdot \boldsymbol{\sigma})\Big](\mathbf{id} - \mathbf{X}_{\boldsymbol{\omega}}) \\
&= \Big(\hat{\mathbf{A}} \circ \hat{\boldsymbol{\Sigma}}^{-1}\Big)(\boldsymbol{\sigma} - \mathbf{X}_{\boldsymbol{\omega}} \cdot \boldsymbol{\sigma}) + \mathbf{X}_{\boldsymbol{\omega}}\Big[\Big(\hat{\mathbf{A}} \circ \hat{\boldsymbol{\Sigma}}^{-1}\Big)(\boldsymbol{\sigma})\Big] - \Big[\Big(\hat{\mathbf{A}} \circ \hat{\boldsymbol{\Sigma}}^{-1}\Big)(\boldsymbol{\sigma})\Big]\,\mathbf{X}_{\boldsymbol{\omega}} \\
&= \bar{\mathbf{a}}(\boldsymbol{\sigma} - \mathbf{X}_{\boldsymbol{\omega}} \cdot \boldsymbol{\sigma}, \mathbf{1}) + \mathbf{X}_{\boldsymbol{\omega}}\bar{\mathbf{a}}(\boldsymbol{\sigma}, \mathbf{1}) - \bar{\mathbf{a}}(\boldsymbol{\sigma}, \mathbf{1})\,\mathbf{X}_{\boldsymbol{\omega}} \\
&= \mathbf{a}^0 - (D_{\boldsymbol{\sigma}}\bar{\mathbf{a}})(\boldsymbol{\sigma}, \mathbf{1}) \cdot (\mathbf{X}_{\boldsymbol{\omega}} \cdot \boldsymbol{\sigma}) + \mathbf{X}_{\boldsymbol{\omega}}\mathbf{a}^0 - \mathbf{a}^0\mathbf{X}_{\boldsymbol{\omega}},
\end{aligned} \tag{B.76}$$

from which it is apparent that

$$(D_{\mathbf{R}}\bar{\mathbf{a}})\big(\boldsymbol{\sigma}^0, \mathbf{1}\big) \cdot \boldsymbol{\omega} = \mathbf{X}_{\boldsymbol{\omega}}\mathbf{a}^0 - \mathbf{a}^0\mathbf{X}_{\boldsymbol{\omega}} - (D_{\boldsymbol{\sigma}}\bar{\mathbf{a}})\big(\boldsymbol{\sigma}^0, \mathbf{1}\big) \cdot \big(\mathbf{X}_{\boldsymbol{\omega}} \cdot \boldsymbol{\sigma}^0\big)\,. \tag{B.77}$$

Substituting this into eq.(B.75), the perturbation to the elastic tensor is

$$\mathbf{a}^1 = \mathbf{X}_{\boldsymbol{\omega}}\mathbf{a}^0 - \mathbf{a}^0\mathbf{X}_{\boldsymbol{\omega}} + (D_{\boldsymbol{\sigma}}\bar{\mathbf{a}})\big(\boldsymbol{\sigma}^0, \mathbf{1}\big) \cdot \big(\boldsymbol{\sigma}^1 - \mathbf{X}_{\boldsymbol{\omega}} \cdot \boldsymbol{\sigma}^0\big)\,. \tag{B.78}$$

Calculation of $D_{\boldsymbol{\sigma}}\bar{\mathbf{a}}\big(\boldsymbol{\sigma}^0, \mathbf{1}\big)$ requires us to find $D\hat{\mathbf{A}}(\mathbf{1})$ and $D\hat{\boldsymbol{\Sigma}}(\mathbf{1})$. They are evaluated most conveniently by forming explicit binomial expansions of $\hat{\boldsymbol{\Sigma}}$ and $\hat{\mathbf{A}}$ about $\mathbf{U} = \mathbf{1} + \mathbf{u}$. At zeroth order

$$\hat{\boldsymbol{\Sigma}}(\mathbf{1}) = \boldsymbol{\sigma}^0 = 2DV(\mathbf{1}) \tag{B.79}$$

$$\hat{\mathbf{A}}(\mathbf{1}) = \mathbf{a}^0 = 4D^2V(\mathbf{1}) + \mathbf{R}_{\hat{\boldsymbol{\Sigma}}(\mathbf{1})}, \tag{B.80}$$

and it is useful to define

$$\mathbf{c}^0 = 4D^2V(\mathbf{1}) = \hat{\mathbf{A}}(\mathbf{1}) - \mathbf{R}_{\hat{\boldsymbol{\Sigma}}(\mathbf{1})}. \tag{B.81}$$

We showed in Appendix B.2 that

$$D\hat{\boldsymbol{\Sigma}}(\mathbf{1}) = \mathbf{c}^0 + \overline{\mathbf{X}}_{\boldsymbol{\sigma}^0} - \boldsymbol{\sigma}^0 \otimes \mathbf{1}. \tag{B.82}$$

In the same manner, $\hat{\mathbf{A}}$ expands as

$$\begin{aligned}
\hat{\mathbf{A}}(\mathbf{1} + \mathbf{u}) &= 4(1 - \mathrm{tr}(\mathbf{u}))(\mathbf{id} + \mathbf{X}_{\mathbf{u}})\big[D^2V(\mathbf{1}) + 2D^3V(\mathbf{1}) \cdot \mathbf{u}\big](\mathbf{id} + \mathbf{X}_{\mathbf{u}}) + \mathbf{R}_{\hat{\boldsymbol{\Sigma}}(\mathbf{1}+\mathbf{u})} \\
&= \mathbf{c}^0 + 8D^3V(\mathbf{1}) \cdot \mathbf{u} + \mathbf{X}_{\mathbf{u}}\mathbf{c}^0 + \mathbf{c}^0\mathbf{X}_{\mathbf{u}} - \mathbf{c}^0\mathrm{tr}(\mathbf{u}) + \mathbf{R}_{\boldsymbol{\sigma}^0} + \mathbf{R}_{D\hat{\boldsymbol{\Sigma}}(\mathbf{1})\cdot\mathbf{u}},
\end{aligned} \tag{B.83}$$

so its derivative at the identity is given by

$$D\hat{\mathbf{A}}(\mathbf{1})\cdot\mathbf{u} = \mathbf{R}_{D\hat{\boldsymbol{\Sigma}}(\mathbf{1})\cdot\mathbf{u}} + 8D^3V(\mathbf{1})\cdot\mathbf{u} + \mathbf{X}_{\mathbf{u}}\mathbf{c}^0 + \mathbf{c}^0\mathbf{X}_{\mathbf{u}} - \mathbf{c}^0\mathrm{tr}(\mathbf{u}) \tag{B.84}$$

for any $\mathbf{u}$.

Now we can compute $D_{\boldsymbol{\sigma}}\bar{\mathbf{a}}\big(\boldsymbol{\sigma}^0,\mathbf{1}\big)$ by writing

$$\begin{aligned}\bar{\mathbf{a}}\big(\boldsymbol{\sigma}^0+\boldsymbol{\Sigma},\mathbf{1}\big) &= \hat{\mathbf{A}}\Big[\hat{\boldsymbol{\Sigma}}^{-1}\big(\boldsymbol{\sigma}^0+\boldsymbol{\Sigma}\big)\Big]\\ &= \hat{\mathbf{A}}\Big[\hat{\boldsymbol{\Sigma}}^{-1}\big(\boldsymbol{\sigma}^0\big)+\Big[D\Big(\hat{\boldsymbol{\Sigma}}^{-1}\Big)\Big]\big(\boldsymbol{\sigma}^0\big)\cdot\boldsymbol{\Sigma}\Big]\\ &= \hat{\mathbf{A}}\Big\{\mathbf{1}+\Big[D\hat{\boldsymbol{\Sigma}}(\mathbf{1})\Big]^{-1}\cdot\boldsymbol{\Sigma}\Big\}\\ &= \hat{\mathbf{A}}(\mathbf{1})+D\hat{\mathbf{A}}(\mathbf{1})\cdot\Big\{\Big[D\hat{\boldsymbol{\Sigma}}(\mathbf{1})\Big]^{-1}\cdot\boldsymbol{\Sigma}\Big\},\end{aligned} \tag{B.85}$$

valid for small symmetric $\boldsymbol{\Sigma}$, where we have used the identity

$$D\Big(\hat{\boldsymbol{\Sigma}}^{-1}\Big)\big(\boldsymbol{\sigma}^0\big) = \Big\{D\hat{\boldsymbol{\Sigma}}\Big[\hat{\boldsymbol{\Sigma}}^{-1}\big(\boldsymbol{\sigma}^0\big)\Big]\Big\}^{-1} = \Big[D\hat{\boldsymbol{\Sigma}}(\mathbf{1})\Big]^{-1}. \tag{B.86}$$

Thus,

$$(D_{\boldsymbol{\sigma}}\bar{\mathbf{a}})\big(\boldsymbol{\sigma}^0,\mathbf{1}\big)\cdot\big(\boldsymbol{\sigma}^1-\mathbf{X}_{\boldsymbol{\omega}}\cdot\boldsymbol{\sigma}^0\big) = D\hat{\mathbf{A}}(\mathbf{1})\cdot\Big\{\Big[D\hat{\boldsymbol{\Sigma}}(\mathbf{1})\Big]^{-1}\cdot\big(\boldsymbol{\sigma}^1-\mathbf{X}_{\boldsymbol{\omega}}\cdot\boldsymbol{\sigma}^0\big)\Big\}, \tag{B.87}$$

and we can combine this with eqs. (B.84), (B.82) and (B.78) to write the perturbation to the elastic tensor as

$$\mathbf{a}^1 = \mathbf{X}_{\boldsymbol{\omega}}\mathbf{a}^0 - \mathbf{a}^0\mathbf{X}_{\boldsymbol{\omega}} + \mathbf{X}_{\mathbf{u}}\mathbf{c}^0 + \mathbf{c}^0\mathbf{X}_{\mathbf{u}} - \mathbf{c}^0\mathrm{tr}(\mathbf{u}) + 8D^3\tilde{V}(\mathbf{1})\cdot\mathbf{u} + \mathbf{R}_{(\boldsymbol{\sigma}^1-\mathbf{X}_{\boldsymbol{\omega}}\cdot\boldsymbol{\sigma}^0)}, \tag{B.88}$$

with

$$\mathbf{u} = \big(\mathbf{c}^0+\overline{\mathbf{X}}_{\boldsymbol{\sigma}^0}-\boldsymbol{\sigma}^0\otimes\mathbf{1}\big)^{-1}\cdot\big(\boldsymbol{\sigma}^1-\mathbf{X}_{\boldsymbol{\omega}}\cdot\boldsymbol{\sigma}^0\big). \tag{B.89}$$

A final simplification is obtained by noting that

$$\mathbf{X}_{\boldsymbol{\omega}}\mathbf{a}^0 - \mathbf{a}^0\mathbf{X}_{\boldsymbol{\omega}} = \mathbf{X}_{\boldsymbol{\omega}}\mathbf{c}^0 - \mathbf{c}^0\mathbf{X}_{\boldsymbol{\omega}} + \mathbf{X}_{\boldsymbol{\omega}}\mathbf{R}_{\boldsymbol{\sigma}^0} - \mathbf{R}_{\boldsymbol{\sigma}^0}\mathbf{X}_{\boldsymbol{\omega}}. \tag{B.90}$$

It is then readily shown that

$$\mathbf{X}_{\boldsymbol{\omega}}\mathbf{R}_{\boldsymbol{\sigma}^0} - \mathbf{R}_{\boldsymbol{\sigma}^0}\mathbf{X}_{\boldsymbol{\omega}} = \mathbf{R}_{\mathbf{X}_{\boldsymbol{\omega}}\cdot\boldsymbol{\sigma}^0}, \tag{B.91}$$

which partially cancels with the final term in eq.(B.88). Thus, our final expression for the

perturbation to the elastic tensor is

$$\begin{aligned}
\mathsf{a}^1 &= \mathsf{c}^1 + \mathsf{R}_{\boldsymbol{\sigma}^1} \\
\mathsf{c}^1 &= \mathsf{X}_{\mathbf{u}+\boldsymbol{\omega}}\mathsf{c}^0 + \mathsf{c}^0\mathsf{X}_{\mathbf{u}-\boldsymbol{\omega}} - \mathsf{c}^0\mathrm{tr}(\mathbf{u}) + 8D^3\tilde{V}(\mathbf{1})\cdot\mathbf{u} \\
\mathbf{u} &= \left(\mathsf{c}^0 + \overline{\mathsf{X}}_{\boldsymbol{\sigma}^0} - \boldsymbol{\sigma}^0\otimes\mathbf{1}\right)^{-1}\cdot\left(\boldsymbol{\sigma}^1 - \mathsf{X}_{\boldsymbol{\omega}}\cdot\boldsymbol{\sigma}^0\right).
\end{aligned} \tag{B.92}$$

Note that the arbitrary antisymmetric matrix $\boldsymbol{\omega}$ insinuates itself implicitly via the definition of $\mathbf{u}$, as well as appearing explicitly in the expression for $\mathbf{c}^1$. When the background material is isotropic $\boldsymbol{\omega}$ can be set to zero without loss of generality.

B.3.2 Isotropic, hydrostatically pre-stressed background

For a zeroth-order hydrostatic stress and elastic tensor given by

$$\begin{aligned}
\boldsymbol{\sigma}^0 &= -p^0\mathbf{1} \\
\mathbf{c}^0 &= \lambda\mathbf{1}\otimes\mathbf{1} + 2\mu\overline{\mathbf{id}},
\end{aligned} \tag{B.93}$$

the perturbation to the stress satisfies

$$\begin{aligned}
\boldsymbol{\sigma}^1 &= \left(\mathbf{c}^0 + \overline{\mathsf{X}}_{\boldsymbol{\sigma}^0} - \boldsymbol{\sigma}^0\otimes\mathbf{1}\right)\cdot\mathbf{u} \\
&= \left(\lambda\mathbf{1}\otimes\mathbf{1} + 2\mu\overline{\mathbf{id}} - 2p^0\overline{\mathbf{id}} + p^0\mathbf{1}\otimes\mathbf{1}\right)\cdot\mathbf{u} \\
&= \tilde{\lambda}\mathrm{tr}(\mathbf{u})\,\mathbf{1} + 2\tilde{\mu}\mathbf{u},
\end{aligned} \tag{B.94}$$

with

$$\tilde{\lambda} = \lambda + p^0 \tag{B.95a}$$

$$\tilde{\mu} = \mu - p^0. \tag{B.95b}$$

It follows easily that

$$\mathrm{tr}\left(\boldsymbol{\sigma}^1\right) = \left(3\tilde{\lambda} + 2\tilde{\mu}\right)\mathrm{tr}(\mathbf{u}), \tag{B.96}$$

from which

$$\mathbf{u} = \frac{1}{2\tilde{\mu}}\left[\boldsymbol{\sigma}^1 - \frac{\tilde{\lambda}}{3\tilde{\lambda} + 2\tilde{\mu}}\mathrm{tr}\left(\boldsymbol{\sigma}^1\right)\mathbf{1}\right]. \tag{B.97}$$

Next, we split the stress into its hydrostatic and deviatoric components. Writing

$$\boldsymbol{\sigma}^1 = -p^1\mathbf{1} + \boldsymbol{\tau}^1, \tag{B.98}$$

with

$$\mathrm{tr}\left(\boldsymbol{\tau}^1\right) = 0, \tag{B.99}$$

we find that

$$\mathbf{u} = -x\mathbf{1} + \frac{1}{2\tilde{\mu}}\boldsymbol{\tau}^1, \tag{B.100}$$

where we define the shorthand

$$x \equiv \frac{p^1}{3\tilde{\lambda} + 2\tilde{\mu}}. \tag{B.101}$$

Let us now turn to the expression for $\mathbf{c}^1$, which is given by

$$\mathbf{c}^1 = \mathbf{X}_\mathbf{u}\mathbf{c}^0 + \mathbf{c}^0\mathbf{X}_\mathbf{u} - \mathrm{tr}(\mathbf{u})\,\mathbf{c}^0 + 8D^3\tilde{V}(\mathbf{1})\cdot\mathbf{u} \tag{B.102}$$

in the isotropic case. For the third-derivative term, we follow the same philosophy as Murnaghan (1937), considering a Taylor-expansion of the strain-energy function $\tilde{V}$ up to third-order in the *scalar-invariants of* $\mathbf{C}$. The most general such expression is, in index-notation,

$$[8D^3\tilde{V}(\mathbf{1})]_{ijklmn}C_{ij}C_{kl}C_{mn} = \zeta_1\mathrm{tr}(\mathbf{C})^3 + 3\zeta_2\mathrm{tr}(\mathbf{C})\,\mathrm{tr}\big(\mathbf{C}^2\big) + 2\zeta_3\mathrm{tr}\big(\mathbf{C}^3\big)\,, \tag{B.103}$$

where we have defined the constants ζ_1, ζ_2 and ζ_3. This expression should be compared with Murnaghan (1937, p.250, 2nd equation from bottom), wherein the Murnaghan constants l, m and n are introduced, as well as the bottom equation of p.240 of that paper, where the scalar-invariants of a tensor are defined. Our constants ζ_1, ζ_2 and ζ_3, which we have found convenient to use when performing calculations, are equivalent to Murnaghan's with

$$\zeta_1 = 2l - 2m + n \tag{B.104a}$$

$$\zeta_2 = 2m - n \tag{B.104b}$$

$$\zeta_3 = n, \tag{B.104c}$$

and we shall simply refer to the $\{\zeta_i\}$ as 'the Murnaghan constants'. Using our operator notation, the expression for the third-derivative term in $\mathbf{c}^1$ is

$$8D^3\tilde{V}(\mathbf{1})\cdot\mathbf{u} = \zeta_1\mathrm{tr}(\mathbf{u})\,\mathbf{1}\otimes\mathbf{1} + \zeta_2\mathrm{tr}(\mathbf{u})\,\overline{\mathbf{id}} + \zeta_2(\mathbf{1}\otimes\mathbf{u} + \mathbf{u}\otimes\mathbf{1}) + \zeta_3\overline{\mathbf{X}}_\mathbf{u}, \tag{B.105}$$

where we have used bars to mark symmetrisation of certain operators (see eq.B.32). With $\mathbf{c}^0$ given above, and bearing in mind that

$$\mathbf{X}_\mathbf{u}(\mathbf{1}\otimes\mathbf{1}) = 2\mathbf{u}\otimes\mathbf{1}, \tag{B.106}$$

$$\mathbf{X}_\mathbf{u}\overline{\mathbf{id}} = \overline{\mathbf{X}}_\mathbf{u}, \tag{B.107}$$

we obtain

$$\mathbf{c}^1 = (\zeta_1 - \lambda)\,\mathrm{tr}(\mathbf{u})\,\mathbf{1}\otimes\mathbf{1} + (\zeta_2 - 2\mu)\,\mathrm{tr}(\mathbf{u})\,\overline{\mathbf{id}} + (2\lambda + \zeta_2)(\mathbf{1}\otimes\mathbf{u} + \mathbf{u}\otimes\mathbf{1}) + (4\mu + \zeta_3)\,\overline{\mathbf{X}}_\mathbf{u}. \tag{B.108}$$

We can now substitute in our expression for $\mathbf{u}$ in terms of p^1 and $\boldsymbol{\tau}^1$, yielding

$$\begin{aligned}\mathsf{c}^1 = &-\frac{\lambda+3\zeta_1+2\zeta_2}{3\lambda+2\mu+p^0}p^1\mathbf{1}\otimes\mathbf{1} - \frac{2\mu+3\zeta_2+2\zeta_3}{3\lambda+2\mu+p^0}p^1\overline{\mathsf{id}} \\ &+ \frac{2\lambda+\zeta_2}{2(\mu-p^0)}\big(\mathbf{1}\otimes\boldsymbol{\tau}^1+\boldsymbol{\tau}^1\otimes\mathbf{1}\big) + \frac{4\mu+\zeta_3}{2(\mu-p^0)}\overline{\mathsf{X}}_{\boldsymbol{\tau}^1}.\end{aligned} \tag{B.109}$$

With this, we may write the perturbation to first elastic tensor as

$$\mathsf{a}^1 = cp^1\mathbf{1}\otimes\mathbf{1} + 2dp^1\overline{\mathsf{id}} + a\big(\mathbf{1}\otimes\boldsymbol{\tau}^1+\boldsymbol{\tau}^1\otimes\mathbf{1}\big) + 2b\overline{\mathsf{X}}_{\boldsymbol{\tau}^1} - p^1\mathsf{id} + \mathsf{R}_{\boldsymbol{\tau}^1}, \tag{B.110}$$

where a, b, c and d are given in terms of the Murnaghan constants as

$$a \equiv \frac{\lambda+\frac{1}{2}\zeta_2}{\mu-p^0} \tag{B.111}$$

$$b \equiv \frac{\mu+\frac{1}{4}\zeta_3}{\mu-p^0} \tag{B.112}$$

$$c \equiv -\frac{\lambda+3\zeta_1+2\zeta_2}{3\kappa+p^0} \tag{B.113}$$

$$d \equiv -\frac{\mu+\frac{3}{2}\zeta_2+\zeta_3}{3\kappa+p^0}. \tag{B.114}$$

The first elastic tensor is written in index notation as

$$\begin{aligned}\mathsf{a}_{ijkl} = &\left(\kappa-\frac{2}{3}\mu+p^1c\right)\delta_{ij}\delta_{kl} + \big(\mu+p^1d\big)\big(\delta_{ik}\delta_{jl}+\delta_{il}\delta_{jk}\big) - \big(p^0+p^1\big)\,\delta_{ik}\delta_{jl} \\ &+ a\big(\delta_{ij}\tau^1_{kl}+\delta_{kl}\tau^1_{ij}\big) + b\big(\delta_{ik}\tau^1_{jl}+\delta_{jl}\tau^1_{ik}+\delta_{il}\tau^1_{jk}+\delta_{jk}\tau^1_{il}\big) + \delta_{ik}\tau^1_{jl}.\end{aligned} \tag{B.115}$$

B.3.3 Transversely-isotropic, 'quasi-hydrostatically' pre-stressed background

The transversely-isotropic calculation is more intricate than the isotropic one for a number of reasons. Firstly, and perhaps most simply remedied, we can no longer ignore the arbitrary antisymmetric matrix $\boldsymbol{\omega}$. Secondly, the stress-strain relationship

$$\mathbf{u} = \big(\mathbf{c}^0 + \overline{\mathsf{X}}_{\boldsymbol{\sigma}^0} - \boldsymbol{\sigma}^0\otimes\mathbf{1}\big)^{-1}\cdot\big(\boldsymbol{\sigma}^1 - \mathsf{X}_{\boldsymbol{\omega}}\cdot\boldsymbol{\sigma}^0\big) \tag{B.116}$$

is not as easily inverted for a transversely-isotropic elastic tensor. Thirdly, there are many more terms to keep track of.

Let us begin by recalling the stress-free transversely-isotropic elastic-tensor given in eq.(3.148):

$$\begin{aligned}\mathsf{a}_{ijkl} = \mathsf{c}_{ijkl} = &\lambda\delta_{ij}\delta_{kl} + \mu(\delta_{ik}\delta_{jl}+\delta_{il}\delta_{jk}) + 8\gamma\nu_i\nu_j\nu_k\nu_l \\ &+ 4\beta(\nu_i\nu_j\delta_{kl}+\delta_{ij}\nu_k\nu_l) - \alpha(\nu_i\nu_k\delta_{jl}+\nu_j\nu_k\delta_{il}+\nu_j\nu_l\delta_{ik}+\nu_i\nu_l\delta_{jk})\,.\end{aligned} \tag{B.117}$$

For the remainder of the calculation we will switch to our 'operator-based' notation. We also introduce a shorthand that is standard in many areas of physics, whereby a symmetric expression

is written as

$$(\text{symmetric object}) = (\text{not-necessarily-symmetric object}) + h.c., \tag{B.118}$$

an example being

$$\left(\mathbf{1} \otimes \boldsymbol{\tau}^1 + \boldsymbol{\tau}^1 \otimes \mathbf{1}\right) = \mathbf{1} \otimes \boldsymbol{\tau}^1 + h.c.. \tag{B.119}$$

It will allow us to avoid significant clutter later on. (Here, *h.c.* technically stands for 'hermitian conjugate'.) We can now rewrite the zeroth-order elastic tensor as

$$\mathbf{c}^0 = \lambda \mathbf{1} \otimes \mathbf{1} + 2\mu \overline{\mathbf{id}} + 8\gamma \mathbf{N} \otimes \mathbf{N} + 4\beta(\mathbf{1} \otimes \mathbf{N} + h.c.) - 2\alpha \overline{\mathbf{X}}_{\mathbf{N}}, \tag{B.120}$$

and the pre-stress (eq.3.151) as

$$\boldsymbol{\sigma}^0 = -\left(p^0 + \frac{q^0}{3}\right) \mathbf{1} + q^0 \mathbf{N}. \tag{B.121}$$

$\mathbf{N}$ satisfies the relations

$$\mathrm{tr}(\mathbf{N}) = 1, \tag{B.122}$$

and

$$\mathbf{N}^n = \mathbf{N} \tag{B.123}$$

for positive integer n, from which it follows by induction that

$$\mathbf{X}_{\mathbf{N}}^n = \mathbf{X}_{\mathbf{N}} + (2^n - 2)\, \mathbf{N} \otimes \mathbf{N}. \tag{B.124}$$

It is useful to note that

$$\overline{\mathbf{X}}_{\boldsymbol{\sigma}^0} - \boldsymbol{\sigma}^0 \otimes \mathbf{1} = -2\left(p^0 + \frac{q^0}{3}\right) \overline{\mathbf{id}} + q^0 \overline{\mathbf{X}}_{\mathbf{N}} + \left(p^0 + \frac{q^0}{3}\right) \mathbf{1} \otimes \mathbf{1} - q^0 \mathbf{N} \otimes \mathbf{1}, \tag{B.125}$$

for now we can rewrite the stress-strain relationship (eq.B.116) as

$$\begin{aligned} \boldsymbol{\sigma}^1 - \mathbf{X}_{\boldsymbol{\omega}} \cdot \boldsymbol{\sigma}^0 &= \left[\mathbf{c}^0 - 2\left(p^0 + \frac{q^0}{3}\right) \overline{\mathbf{id}} + q^0 \overline{\mathbf{X}}_{\mathbf{N}} + \left(p^0 + \frac{q^0}{3}\right) \mathbf{1} \otimes \mathbf{1} - q^0 \mathbf{N} \otimes \mathbf{1}\right] \cdot \mathbf{u} \\ &= \tilde{\lambda} \mathrm{tr}(\mathbf{u})\, \mathbf{1} + 2\tilde{\mu} \mathbf{u} + 8\tilde{\gamma} \langle \mathbf{N}, \mathbf{u} \rangle\, \mathbf{N} - 2\tilde{\alpha} \overline{\mathbf{X}}_{\mathbf{N}} \cdot \mathbf{u} + 4\tilde{\beta} \langle \mathbf{N}, \mathbf{u} \rangle\, \mathbf{1} + 4\tilde{\beta}' \mathrm{tr}(\mathbf{u})\, \mathbf{N}, \end{aligned} \tag{B.126}$$

with

$$\tilde{\lambda} = \lambda + p^0 + \frac{q^0}{3} \tag{B.127a}$$

$$\tilde{\mu} = \mu - p^0 - \frac{q^0}{3} \tag{B.127b}$$

$$\tilde{\gamma} = \gamma \tag{B.127c}$$

$$\tilde{\alpha} = \alpha - \frac{q^0}{2} \tag{B.127d}$$

$$\tilde{\beta} = \beta \tag{B.127e}$$

$$\tilde{\beta}' = \beta - \frac{q^0}{4}. \tag{B.127f}$$

We are now in position to solve for $\mathbf{u}$ in terms of $\boldsymbol{\sigma}^1$ and $\boldsymbol{\omega}$. In the isotropic case we could invert for $\mathbf{u}$ simply by writing $\mathrm{tr}(\mathbf{u})$ in terms of $\mathrm{tr}\big(\boldsymbol{\sigma}^1\big)$. Here, by analogy, we take not only the trace of both sides, but also the inner product with $\mathbf{N}$, to find that

$$\begin{pmatrix} \mathrm{tr}\big(\boldsymbol{\sigma}^1\big) \\ \big\langle \mathbf{N}, \boldsymbol{\sigma}^1 \big\rangle \end{pmatrix} = \begin{pmatrix} 3\tilde{\lambda} + 2\tilde{\mu} + 4\tilde{\beta}' & 8\tilde{\gamma} - 4\tilde{\alpha} + 12\tilde{\beta} \\ \tilde{\lambda} + 4\tilde{\beta}' & 2\tilde{\mu} + 8\tilde{\gamma} - 4\tilde{\alpha} + 4\tilde{\beta} \end{pmatrix} \begin{pmatrix} \mathrm{tr}(\mathbf{u}) \\ \langle \mathbf{N}, \mathbf{u} \rangle \end{pmatrix}. \tag{B.128}$$

Note that $\boldsymbol{\omega}$ is not present here because

$$\mathrm{tr}\big(\mathbf{X}_{\boldsymbol{\omega}} \cdot \boldsymbol{\sigma}^0\big) = \big\langle \mathbf{1}, \mathbf{X}_{\boldsymbol{\omega}} \cdot \boldsymbol{\sigma}^0 \big\rangle = \big\langle \mathbf{X}_{\boldsymbol{\omega}}^T \cdot \mathbf{1}, \boldsymbol{\sigma}^0 \big\rangle, \tag{B.129}$$

which vanishes due to the antisymmetry of $\boldsymbol{\omega}$. By the same token,

$$\big\langle \mathbf{N}, \mathbf{X}_{\boldsymbol{\omega}} \cdot \boldsymbol{\sigma}^0 \big\rangle = -\left(p^0 + \frac{q^0}{3}\right) \langle \mathbf{N}, \mathbf{X}_{\boldsymbol{\omega}} \cdot \mathbf{1} \rangle + q^0 \langle \mathbf{N}, \mathbf{X}_{\boldsymbol{\omega}} \cdot \mathbf{N} \rangle = 0, \tag{B.130}$$

with the second term vanishing due to the antisymmetry of the operator $\mathbf{X}_{\boldsymbol{\omega}}$ (which obviously follows from that of $\boldsymbol{\omega}$). Thus, both $\mathrm{tr}(\mathbf{u})$ and $\langle \mathbf{N}, \mathbf{u} \rangle$ can be written in terms of known quantities wherever they appear.

Now, in a further step reminiscent of the isotropic case, we move most of the terms in eq.(B.126) over to the left hand side, giving

$$2\tilde{\mu}\mathbf{u} - 2\tilde{\alpha}\mathbf{X}_{\mathbf{N}} \cdot \mathbf{u} = 2\tilde{\mu}\boldsymbol{\Sigma}', \tag{B.131}$$

where $\boldsymbol{\Sigma}'$ is a shorthand defined as

$$\boldsymbol{\Sigma}' = \frac{1}{2\tilde{\mu}} \Big[\boldsymbol{\sigma}^1 - \mathbf{X}_{\boldsymbol{\omega}} \cdot \boldsymbol{\sigma}^0 - \tilde{\eta}\mathbf{1} - \tilde{\theta}\mathbf{N} \Big], \tag{B.132}$$

with

$$\begin{pmatrix} \tilde{\eta} \\ \tilde{\theta} \end{pmatrix} = \begin{pmatrix} \tilde{\lambda} & 4\tilde{\beta} \\ 4\tilde{\beta}' & 8\tilde{\gamma} \end{pmatrix} \begin{pmatrix} \mathrm{tr}(\mathbf{u}) \\ \langle \mathbf{N}, \mathbf{u} \rangle \end{pmatrix}. \tag{B.133}$$

We are left to solve the equation

$$\left(\mathbf{id} - \frac{\tilde{\alpha}}{\tilde{\mu}}\mathbf{X_N}\right) \cdot \mathbf{u} = \boldsymbol{\Sigma}'. \tag{B.134}$$

It is readily verified that the necessary inverse operator is

$$\left(\mathbf{id} - \frac{\tilde{\alpha}}{\tilde{\mu}}\mathbf{X_N}\right)^{-1} = \mathbf{id} + \tilde{P}\mathbf{X_N} + \tilde{Q}\mathbf{N} \otimes \mathbf{N}, \tag{B.135}$$

with

$$\tilde{P} = \frac{\frac{\tilde{\alpha}}{\tilde{\mu}}}{1 - \frac{\tilde{\alpha}}{\tilde{\mu}}} \tag{B.136a}$$

$$\tilde{Q} = \frac{2\frac{\tilde{\alpha}}{\tilde{\mu}}}{1 - 2\frac{\tilde{\alpha}}{\tilde{\mu}}}\tilde{P}, \tag{B.136b}$$

from which it follows that

$$\mathbf{u} = \boldsymbol{\Sigma}' + \tilde{P}\mathbf{X_N} \cdot \boldsymbol{\Sigma}' + \tilde{Q}\langle \mathbf{N}, \boldsymbol{\Sigma}' \rangle \, \mathbf{N}. \tag{B.137}$$

This procedure seems to break down when $\tilde{\mu}$ equals $\tilde{\alpha}$ or $2\tilde{\alpha}$, but the physical significance of these cases is not yet clear to the present authors. From here, with the help of the identity

$$\mathbf{X_N}\mathbf{X}_{\boldsymbol{\omega}} \cdot \mathbf{N} = \mathbf{X}_{\boldsymbol{\omega}} \cdot \mathbf{N}, \tag{B.138}$$

it is a matter of relatively straightforward algebra to find that

$$2\tilde{\mu}\mathbf{u} = \boldsymbol{\sigma}^1 - \tilde{\eta}\mathbf{1} + \tilde{P}\mathbf{X_N} \cdot \boldsymbol{\sigma}^1 + \tilde{R}\mathbf{N} - q^0(1 + \tilde{P})\mathbf{X}_{\boldsymbol{\omega}} \cdot \mathbf{N}, \tag{B.139}$$

with

$$\tilde{R} = \tilde{Q}\Big(\langle \mathbf{N}, \boldsymbol{\sigma}^1 \rangle - \tilde{\eta} - \tilde{\theta}\Big) - \tilde{\theta} - 2\tilde{P}\Big(\tilde{\eta} + \tilde{\theta}\Big). \tag{B.140}$$

We now have an expression for $\mathbf{u}$ in terms of:

(1). the transversely-isotropic constants λ, μ, α, β and γ, as well as $\boldsymbol{\nu}$;

(2). the constants p^0 and q^0 which define the equilibrium stress-state;

(3). the perturbation to the stress $\boldsymbol{\sigma}^1$;

(4). an antisymmetric matrix $\boldsymbol{\omega}$ 'pointing' in an arbitrary direction in the plane perpendicular to the unperturbed symmetry-axis.

This is to be substituted into the expression

$$\mathbf{c}^1 = \mathbf{X}_{\mathbf{u}+\boldsymbol{\omega}}\mathbf{c}^0 + \mathbf{c}^0\mathbf{X}_{\mathbf{u}-\boldsymbol{\omega}} - \mathbf{c}^0\mathrm{tr}(\mathbf{u}) + 8D^3\tilde{V}(\mathbf{1}) \cdot \mathbf{u} \tag{B.141}$$

for the perturbed elastic tensor.

In order to make progress we must parametrise the third derivatives of the transversely-isotropic strain-energy function. As stated in the main text, such a strain-energy function will generally depend on $\mathbf{C}$ not only through the invariants I_1, I_2 and I_3 defined in eq.(3.131), but also through the terms (e.g. Holzapfel, 2000)

$$\langle \boldsymbol{\nu}, \mathbf{C}\cdot\boldsymbol{\nu}\rangle = \langle \mathbf{N}, \mathbf{C}\rangle \tag{B.142}$$

$$\langle \boldsymbol{\nu}, \mathbf{C}^2\cdot\boldsymbol{\nu}\rangle = \langle \mathbf{N}, \mathbf{C}^2\rangle = \frac{1}{2}\langle \mathbf{C}, \mathbf{X}_{\mathbf{N}}\cdot\mathbf{C}\rangle\,. \tag{B.143}$$

The third order terms of $\tilde{V}$'s Taylor-series about the identity therefore satisfy

$$\begin{aligned}[8D^3\tilde{V}(\mathbf{1})]_{ijklmn}C_{ij}C_{kl}C_{mn} = {}& \zeta_1\mathrm{tr}(\mathbf{C})^3 + 3\zeta_2\mathrm{tr}(\mathbf{C})\,\mathrm{tr}\big(\mathbf{C}^2\big) + 2\zeta_3\mathrm{tr}\big(\mathbf{C}^3\big)\\ &+ 3\zeta_4\mathrm{tr}(\mathbf{C})\langle\mathbf{C},\mathbf{N}\rangle^2 + 3\zeta_5\mathrm{tr}(\mathbf{C})\langle\mathbf{C},\mathbf{X}_{\mathbf{N}}\cdot\mathbf{C}\rangle\\ &+ 3\zeta_6\mathrm{tr}\big(\mathbf{C}^2\big)\langle\mathbf{C},\mathbf{N}\rangle + 3\zeta_7\langle\mathbf{C},\mathbf{N}\rangle\langle\mathbf{C},\mathbf{X}_{\mathbf{N}}\cdot\mathbf{C}\rangle\\ &+ 3\zeta_8\mathrm{tr}(\mathbf{C})^2\langle\mathbf{C},\mathbf{N}\rangle + \zeta_9\langle\mathbf{C},\mathbf{N}\rangle^3\,,\end{aligned} \tag{B.144}$$

for some material-dependent constants $\{\zeta_i\}$, so that the corresponding term in the elastic tensor is

$$\begin{aligned}8D^3\tilde{V}(\mathbf{1})\cdot\mathbf{u} = {}& \zeta_1\mathrm{tr}(\mathbf{u})\,\mathbf{1}\otimes\mathbf{1}\\ &+ \zeta_2\big[\mathrm{tr}(\mathbf{u})\,\overline{\mathbf{id}} + (\mathbf{1}\otimes\mathbf{u} + h.c.)\big]\\ &+ \zeta_3\overline{\mathbf{X}}_{\mathbf{u}}\\ &+ \zeta_4[\langle\mathbf{N},\mathbf{u}\rangle(\mathbf{1}\otimes\mathbf{N} + h.c.) + \mathrm{tr}(\mathbf{u})\,\mathbf{N}\otimes\mathbf{N}]\\ &+ \zeta_5[\mathbf{1}\otimes(\mathbf{X}_{\mathbf{N}}\cdot\mathbf{u}) + h.c.) + \mathrm{tr}(\mathbf{u})\,\mathbf{X}_{\mathbf{N}}]\\ &+ \zeta_6[\mathbf{N}\otimes\mathbf{u} + h.c.) + \langle\mathbf{N},\mathbf{u}\rangle\,\mathbf{id}]\\ &+ \zeta_7[\mathbf{N}\otimes(\mathbf{X}_{\mathbf{N}}\cdot\mathbf{u}) + h.c.) + \langle\mathbf{N},\mathbf{u}\rangle\,\mathbf{X}_{\mathbf{N}}]\\ &+ \zeta_8[\langle\mathbf{N},\mathbf{u}\rangle\,\mathbf{1}\otimes\mathbf{1} + \mathrm{tr}(\mathbf{u})(\mathbf{1}\otimes\mathbf{N} + h.c.)]\\ &+ \zeta_9\langle\mathbf{N},\mathbf{u}\rangle\,\mathbf{N}\otimes\mathbf{N}\\ = {}& (\zeta_1\mathrm{tr}(\mathbf{u}) + \zeta_8\langle\mathbf{N},\mathbf{u}\rangle)\,\mathbf{1}\otimes\mathbf{1} + (\zeta_2\mathrm{tr}(\mathbf{u}) + \zeta_6\langle\mathbf{N},\mathbf{u}\rangle)\,\overline{\mathbf{id}} + \zeta_2(\mathbf{1}\otimes\mathbf{u} + h.c.) + \zeta_3\overline{\mathbf{X}}_{\mathbf{u}}\\ &+ (\zeta_8\mathrm{tr}(\mathbf{u}) + \zeta_4\langle\mathbf{N},\mathbf{u}\rangle)(\mathbf{1}\otimes\mathbf{N} + h.c.) + (\zeta_4\mathrm{tr}(\mathbf{u}) + \zeta_9\langle\mathbf{N},\mathbf{u}\rangle)\,\mathbf{N}\otimes\mathbf{N}\\ &+ \zeta_5[\mathbf{1}\otimes(\mathbf{X}_{\mathbf{N}}\cdot\mathbf{u}) + h.c.] + \zeta_6(\mathbf{N}\otimes\mathbf{u} + h.c.)\\ &+ \zeta_7[\mathbf{N}\otimes(\mathbf{X}_{\mathbf{N}}\cdot\mathbf{u}) + h.c.] + (\zeta_5\mathrm{tr}(\mathbf{u}) + \zeta_7\langle\mathbf{N},\mathbf{u}\rangle)\,\overline{\mathbf{X}}_{\mathbf{N}}.\end{aligned} \tag{B.145}$$

Whilst for an isotropic solid we needed three extra material-dependent constants to parametrise the third derivatives, here we need nine (see e.g. Clayton, 2011, Table A9).

With this, we are ready to write down an expression for the elastic tensor's perturbation.

Observe that

$$\mathbf{X}_{\mathbf{u}}\mathbf{c}^0 = \big(\mathbf{c}^0\mathbf{X}_{\mathbf{u}}\big)^T \tag{B.146}$$

$$\mathbf{X}_{\boldsymbol{\omega}}\mathbf{c}^0 = \big(\mathbf{c}^0\mathbf{X}_{(-\boldsymbol{\omega})}\big)^T . \tag{B.147}$$

Thus,

$$\begin{aligned}\mathbf{c}^1 = \operatorname{tr}(\mathbf{u})\big[(\zeta_1-\lambda)\,\mathbf{1}\otimes\mathbf{1} + (\zeta_2-2\mu)\,\overline{\mathbf{id}} + (\zeta_4-8\gamma)\,\mathbf{N}\otimes\mathbf{N} + (\zeta_5+2\alpha)\,\overline{\mathbf{X}}_{\mathbf{N}} + (\zeta_8-4\beta)(\mathbf{1}\otimes\mathbf{N}+h.c.)\big]\\ + \langle\mathbf{N},\mathbf{u}\rangle\big[\zeta_8\mathbf{1}\otimes\mathbf{1} + \zeta_6\overline{\mathbf{id}} + \zeta_9\mathbf{N}\otimes\mathbf{N} + \zeta_7\overline{\mathbf{X}}_{\mathbf{N}} + \zeta_4(\mathbf{1}\otimes\mathbf{N}+h.c.)\big]\\ + (\zeta_3+4\mu)\,\overline{\mathbf{X}}_{\mathbf{u}} + (\zeta_2+2\lambda)(\mathbf{1}\otimes\mathbf{u}+h.c.) + (\zeta_6+8\beta)(\mathbf{N}\otimes\mathbf{u}+h.c.)\\ + (\zeta_5+4\beta)[\mathbf{1}\otimes(\mathbf{X}_{\mathbf{N}}\cdot\mathbf{u})+h.c.] + (\zeta_7+8\gamma)[\mathbf{N}\otimes(\mathbf{X}_{\mathbf{N}}\cdot\mathbf{u})+h.c.] - 2\alpha\big(\overline{\mathbf{X}}_{\mathbf{u}}\overline{\mathbf{X}}_{\mathbf{N}}+h.c.\big)\\ + 4\mu\overline{\mathbf{X}}_{\boldsymbol{\omega}} + 8\gamma[\mathbf{N}\otimes(\mathbf{X}_{\boldsymbol{\omega}}\cdot\mathbf{N})+h.c.] + 4\beta[\mathbf{1}\otimes(\mathbf{X}_{\boldsymbol{\omega}}\cdot\mathbf{N})+h.c.] - 2\alpha\big(\overline{\mathbf{X}}_{\boldsymbol{\omega}}\overline{\mathbf{X}}_{\mathbf{N}}+h.c.\big) .\end{aligned} \tag{B.148}$$

It is now a matter of tedious algebra to complete the calculation. The nontrivial identities that we need are:

$$\mathbf{X}_{\mathbf{N}}^2 = \mathbf{X}_{\mathbf{N}} + 2\mathbf{N}\otimes\mathbf{N} \tag{B.149}$$

$$\mathbf{X}_{\mathbf{N}}\mathbf{X}_{\boldsymbol{\omega}}\cdot\mathbf{N} = \mathbf{X}_{\boldsymbol{\omega}}\cdot\mathbf{N} \tag{B.150}$$

$$\mathbf{X}_{(\mathbf{X}_{\boldsymbol{\omega}}\cdot\mathbf{N})} = \mathbf{X}_{\boldsymbol{\omega}}\mathbf{X}_{\mathbf{N}} + h.c. \tag{B.151}$$

$$\overline{\mathbf{X}}_{\mathbf{X}_{\mathbf{N}}\cdot\boldsymbol{\sigma}^1}\overline{\mathbf{X}}_{\mathbf{N}} + h.c. = \overline{\mathbf{X}}_{\mathbf{X}_{\mathbf{N}}\cdot\boldsymbol{\sigma}^1} + 2\big[\mathbf{N}\otimes\big(\mathbf{X}_{\mathbf{N}}\cdot\boldsymbol{\sigma}^1\big)+h.c.\big] + 2\big\langle\mathbf{N},\boldsymbol{\sigma}^1\big\rangle\,\overline{\mathbf{X}}_{\mathbf{N}}. \tag{B.152}$$

Finally, the perturbation to the elastic tensor is given by

$$\begin{aligned}\mathbf{c}^1 = \eta_1\mathbf{1}\otimes\mathbf{1} + \eta_2\overline{\mathbf{id}} + \eta_3\mathbf{N}\otimes\mathbf{N} + \eta_4(\mathbf{1}\otimes\mathbf{N}+h.c.) + \eta_5\overline{\mathbf{X}}_{\mathbf{N}}\\ + \eta_6\overline{\mathbf{X}}_{\boldsymbol{\sigma}^1} + \eta_7\big(\mathbf{1}\otimes\boldsymbol{\sigma}^1+h.c.\big) + \eta_8\big(\mathbf{N}\otimes\boldsymbol{\sigma}^1+h.c.\big) + \eta_9\big[\mathbf{1}\otimes\big(\mathbf{X}_{\mathbf{N}}\cdot\boldsymbol{\sigma}^1\big)+h.c.\big]\\ + \eta_{10}\big[\mathbf{N}\otimes\big(\mathbf{X}_{\mathbf{N}}\cdot\boldsymbol{\sigma}^1\big)+h.c.\big] + \eta_{11}\overline{\mathbf{X}}_{\mathbf{X}_{\mathbf{N}}\cdot\boldsymbol{\sigma}^1} + \eta_{12}\big(\overline{\mathbf{X}}_{\boldsymbol{\sigma}^1}\overline{\mathbf{X}}_{\mathbf{N}}+h.c.\big)\\ + \eta_{13}\overline{\mathbf{X}}_{\boldsymbol{\omega}} + \eta_{14}[\mathbf{1}\otimes(\mathbf{X}_{\boldsymbol{\omega}}\cdot\mathbf{N})+h.c.] + \eta_{15}[\mathbf{N}\otimes(\mathbf{X}_{\boldsymbol{\omega}}\cdot\mathbf{N})+h.c.] + \eta_{16}\big(\overline{\mathbf{X}}_{\boldsymbol{\omega}}\overline{\mathbf{X}}_{\mathbf{N}}+h.c.\big) .\end{aligned} \tag{B.153}$$

The $\{\eta_i\}$ are defined as

$$2\tilde{\mu}\eta_1 = 2\tilde{\mu}[(\zeta_1-\lambda)\operatorname{tr}(\mathbf{u}) + \zeta_8\langle\mathbf{N},\mathbf{u}\rangle] - [2\tilde{\eta}(\zeta_2+2\lambda)] \tag{B.154a}$$

$$2\tilde{\mu}\eta_2 = 2\tilde{\mu}[(\zeta_2-2\mu)\operatorname{tr}(\mathbf{u}) + \zeta_6\langle\mathbf{N},\mathbf{u}\rangle] - [2\tilde{\eta}(\zeta_3+4\mu)] \tag{B.154b}$$

$$\begin{aligned}2\tilde{\mu}\eta_3 = 2\tilde{\mu}[(\zeta_4-8\gamma)\operatorname{tr}(\mathbf{u}) + \zeta_9\langle\mathbf{N},\mathbf{u}\rangle]\\ + \Big[2\tilde{R}(\zeta_6+8\beta) - 8\alpha\tilde{R} + \Big(4\tilde{R} - 4\tilde{\eta} + 4\tilde{P}\big\langle\mathbf{N},\boldsymbol{\sigma}^1\big\rangle\Big)(\zeta_7+8\gamma)\Big]\end{aligned} \tag{B.154c}$$

$$\begin{aligned}2\tilde{\mu}\eta_4 = 2\tilde{\mu}[(\zeta_8-4\beta)\operatorname{tr}(\mathbf{u}) + \zeta_4\langle\mathbf{N},\mathbf{u}\rangle]\\ + \Big[\tilde{R}(\zeta_2+2\lambda) - \tilde{\eta}(\zeta_6+8\beta) + \Big(2\tilde{P}\big\langle\mathbf{N},\boldsymbol{\sigma}^1\big\rangle + 2\tilde{R} - 2\tilde{\eta}\Big)(\zeta_5+4\beta)\Big]\end{aligned} \tag{B.154d}$$

$$2\tilde{\mu}\eta_5 = 2\tilde{\mu}[(\zeta_5+2\alpha)\operatorname{tr}(\mathbf{u}) + \zeta_7\langle\mathbf{N},\mathbf{u}\rangle] + \Big[\tilde{R}(\zeta_3+4\mu) - 2\alpha\Big(2\tilde{R} - 4\tilde{\eta} + 2\tilde{P}\big\langle\mathbf{N},\boldsymbol{\sigma}^1\big\rangle\Big)\Big] \tag{B.154e}$$

$$2\tilde{\mu}\eta_6 = \zeta_3 + 4\mu \tag{B.154f}$$

$$2\tilde{\mu}\eta_7 = \zeta_2 + 2\lambda \tag{B.154g}$$

$$2\tilde{\mu}\eta_8 = \zeta_6 + 8\beta \tag{B.154h}$$

$$2\tilde{\mu}\eta_9 = \tilde{P}(\zeta_2 + 2\lambda) + \Big(1 + \tilde{P}\Big)(\zeta_5 + 4\beta) \tag{B.154i}$$

$$2\tilde{\mu}\eta_{10} = \tilde{P}(\zeta_6 + 8\beta - 4\alpha) + \Big(1 + \tilde{P}\Big)(\zeta_7 + 8\gamma) \tag{B.154j}$$

$$2\tilde{\mu}\eta_{11} = \tilde{P}(\zeta_3 + 4\mu - 2\alpha) \tag{B.154k}$$

$$2\tilde{\mu}\eta_{12} = -2\alpha \tag{B.154l}$$

$$2\tilde{\mu}\eta_{13} = 8\mu\tilde{\mu} \tag{B.154m}$$

$$2\tilde{\mu}\eta_{14} = 8\beta\tilde{\mu} - q^0\Big(1 + \tilde{P}\Big)(\zeta_2 + \zeta_5 + 2\lambda + 4\beta) \tag{B.154n}$$

$$2\tilde{\mu}\eta_{15} = 16\gamma\tilde{\mu} - q^0\Big(1 + \tilde{P}\Big)(\zeta_6 + \zeta_7 - 4\alpha + 8\beta + 8\gamma) \tag{B.154o}$$

$$2\tilde{\mu}\eta_{16} = -\Big[4\alpha\tilde{\mu} + q^0\Big(1 + \tilde{P}\Big)(\zeta_3 + 4\mu - 2\alpha)\Big], \tag{B.154p}$$

definitions which should in turn be combined with the earlier definitions eqs. (B.127), (B.128), (B.133), (B.136), (B.140) and (B.144). The perturbation to the elastic tensor is given in terms of

(1). the transversely-isotropic constants λ, μ, α, β and γ, as well as $\boldsymbol{\nu}$;

(2). the constants p^0 and q^0 which parametrise the zeroth-order equilibrium stress;

(3). the nine constants $\{\zeta_i\}$ defined in eq.(B.144), which parametrise the third derivatives of a transversely-isotropic strain-energy function about equilibrium;

(4). the small induced stress $\boldsymbol{\sigma}^1$;

(5). the arbitrary 2-parameter antisymmetric matrix $\boldsymbol{\omega}$.

B.4 The isotropic elastic moduli, their pressure-derivatives, and wave speeds

Working under the assumption of isotropic background states, this section compares our linearised theory with the theories of Dahlen (1972b) and Tromp & Trampert (2018). We demonstrate that the theories are compatible for certain choices of parameter and, moreover, that our parameters c and d are not readily comparable with Tromp & Trampert's κ' and μ'. For this section we will work in the notation of Section 4.1, using the Lamé parameter λ interchangeably with κ.

Recall from Section 4.1 that the most general isotropic elastic tensor $\boldsymbol{\Xi}$ is written, upon inducing an incremental stress, as

$$\begin{aligned}\Xi_{ijkl} = &\left(\kappa - \frac{2}{3}\mu + \Delta p^0 c\right)\delta_{ij}\delta_{kl} + \big(\mu + \Delta p^0 d\big)(\delta_{ik}\delta_{jl} + \delta_{il}\delta_{jk}) \\ &+ a\big(\delta_{ij}\Delta\tau^0_{kl} + \delta_{kl}\Delta\tau^0_{ij}\big) + b\big(\delta_{ik}\Delta\tau^0_{jl} + \delta_{il}\Delta\tau^0_{jk} + \delta_{jk}\Delta\tau^0_{il} + \delta_{jl}\Delta\tau^0_{ik}\big)\end{aligned} \tag{B.155}$$

and that we then obtained Tromp & Trampert's $\boldsymbol{\Xi}$ by setting

$$c = -2a \tag{B.156}$$

$$d = -2b \tag{B.157}$$

and

$$a = \frac{1}{2} + \frac{1}{3}\mu' - \frac{1}{2}\kappa' \tag{B.158}$$

$$b = -\frac{1}{2} - \frac{1}{2}\mu' \tag{B.159}$$

with the constants κ' and μ' interpreted as adiabatic pressure-derivatives of the elastic moduli. These equations can be considered as a four-dimensional system

$$c = \lambda' - 1 \tag{B.160a}$$

$$d = \mu' + 1 \tag{B.160b}$$

$$c = -2a \tag{B.160c}$$

$$d = -2b \tag{B.160d}$$

parametrised by λ' and μ', where

$$\lambda' \equiv \kappa' - \frac{2}{3}\mu'. \tag{B.161}$$

But in eqs.(3.143) we showed that a, b, c and d are given in terms of the *three* Murnaghan constants. Under what conditions are the two theories compatible?

Eqs.(B.160c,B.160d) just constrain eqs.(3.143), effectively fixing two of the Murnaghan constants. Let us define two shorthands

$$y = \frac{\lambda + p^0}{\mu - p^0} \tag{B.162}$$

$$z = \frac{2\lambda + \mu + p^0}{\mu - p^0}. \tag{B.163}$$

The explicit forms of eqs.(3.143) can then be used to write eqs.(B.160c,B.160d) as

$$\begin{pmatrix} 1 & -y & 0 \\ 0 & 1 & -y \end{pmatrix} \begin{pmatrix} \zeta_1 \\ \zeta_2 \\ \zeta_3 \end{pmatrix} = z \begin{pmatrix} \lambda \\ 2\mu \end{pmatrix}, \tag{B.164}$$

after which we may solve for $\zeta_{2,3}$ in terms of ζ_1, finding that

$$\begin{pmatrix} \zeta_2 \\ \zeta_3 \end{pmatrix} = \frac{1}{y^2} \begin{pmatrix} -y & 0 \\ 1 & -y \end{pmatrix} \begin{pmatrix} z & 0 & -1 \\ 0 & 2z & 0 \end{pmatrix} \begin{pmatrix} \lambda \\ \mu \\ \zeta_1 \end{pmatrix}. \tag{B.165}$$

This expression is written in a rather strange way, but we have found it highly amenable to algebraic manipulation. One free parameter, ζ_1, remains with which to satisfy eqs.(B.160a,B.160b). Using eqs.(3.143) once again, after some algebra we find from eqs.(B.160a,B.160b) that the constants λ' and μ' are given by

$$\begin{pmatrix}\lambda'\\ \mu'\end{pmatrix} = \begin{pmatrix}1\\ -1\end{pmatrix} - \frac{1}{3\kappa + p^0}\begin{pmatrix} 1-2\frac{z}{y} & 0 & 3+\frac{2}{y} \\ -\left(\frac{3}{2}y+1\right)\frac{z}{y^2} & 1-2\frac{z}{y} & \left(\frac{3}{2}y+1\right)\frac{1}{y^2}\end{pmatrix}\begin{pmatrix}\lambda\\ \mu\\ \zeta_1\end{pmatrix}. \tag{B.166}$$

As ζ_1 is arbitrary, this shows that there exists a one-parameter family of values of λ' and μ' whereby both eqs.(B.160) and eqs.(3.143) are satisfied and Tromp & Trampert's theory thus agrees with ours. Moreover, this will hold for any physically allowed λ, μ and p^0. It formalises our earlier assertion that their theory is valid for a certain class of isotropic materials. The theory of Dahlen (1972b) is formally obtained from that of Tromp & Trampert (2018) by setting $\kappa' = \mu' = 0$. However, now that two free parameters have been removed, eq.(B.166) reduces to the expression

$$f\big(\lambda, \mu, p^0\big) = 0 \tag{B.167}$$

for some real-valued function f, and the elastic moduli themselves are constrained.

One small puzzle remains. From looking at eq.(B.155), our two constants c and d might be thought to represent the pressure-derivatives of the elastic moduli, but eqs.(B.160a,B.160b) make clear that they cannot be equivalent to Tromp & Trampert's κ' and μ'. In order to better understand this discrepancy we should focus on the pressure dependence of P- and S-wave speeds. We can do that by neglecting deviatoric stress increments and considering the Christoffel operator (defined in eq.3.56 and written here with $\hat{\mathbf{k}}$ substituted for $\hat{\mathbf{p}}$)

$$\rho B_{jl} = \left[\left(\kappa + \frac{1}{3}\mu\right) + \Delta p^0(c+d)\right]\hat{k}_j\hat{k}_l + \big[\mu - \Delta p^0(1-d)\big]\,\delta_{jl} + (\text{deviatoric})\,. \tag{B.168}$$

This gives wave speeds of

$$\rho c_P^2 = \big[\big(\lambda + \Delta p^0 c\big) + 2\big(\mu + \Delta p^0 d\big)\big] - \Delta p^0 \tag{B.169}$$

$$\rho c_S^2 = \big[\mu + \Delta p^0 d\big] - \Delta p^0. \tag{B.170}$$

The wave speeds' dependence on Δp^0 comes not only from terms in c and d that belong to $\boldsymbol{\Xi}$, but also from the term $\Delta T^0_{ik}\delta_{jl}$ that is added to $\boldsymbol{\Xi}$ in order to form $\boldsymbol{\Lambda}$ (and hence the Christoffel operator). The construction of the theories of Dahlen, Tromp and Trampert is such that the hydrostatic contribution of $\Delta T^0_{ik}\delta_{jl}$ is always cancelled out. For example, the components of Tromp & Trampert's $\boldsymbol{\Lambda}$ are found to be

$$\Lambda_{ijkl} = \big(\lambda + \Delta p^0\lambda'\big)\,\delta_{ij}\delta_{kl} + \big(\mu + \Delta p^0\mu'\big)(\delta_{ik}\delta_{jl} + \delta_{il}\delta_{jk}) + \Delta p^0(\delta_{il}\delta_{jk} - \delta_{ij}\delta_{kl}) + (\text{deviatoric})\,. \tag{B.171}$$

The third term vanishes upon contraction with $\hat{k}_i\hat{k}_k$ and can therefore be neglected when forming the Christoffel operator. This leaves us with the neatly defined elastic moduli and derivatives within the first two terms, and we ultimately arrive at Tromp & Trampert's "quasi-classical" expressions for the wave speeds

$$\rho c_P^2 = \left(\lambda + \lambda' \Delta p^0\right) + 2\left(\mu + \mu' \Delta p^0\right) \tag{B.172}$$

$$\rho c_S^2 = \left(\mu + \mu' \Delta p^0\right). \tag{B.173}$$

In effect, by using this definition of the elastic moduli's pressure derivatives one is "redefining" the elastic moduli in order to subsume the pressure-dependence introduced by $\Delta T^0_{ik}\delta_{jl}$.

Bibliography

Agnew, D., 2015. Earth tides, in *Treatise on Geophysics*, pp. 151–178, Elsevier.

Akbarashrafi, F., Al-Attar, D., Deuss, A., Trampert, J., & Valentine, A. P., 2017. Exact free oscillation spectra, splitting functions and the resolvability of earth's density structure, *Geophysical Journal International*, **213**(1), 58–76.

Al-Attar, D. & Crawford, O., 2016. Particle relabelling transformations in elastodynamics, *Geophysical Journal International*, **205**(1), 575–593.

Al-Attar, D. & Tromp, J., 2014. Sensitivity kernels for viscoelastic loading based on adjoint methods, *Geophysical Journal International*, **196**(1), 34–77.

Al-Attar, D. & Woodhouse, J. H., 2010. On the parametrization of equilibrium stress fields in the earth, *Geophysical Journal International*, **181**(1), 567–576.

Al-Attar, D., Woodhouse, J. H., & Deuss, A., 2012. Calculation of normal mode spectra in laterally heterogeneous earth models using an iterative direct solution method, *Geophysical Journal International*, **189**(2), 1038–1046.

Al-Attar, D., Crawford, O., Valentine, A. P., & Trampert, J., 2018. Hamilton's principle and normal mode coupling in an aspherical planet with a fluid core, *Geophysical Journal International*.

Backus, G. E., 1962. Long-wave elastic anisotropy produced by horizontal layering, *Journal of Geophysical Research*, **67**(11), 4427–4440.

Backus, G. E., 1967. Converting vector and tensor equations to scalar equations in spherical coordinates, *Geophysical Journal International*, **13**(1-3), 71–101.

Balmino, G., 1994. Gravitational potential harmonics from the shape of an homogeneous body, *Celestial Mechanics & Dynamical Astronomy*, **60**(3), 331–364.

Barnett, C. T., 1976. Theoretical modeling of the magnetic and gravitational fields of an arbitrarily shaped three-dimensional body, *GEOPHYSICS*, **41**(6), 1353–1364.

Beer, G. & Meek, J. L., 1981. "infinite domain" elements, *International Journal for Numerical Methods in Engineering*, **17**(1), 43–52.

Bender, C. M. & Orszag, S. A., 2013. *Advanced mathematical methods for scientists and engineers I: Asymptotic methods and perturbation theory*, Springer Science & Business Media.

Bettess, P., 1977. Infinite elements, *International Journal for Numerical Methods in Engineering*, **11**(1), 53–64.

Birch, F., 1952. Elasticity and constitution of the earth's interior, *Journal of Geophysical Research*, **57**(2), 227–286.

Bonet, J. & Burton, A., 1998. A simple orthotropic, transversely isotropic hyperelastic constitutive equation for large strain computations, *Computer Methods in Applied Mechanics and Engineering*, **162**(1-4), 151–164.

Boyd, J. P., 2001. *Chebyshev and Fourier spectral methods*, Courier Corporation.

Buffett, B. A., 2010. Tidal dissipation and the strength of the earth's internal magnetic field, *Nature*, **468**(7326), 952–954.

Capdeville, Y. & Métivier, L., 2018. Elastic full waveform inversion based on the homogenization method: theoretical framework and 2-d numerical illustrations, *Geophysical Journal International*, **213**(2), 1093–1112.

Chaljub, E. & Valette, B., 2004. Spectral element modelling of three-dimensional wave propagation in a self-gravitating earth with an arbitrarily stratified outer core, *Geophysical Journal International*, **158**(1), 131–141.

Chambat, F. & Valette, B., 2005. Earth gravity up to second order in topography and density, *Physics of the Earth and Planetary Interiors*, **151**(1-2), 89–106.

Chambat, F., Ricard, Y., & Valette, B., 2010. Flattening of the earth: further from hydrostaticity than previously estimated, *Geophysical Journal International*, **183**(2), 727–732.

Clairaut, A. C., 1743. *Théorie de la figure de la terre, tirée des principes de l'hydrostatique*, chez David fils, libraire, ruë Saint-Jacques à la plume d'or.

Clayton, J. D., 2011. *Nonlinear Mechanics of Crystals*, Springer Netherlands.

Coleman, B. D. & Noll, W., 1961. Foundations of linear viscoelasticity, *Reviews of Modern Physics*, **33**(2), 239–249.

Crawford, O., 2018. *On the Viscoelastic Deformation of the Earth*, Ph.D. thesis, University of Cambridge.

Crawford, O., Al-Attar, D., Tromp, J., & Mitrovica, J. X., 2016. Forward and inverse modelling of post-seismic deformation, *Geophysical Journal International*, **208**(2), 845–876.

Crawford, O., Al-Attar, D., Tromp, J., Mitrovica, J. X., Austermann, J., & Lau, H. C. P., 2018. Quantifying the sensitivity of post-glacial sea level change to laterally varying viscosity, *Geophysical Journal International*, **214**(2), 1324–1363.

Cupillard, P. & Capdeville, Y., 2018. Non-periodic homogenization of 3-d elastic media for the seismic wave equation, *Geophysical Journal International*, **213**(2), 983–1001.

Dahlen, F. & Tromp, J., 1998. *Theoretical global seismology*, Princeton university press.

Dahlen, F. A., 1972a. Elastic dislocation theory for a self-gravitating elastic configuration with an initial static stress field, *Geophysical Journal International*, **28**(4), 357–383.

Dahlen, F. A., 1972b. Elastic velocity anisotropy in the presence of an anisotropic initial stress, *Bulletin of the Seismological Society of America*, **62**(5), 1183–1193.

Dahlen, F. A., 1976. The passive influence of the oceans upon the rotation of the earth, *Geophysical Journal International*, **46**(2), 363–406.

Dahlen, F. A. & Smith, M. L., 1975. The influence of rotation on the free oscillations of the earth, *Philosophical Transactions of the Royal Society A: Mathematical, Physical and Engineering Sciences*, **279**(1292), 583–624.

Dehant, V., 2013. Core undertones in an elliptical uniformly rotating earth, *Structure and Dynamics of Earth's Deep Interior*, pp. 29–34.

Dehant, V. & Mathews, P. M., 2015. *Precession, nutation and wobble of the Earth*, Cambridge University Press.

Destrade, M. & Ogden, R. W., 2012. On stress-dependent elastic moduli and wave speeds, *IMA Journal of Applied Mathematics*, **78**(5), 965–997.

Dziewonski, A. M. & Anderson, D. L., 1981. Preliminary reference earth model, *Physics of the Earth and Planetary Interiors*, **25**(4), 297–356.

Egle, D. M. & Bray, D. E., 1976. Measurement of acoustoelastic and third-order elastic constants for rail steel, *The Journal of the Acoustical Society of America*, **60**(3), 741–744.

Friedlander, F. G., Friedlander, G., Joshi, M. S., Joshi, M., & Joshi, M. C., 1998. *Introduction to the Theory of Distributions*, Cambridge University Press.

Fu, Y., Argus, D. F., Freymueller, J. T., & Heflin, M. B., 2013. Horizontal motion in elastic response to seasonal loading of rain water in the amazon basin and monsoon water in southeast asia observed by GPS and inferred from GRACE, *Geophysical Research Letters*, **40**(23), 6048–6053.

Garnero, E. J., McNamara, A. K., & Shim, S.-H., 2016. Continent-sized anomalous zones with low seismic velocity at the base of earth's mantle, *Nature Geoscience*, **9**(7), 481–489.

Gharti, H. N. & Tromp, J., 2017. A spectral-infinite-element solution of poisson's equation: an application to self gravity.

Gharti, H. N., Tromp, J., & Zampini, S., 2018. Spectral-infinite-element simulations of gravity anomalies, *Geophysical Journal International*, **215**(2), 1098–1117.

Gharti, H. N., Langer, L., & Tromp, J., 2019. Spectral-infinite-element simulations of earthquake-induced gravity perturbations, *Geophysical Journal International*, **217**(1), 451–468.

Giardini, D., Li, X.-D., & Woodhouse, J. H., 1987. Three-dimensional structure of the earth from splitting in free-oscillation spectra, *Nature*, **325**(6103), 405–411.

Gower, A. L., Shearer, T., & Ciarletta, P., 2017. A new restriction for initially stressed elastic solids, *The Quarterly Journal of Mechanics and Applied Mathematics*, **70**(4), 455–478.

Gurtin, M. E., Fried, E., & Anand, L., 2010. *The mechanics and thermodynamics of continua*, Cambridge University Press.

Gutenberg, B., 1913. Uber die konstitution des erdinnern, erschlossen aus erdbebenbeobachtungen, *Phys. Z*, **14**, 1217–1218.

Hara, T., Tsuboi, S., & Geller, R. J., 1993. Inversion for laterally heterogeneous upper mantle s-wave velocity structure using iterative waveform inversion, *Geophysical Journal International*, **115**(3), 667–698.

Holzapfel, G., 2000. *Nonlinear Solid Mechanics: A Continuum Approach for Engineering*, John Wiley and Sons, Chichester, UK.

Houser, C., Masters, G., Shearer, P., & Laske, G., 2008. Shear and compressional velocity models of the mantle from cluster analysis of long-period waveforms, *Geophysical Journal International*, **174**(1), 195–212.

Hubbard, W. B., 2012. High-precision maclaurin-based models of rotating liquid planets, *The Astrophysical Journal*, **756**(1), L15.

Hubbard, W. B., 2013. Concentric maclaurin spheroid models of rotating liquid planets, *The Astrophysical Journal*, **768**(1), 43.

Hughes, D. S. & Kelly, J. L., 1953. Second-order elastic deformation of solids, *Physical Review*, **92**(5), 1145–1149.

Iserles, A., 2009. *A first course in the numerical analysis of differential equations*, no. 44, Cambridge university press.

Ishii, M. & Tromp, J., 1999. Normal-mode and free-air gravity constraints on lateral variations in velocity and density of earth's mantle, *Science*, **285**(5431), 1231–1236.

Ishii, M. & Tromp, J., 2001. Even-degree lateral variations in the earth's mantle constrained by free oscillations and the free-air gravity anomaly, *Geophysical Journal International*, **145**(1), 77–96.

Ishii, M. & Tromp, J., 2004. Constraining large-scale mantle heterogeneity using mantle and inner-core sensitive normal modes, *Physics of the Earth and Planetary Interiors*, **146**(1-2), 113–124.

Jeffreys, H., 1924. *The Earth: its origin, history and physical constitution*, University Press.

Jeffreys, H., 1939. THE TIMES OF THE CORE WAVES (second paper), *Geophysical Journal International*, **4**, 594–615.

Jeffreys, H., 1949. Dynamic effects of a liquid core, *Monthly Notices of the Royal Astronomical Society*, **109**(6), 670–687.

Jobert, N., 1976. Propagation of surface waves on an ellipsoidal earth, *pure and applied geophysics*, **114**(5), 797–804.

Kaula, W. M., 1964. Tidal dissipation by solid friction and the resulting orbital evolution, *Reviews of Geophysics*, **2**(4), 661.

Koelemeijer, P., Deuss, A., & Ritsema, J., 2017. Density structure of earth's lowermost mantle from stoneley mode splitting observations, *Nature Communications*, **8**(1).

Komatitsch, D. & Tromp, J., 1999. Introduction to the spectral element method for three-dimensional seismic wave propagation, *Geophysical Journal International*, **139**(3), 806–822.

Kopeikin, S., Efroimsky, M., & Kaplan, G., 2011. *Relativistic celestial mechanics of the solar system*, John Wiley & Sons.

Kuo, C. & Romanowicz, B., 2002. On the resolution of density anomalies in the earth's mantle using spectral fitting of normal-mode data, *Geophysical Journal International*, **150**(1), 162–179.

Kustowski, B., Ekström, G., & Dziewoński, A. M., 2008. Anisotropic shear-wave velocity structure of the earth's mantle: A global model, *Journal of Geophysical Research*, **113**(B6).

Lamb, H., 1881. On the vibrations of an elastic sphere, *Proceedings of the London Mathematical Society*, **s1-13**(1), 189–212.

Lambeck, K., 2005. *The Earth's variable rotation: geophysical causes and consequences*, Cambridge University Press.

Landau, L. D. & Lifshitz, E. M., 1976. *Mechanics: Volume 1*, vol. 1, Butterworth-Heinemann.

Latychev, K., Mitrovica, J. X., Tromp, J., Tamisiea, M. E., Komatitsch, D., & Christara, C. C., 2005. Glacial isostatic adjustment on 3-d earth models: a finite-volume formulation, *Geophysical Journal International*, **161**(2), 421–444.

Lau, H. C., Yang, H.-Y., Tromp, J., Mitrovica, J. X., Latychev, K., & Al-Attar, D., 2015. A normal mode treatment of semi-diurnal body tides on an aspherical, rotating and anelastic earth, *Geophysical Journal International*, **202**(2), 1392–1406.

Lau, H. C., Faul, U., Mitrovica, J. X., Al-Attar, D., Tromp, J., & Garapić, G., 2016. Anelasticity across seismic to tidal timescales: a self-consistent approach, *Geophysical Journal International*, **208**(1), 368–384.

Lau, H. C. P., Mitrovica, J. X., Davis, J. L., Tromp, J., Yang, H.-Y., & Al-Attar, D., 2017. Tidal tomography constrains earth's deep-mantle buoyancy, *Nature*, **551**(7680), 321–326.

Lehmann, I., 1936. P', bur. centr. seismol. int. a., *Travaux Scientifiques*, **14**, 87–115.

Leng, K., Nissen-Meyer, T., & van Driel, M., 2016. Efficient global wave propagation adapted to 3-d structural complexity: a pseudospectral/spectral-element approach, *Geophysical Journal International*, **207**(3), 1700–1721.

Leng, K., Nissen-Meyer, T., van Driel, M., Hosseini, K., & Al-Attar, D., 2019. Axisem3d: broadband seismic wavefields in 3-d global earth models with undulating discontinuities, *Geophysical Journal International*.

Lin, Y. & Ogilvie, G. I., 2017. Tidal interactions in spin–orbit misaligned systems, *Monthly Notices of the Royal Astronomical Society*, **468**(2), 1387–1397.

Lock, S. J. & Stewart, S. T., 2017. The structure of terrestrial bodies: Impact heating, corotation limits, and synestias, *Journal of Geophysical Research: Planets*, **122**(5), 950–982.

Lognonné, P., 1991. Normal modes and seismograms in an anelastic rotating earth, *Journal of Geophysical Research: Solid Earth*, **96**(B12), 20309–20319.

Lognonné, P. & Romanowicz, B., 1990. Modelling of coupled normal modes of the earth: the spectral method, *Geophysical Journal International*, **102**(2), 365–395.

Love, A. E. H., 1911. *Some Problems of Geodynamics: Being an Essay to which the Adams Prize in the University of Cambridge was Adjudged in 1911*, CUP Archive.

Maitra, M. & Al-Attar, D., 2019. A non-perturbative method for gravitational potential calculations within heterogeneous and aspherical planets, *Geophysical Journal International*, **219**(2), 1043–1055.

Maitra, M. & Al-Attar, D., 2020. On the stress dependence of the elastic tensor, *Geophysical Journal International*, **225**(1), 378–415.

Marsden, J. E. & Hughes, T. J., 1994. *Mathematical foundations of elasticity*, Courier Corporation.

Martinec, Z., Pěč, K., & Burša, M., 1989. The phobos gravitational field modeled on the basis of its topography, *Earth, Moon and Planets*, **45**(3), 219–235.

Masters, G., Laske, G., Bolton, H., & Dziewonski, A., 2000. The relative behavior of shear velocity, bulk sound speed, and compressional velocity in the mantle: Implications for chemical and thermal structure, in *Earth's Deep Interior: Mineral Physics and Tomography From the Atomic to the Global Scale*, pp. 63–87, American Geophysical Union.

McNamara, A. K., 2019. A review of large low shear velocity provinces and ultra low velocity zones, *Tectonophysics*, **760**, 199–220.

Medina, F. & Taylor, R. L., 1983. Finite element techniques for problems of unbounded domains, *International Journal for Numerical Methods in Engineering*, **19**(8), 1209–1226.

Métivier, L., Greff-Lefftz, M., & Diament, M., 2006. Mantle lateral variations and elastogravitational deformations - i. numerical modelling, *Geophysical Journal International*, **167**(3), 1060–1076.

Mitrovica, J. X., Wahr, J., Matsuyama, I., & Paulson, A., 2005. The rotational stability of an ice-age earth, *Geophysical Journal International*, **161**(2), 491–506.

Moulik, P. & Ekström, G., 2016. The relationships between large-scale variations in shear velocity, density, and compressional velocity in the earth's mantle, *Journal of Geophysical Research: Solid Earth*, **121**(4), 2737–2771.

Munk, W. & McDonald, G., 1960. The rotation of the earth, a geophys. discussion, monograph.

Murnaghan, F. D., 1937. Finite deformations of an elastic solid, *American Journal of Mathematics*, **59**(2), 235.

Nakiboglu, S., 1982. Hydrostatic theory of the earth and its mechanical implications, *Physics of the Earth and Planetary Interiors*, **28**(4), 302–311.

Noll, W., 1965. Proof of the maximality of the orthogonal group in the unimodular group, *Archive for Rational Mechanics and Analysis*, **18**(2), 100–102.

Noll, W., 1974. *A new mathematical theory of simple materials*, Springer.

Ogden, R. & Singh, B., 2011. Propagation of waves in an incompressible transversely isotropic elastic solid with initial stress: Biot revisited, *Journal of Mechanics of Materials and Structures*, **6**(1-4), 453–477.

Oldham, R. D., 1906. The constitution of the interior of the earth, as revealed by earthquakes, *Quarterly Journal of the Geological Society*, **62**(1-4), 456–475.

Panning, M. & Romanowicz, B., 2006. A three-dimensional radially anisotropic model of shear velocity in the whole mantle, *Geophysical Journal International*, **167**(1), 361–379.

Parker, R. L., 1973. The rapid calculation of potential anomalies, *Geophysical Journal International*, **31**(4), 447–455.

Parker, R. L. & Shure, L., 1985. Gravitational and magnetic fields of some simple solids of revolution, *Geophysical Journal International*, **80**(3), 631–647.

Payan, C., Garnier, V., Moysan, J., & Johnson, P. A., 2009. Determination of third order elastic constants in a complex solid applying coda wave interferometry, *Applied Physics Letters*, **94**(1), 011904.

Peltier, W. R., 1974. The impulse response of a maxwell earth, *Reviews of Geophysics*, **12**(4), 649.

Peter, D., Komatitsch, D., Luo, Y., Martin, R., Goff, N. L., Casarotti, E., Loher, P. L., Magnoni, F., Liu, Q., Blitz, C., Nissen-Meyer, T., Basini, P., & Tromp, J., 2011. Forward and adjoint simulations of seismic wave propagation on fully unstructured hexahedral meshes, *Geophysical Journal International*, **186**(2), 721–739.

Phinney, R. A. & Burridge, R., 1973. Representation of the elastic - gravitational excitation of a spherical earth model by generalized spherical harmonics, *Geophysical Journal International*, **34**(4), 451–487.

Poisson, E. & Will, C. M., 2014. Gravity, *Gravity*.

Rajeev, S. G., 2013. *Advanced mechanics: from Euler's determinism to Arnold's chaos*, OUP Oxford.

Rekier, J., Triana, S. A., Trinh, A., & Dehant, V., 2020. Inertial modes of a freely rotating ellipsoidal planet and their relation to nutations, *The Planetary Science Journal*, **1**(1), 20.

Ritsema, J., van Heijst, H. J., & Woodhouse, J. H., 1999. Complex shear wave velocity structure imaged beneath africa and iceland, *Science*, **286**(5446), 1925–1928.

Ritsema, J., van Heijst, H. J., & Woodhouse, J. H., 2004. Global transition zone tomography, *Journal of Geophysical Research: Solid Earth*, **109**(B2).

Ritsema, J., Deuss, A., van Heijst, H. J., & Woodhouse, J. H., 2010. S40rts: a degree-40 shear-velocity model for the mantle from new rayleigh wave dispersion, teleseismic traveltime and normal-mode splitting function measurements, *Geophysical Journal International*, **184**(3), 1223–1236.

Rogister, Y. & Valette, B., 2009. Influence of liquid core dynamics on rotational modes, *Geophysical Journal International*, **176**(2), 368–388.

Saad, Y., 2003. *Iterative methods for sparse linear systems*, vol. 82, siam.

Simmons, N. A., Forte, A. M., & Grand, S. P., 2009. Joint seismic, geodynamic and mineral physical constraints on three-dimensional mantle heterogeneity: Implications for the relative importance of thermal versus compositional heterogeneity, *Geophysical Journal International*, **177**(3), 1284–1304.

Smith, M. L., 1974. The scalar equations of infinitesimal elastic-gravitational motion for a rotating, slightly elliptical earth, *Geophysical Journal International*, **37**(3), 491–526.

Smith, M. L., 1977. Wobble and nutation of the earth, *Geophysical Journal International*, **50**(1), 103–140.

Stacey, F. D., 1992. *Physics of the Earth*, Brookfield Press.

Stone, M. & Goldbart, P., 2009. *Mathematics for physics: a guided tour for graduate students*, Cambridge University Press.

Su, W.-j. & Dziewonski, A. M., 1997. Simultaneous inversion for 3-d variations in shear and bulk velocity in the mantle, *Physics of the Earth and Planetary Interiors*, **100**(1-4), 135–156.

Tackley, P. J., 2011. Living dead slabs in 3-d: The dynamics of compositionally-stratified slabs entering a "slab graveyard" above the core-mantle boundary, *Physics of the Earth and Planetary Interiors*, **188**(3-4), 150–162.

Takeuchi, N., 2005. Finite boundary perturbation theory for the elastic equation of motion, *Geophysical Journal International*, **160**(3), 1044–1058.

Thomson, W., 1863. XXVII. on the rigidity of the earth, *Philosophical Transactions of the Royal Society of London*, **153**, 573–582.

Triana, S. A., Rekier, J., Trinh, A., & Dehant, V., 2019. The coupling between inertial and rotational eigenmodes in planets with liquid cores, *Geophysical Journal International*, **218**(2), 1071–1086.

Tromp, J. & Trampert, J., 2018. Effects of induced stress on seismic forward modelling and inversion, *Geophysical Journal International*, **213**(2), 851–867.

Tromp, J., Marcondes, M. L., Wentzcovitch, R. M. M., & Trampert, J., 2019. Effects of induced stress on seismic waves: Validation based on ab initio calculations, *Journal of Geophysical Research: Solid Earth*, **124**(1), 729–741.

Truesdell, C. & Noll, W., 2004. *The Non-Linear Field Theories of Mechanics*, Springer Berlin Heidelberg, Berlin, Heidelberg.

Valette, B., 1989a. Spectre des vibrations propres d'un corps élastique, auto-gravitant, en rotation uniforme et contenant une partie fluide, *CR Acad. Sci. Paris*, **309**(Série I), 419–422.

Valette, B., 1989b. Etude d'une classe de problèmes spectraux, *Comptes rendus de l'Académie des sciences. Série 1, Mathématique*, **309**(12), 785–788.

van Driel, M., Kemper, J., & Boehm, C., 2021. On the modelling of self-gravitation for full 3-d global seismic wave propagation, *Geophysical Journal International*, **227**(1), 632–643.

Van Loan, C. F. & Golub, G. H., 1983. *Matrix computations*, Johns Hopkins University Press.

Wahr, J. M., 1981a. The forced nutations of an elliptical, rotating, elastic and oceanless earth, *Geophysical Journal of the Royal Astronomical Society*, **64**(3), 705–727.

Wahr, J. M., 1981b. Body tides on an elliptical, rotating, elastic and oceanless earth, *Geophysical Journal of the Royal Astronomical Society*, **64**(3), 677–703.

Wahr, J. M., 1981c. A normal mode expansion for the forced response of a rotating earth, *Geophysical Journal of the Royal Astronomical Society*, **64**(3), 651–675.

Waldvogel, J., 1979. The newtonian potential of homogeneous polyhedra, *Zeitschrift für angewandte Mathematik und Physik ZAMP*, **30**(2), 388–398.

Walton, K., 1974. The seismological effects of elastic pre-straining within the earth, *Geophysical Journal International*, **36**(3), 651–671.

Werner, R. A., 1994. The gravitational potential of a homogeneous polyhedron or don't cut corners, *Celestial Mechanics and Dynamical Astronomy*, **59**(3), 253–278.

Woodhouse, J. & Deuss, A., 2015. Theory and observations - earth's free oscillations, *Treatise on Geophysics*, pp. 79–115.

Woodhouse, J. H., 1976. On rayleigh's principle, *Geophysical Journal International*, **46**(1), 11–22.

Woodhouse, J. H. & Dahlen, F. A., 1978. The effect of a general aspherical perturbation on the free oscillations of the earth, *Geophysical Journal International*, **53**(2), 335–354.

Woodhouse, J. H. & Giardini, D., 1985. Inversion for the splitting function of isolated low order normal mode multiplets, *Eos Trans. AGU*, **66**, 300.

Woodhouse, J. H. & Girnius, T. P., 1982. Surface waves and free oscillations in a regionalized earth model, *Geophysical Journal International*, **68**(3), 653–673.

Yang, H.-Y. & Tromp, J., 2015. Synthetic free-oscillation spectra: an appraisal of various mode-coupling methods, *Geophysical Journal International*, **203**(2), 1179–1192.